department
Mobility and
Public Works

Numerical modelling of the extreme wave climate in the Belgian harbours

PART 3: MARINA OF BLANKENBERGE

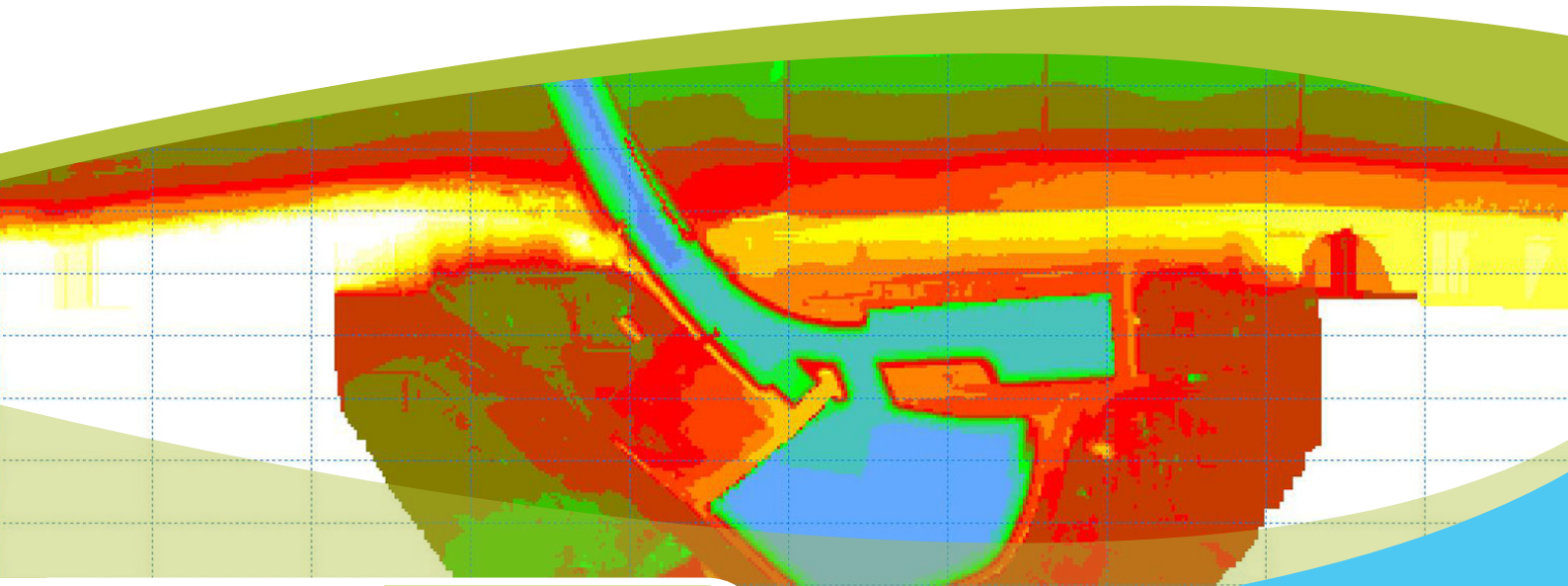

769_03 WL Rapporten

flanders
HYDRAULICS RESEARCH

IMDC
International Marine & Dredging Consultants

Vlaamse overheid

flanders
HYDRAULICS RESEARCH

Numerical modelling of the extreme wave climate in the Belgian harbours

Part 3: Marina of Blankenberge

Suzuki, T.; Gruwez, V.; Bolle, A.; Verwaest, T.; Mostaert, F.

May 2012

WL2012R769_03_3rev2_0

I/RA/11273/12.045/VGR

This publication is cited as:

Suzuki, T.; Gruwez, V.; Bolle, A.; Verwaest, T.; Mostaert, F. (2012). Numerical modelling of the extreme wave climate in the Belgian harbours: Part 3: Marina of Blankenberge. Version 2_0. WL Rapporten, 769_03_3. Flanders Hydraulics Research & IMDC: Antwerp, Belgium

I/RA/11273/12.045/VGR. IMDC, Antwerp, Belgium

Waterbouwkundig Laboratorium

Flanders Hydraulics Research

Berchemlei 115
B-2140 Antwerp
Tel. +32 (0)3 224 60 35
Fax +32 (0)3 224 60 36
E-mail: waterbouwkundiglabo@vlaanderen.be
www.watlab.be

International Marine and Dredging Consultants

Coveliersstraat 15
B-2600 Antwerp
Tel. +32 (0)3 270 92 95
Tel. +32 (0)3 235 67 11
info@imdc.be
www.imdc.be

Document identification

Title:	Numerical modelling of the extreme wave climate in the Belgian harbours: Part 3: Marina of Blankenberge		
Customer:	Coastal Division, VO	Ref.:	WL2012R769_03_3rev2_0 I/RA/11273/12.045/VGR
Trefwoorden (3-5):	Numerical wave modelling, Extreme wave climate, Harbour of Blankenberge, SWASH, Mike 21 BW, SWAN		
Text (p.):	100	Tables (p.):	/
Appendices (p.):	50	Figures (p.):	/
Confidentiality:	☐ Yes	Exceptions:	☐ Customer ☐ Internal ☐ Flemish government
		Resleased as from	
	☒ No		☒ Available online

Approval

Authors	Revisor	Project leader	Division head
Tomohiro Suzuki (WL, UGent) Vincent Gruwez (IMDC)	Annelies Bolle (IMDC)	Toon Verwaest	Frank Mostaert

Revisions

No	Date	Description	Author
1_0	20/03/2012	Concept version	Suzuki, T.; Gruwez, V.
1_1	21/03/2012	Revision	Bolle, A.
2_0	15/05/2012	Final version	Suzuki, T.; Gruwez, V.

Abstract

The design of water and wave retaining walls and flood risk analyses need hydrodynamic boundary conditions. These boundary conditions are needed during a storm with return period 1000yrs and during the super storms which were defined in the risk analysis study. The modelling of the extreme wave climate is decoupled to the wave penetration and the lacal generation of waves by the extreme wind speed. The wave penetration is modelled with Mike 21 BW as was done for Oostende and Zeebrugge. MILDwave is not used this time because non-linear effects (e.g. long wave generation, wave setup) are too important in this case. Instead another nonlinear model SWASH is applied. The modelling of local generation of waves by wind is still done with the spectral model SWAN.

First the bathymetry files are created based on the dredging plan of Blankenberge marina, and all the suitable settings used for the Mike 21 BW and the SWASH are investigated. Since SWASH model does not have so much application examples, Wenduine physical model is used to validate the model. Consequently, a sensitivity analysis is conducted for both models to study which parameter is important for the wave climate inside the marina. The most severe offshore wave direction for the design of the wave retaining walls is decided based on the 1000 year storm. After the calculation of the wave penetration in the case of 1000 year storm and +7.9 mTAW storm, locally generated wind waves are also simulated by SWAN. All extreme wind speeds and directions for the 1000-year storm and the super storms are modelled. Finally, long and short wave energy of the wave penetration models is separated and a superposition of the short wave energy and the SWAN model is done to obtain the total extreme wave climate in the marina of Blankenberge. The maximum surface elevation of the long wave energy and the wave setup provide an increase of the still water level to take into account for design purpose.

Table of Contents

List of Tables

List of Figures

1 Introduction

1.1 The assignment

On the 10th of July 2009 the contract extension 1 of act 16EB/04/18 “Wave Modelling Flemish and Dutch Coast” (in Dutch: “Golfmodellering Vlaamse en Nederlandse kust”) was established. This act contains the study of the extreme wave climate in the Belgian harbours and is performed by IMDC (International Marine & Dredging Consultants nv) in cooperation with Flanders Hydraulics Research.

1.2 Aim of the study

During a super storm primarily the waves determine the forces and overtopping that is occurring on the wave retaining walls. The aim of this study is to determine the wave climate in the Belgian harbours during such super storms by detailed wave modelling. In the current report the harbour of Blankenberge is considered. The purpose of this report can be summarized as:

- A detailed description of the model set-up, performing sensitivity analyses, an analysis of the wave setdown/-up and the generation of long waves and the resulting oscillations in the harbour, comparison of the model results and a validation with field measurements;
- Set-up of the wave model for the modelling of locally generated waves by extreme wind speeds;
- Combining the wave penetration results with the locally generated waves to obtain the total extreme wave climate in the harbour along the trajectory of the retaining walls (cf. Figure 1-1).

The same methodology which was developed by Gruwez et al. (2011) for the harbour of Oostende and which was applied for the harbour of Zeebrugge (Gruwez et al., 2012) is used for the harbour of Blankenberge. However, some specific adjustments are needed for the Blankenberge case.

Figure 1-1: Trajectory of the water and wave retaining walls in the harbour of Blankenberge (Coastal Division, 2011). Along the western part of the northern quay, there already exist some walls.

1.3 Overview

Within the present study, previously the following reports have been published (in Dutch):

- Deelopdracht 1: Inventarisatie Voorbereiding tijdreeksen met randvoorwaarden (Deelrapport 1 : I/RA/11273/05.106/CMA)
- Deelopdracht 2: Voortzetting validatie numeriek model (Deelrapport 2: I/RA/11273/06.057/SDO)
- Deelopdracht 3: Opstellen van de post processing tools (I/RA/11273/09.051/SDO)
- Deelopdracht 4: Technisch wetenschappelijke bijstand
    - Traject golfklimaat (Deelrapport 4: I/RA/11273/08.064/SDO)
    - Traject Onderzoek (Deelrapport 4: I/RA/11273/09.007/SDO)
    - Eindrapport (Deelrapport 4: I/RA/11273/09.030/SDO)
- Deelopdracht 5: Rapportage jaargemiddelde golfklimaat (Deelrapport 5: I/RA/11273/09.091/SDO)
- Bijakte: Numerieke modellering van het extreem golfklimaat in de Belgische havens
    - Harbour of Oostende (WL ref.: WL2011R769_03rev2_0, IMDC ref. : I/RA/11273/11.113/VGR)
    - Harbour of Zeebrugge (WL ref.: WL2012R769_03_2rev2_0, IMDC ref. : I/RA/11273/12.016/VGR)
    - Harbour of Blankenberge (the current report)

1.4 Structure of the report

In Chapter 2 a short overview of the applied wave models is given.

Chapter 3 discusses the set-up of the different wave penetration models. It also contains some sensitivity analyses, influence studies, a comparison of the different wave models and a validation with field measurements.

In Chapter 4 the wave model for the simulation of the locally generated waves by extreme wind is set up. These results are then combined with the wave penetration models results to obtain the total extreme wave climate in the harbour along predefined quay wall zones in Chapter 5.

The general conclusions will then follow in Chapter 6.

2 Numerical wave models

For the previous harbour cases Oostende (Gruwez et al., 2011) and Zeebrugge (Gruwez et al., 2012), the wave penetration was modelled with both the linear modal MILDwave (Troch, 1998) and non-linear model Mike 21 BW. The water depth was sufficiently high in the areas of interest, so that non-linear effects were negligible. In the case of the marina of Blankenberge however, the water is quite shallow and very shallow areas on the beaches next to the harbour and on the harbour dams occur. This causes an increase of the importance of the non-linear effects such as wave-wave-interactions and wave setdown/-up. From the field measurements (IMDC, 2011) it was also clear that short wave penetration was inferior to wave-wave interaction generated long wave penetration and resulting resonance effects. This explains why in this case only non-linear phase resolving wave models were used. It is however possible to determine the resonance frequencies of the marina with the linear model MILDwave (Comm. Troch, 2011) although it is not yet practical (no user defined spectrum can be specified).

The Boussinesq equations model Mike 21 BW and the Non-Linear-Shallow-Water-Equations model SWASH were chosen. A short overview of the chosen wave models together with their characteristics and which physical (wave) processes can be simulated, are given in Table 2-1. Although SWASH is more stable and can simulate wave run-up, wave breaking and wave transmission simultaneously with a much more robust numerical stability than Mike 21 BW, it is still the first application of the SWASH model for wave penetration in a harbour. That is why a validation with the known and well validated model Mike 21 BW and field measurements is important.

Local generation of waves by wind is modelled with the spectral model SWAN (TUDelft, 2010).

Table 2-1: Overview of the chosen wave models and their characteristics.

	Mike 21 BW	**SWASH**	**SWAN**
Type	Non-linear	Non-linear	Spectral
Equations	Boussinesq equations Madsen et al. (1991, 1992)	NLSW Zijlema et al. (2011)	Action balance equation Booij et al. (1999)
Domain	Time	Time	Frequency
Physical processes			
Refraction & shoaling	X	X	X
Diffraction	X	X	X (except combined with reflection)
(partial) Reflection	X Brorsen (1998, 2000)	X	X (no standing waves)
Wave breaking	X	X	X
Non-linear wave-wave interactions	X	X	X (no sub harmonics)
Wave generation by wind	-	X (not yet functional)	X

3 Wave penetration: phase resolving wave models

3.1 Bathymetry

3.1.1 Introduction

The method to create the bathymetry file for the Blankenberge models is introduced in this section. The bathymetry files are used in numerical model simulations (e.g. SWASH, Mike21BW and SWAN) based on the Cartesian coordinate system by changing local settings such as the domain size, the sponge layer's thickness and the local depth for each numerical models.

It is noted that the navigation channel is prone to sedimentation by sand arriving from transport on the neighbouring beaches and shore face in storm conditions. Severe storms can result in blockage of the marina entrance. However, the sedimentation of navigation channel is not taken into account in this study.

3.1.2 Original data

Original data for the creation of the bathymetry files for Blankenberge are listed below. Table 3-1 shows the overview of the original bathymetry data. Figure 3-1 shows the plan view of the bathymetry inside the harbor and Figure 3-2 shows the plan view of the bathymetry of the new land.

- Offshore bathymetry data : "110520_BKBZB_lat.txt" (Afdeling Kust, 2011a)
- Beach level : "strandlodingen_2008_part1_WGS84_TAW.xyz" and "*_part2_*" (Afdeling Kust, 2011a)
- Land level : "2009_stra_Blankenberge_maa.txt" (Afdeling Kust, 2011a)
- Bathymetry inside the harbour : "blankenberge in wgs84 utm31.pdf" (Afdeling Kust, 2011b), shown in Figure 3-1.
- Land level of the new land : "plan 2-3_aangepast na aanbesteding_v6.pdf" (Afdeling Kust, 2011c), shown in Figure 3-2.

Table 3-1: Original bathymetry data

Data	Measurement year	Reference level	XY coordinates
Offshore depth data	2011	LAT (0.32 m below TAW)*	UTM31WGS84
Beach level	2008	TAW	UTM31WGS84
Land level	2009	TAW**	Lambert72
Land level of the new land	Plan view	TAW	UTM31WGS84
Depth inside the harbor	Plan view	LAT (0.32 m below TAW)	UTM31WGS84

* based on Getijtafels LAT 2012-LR.pdf , and personal communication with Afdeling Kust by email on 01/13/2012.

** personal communication with Afdeling Kust by email on 02/12/2011.

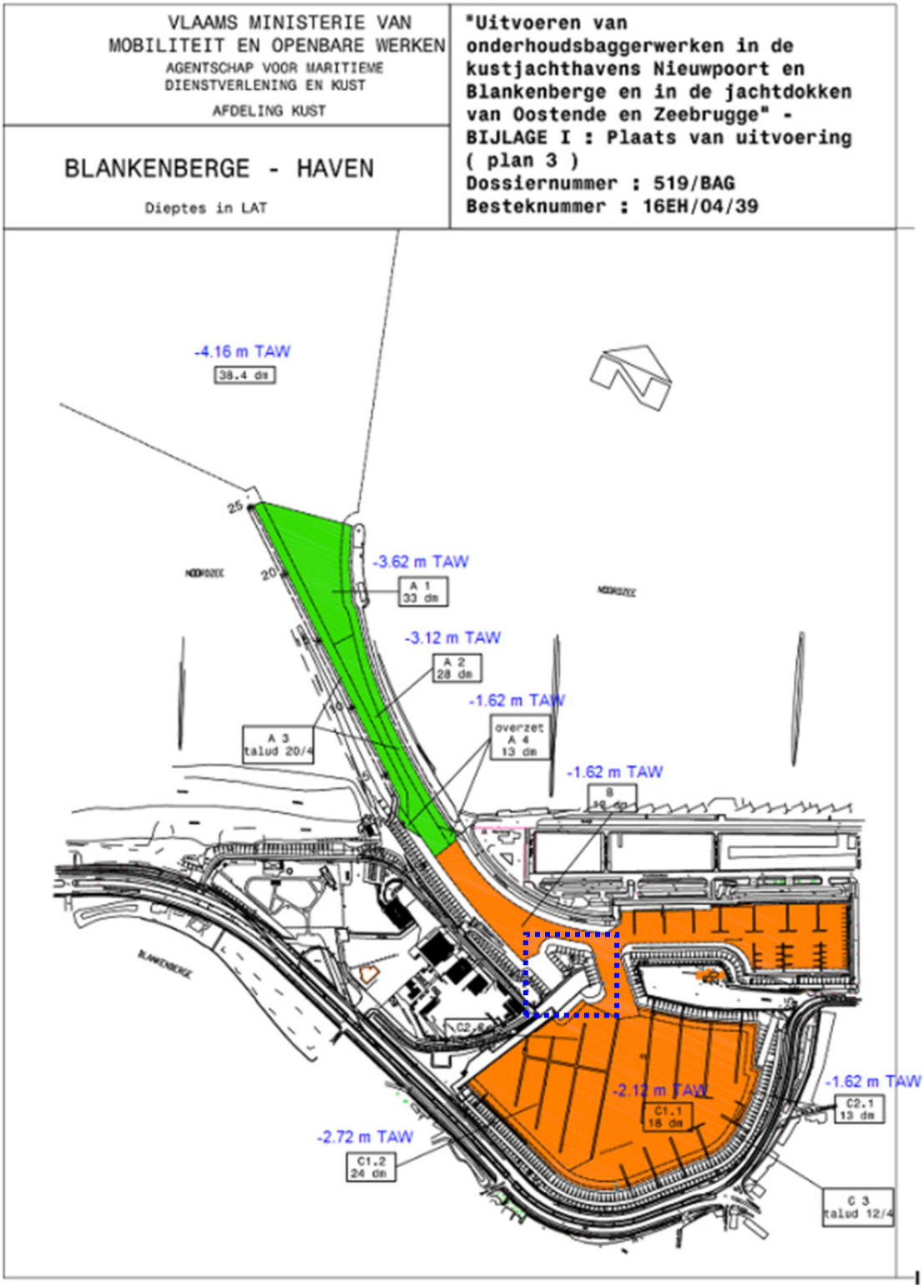

Figure 3-1: Bathymetry inside the harbour, “blankenberge in wgs84 utm31.pdf” (Afdeling Kust, 2011). It is noted that the new land is to be located inside the blue dotted box.

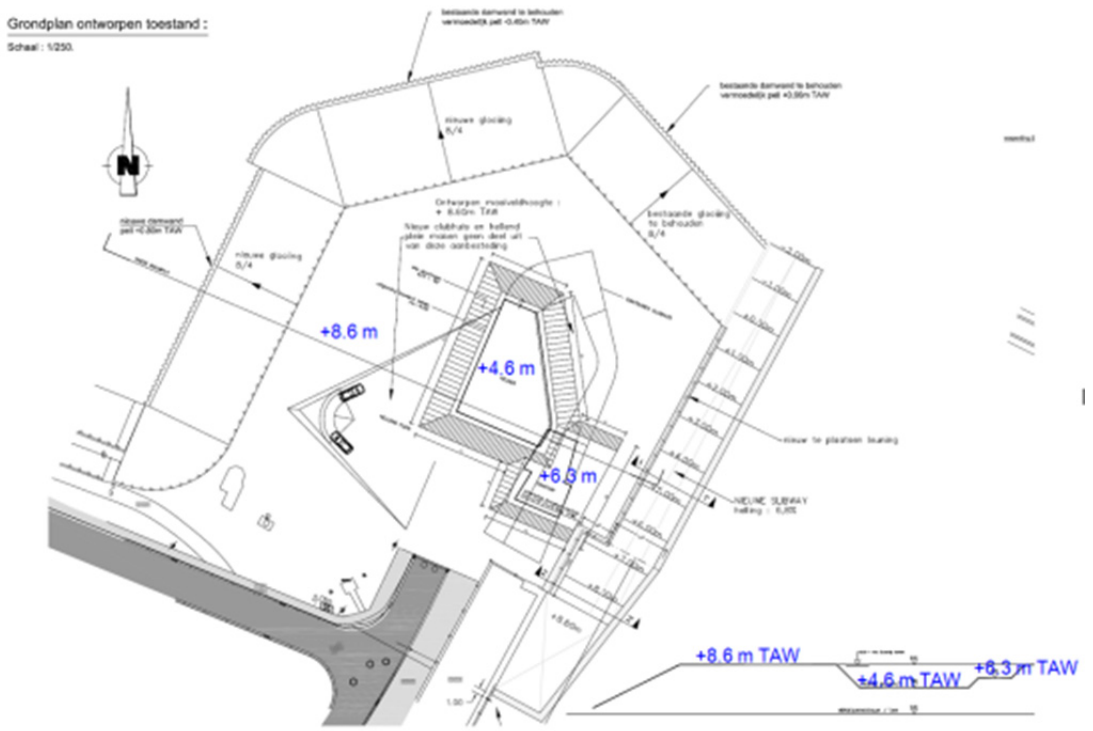

Figure 3-2: Bathymetry of the new land, “plan 2-3_aangepast na aanbesteding_v6.pdf” (Afdeling Kust, 2011).

3.1.3 Data management

Reference level

TAW (Tweede Algemene Waterpassing; Belgian standard datum level, situated near MLLWS) is used as a reference level for the bathymetry. LAT (Lowest Astronomical tide) is converted to TAW by using the relationship between LAT and TAW below.

- Level in TAW = Level in LAT - 0.32 m (e.g. 0 m TAW = 0.32 m LAT; -2.12 m TAW = -1.8 m LAT)

XY coordinates

UTM31WGS84 format is used as a reference for XY (horizontal) coordinates for the bathymetry. Lambert 72 format is converted into UTM31WGS84 format by ArcGIS.

Data extraction from CAD data

The CAD data (Bathymetry inside the harbour and the new land, shown in Figure 3-1 and Figure 3-2) are used to make the bathymetry inside/around the harbour. Since it is required to extract the bathymetry from the CAD data, the extraction of the bathymetry data has been made by the method as shown below.

1. Define the boundary of each depth. The defined areas are shown in Figure 3-2. The slope gradient of the transitions between each depth are set as 1/10 by considering the realistic dredging operations.
2. In CAD, additional depth points are allotted inside the defined areas. An offset from boundary of the defined area is used to get more points inside the enclosed area.
3. Extract these data by the “List” function of AutoCAD.

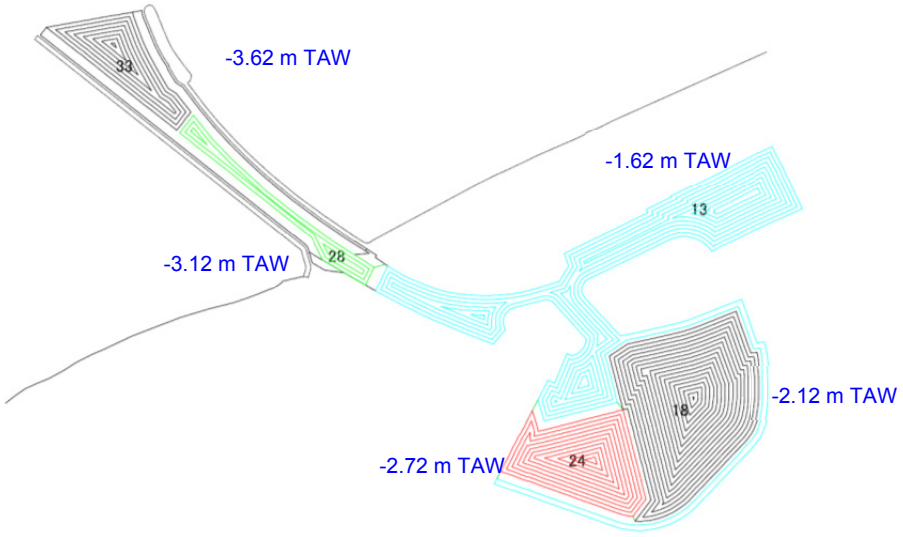

Figure 3-3: Bathymetry points inside the harbour. It is noted that all the points are located on the lines.

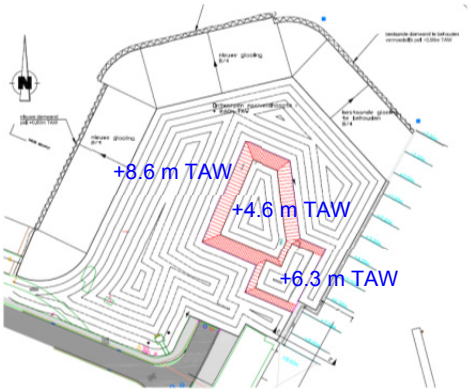

Figure 3-4: Bathymetry points around the new land.

Grid size

The grid size of the created bathymetry file is 2 m both in x- and y- axes.

Pier structures at the entrance channel

Pier structures are not included in the bathymetry file. The pier structures consist of wooden piles, therefore it is assumed that these are destroyed during super storms.

Bathymetry file creation

The flow of the bathymetry data creation for Blankenberge is shown below.

1. XY coordinate format change from Lambert72 to UTM31.
   - “2009_stra_Blankenberge_maa.txt” (Lambert72) to “a_utm31wgs84.txt” (UTM31)
2. The level format is changed from LAT to TAW and all the file are merged into one bathymetry file, BLK_A0.xyz (level, TAW)

- a_utm31wgs84.txt (level, TAW)
- 110520_BKBZB_lat.txt (depth, LAT)
- strandlodingen_2008_part1_WGS84_TAW.xyz (level, TAW)*
- strandlodingen_2008_part1_WGS84_TAW.xyz (level, TAW)*

  *the data between x=507000 to 509000 are used since the file size is too large.
- BLK_DEP.txt (level, LAT) from CAD

3. Creation of the bathymetry is done by Mike Zero.
4. Output the created bathymetry file.

Created bathymetry file

The bathymetry created based on the original data detailed in § 3.1.2 is shown in Figure 3-5. 'Define working area – Type' in Mike Zero is: UTM31, Projection (507300, 5683750), Grid (2.0, 2.0), Points (1000,600), Orientation -22.5°(NNW). Interpolation has been done with a diameter of 5 m by bilinear interpolation.

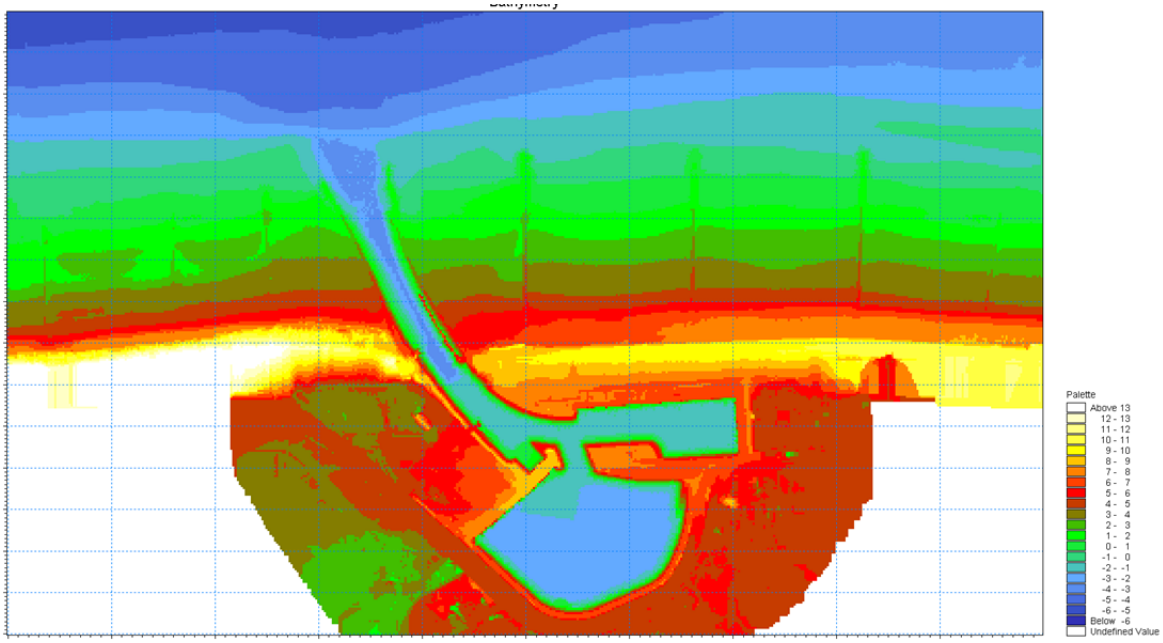

Figure 3-5: Created bathymetry by Mikezero. It is noted that the new land has not been reflected in this figure.

The same bathymetry data is used for all the numerical models.

3.2 Hydrodynamic boundary conditions

The hydrodynamic boundary conditions are shown in Table 3-2. The conditions of the 1000 year storm and those of the super storms are determined in Annex 1. The conditions of the validation runs are field measurements of the wave buoy located just outside the marina of Blankenberge (coordinates: N51°19'02", E03°06'05"). These conditions are taken from the measurement campaign of 2010-2011 (IMDC, 2011) during some of the highest field measurements in the marina (short wave penetration). The choice of the validation conditions is discussed further in §3.6.

Table 3-2: The hydrodynamic boundary conditions and calculation cases

Type	SWL	σ [°]	d_{max} [m]	H_{m0} [m]	T_p [s]	Wave direction [-]			
						N	**NNW**	**NW**	**WNW**
Validation	+4.91	30	9.91	2.3	9.1	-	X	-	-
	+4.97	30	9.97	2.3	8.5	-	-	X	-
	+4.55	30	9.55	2.5	8.5	-	X	-	-
	+4.61	30	9.61	2.7	8.5	X	-	-	-
1000 year storm	+7.10	0	12.1	4.5	12.0	-	X[1]	-	-
	+7.10	15	12.1	4.5	12.0	X	X	X	X
	+7.10	30	12.1	4.5	12.0	-	X[1]	-	-
Super storms	+7.90	0	12.9	5.0	12.0	-	-	-	-
	+7.90	15	12.9	5.0	12.0	-	X	-	-
	+7.90	30	12.9	5.0	12.0	-	-	-	-
	+7.40	15	12.9	4.7	12.0	-	-	-	-
	+6.90	15	12.9	4.5	12.0	-	-	-	-
	+6.40	15	12.9	4.3	12.0	-	-	-	-

[1]: Result only with older version of model, which is only useful for relative comparison.

Based on each of these wave conditions a JONSWAP spectrum is made. This spectrum is then used to generate a time series which is imposed at the wave generating boundary/wave generation line.

Directional spreading

The directional spreading for the short crested wave simulations is determined for both models from the directional distribution function (DHI, 2009; SWASH User Manual, 2011):

$$D_n(\theta) = \cos^n(\theta - \theta_{main})$$

With n the directional spreading index;
θ the wave direction;
θ_{main} the main wave direction.

The corresponding directional spreadings σ for the applied directional spreading indices n are shown in Table 3-3. The relation is determined by equation $\sigma = \sqrt{\frac{2}{(s+1)}}$ with $s = 2n + 1$.

Table 3-3: The directional spreading applied in the Mike 21 BW model, for SWASH see Table 3-8.

n [-]	σ (approximate value) [°]
13	**15**
2	**30**

The influence of the directional spreading will be discussed in §3.5.4.

To determine a realistic value of the directional spreading the spreading parameter s_{max} can be estimated by Goda (2010) by the following method.

1. Calculate the deep water wave steepness, Ho/Lo. Ho is the offshore significant wave height and Lo is the offshore peak wave period. In this study, wave conditions for 8m super storm (Verwaest et al. 2008) are used. The off-shore significant wave height Ho is 8.39 m and the offshore peak period To is 12.7 s, which gives as deep water wave steepness Ho/Lo = 0.33.

   To=12.7s → Lo=1.56 T^2= 252 m → Ho/Lo = 8.39/252 = 0.33

2. Estimate the spreading parameter smax offshore from the diagram of Goda (2010), shown in Figure 3-6. It gives smax,o~10 when Ho/Lo = 0.33 is applied.

   Ho/Lo = 0.33 → smax,o ~ 10

3. Estimate the spreading parameter smax from the diagram of Goda (2010), shown in Figure 3-6. In this study, the water depth at the calculation boundary is 13 m (at -5m TAW). It gives smax~50 when the relative water depth h/Lo = 0.05 is applied.

   h/Lo = 0.05 → smax ~ 50

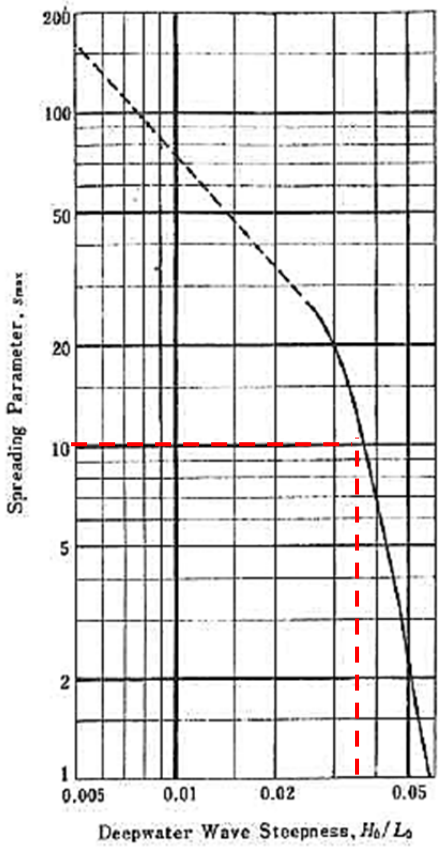

Figure 3-6: Goda's (2010) diagram for the estimation of spreading parameter in offshore

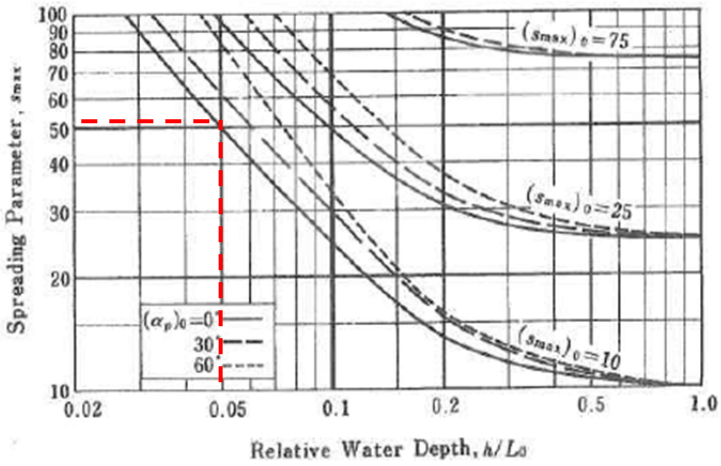

Figure 3-7: Goda's (2010) diagram for the estimation of spreading parameter in shallow water

The directional spreading is determined by equation $\sigma = \sqrt{\frac{2}{(s+1)}}$ with $s = 2m + 1$.

If the s_{max} value can be directly translated to s value in the equation, the directional spreading in this case is 11 degree. Taking into account the directional spreading value used in previous studies for the Flemish coast, it is determined to use directional spreading =15° for this study.

3.3 Setting up the Mike 21 BW model

3.3.1 Introduction

The Mike 21 BW model is set up according to the same method previously followed by Gruwez et al. (2011; 2012) for the harbours of Oostende and Zeebrugge.

3.3.2 Bathymetry, harbour geometry and calculation domain

The bathymetry made in §3.1 is adapted for use in the Mike 21 BW model:

- A minimum water depth of 1.5m (1.0m in case of the validation simulations) is employed so that the wave runup does not have to be modelled (notorious for its numerical instabilities);
- A land boundary is defined corresponding to the intersection of land and still water level (if necessary increased with the wave setup) in case of slopes and along the quay walls;
- The slopes of the harbour dams are smoothed and the slope and crest is adapted to comply with the original plans (Dienst der Kust, 1956).

The slopes of the dikes in the marina (~1/2) are included in the bathymetry made in §3.1. Although they are – strictly speaking – too steep to be used in the Mike 21 BW model (max. slope = 1/3), the slopes are preserved in the bathymetry to account for the refraction of the waves.

The size of the calculation domain makes sure that:

- The area of interest is included;
- It is as small as possible to limit the calculation time;
- Enough space is available for the development of the incoming waves (usually two wave lengths between the wave generation line and the start of the real bathymetry) and absorption of the outgoing waves (provided by sponge layers of usually one or two wave lengths wide (DHI, 2009));
- A sufficiently wide area of the beach on both sides of the marina is included to allow generation of long waves due to non-linear wave-wave interactions. These bound long waves become free long waves when reflected on the beach and enter the marina by refraction and diffraction;
- The shadow zone created by changing the wave direction and/or the directional spreading does not reach the area of interest. In other words the total imposed wave energy is allowed to reach the entrance of the harbour at all times.

Two calculation domains are made:

1. NNW orientation (cf. Figure 3-8): for simulation of wave directions NW, NNW and N;
2. WNW orientation (cf. Figure 3-9): for simulation of wave directions W and WNW.

All levels are given relative to the reference level TAW [m TAW].

The longitudinal and cross sections along which the results will be analysed are given in Figure 3-8. The output points are given in Figure 3-10 and Figure 3-11.

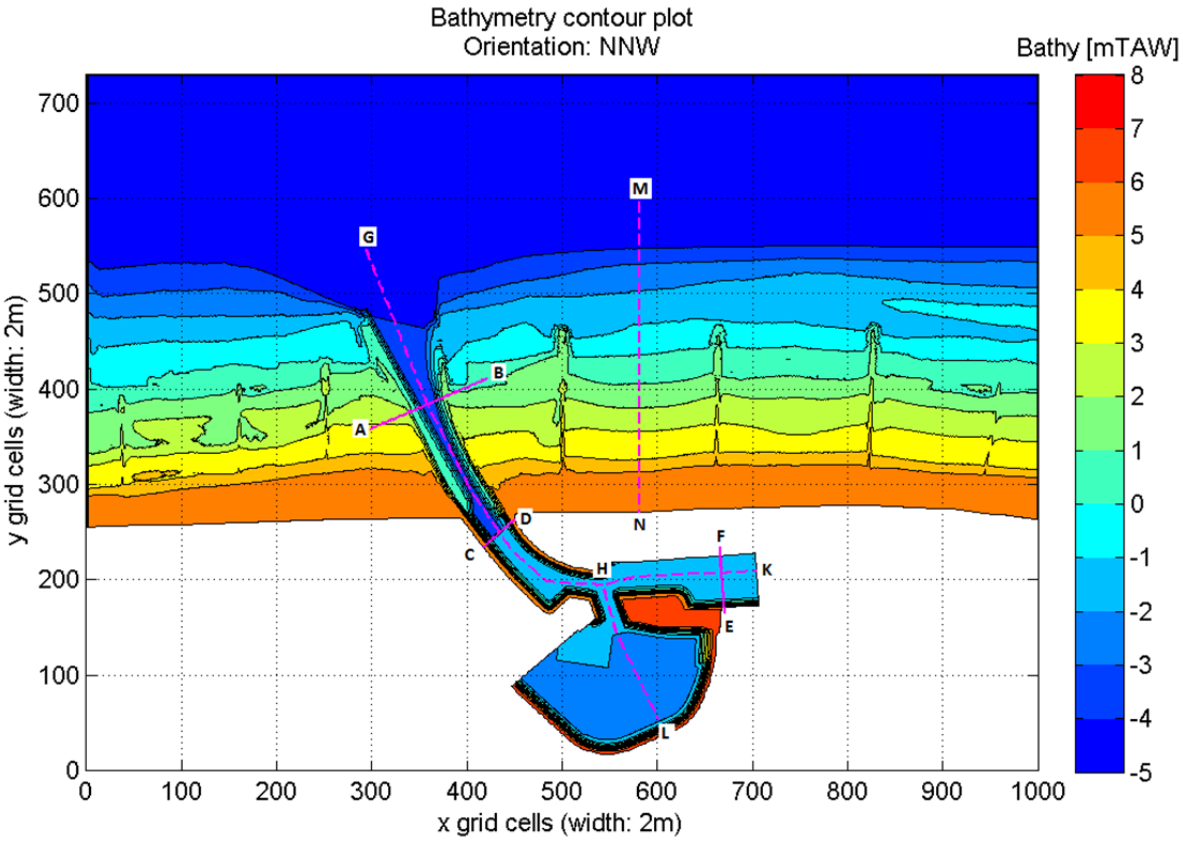

Figure 3-8: Overview of the bathymetry within the calculation domain (orientation NNW). Indication of the longitudinal sections GH, HK and HL and cross sections AB, CD, EF and MN.

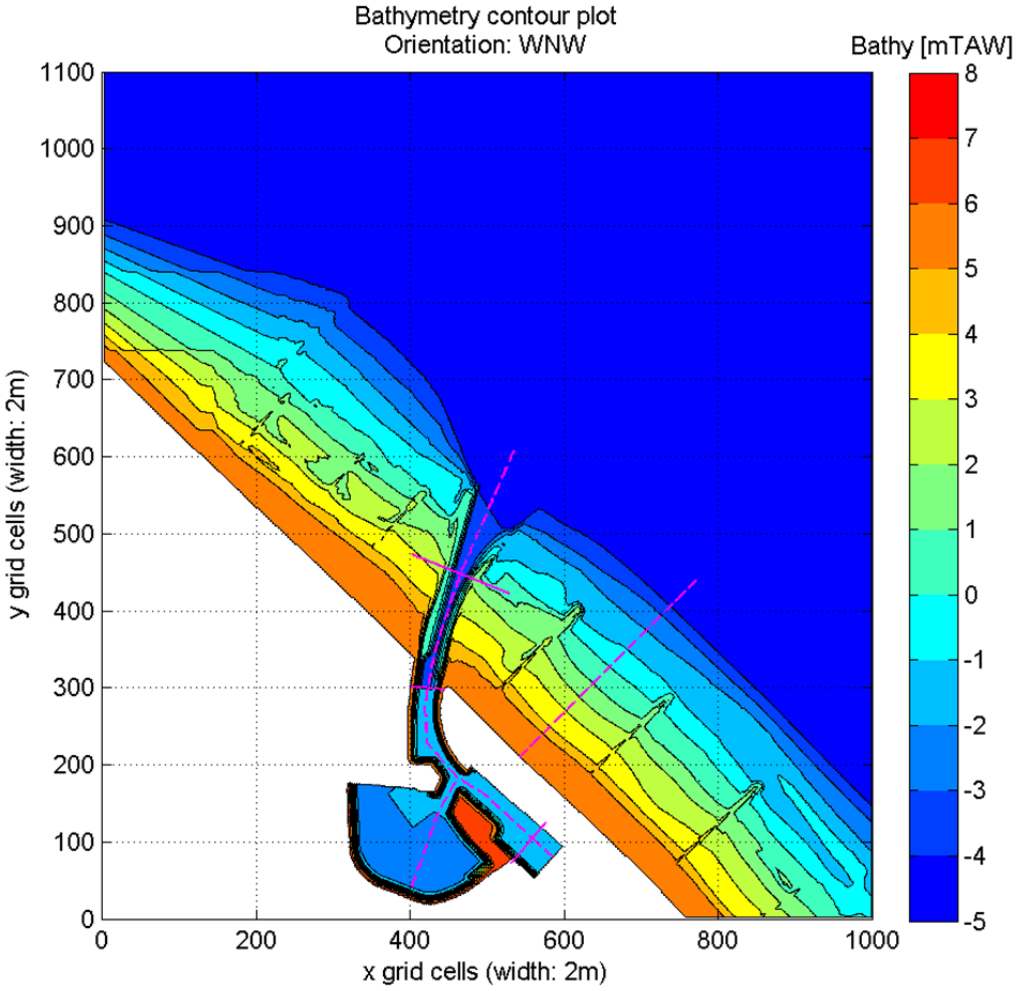

Figure 3-9: Overview of the bathymetry within the calculation domain (orientation WNW). Indication of the longitudinal sections GH, HK and HL and cross sections AB, CD, EF and MN.

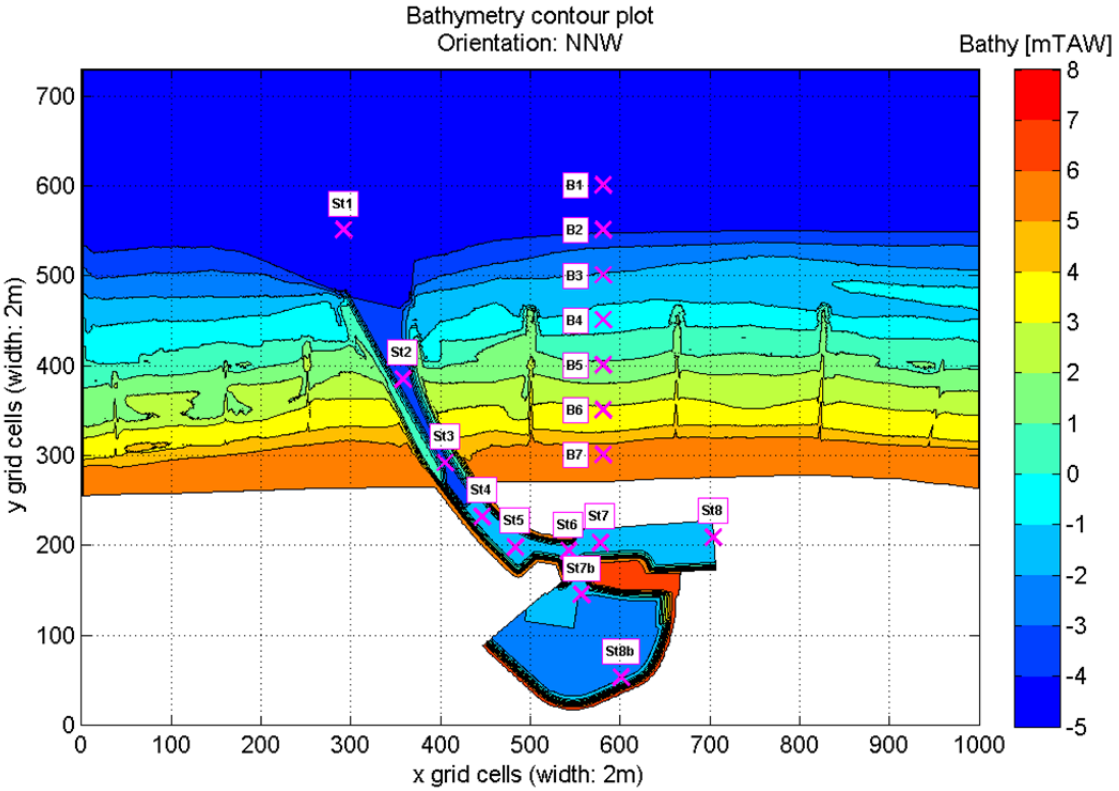

Figure 3-10: Overview of the bathymetry within the calculation domain (orientation NNW). Indication of output points along the longitudinal sections.

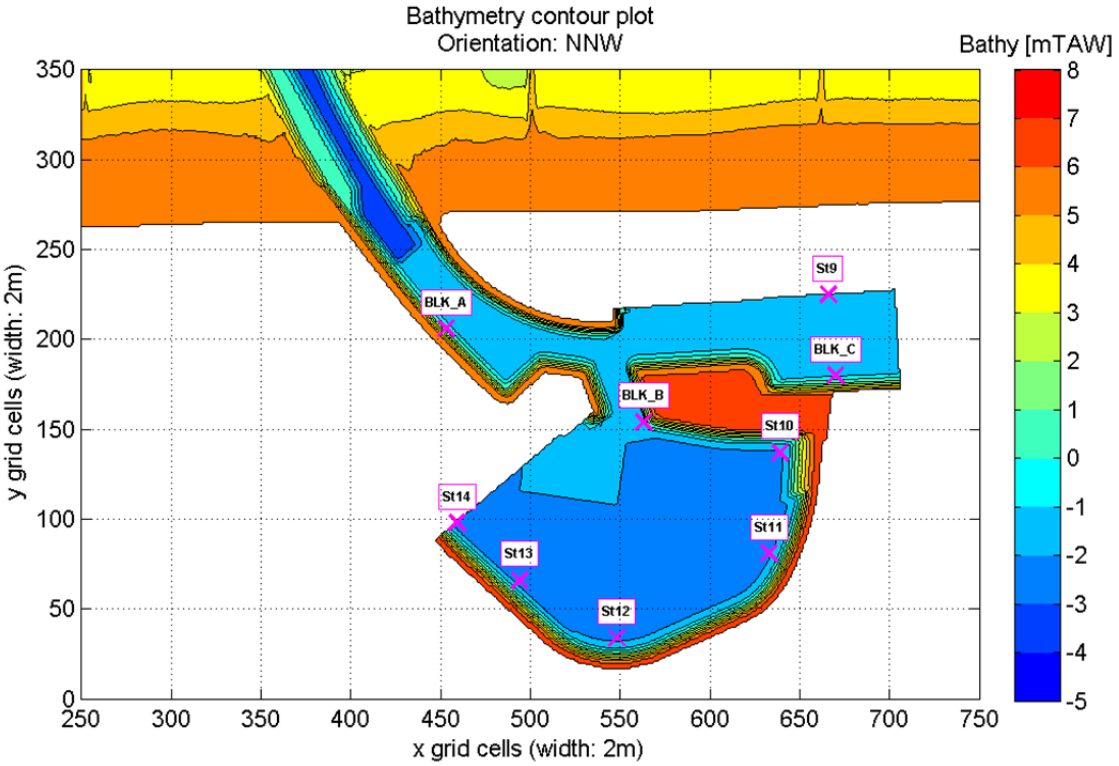

Figure 3-11: Zoom to the bathymetry of the marina (orientation NNW). Indication of output points inside the marina of Blankenberge.

3.3.3 Spectrum cut-off frequency

A JONSWAP spectrum is made based on each of the wave conditions given in Table 3-2. In Mike 21 BW a cutoff-frequency has to be chosen to prevent numerical instabilities caused by very short waves (DHI, 2009). The relation of the maximum water depth in the calculation domain and the deep water wave length of the shortest wave may not exceed 0.5 (when using the Boussinesq equations including the deep water correction terms). The lowest upper boundary of this cutoff-frequency is determined by the conditions with the largest water depth, i.e. for SWL = +7.90mTAW. For a wave with period 4.10s this conditions is fulfilled:

$$\frac{d_{max}}{L_0} = \frac{12.90}{26.22} = 0.49 \leq 0.50$$

To provide some extra room for the numerical stability a minimum wave period of 5.5s is chosen. Although a higher cutoff-frequency can be used for lower water levels the cutoff-frequency of 0.182Hz (=1/5.5s) is used for all extreme storm simulations (1000yr and super storm conditions) out of practical considerations. For the validation runs the water level is much lower and the peak period is also lower. For these cases a higher cutoff-frequency of 0.250Hz (=1/4.0s) is used.

The spectrum is truncated for frequencies higher than the cutoff-frequency. This causes a minor loss of wave energy and therefore also of the significant wave height. Mike 21 BW provides the ability to rescale the spectrum so that the imposed significant wave height is respected. However, it was chosen not to apply this because:

- Then the specific shape of the JONSWAP spectrum is preserved;
- The loss of wave energy is indeed minor.

3.3.4 Grid size, time step and simulation period

Grid size

A discretisation is needed to a finite number of calculation points within the calculation domain. This discretisation results in a regular rectangular grid. The grid cell size in x and y direction is chosen such that (DHI, 2009):

- The shortest wave length in the calculation domain (T_{min} = 4.0s and d_{min} ≈ 1.5m => L_{min} = 14.4m) has a resolution of 7 to 10 grid points:
$$\frac{\mathrm{L_{min}}}{7 \text{ to } 10} \approx 2.06\mathrm{m} \text{ to } 1.44\mathrm{m}$$
- The most energetic waves in the calculation domain have a resolution of 20 to 40 grid points per wave length in the breaking zone:
$$\frac{\mathrm{L_p}}{20 \text{ to } 40} \approx 2.3\mathrm{m} \text{ to } 2.1\mathrm{m}$$
- The complexities of the bathymetry and harbour geometry are sufficiently represented.

From these conditions a practical choice is made for the grid cell dimensions:

$$\boxed{\Delta x = \Delta y = 2.0m}$$

Time step

In Mike 21 BW the time step has to meet the following conditions (DHI, 2009):

- The smallest wave period (=4.0s) has to contain 25-35 time steps;
- The time step should satisfy the Courant-criterion:
$$\Delta t \leq \frac{\Delta x}{C}$$
- When wave breaking is enabled, the time step is typically 0.05s-0.10s according to experience from DHI (2009).

The upper boundaries of the time step are summarised in Table 3-4.

Table 3-4: Upper boundaries for the time step Δt in Mike 21 BW based on the conditions given by DHI (2009)

Frequency	f [Hz]	T [s]	L0 [m]	Ld_{max} [m]	C [m/s]	Δt_{max} [s]	T/25 [s]	T/35 [s]
f_p	0.083	12.0	225.0	127.0	10.6	0.19	0.48	0.34
$f_{max,1}$	0.182	5.5	47.2	44.7	8.1	0.25	0.22	0.16
$f_{max,2}$	0.250	4.0	25.0	25.0	6.3	0.32	0.16	0.11

Based on these conditions a time step of $\boxed{\Delta t = 0.05s}$ is chosen because wave breaking will be included in al simulations (cf. §3.3.6).

Simulation period

For the calculation of the statistical parameters (such as the significant wave height Hm0) the simulation period has to be at least 15min to 20min long. This corresponds to approximately 100 waves. Because also long waves are considered in the case of Blankenberge a longer simulation period of 40min is used corresponding with 200 waves (for T_p = 12.0s).

In addition to this a warm-up period is needed to allow enough time for the shortest wave (T = 4.0s, L = 25.0m => C = L/T = 6.3m/s) to reach the furthest location in the calculation domain (DHI, 2009). The longest distance a wave has to propagate in the calculation domain is about 1200m. The minimal warm-up time needed is then:

$$\frac{1200}{6.3} = 190s \approx 3.2min$$

A total simulation time of 45min is chosen for all Mike 21 BW simulations. In §3.5.5 the influence of a longer time series of 80min is investigated.

3.3.5 Wave generation and absorption

In Mike 21 BW waves are generated in the calculation domain by an internal wave generation line. A time series of surface elevations is made based on the JONSWAP spectrum from §3.2. This time series is imposed on the wave generation line. Waves propagate to both sides of this line perpendicular or with an angle to this line. The wave generation line is placed in constant water depth of -5mTAW over a distance of at least one or two wave lengths from the real bathymetry. Behind the wave generation line there is one wave length space for the sponge layers which absorb:

- The wave energy coming from the wave generation line directly;
- The wave energy reflected from the beach and marina.

At the sides of the calculation domain a thin layered sponge layer is placed which absorbs most of the incoming wave energy in case of an oblique incident wave direction and/or directional spreading. A thin layered sponge layer (absorption coefficient μ_{MIKE} = 1.60 → Cr ≈ 0.10, with transition layers of μ_{MIKE}=1.1 and 1.3) is used to keep the calculation domain (and therefore the calculation time) as small as possible (cf. Figure 3-12).

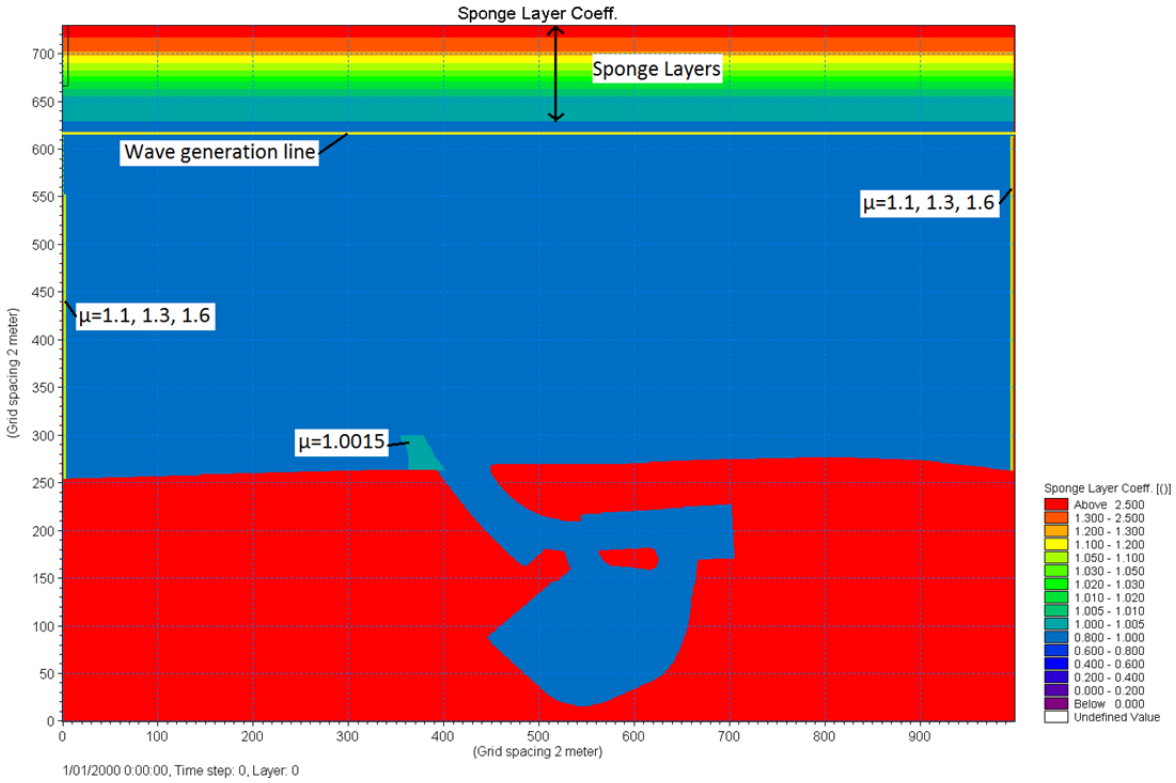

Figure 3-12: Position of the wave generation line and sponge layers in the Mike 21 BW model (orientation: NNW)

3.3.6 Physical processes

Wave breaking

Wave breaking occurs when the significant wave height exceeds half of the local water depth ($H_s \geq 0.5 * h$). Very shallow areas occur on the beach, the harbour dams and in the marina on the slopes of the dikes. Moreover, wave breaking is not only an important dissipative process but is also important for freeing bound long waves.

Wave breaking is included in the Mike 21 BW model. The default values for the parameters of the wave breaking module are applied.

Wave run-up

Although Mike 21 BW is able to model wave run-up it is not included. Including wave run-up would increase the chance of numerical instability too much, certainly in the case of a very complicated bathymetry.

Wave transmission

Because most of the harbour dams are below SWL a lot of wave transmission occurs at these locations. The piers along the harbour dams could be a cause of dissipation for waves propagating over the harbour dams. In case of the 1000yr storm and the super storms it is assumed the pier structure will have failed and disappeared. Only in case of the validation runs the piers could possibly have an effect on the transmitted waves. This could be modelled using a sponge layer (or porosity layer) but it was chosen not to do this.

Another area of possible wave transmission is just east of the marina entrance where the crest level of the dike is around +9.00mTAW. Due to wave set-up the water level can reach this level and wave transmission could occur. Without wave run-up this is impossible to simulate with Mike 21 BW. Sponge layers could be used in coordination with a minimal water depth, but this would have to be calibrated.

The parking area between the two yacht harbours in the marina is not safeguarded by a storm wave retaining wall (cf.). The level of this area is approximately at +7.50mTAW. During some of the super storm conditions (e.g. +7.90mTAW) this area will even be flooded and therefore also wave transmission can occur. In case this area is flooded a minimum water depth of 0.5m made and a sponge layer is added.

Bottom friction

Bottom friction has an important dissipative effect on long waves (T>30.0s). The coefficient of Chézy C determines the bottom friction in Mike 21 BW. A value of C=73 is chosen for the complete calculation domain. This corresponds approximately to a coefficient of Manning of 0.02 (as used for the SWASH model) using the relation (DHI, 2009):

$$M = \frac{h^{-1/6}}{C}$$

An artificially high bottom friction is also used in numerically unstable areas (cf. §3.3.7).

Miscellaneous

Because of the many shallow areas in this model the following physical processes are also very important:

- Wave setdown/-up;
- Non-linear wave-wave interactions.

These physical processes are modelled intrinsically by the applied (weakly) non-linear Boussinesq equations in Mike 21 BW.

3.3.7 Numerical stability

Introduction

Experience with the Mike 21 BW model has taught that it is a wave model with a very sensitive numerical stability. The numerical instability manifests itself as a so called “blow-up” or negative water depth due to an abnormal and uncontrollable increase of a local surface elevation. In §3.3.6 it was already decided to not include wave run-up in the model to prevent increased numerical instability and limit the calculation time. In this chapter the additional measures are discussed to obtain a numerically stable model with Mike 21 BW.

The areas with the most sensitive numerical stability include:

- The most shallow parts of the beach on either side of the marina entrance;
- The shallow parts on the harbour dams and where wave concentration occurs due to the effect of the navigation channel.

These types of areas correspond with the types which were observed in the case of Oostende (Gruwez, 2011). The same measures as in the case of Oostende are taken to obtain a numerically stable model.

Time extrapolation factor

This factor has no effect for value 1.0. When including wave breaking DHI (2009) recommends a value of 0.8-0.9. For a value of 0.8 all Mike 21 BW models made in this study are stable. Using a time-extrapolation factor however causes some numerical dissipation (DHI, 2009). In §3.5.2 this dissipative effect is evaluated.

Bottom friction

In many cases a blow-up is prevented by introducing some extra wave dissipation by an artificially high bottom friction in the very shallow areas of the model (Chézy number of C = 11 $m^{1/2}/s$, cf. Figure 3-14, or a corresponding Manning number of approximately 0.10 $s/m^{1/3}$).

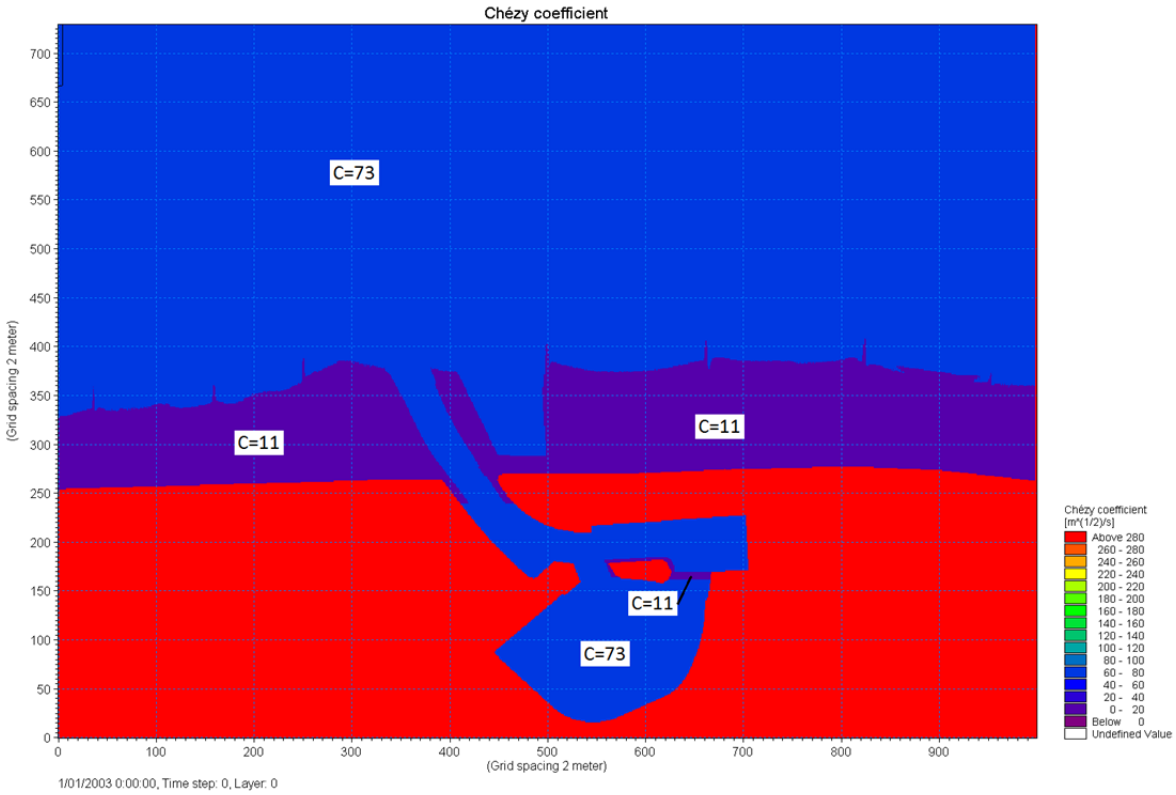

Figure 3-13: Bottom friction map with indication of the artificially high bottom friction (C = 11 $m^{1/2}/s$) in the very shallow areas of the calculation domain.

Low-pass filter

Although the extra bottom friction improves the numerical stability, still blow-ups occur in the smallest water depths (= 1.50m). An explicit numerical low-pass filter is introduced in the areas indicated in Figure 3-14. The low-pass filter dissipates the wave energy in the area where the surface roller cannot be resolved (DHI, 2009).

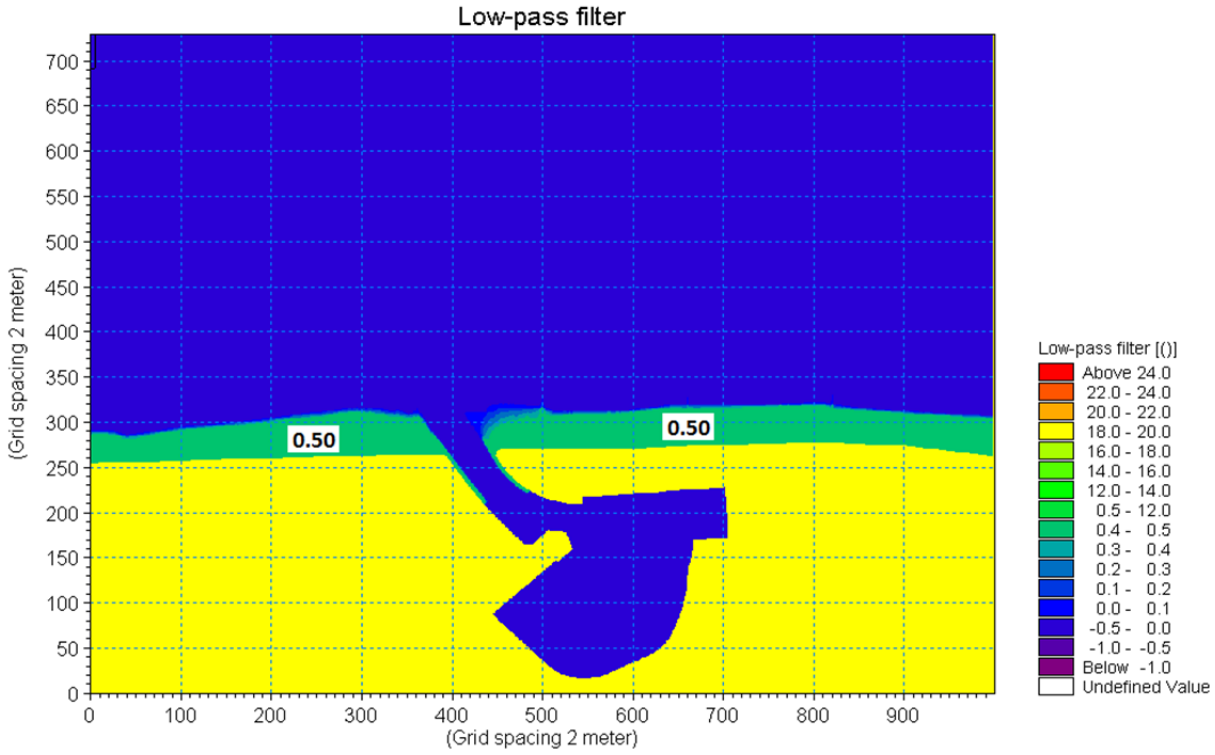

Figure 3-14: Filter coefficient map with indication of the low-pass filter areas (green).

Sponge layers

When even extra bottom friction and a low-pass filter are insufficient a sponge layer can be used to introduce even more dissipation. This is used as a last resort because it can be the most dissipative measure. This method is recommended by DHI (2009) as a last resort to remove blow-ups.

Figure 3-12 shows the areas where the sponge layers for numerical stability are included (μ_{MIKE} = 1.0015). The sponge layers are positioned on the west bank/beach just outside the entrance of the harbour where they have little to no effect on the wave penetration inside the marina.

Overview

When the water level and/or the wave direction is changed in the model the blow-up sensitive locations also change or new instabilities occur. That is why it is possible that for other SWL-wave direction combinations another set of measure is needed or on other locations to ensure numerical stability.

An overview of the applied measures for each model is given in Table 3-5.

Table 3-5: Overview of the applied measures to obtain numerical stability for each of the Mike 21 BW models.

Type	SWL	σ [°]	d_{max} [m]	H_{m0} [m]	T_p [s]	Measures for numerical stability			
						Time-extrapolation factor [-]	Bottom Friction	Low-pass filter	Extra sponge layers on west beach/bank
Validation	+4.91	30	9.91	2.3	9.1	0.80	X	X	-
	+4.97	30	9.97	2.3	8.5	0.80	X	X	-
	+4.55	30	9.55	2.5	8.5	0.80	X	X	-
	+4.61	30	9.61	2.7	8.5	0.80	X	X	X
1000 year storm	+7.10	0	12.1	4.5	12.0	0.80	X	X	X
	+7.10	15	12.1	4.5	12.0	0.80	X	X	X (except WNW and W)
	+7.10	30	12.1	4.5	12.0	0.80	X	X	X
Super storms	+7.90	15	12.9	5.0	12.0	0.80	X	X	X

3.3.8 Partial reflection

In the previous wave penetration models for the harbours of Oostende and Zeebrugge a one-layered sponge layer was used along the land boundary inside the harbour to model the partial reflection caused by the flooded quay walls and sloping structures (Gruwez et al., 2011; 2012). In the case of the marina of Blankenberge no partial reflection is modelled because:

- Using a sponge layer along the land boundary has an influence on the wave setdown/-up;
- The wave penetration of short waves (T<20s) is very limited in the marina and long wave energy in the marina is dominant (cf. §3.7.3). For long waves even sloping structures cause a reflection of 100%.
- When including the slopes of structures in the bathymetry it was found in the case of Oostende (slope at the “Halve Maan”) that without sponge layer at the crest of the slope the best correspondence with the physical model was found (Gruwez et al., 2011).

Nevertheless, an overview of all structures, their slopes and crest levels is given in Annex 2.

3.4 Setting up the SWASH model

3.4.1 Introduction

Recently a phase-resolving wave propagation model, SWASH (Zijlema et al., 2011), based on the non-linear shallow water equations with a non-hydrostatic pressure model has been developed at the Delft University of Technology. Suzuki et al. (2011) has already demonstrated that this model produces satisfactory results for both wave transformation and wave overtopping for a shallow foreshore topography in their one-dimensional calculation. This model is suitable for the study of long waves/surf beat since it is based on the shallow water equations which can represent bore generation due to wave breaking. The non-hydrostatic pressure term in the equation sustains the frequency dispersion which makes it possible to calculate the wave transformation from offshore.

3.4.2 Governing equations

The governing equations are the shallow water equations including a non-hydrostatic pressure term. The governing equations are shown as follows:

$$\frac{\partial u}{\partial x}+\frac{\partial v}{\partial y}+\frac{\partial w}{\partial z}=0 \tag{1}$$

$$\frac{\partial u}{\partial t}+\frac{\partial u^2}{\partial x}+\frac{\partial vu}{\partial y}+\frac{\partial wu}{\partial z}+\frac{g}{\rho_0}\frac{\partial \zeta}{\partial x}+\frac{g}{\rho_0}\frac{\partial q}{\partial x}+c_f\frac{u|u|}{h}=\frac{1}{h}\left(\frac{\partial h\tau_{xx}}{\partial x}+\frac{\partial h\tau_{xy}}{\partial y}\right) \tag{2}$$

$$\frac{\partial v}{\partial t}+\frac{\partial uv}{\partial x}+\frac{\partial v^2}{\partial y}+\frac{\partial wv}{\partial z}+\frac{g}{\rho_0}\frac{\partial \zeta}{\partial y}+\frac{g}{\rho_0}\frac{\partial q}{\partial y}+c_f\frac{u|u|}{h}=\frac{1}{h}\left(\frac{\partial h\tau_{yx}}{\partial x}+\frac{\partial h\tau_{yy}}{\partial y}\right) \tag{3}$$

$$\frac{\partial w}{\partial t}+\frac{1}{\rho_0}\frac{\partial q}{\partial z}=0 \tag{4}$$

$$\tau_{xx}=2\nu_t\frac{\partial u}{\partial x},\tau_{xy}=\tau_{yx}=\nu_t\left(\frac{\partial v}{\partial x}+\frac{\partial u}{\partial y}\right),\tau_{yy}=2\nu_t\frac{\partial v}{\partial y} \tag{5}$$

where t is time, x and y the horizontal coordinate, z the vertical coordinate, u, v and w the velocity in x-direction, y-direction and z-direction respectively. ζ is the surface elevation from still water level. q is the non-hydrostatic pressure, g the gravitational acceleration, cf is the dimensionless bottom friction coefficient and vt the eddy viscosity.

A full description of the numerical model, boundary conditions, numerical scheme and applications are given in Zijlema et al. (2011).

3.4.3 Previous validation study for SWASH

The SWASH model is a relatively new model, therefore there are not many examples of previous project applications. However, Suzuki et al. (2011) has already conducted a validation against the Wenduine wave overtopping physical model (1D case) (Veale et al. 2011). The bathymetric configurations and wave conditions in Wenduine project are quite similar to the case of Blankenberge, therefore this validation is relevant to this study. Below the validation of the SWASH model from Suzuki et al. (2011) is summarized.

The applicability of SWASH for modelling wave transformation and wave overtopping discharge on a shallow foreshore was investigated. The results from numerical simulations in terms of wave transformation on the shallow foreshore and wave overtopping discharge on the dike crest are compared with physical model data of the same physical test set-up.

Figure 3-15 compares the significant wave height from spectral analysis (Hm0 =4√m0) and wave set-up estimated with the numerical and physical model for Test 1A, shown in Table 3-6. Here the parameters are based on the entire wave spectra, thus including both incident and reflected waves. As can be seen in Figure 3-15, the numerical model results for significant wave height is in very good agreement with data from the physical model. Wave set-up is slightly overestimated, but the trend of the wave set-up is well reproduced.

Figure 3-16 compares the wave spectrum with the numerical and physical model for Test 1A. All the results from the numerical model have a similar wave energy spectrum shape to the physical model spectra.

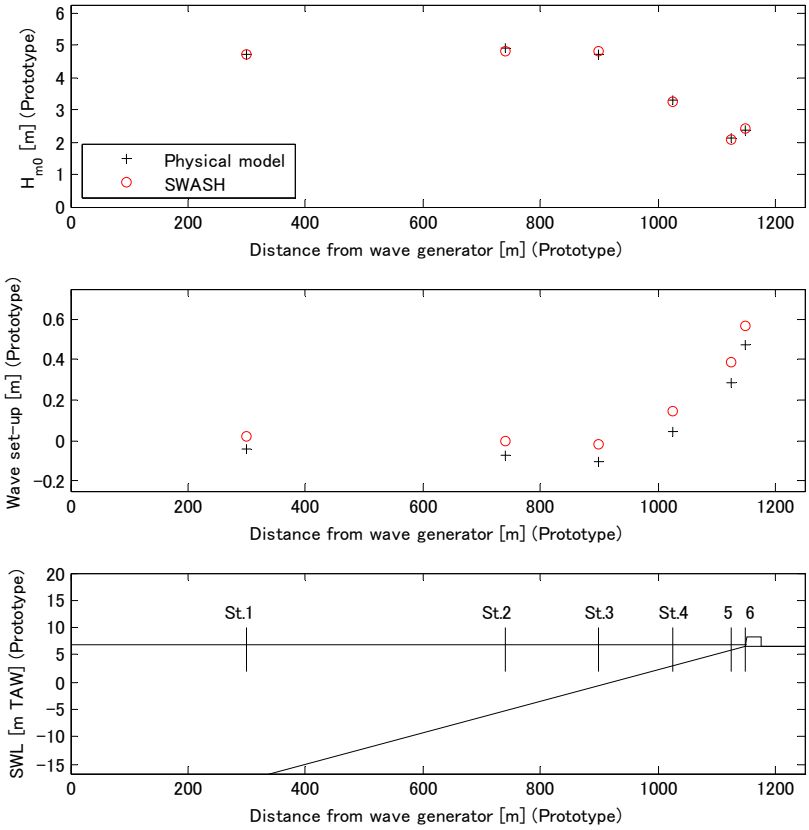

Figure 3-15: Significant wave height and wave set-up result from Suzuki et al. (2011)

Table 3-6: Test program for the physical model test

Test No.	Storm condition	Dike-configuration	Prototype, at -5 m TAW			
			SWL (m TAW)	$H_{m0,i}$ (m)	$T_{m-1,0}$ (s)	T_p (s)
1A	1000 year storm	Dike only (no wall)	6.84	4.75	8.60	11.70

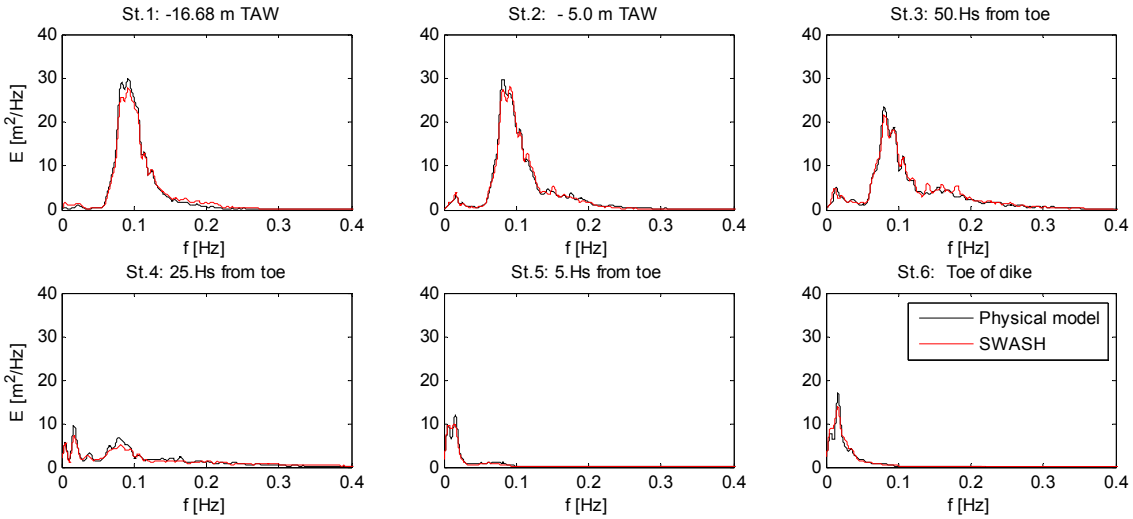

Figure 3-16: Wave energy spectrum at each station for the case of Test 1A.

Wave overtopping discharge estimates from numerical and physical model tests are shown in Table 3-7 for Tests 1A alongside estimates using Equation 5.8 published in EurOtop (2007). The 5% upper and lower confidence limits for discharges estimated with the EurOtop Equation 5.8 are also presented in Table 3-7.

Table 3-7: Wave overtopping discharge obtained from the physical model, SWASH model and Eq. 5.8 in EurOtop (1:25 scale)

Test No.	**Parameter**	**Physical Model**	**SWASH Model**	**EurOtop Eq. 5.8 Lower 5% / Mean / Upper 5%**
1A	$H_{m0,i}$ (m) at $5H_{m0}$ from toe (St.5)	0.073	0.073	-
	$T_{m-1,0}$ (s) at -5 m TAW (St.2)	2.1	2.1	-
	$T_{m-1,0}$ (s) at toe (St.6)	18.7	16.7	-
	Wave setup (m) at toe (St.6)	0.019	0.023	-
	q (l/s/m)	0.58	0.45	0.66 / 1.08 / 1.75

From these results, it is confirmed that the SWASH model is capable to represent one dimensional physical model results.

3.4.4 Bathymetry

Final configurations

Further modifications were carried out for the bathymetry of SWASH model. The modified features from Figure 3-5 are listed below. The final configurations of the bathymetry for NNW is shown in Figure 3-18 (A0 configuration: without the new land) and Figure 3-19 (A1 configuration: with the new land).

- All the rest of the area (blank area) has been filled at the level of +5.0 m TAW
- Apartment buildings are located on the sea dike
- A navigation channel with the level of -4.16m TAW is added in between the area of -3.62 m TAW and -5.0 m TAW as a transition zone .
- Extension of the bathymetry in the long-shore direction (200m)
- Extension of the bathymetry in the cross-shore direction (40 m)
- Offshore depth: -5 m TAW (one wave length:120 m)
- The area which is not completely flat due to the result of interpolated is smoothed.
- The entrance channel is smoothed.
- The east side pier structure is removed at the entrance channel
- Added a seawall around the harbor (height of the wall: +20 m TAW); the position is indicated in Figure 3-17. However, wave overtopping can be severe at the western bank of the entrance channel (severe wave overtoppings were observed in a preliminal calculation with the SWASH model), so the seawall is extended to the western dune. Additionally the end of the seawall at eastern side also extended to the apartment buildings to prevent inundation.

Figure 3-17: Position of a planned new storm surge wall. (blue dot line)

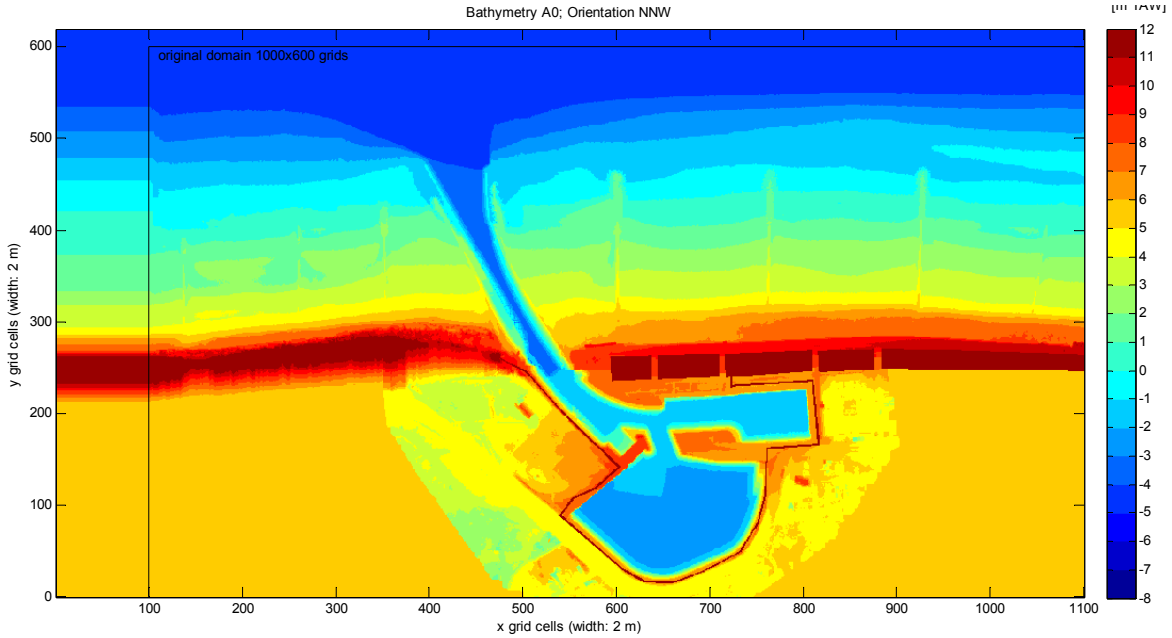

Figure 3-18: Final configuration of the bathymetry for SWASH in the case of A0. The number of the grid is 1100 in x-direction (long-shore direction) and 620 in y-direction (cross-shore direction).

- The new land has been added.

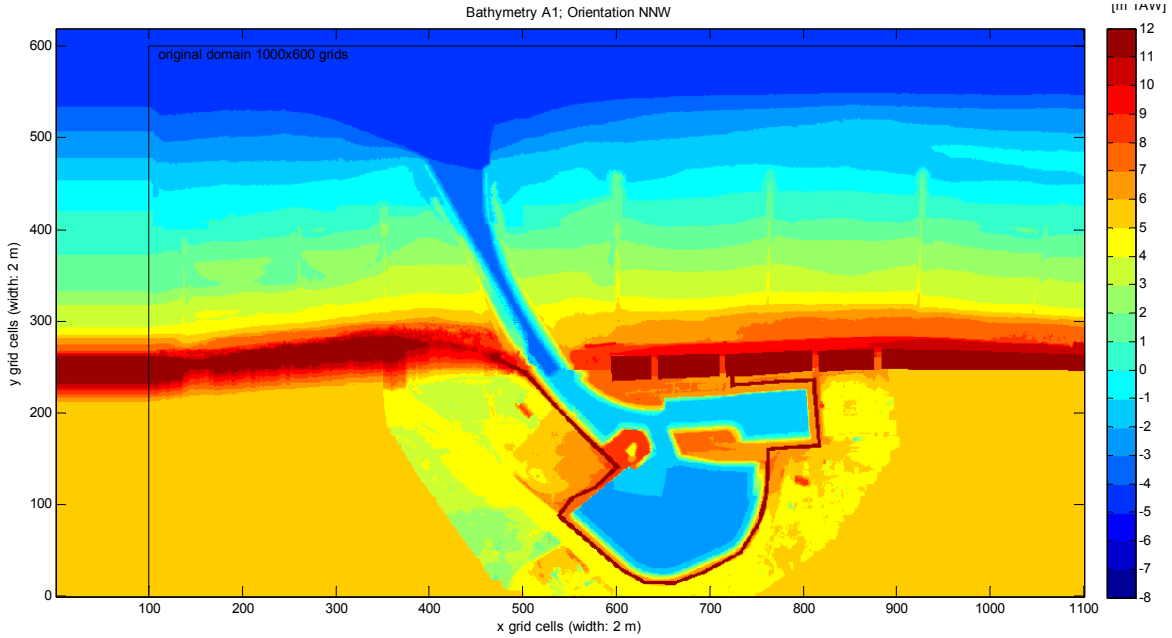

Figure 3-19: Final configuration of the bathymetry for the numerical simulation in the case of A1. The number of the grid cells is 1100 in the x-direction (long-shore direction) and 620 in the y-direction (cross-shore direction).

Input bathymetries for 4 directions (N,NNW, NW and WNW) in SWASH

Four directions (N,NNW, NW and WNW) are required for the wave penetration calculations. The input bathymetries in the SWASH model are shown in Figure 3-20 to Figure 3-23. These bathymetries have been created based on the bathymetry of the direction NNW. The computational grid is rotated to 90 degree anti-clockwise so that the wave boundary of the SWASH model becomes west (the default direction). The domains used by the SWASH model simulations are shown as red boxes. The total domain of these bathymetries is larger than the computation area of the SWASH model for the flexibility. It is noted that the shown bathymetries here are based on a 2 m grid, however, the SWASH model uses a 4 m grid in the actual calculations. These 2 m grid bathymetries are used for the input file of the SWASH model. The SWASH model merges the 2 m grid into a 4 m grid. The actual bathymetries used in the SWASH model are shown in the next section. (In Mike21BW a 2 m grid has been used.)

Wave boundary location

Wave boundary location is set at the west boundary of the red box for the each direction.

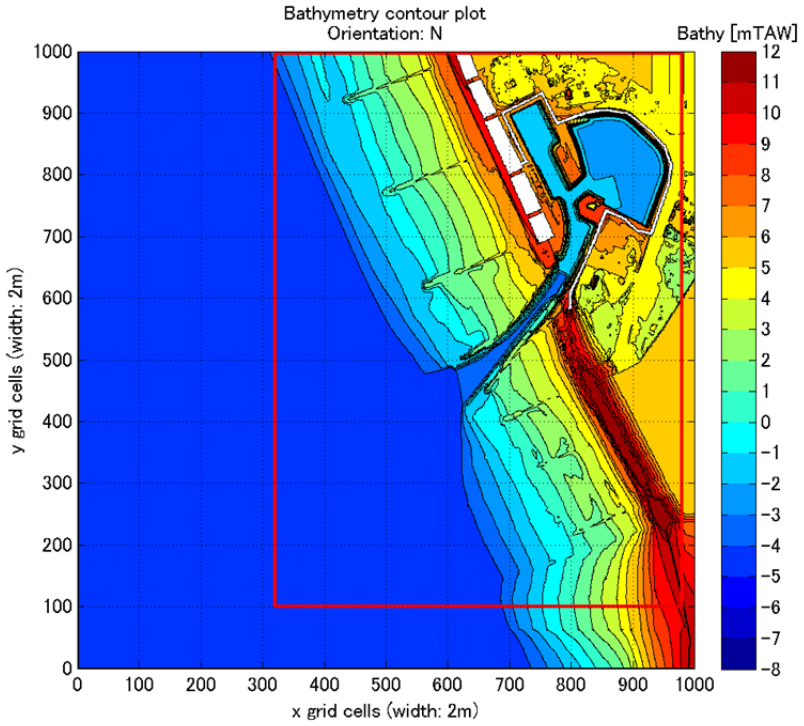

Figure 3-20: Bathymetry for the direction N

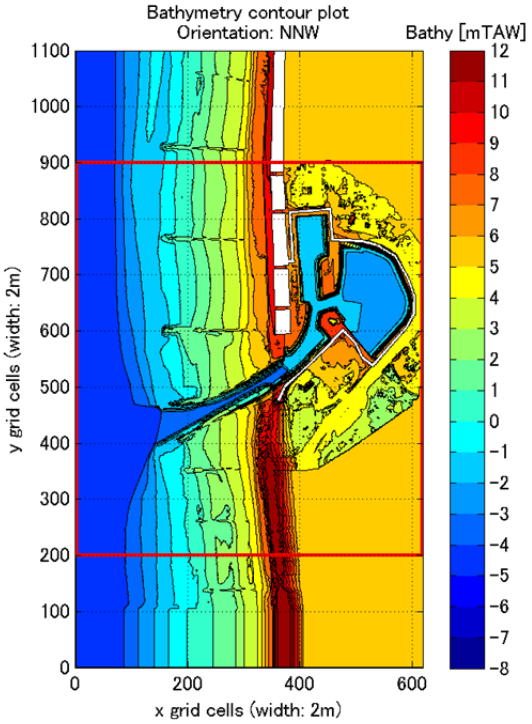

Figure 3-21: Bathymetry for the direction NNW

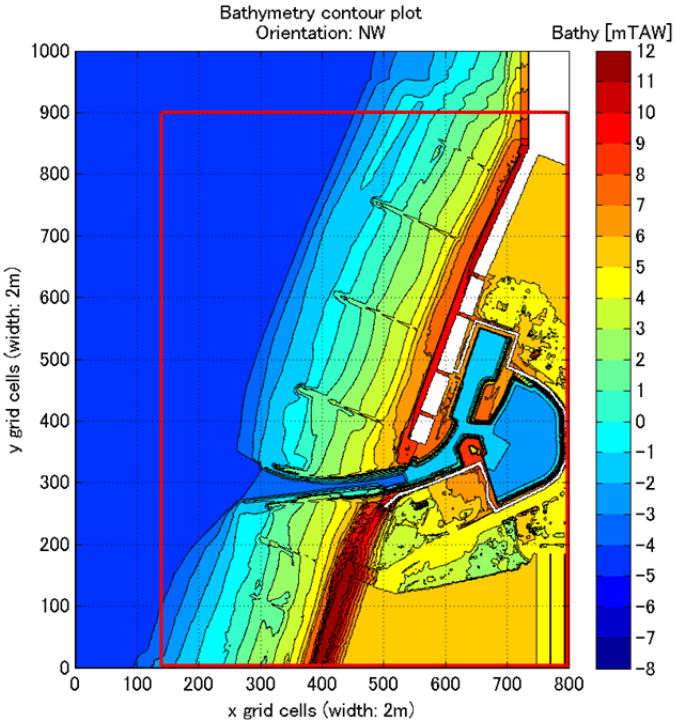

Figure 3-22: Bathymetry for the direction NW

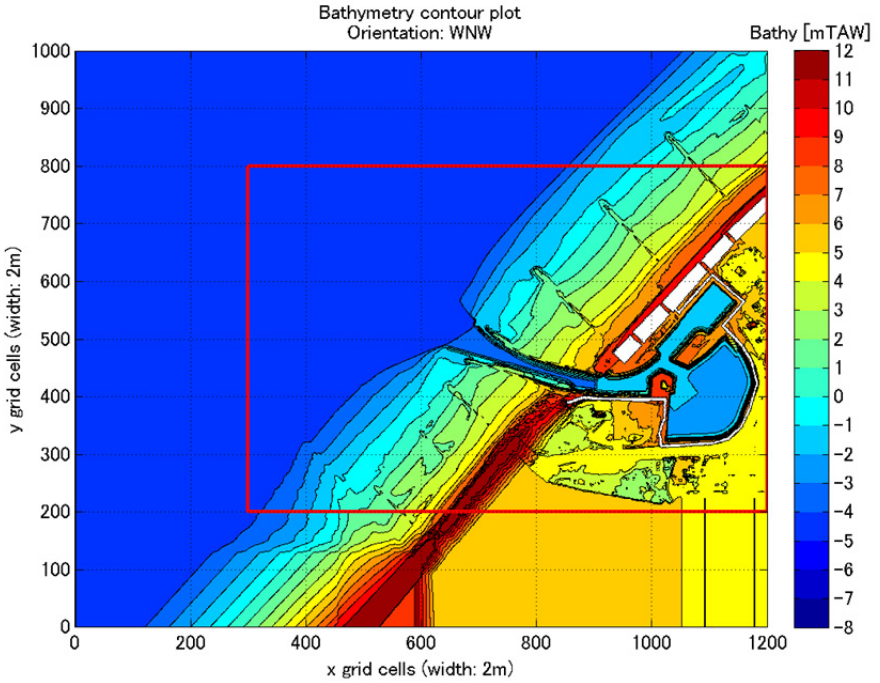

Figure 3-23: Bathymetry for the direction WNW

Bathymetries in the actual calculations in SWASH model

The actual bathymetries used in SWASH are shown in Figure 3-24 to Figure 3-27. Black boxes in these figures show the output location of time series. Due to the limited volume of the output, the output area is limited. From these time series, significant wave height and wave set-up are calculated. Dotted lines (directional spreading: 30 degree) and dashed line (directional spreading: 15 degree) show the area where there is supposed to be no energy loss due to the boundary effect. It can be seen that all the energy from the wave boundary is transmitted towards the entrance of the harbour for all directions.

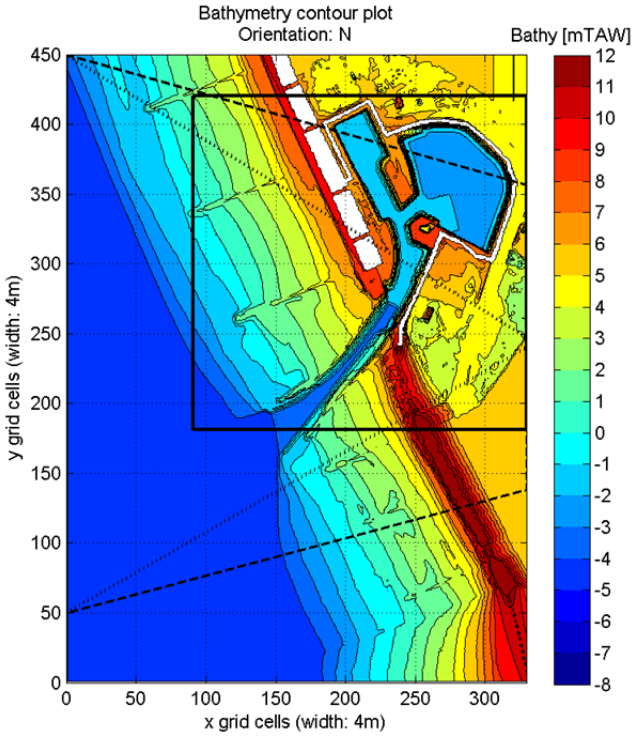

Figure 3-24: Calculation domain for the direction N. A sponge layer is added at 0-50 grids in the y grid cells.

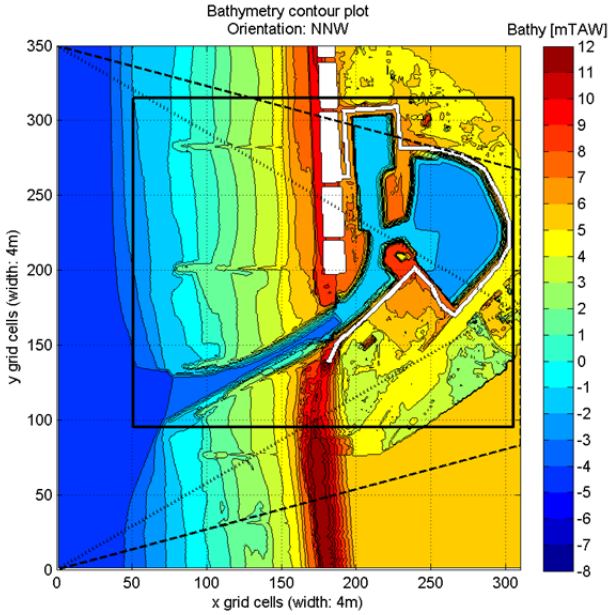

Figure 3-25: Calculation domain for the direction NNW. No sponge layer is added.

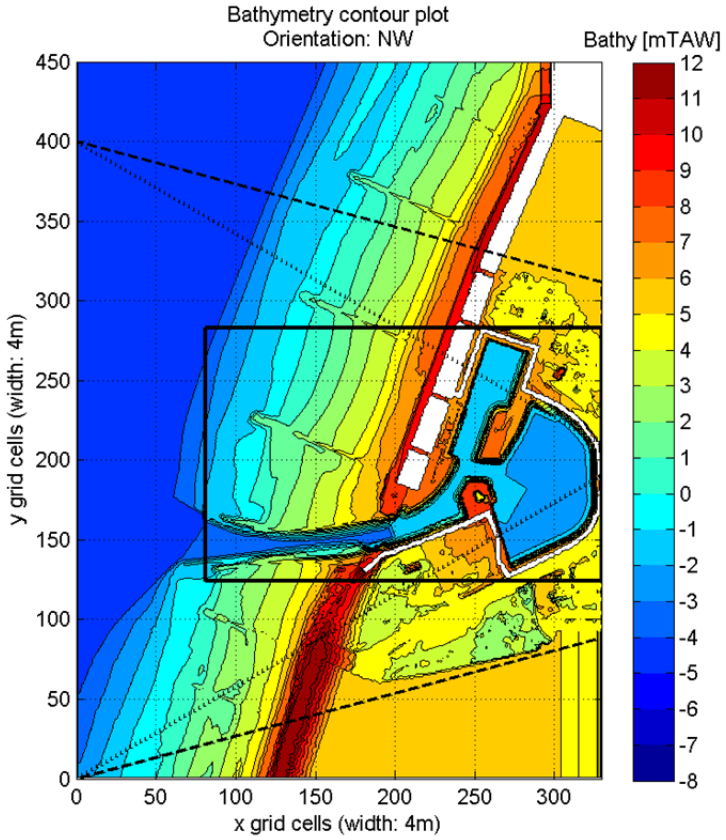

Figure 3-26: Calculation domain for the direction NW. A sponge layer is added at 400-450 grids in the y grid cells.

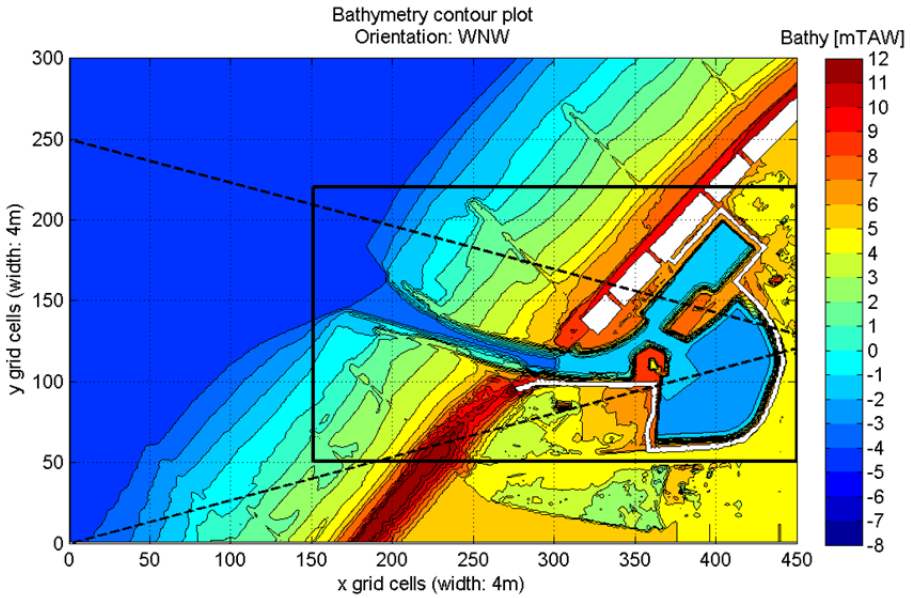

Figure 3-27: Calculation domain for the direction WNW. A sponge layer is added at 450-500 grids in the y grid cells.

Output locations

The output locations are shown in Figure 3-28 to Figure 3-30. These locations correspond with the ones used in the Mike21 BW model.

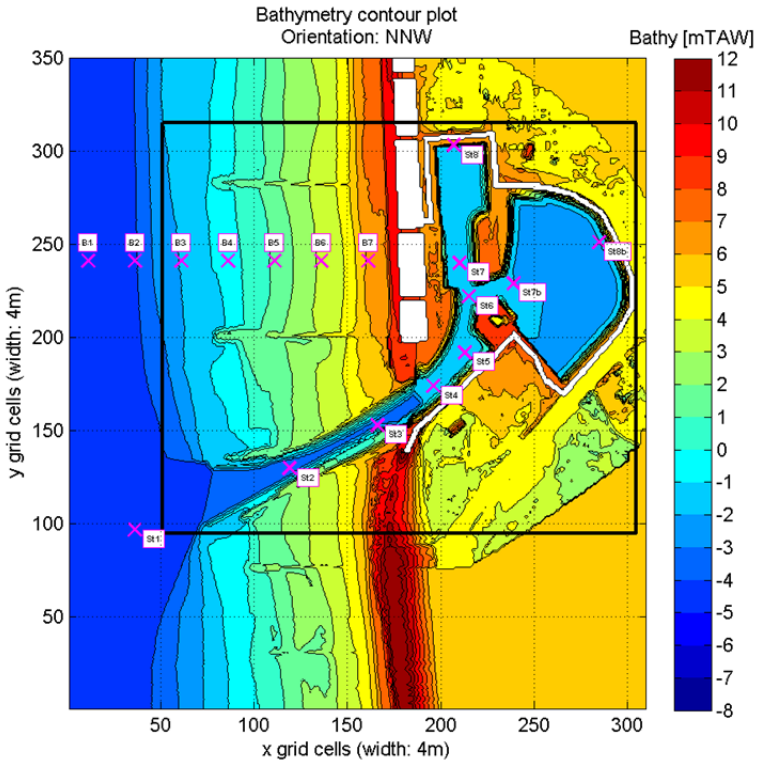

Figure 3-28: Overview of the result output locations (St.1-St.8b, B1-B7).

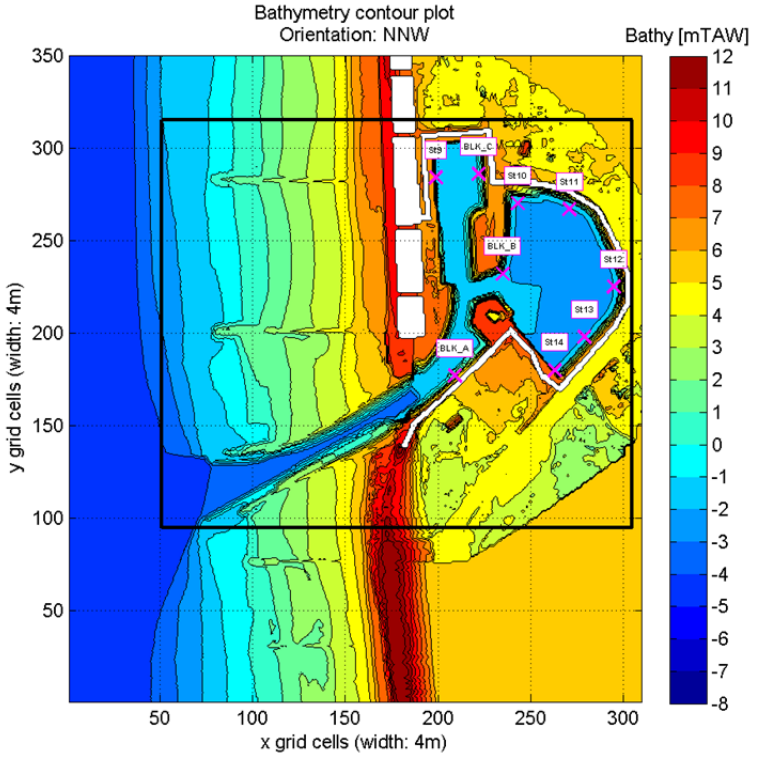

Figure 3-29: Overview of the result output locations (BLK_A-C, St.9-14).

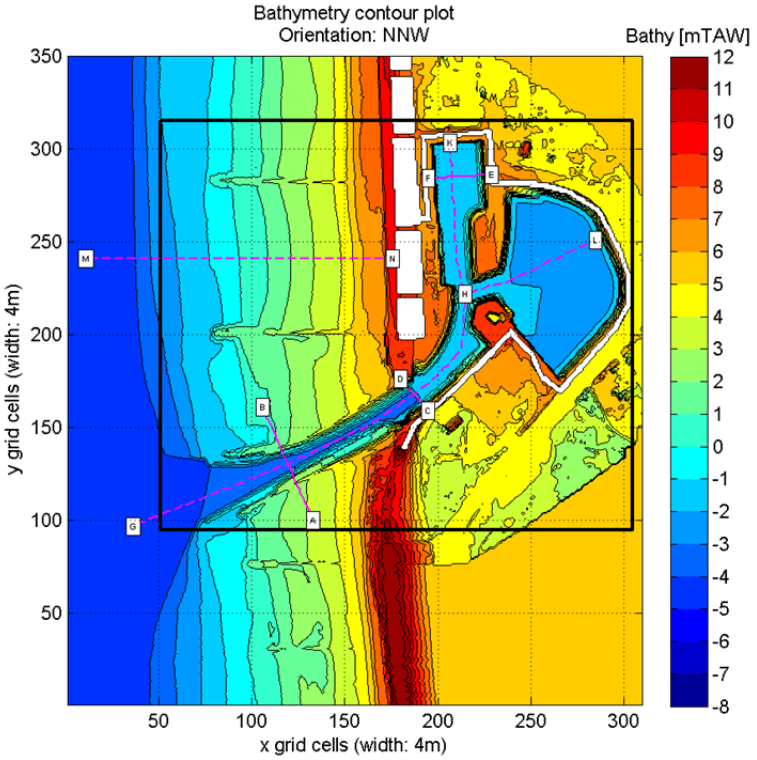

Figure 3-30: Overview of the result output cross-sections (Point A-N).

3.4.5 Hydrodynamic boundary conditions

Water level

From the results of Suzuki et al. (2011) shown in Figure 3-15, it is recognized that the SWASH model gives higher water levels than the physical model. In general, the water level before the wave breaking zone becomes lower than the zero level due to the radiation stress. This wave set-down can be seen in the physical model result in Figure 3-15. The wave set-down calculated by the equation below shows 10 cm wave set-down, which can also be seen in the physical model.

$$d = -\frac{1}{8}\frac{H^2 k}{\sinh 2kd} \tag{6}$$

This effect probably comes from the boundary condition of the SWASH model, namely the weakly reflective wave boundary. However, the other boundary condition in the SWASH model is not going to be implemented in this study. Instead, the lower water level based on the Mike21BW result for wave set-down is used since the result of Mike21BW is more reliable than SWASH in terms of wave set-down as can be seen in Figure 3-31. It is noted that the SWASH model predicts the wave set-up result well even though the wave set-down is somewhat underestimated.

The calculation result of the SWASH 2D model and the Mike21BW 1D/2D models for Blankenberge beach profile is shown in Figure 3-32. The hydrodynamic condition is the '8m super storm' condition, the directional spreading is 15 degree and the wave direction is NNW. The Mike 21 BW model shows a wave set-down at the wave boundary of about 6 cm. The differences between Mike 21 BW and SWASH model is about 10 cm, so it was decided to reduce the water level of the SWASH boundary condition with 10 cm. In the validation cases, the water levels are reduce with 5 cm, since the wave heights are smaller.

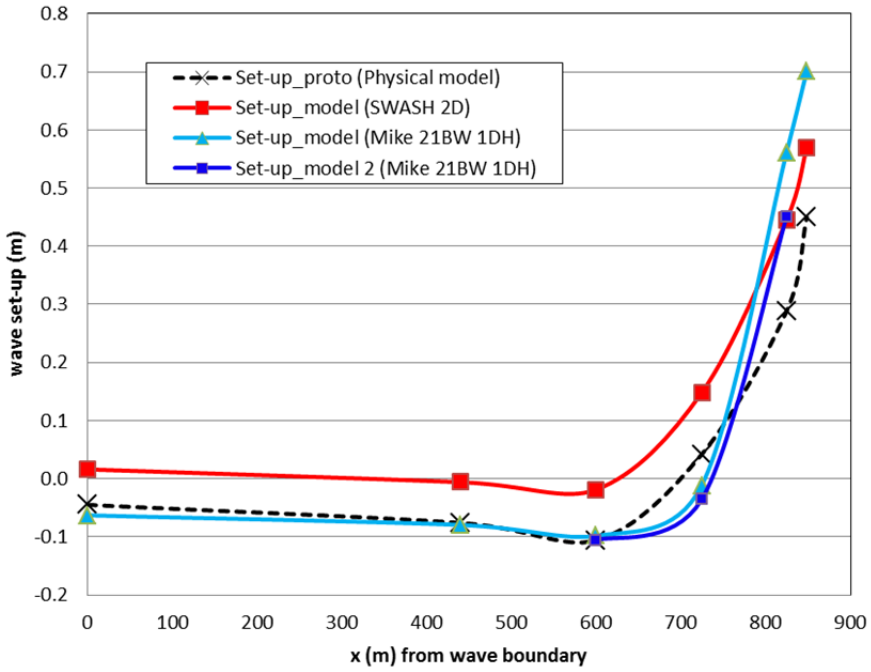

Figure 3-31: Wave set-up of Mike 21 BW and SWASH for Wenduine case

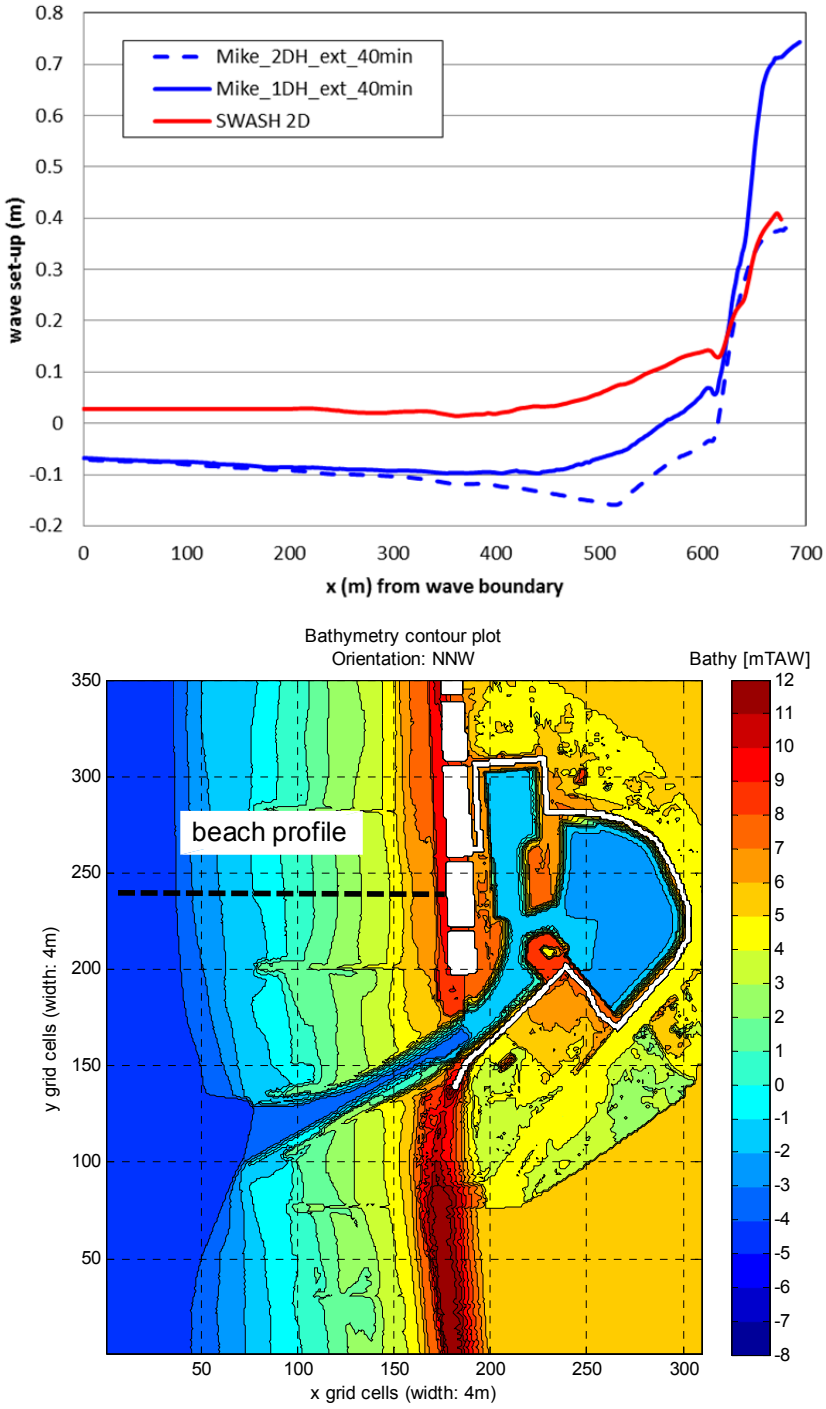

Figure 3-32: Wave model set-up of Mike 21 BW and SWASH for Blankenberge beach profile

Directional spreading

The corresponding directional spreading σ for the applied directional spreading in the SWASH model is shown in Table 3-3.

Table 3-8: m value used in SWASH model

m [-]	**σ [°]**	**σ (value used in this report) [°]**
10	**17.1**	**'15°'**
2	**31.5**	**'30°'**

Hydrodynamic boundary conditions

Table 3-9 shows the hydrodynamic boundary conditions used in the SWASH model. The water level is reduced compared to the hydraulic boundary condition shown in Table 3-2.

Table 3-9: The hydrodynamic boundary conditions and calculation cases used in SWASH

Type	SWL	σ [°]	d_{max} [m]	H_{m0} [m]	T_p [s]	Wave direction [-]			
						N	**NNW**	**NW**	**WNW**
Validation	+4.91	30	9.91	2.3	9.1	-	X	-	-
	+4.97	30	9.97	2.3	8.5	-	-	X	-
	+4.55	30	9.55	2.5	8.5	-	X	-	-
	+4.61	30	9.61	2.7	8.5	X	-	-	-
1000 year storm	+7.10	0	12.1	4.5	12.0	-	X	-	-
	+7.10	15	12.1	4.5	12.0	X	X	X	X
	+7.10	30	12.1	4.5	12.0	-	X	-	-
Super storms	+7.90	0	12.9	5.0	12.0	-	X	-	-
	+7.90	15	12.9	5.0	12.0	-	X	-	-
	+7.90	30	12.9	5.0	12.0	-	X	-	-

Cut-off frequency

A cut-off frequency is not used in the SWASH model while the Mike21BW model needs it due to the computational stability.

3.4.6 Calculation grid, time step and duration of simulation

Calculation grid

The size of calculation grid in the SWASH model is chosen based on the wave length at the boundary of the calculation domain. The depth of each calculation domain (N,NNW, NW and WNW) is set -5m TAW and thus the total water depth at the boundary is 12 m in the case of 1000 year super storm. The peak period of a 1000 year super storm is 12 s and thus the wave length in this case is about 123 m. Zijlema (personal communication, 2011) recommends to use 30-50 grid cells for one wave length. Therefore the recommended grid size is 2.5-4.1 m.

$$\frac{L_p}{30-50} \approx 4.1m - 2.5m$$

In this report, a 4 m grid is chosen for the calculations with the SWASH model. This value is chosen as close to the highest values in the above recommendation to keep the computation time as short as possible.

$$\boxed{\Delta x = \Delta y = 4.0m}$$

A comparison between a 1 m grid and a 4 m grid calculation has been made to check the validity of the grid size and the result is shown in Figure 3-33. It is noted that the 1 m grid calculation is from Suzuki et al. (2011). It is confirmed that the 4 m grid reproduced similar wave height and wave set-up as obtained in 1 m grid. The slight difference of the wave set-up at St.5 and St.6 is due to the local bottom level which is slightly different due to the respective grid resolutions.

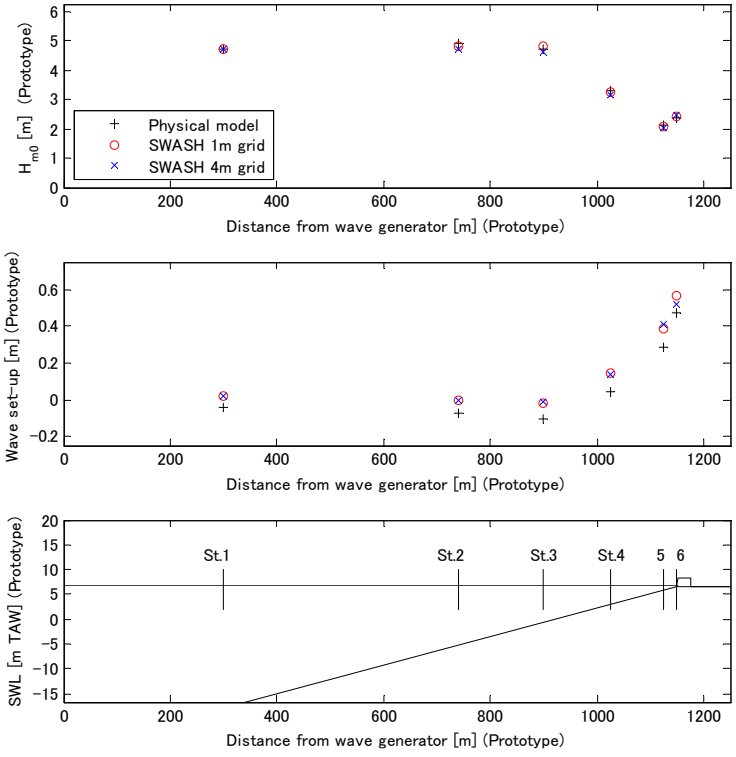

Figure 3-33: Intercomparison between 1m grid calculation and 4m grid calculation in the case of Wenduine physical model

Time step

The time step in the SWASH model is automatically determined based on the Courant-Friedrichs-Lewy (CFL) number associated with the long wave speed, when time integration is explicit. The initial time step used in the calculations in this report is set as 0.02 s. The time step is halved when this number becomes larger than a pre-set constant [cflhig] < 1, and the time step is doubled when this number is smaller than another constant [cfllow], which is small enough to be sure the time step can be doubled (SWASH user manual; version 1.05, 2011).

In this study, explicit time integration is used for all the calculations.

Duration of simulation

For the calculation of the statistical parameters (such as the significant wave height H_{m0}) the simulation period has to be at least 15 min to 20 min long. This corresponds to approximately 100 waves. Because also long waves are considered in the case of Blankenberge a longer simulation period of 40 min is used corresponding with 200 waves (for T_p = 12.0s).

In addition to this a warm-up period is needed to allow enough time also for the shorter wave (e.g. T = 6.0 s, L = 46.0m => Cg = 5.6 m/s) to reach the furthest location in the calculation domain. The longest distance a wave has to propagate in the calculation domain is about 1200 m. The minimal warm-up time needed is then:

$$\frac{1200}{5.6} = 214s \approx 3.5\,\text{min}$$

A total simulation time of 45 min (warm up time: 5 min, analysis time: 40 min) is chosen for all SWASH simulations. This is the same as used in the Mike 21 BW calculations.

Table 3-10: Frequency and group velocity

Frequency	f [Hz]	T [s]	Minimum Depth [m]	Wave length [m]	Wave celerity [m/s]	Group celerity [m/s]	Distance [m]	Wating time [s]
$f_{p,1/2}$	0.042	24.0	8.7	219	9.1	9.0	1200	133
f_p	0.083	12.0	8.7	106	8.9	8.2	1200	146
$f_{p,2}$	0.166	6.0	8.7	46	7.7	5.6	1200	214

3.4.7 Wave generation and absorption

Wave generation

SWASH uses a weakly reflective boundary, so that the reflected waves from the harbour do not influence the wave generation. With this method, there is no need to put a sponge layer behind the wave boundary as used in Mike 21 BW.

Sponge Layer

Sponge layers are used in the calculation domain to absorb the energy of reflected waves from the harbour and beach. The position is shown in in Figure 3-24 to Figure 3-27.

3.4.8 Physical processes

Bottom friction

The SWASH model employs bottom friction with the following expression, where n is the Manning's roughness coefficient, and h is the total depth.

$$c_f = \frac{n^2 g}{h^{1/3}} \tag{7}$$

In this study, a global Manning's roughness coefficient of n=0.02 is applied. (The same setting has been chosen in the Mike 21 BW model.)

Wave breaking

By considering the similarity between breaking waves and bores or moving hydraulic jumps, energy dissipation due to wave breaking is inherently accounted for. However, at the front face of the breaking wave, pressure must be hydrostatic. Hence, steep bore-like wave fronts need to be followed and this can be controlled by the vertical speed of the free surface. When this exceeds a fraction of the wave phase speed, as follows:

$$\frac{\partial \zeta}{\partial t} > \alpha \sqrt{gh} \tag{8}$$

the non-hydrostatic pressure is then neglected and remains so at the front face of the breaker. The parameter α > 0 controls the rate of energy dissipation. In general, the lower the α value, the more energy will be dissipated. This parameter depends on the breaker type. Numerical experiments suggest α = 0.4 and α = 0.3 for spilling and plunging breakers, respectively. This approach combined with a proper momentum conservation leads to a correct amount of energy dissipation on the front face of the breaking wave. Moreover, nonlinear wave properties such as asymmetry and skewness are preserved as well (SWASH user manual; version 1.05, 2011).

In this study, α = 0.4 is applied since the wave conditions are categorized as spilling waves.

Horizontal eddy viscosity

The SWASH model employs horizontal eddy viscosities. Three different horizontal viscosity model are available, which are a constant viscosity, the Smagorinsky model and the Prandtl mixing length hypothesis. (SWASH user manual; version 1.05, 2011). The Smagorinsky model can be shown as follows:

$$\nu_t = C_s^2 \Delta x \Delta y \sqrt{2\left(\frac{\partial u}{\partial x}\right)^2 + 2\left(\frac{\partial v}{\partial y}\right)^2 + \left(\frac{\partial v}{\partial x} + \frac{\partial u}{\partial y}\right)^2} \tag{9}$$

In this study, the Smagorinsky model with Cs=0.1 is applied.

Wave run-up, wave overtopping

Wave run-up and wave overtopping (cf. at the eastern bank of the entrance channel) can be simulated with SWASH model since actual land bathymetry is used in the calculations. However, wave overtopping were not simulated at the storm surge wall. The storm surge wall was set enough high not to have wave overtopping.

Wave transmission

Pier structures are not included in the calculations with the SWASH model. This is the same approach as used in Mike 21 BW simulations.

Miscellaneous

Because of the many shallow areas in this model the following physical processes are also very important:

- Wave set-down/-up;
- Non-linear wave-wave interactions.

These physical processes are modelled intrinsically by the non-linear shallow water equations in SWASH model.

3.4.9 Numeric

Layers and frequency dispersion

The model improves its frequency dispersion by simply increasing the number of vertical layers. In order to resolve the frequency dispersion up to an acceptable level of accuracy, a compact difference scheme for the approximation of vertical gradient of the non-hydrostatic pressure is applied in conjunction with a vertical terrain-following grid, permitting more resolution near the free surface as well as near the bottom. This scheme receives good linear dispersion up to $k*d \approx 7$ and $k*d \approx 3$ with two equidistant layers at 1% error in phase velocity of standing and progressive waves, respectively (k and d are the wave number and still water depth, respectively). The model improves its frequency dispersion by simply increasing the number of vertical layers (SWASH user manual; version 1.05, 2011).

In this study, one layer is used since k*d values less than one in which frequency dispersion is still applied is supposed to be relatively accurate. To prove that, a calculation with the one layer is shown below.

Figure 3-34 shows one layer calculations with non-hydrostatic pressure and hydrostatic pressure. The SWASH model result with one layer and the non-hydrostatic pressure shows a good agreement with the physical model test. This proves that the one layer mode gives a good frequency dispersion. However, the SWASH model result with one layer and the hydrostatic pressure show a deviation from the physical model data. This indicates that the NLSW equation model with the assumption of hydrostatic pressure is not capable of representing wave propagation from offshore to dike in this case, with a shallow foreshore. This may be attributed to the fact that the frequency dispersion and non-linear effects were not well predicted by the one layer hydrostatic pressure model.

In this study, the non-hydrostatic pressure is applied to all the calculations.

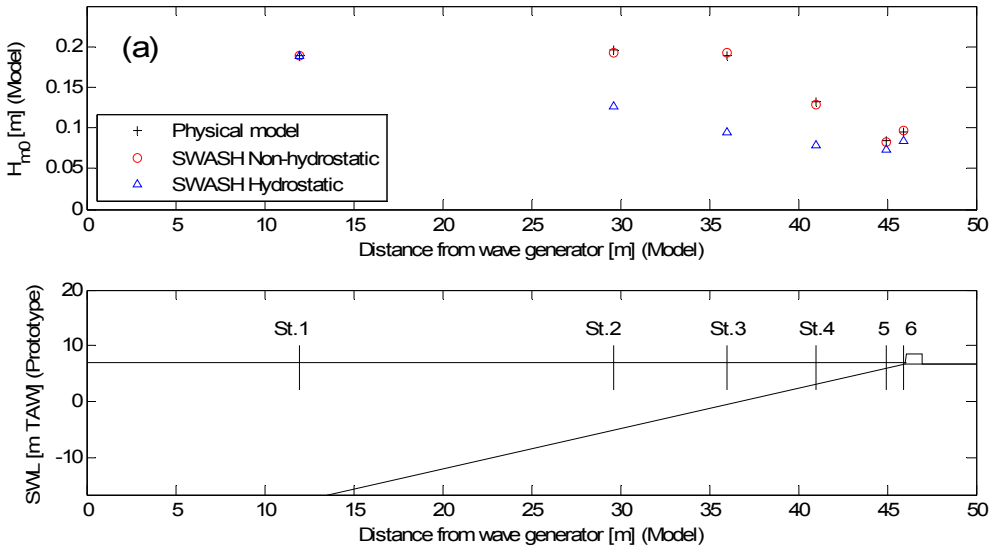

Figure 3-34: Intercomparison between calculations with non-hydrostatic pressure and hydrostatic pressure in the case of Wenduine physical model (Suzuki et al., 2011)

Numerical stability

Calculations sometimes do not converge due to numerical instability. In general, instabilities can be prevented by adding dissipation into a computation. Zijlema (personal communication, 2011) recommends several numerical methods to make a computation more stable. The recommended options are shown below.

- Use one layer mode for the vertical layers
- Add horizontal viscosity; SMAG=0.1
- Use Non-hydrostatic mode and BOX scheme with theta=0.1
- Use stable numerical schemes:
  - CORRDEP + FIRST
  - UPWIND + FIRST
  - UPWIND + MUSCL

A full description of the numerical scheme are given in the SWASH user manual. It is noted that the numerical results can be changed by the different numerical schemes.

In this study, 1 layer mode for the vertical layers, the horizontal viscosity with SMAG=0.1 and the numerical scheme of UPWIND+MUSCL are used to stabilize the simulations.

3.4.10 Partial reflection

Partial reflection is not used in SWASH model since actual bathymetry data is used. Reflection is decided by the actual configuration of the boundary of the structure.

3.5 Sensitivity analyses

3.5.1 Introduction

The sensitivity analyses are performed to test if certain assumptions cause a large under- or overestimation of the wave penetration in the marina. The following sensitivity analyses are performed:

- The influence of the time-extrapolation factor (cf. §3.3.7) is analysed;
- The sensitivity of the wave direction at the boundary;
- The sensitivity of the directional spreading on the wave climate in the marina;
- The sensitivity of the length of the time series on the result of the generated long waves;

The analysis of the results in this chapter and the next (cf. §3.7) is done with the disturbance coefficient K_d:

$$K_d = \frac{H_{m0,loc}}{H_{m0,St1}}$$

with $H_{m0,loc}$ the significant wave height at the considered location [m]
$H_{m0,St1}$ the significant wave height at output location St1 (cf. Figure 3-10) [m]

The influence of a certain change in the wave model will be investigated by:

- The K_d-values in the output locations shown in Figure 3-10 and Figure 3-11. This gives an idea of the sensitivity on the K_d-values along the most important quay wall zones in the marina, where the final results will be determined;
- The longitudinal section GH, which continues along HL in the yacht dock and along HL in the old basin (cf. Figure 3-8). This section follows the – generally – most energetic pathway and will therefore show the biggest influence.
- The cross sections AB, CD and EF (cf. Figure 3-8). Cross section AB can show the influence of the navigation channel in between the two parallel harbour dams. Section CD provides an insight as to how much wave energy enters the harbour and section EF is a cross section of how much wave energy is present in the yacht dock.
- A cross section of the beach MN (cf. Figure 3-8) which provides a good image of the effect on the wave breaking, wave setdown/-up and long wave generation.

When this is insufficient, supplementary results (e.g. contour plots,…) will be consulted to be able to reach a justified conclusion.

3.5.2 Time-extrapolation factor

In the previous harbour studies it was shown that this factor has a numerically stabilising but dissipative effect. This chapter investigates the effect of this factor in the case of Blankenberge. The result of the models with a factor of 0.80 and 0.90 (cf. Table 3-11) are compared.

This analysis was done for the grid orientation of WNW (cf. Figure 3-9), because it is the largest grid of the two.

Table 3-11: Hydrodynamic boundary conditions of the sensitivity analysis “Time-extrapolation factor”.

SWL [mTAW]	d_{max} [m]	H_{m0} [m]	T_p [s]	Richting [-]	Mike 21 BW
+7.10	12.10	4.5	12.0	WNW	X (TEF = 0.80)
+7.10	12.10	4.5	12.0	WNW	X (TEF = 0.90)

From Figure 3-35 it appears that increasing the factor causes no discernible difference in the results of the 2DH model. The dissipative effect is therefore negligible and a time-extrapolation factor of 0.80 is used in all models.

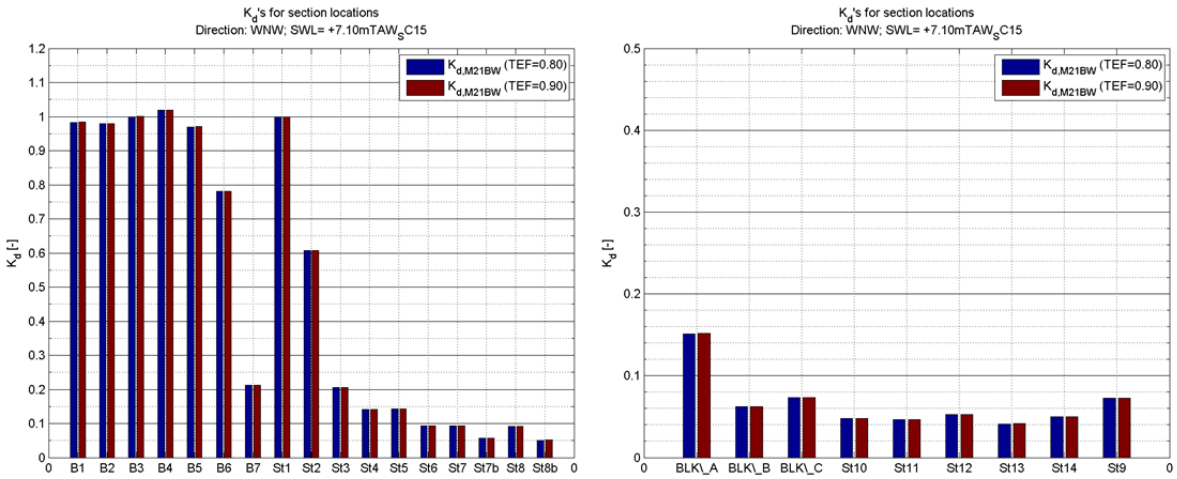

Figure 3-35: K_d-values of some locations along the longitudinal sections and of the locations in the marina. Comparison between the model with time-extrapolation factor 0.80 and 0.90.

3.5.3 Wave directions

Introduction

In this section the influence of the wave direction outside the marina on the wave penetration into the marina is investigated. In addition the wave direction is determined for which the most wave energy reaches the areas in the marina for which storm surge walls have to be designed.

The selected directions are in total five cases, direction N, NNW, NW, WNW and W. It is noted that W is only calculated by the Mike 21 BW model. From previous studies, it is known that the direction NNW gives the most severe wave condition at -5 m TAW (see Annex 1). It is thus expected that the direction NNW has the highest wave height. However, the same wave condition is used for all the wave directions in the sensitivity analysis to confirm which direction is the worst wave direction. The 1000 year storm condition is used for the investigation. The hydrodynamic boundary conditions are summarized in Table 3-12.

Table 3-12: Hydrodynamic boundary conditions for the sensitivity analysis “Wave direction”.

SWL [mTAW]	d_{max} [m]	H_{m0} [m]	T_p [s]	Direction [-]				
+7.10	12.10	4.5	12.0	W*	WNW	NW	NNW	N

*direction W is only calculated by Mike 21 BW model.

Mike 21 BW model results

The K_d contour plots are shown in Figure 3-36. The comparison on the locations is shown in Figure 3-37, and the cross-section is shown in Figure 3-38.

For each direction the following can be observed:

- The highest K_d value inside the marina is observed for direction N.
- The K_d value of WNW and W are not high even though the wave direction is almost parallel to the direction of the entrance channel.

Incoming waves of WNW and W go away to the perpendicular direction to the entrance channel when waves feel the slope of the entrance channel due to refraction. Since WNW and W pass longer channels than N and NNW, the wave energy becomes small inside the marina for these directions.

- The high K_d value of the direction N at the entrance channel can be explained by wave reflection. Incoming waves of the direction N are reflected at the west bank and the new storm surge wall. These reflected waves are again reflected at the east bank. Thus the K_d value of N at the entrance channel becomes high.

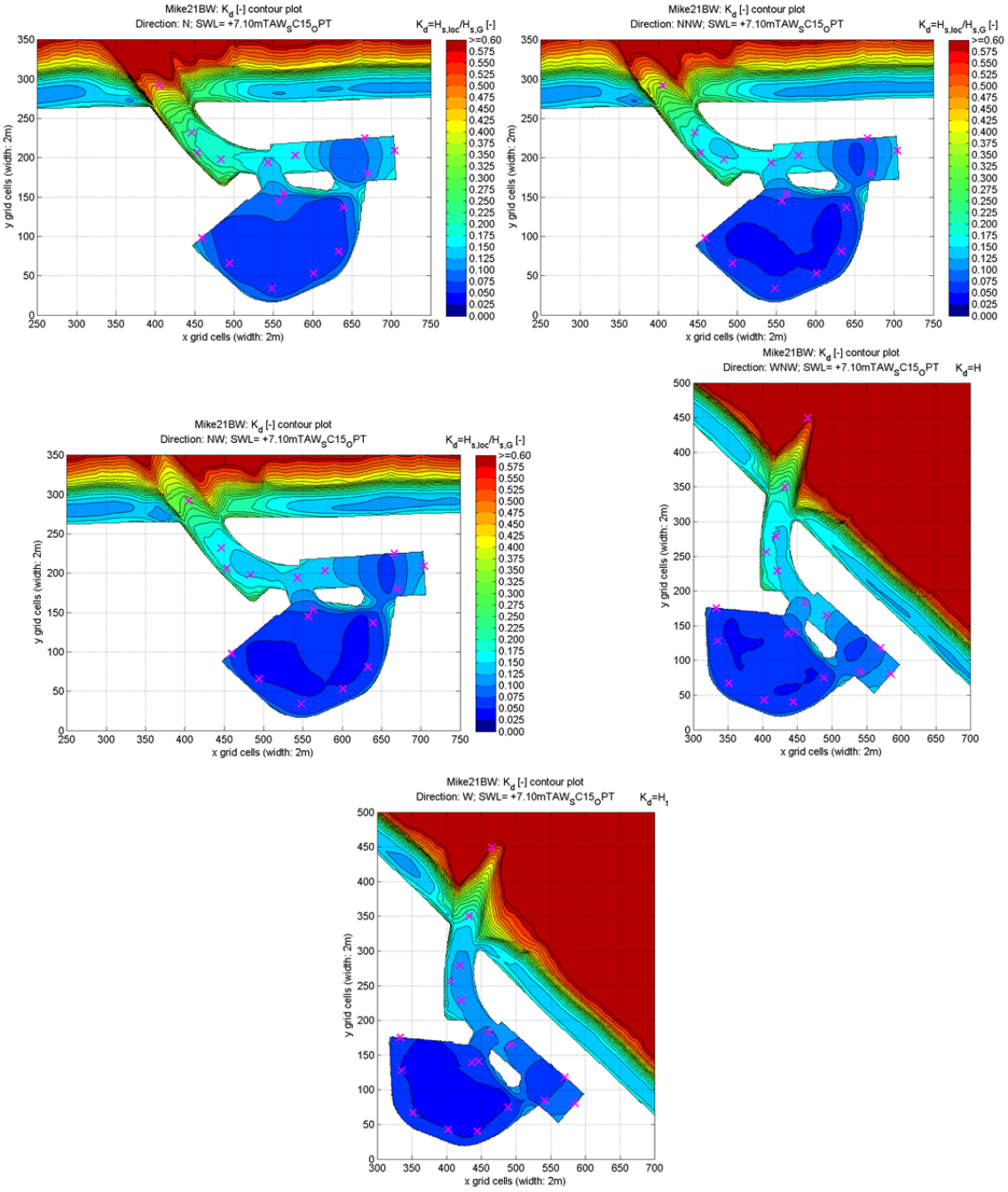

Figure 3-36: K_d contour plot zoomed to marina with indication of output locations. Result of Mike 21 BW. Comparison of wave directions N, NNW, NW,WNW and W.

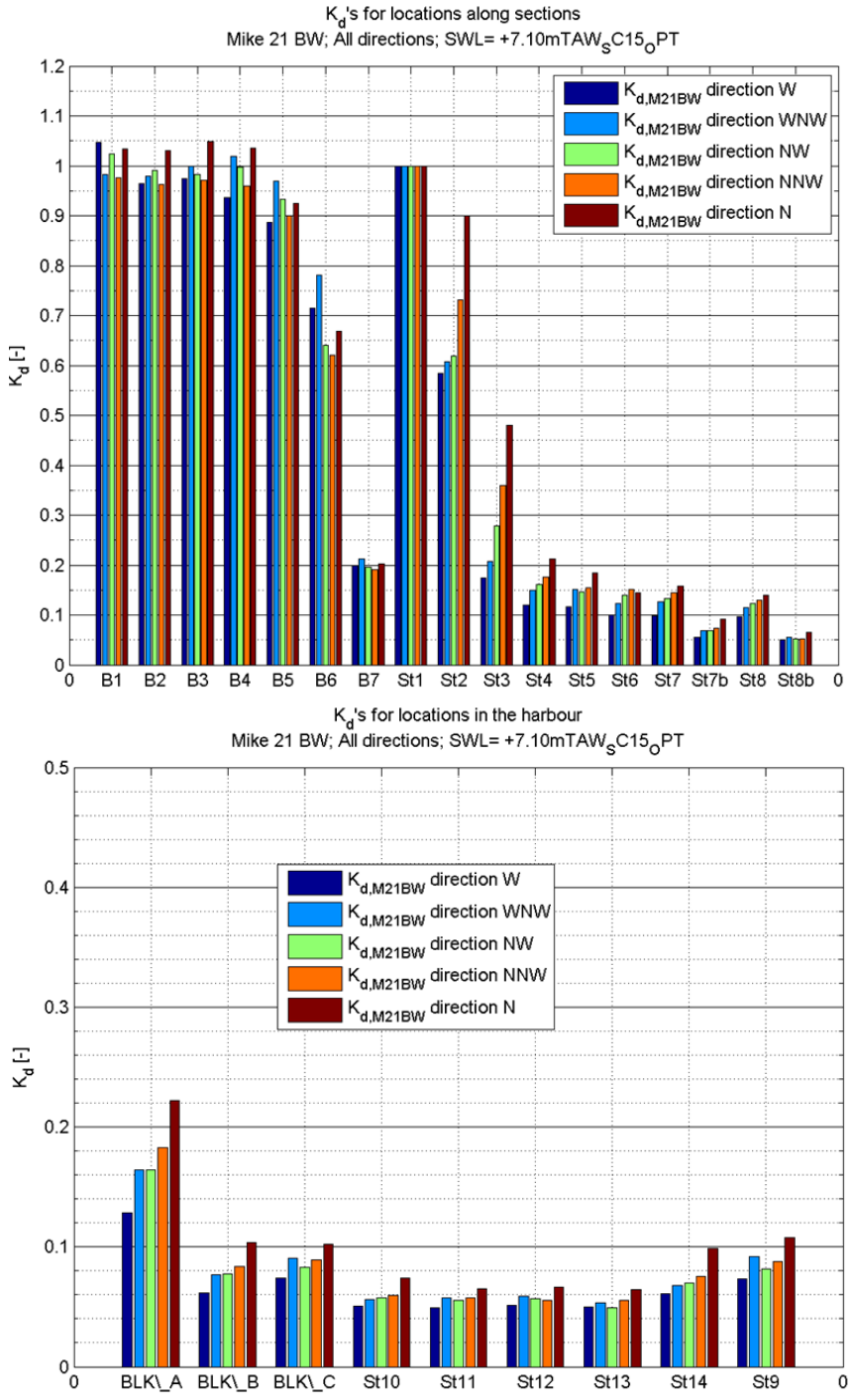

Figure 3-37: K_d-values of the locations along the sections (upper) and in the marina (lower). Result of the Mike 21 BW. Comparison of wave directions W, WNW, NW, NNW and N.

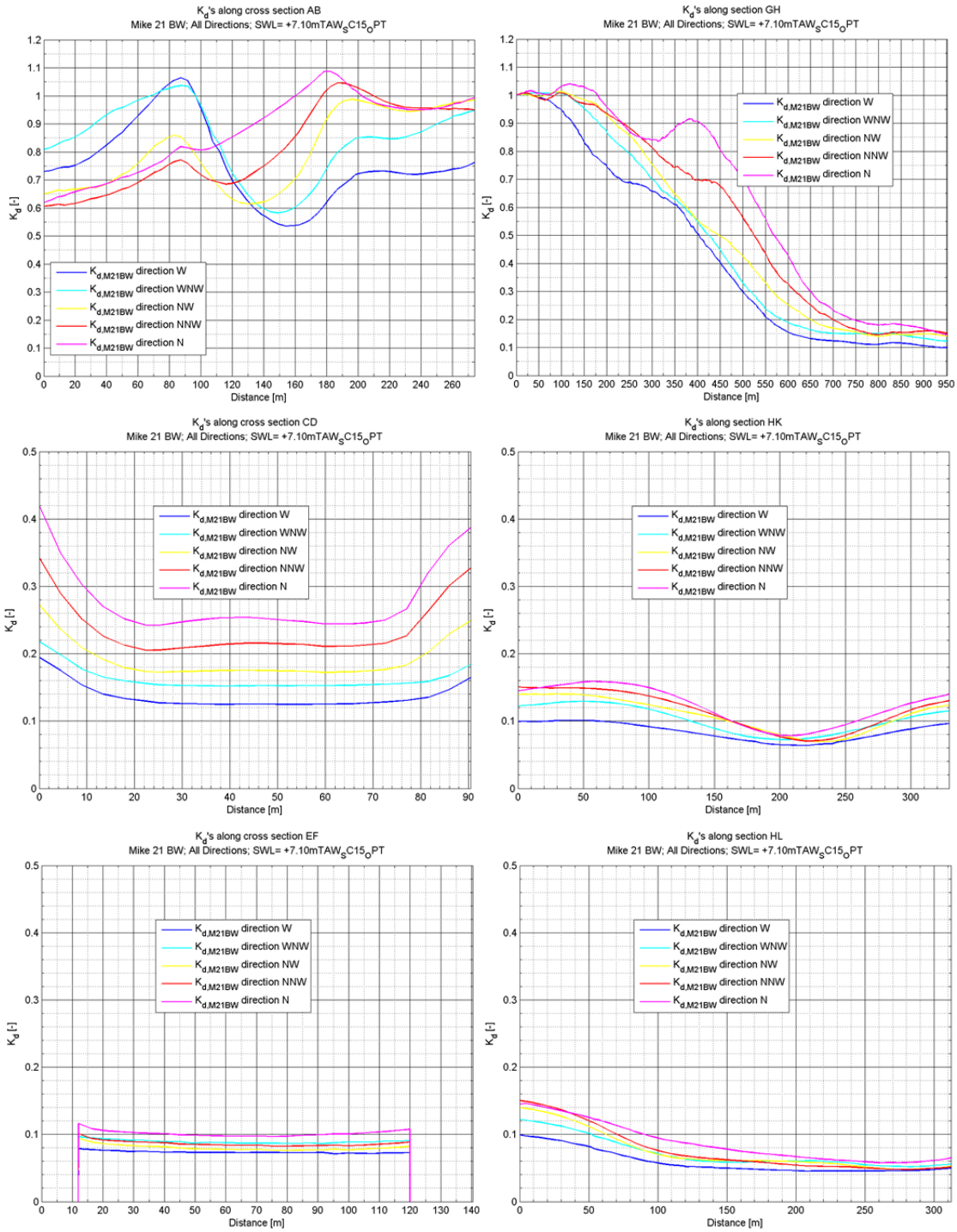

Figure 3-38: Comparison of the evolution of the K_d-value along the longitudinal section GH (HL and HK) and cross sections AB, CD and EF for different wave directions.

SWASH model results

The K_d contour plots are shown in Figure 3-39. The comparison on the locations are shown in Figure 3-40 and the sections in Figure 3-47. Figure 3-42 shows the wave set-up contour plot.

For each direction the following can be observed:

- The wave direction of NNW has the highest K_d value inside the marina while N has the highest K_d value at the entrance channel.
- The K_d value of NW and WNW inside the marina and at the entrance channel are not high even though the wave direction is almost parallel to the direction of the entrance channel. This may be due to the effect of refraction. Incoming waves of NW and WNW disappear when waves feel the slope of the entrance channel. Since NW and WNW pass longer channels than N and NNW, the wave energy becomes small inside the marina in these directions.
- The high K_d value of the direction N at the entrance channel can be explained by wave reflection. Incoming waves of the direction N are reflected at the west bank and the new storm surge wall. These reflected waves are again reflected at the east bank. Thus the K_d value of N at the entrance channel becomes high.
- The high K_d value of NNW can be explained by wave reflection direction. The incoming waves of NNW are reflected at the west bank of the entrance channel almost 45 degrees. The reflected waves go directly into the marina. This can be the reason that the high K_d value is observed in NNW.
- Wave set-up is high at the direction NNW and NW.

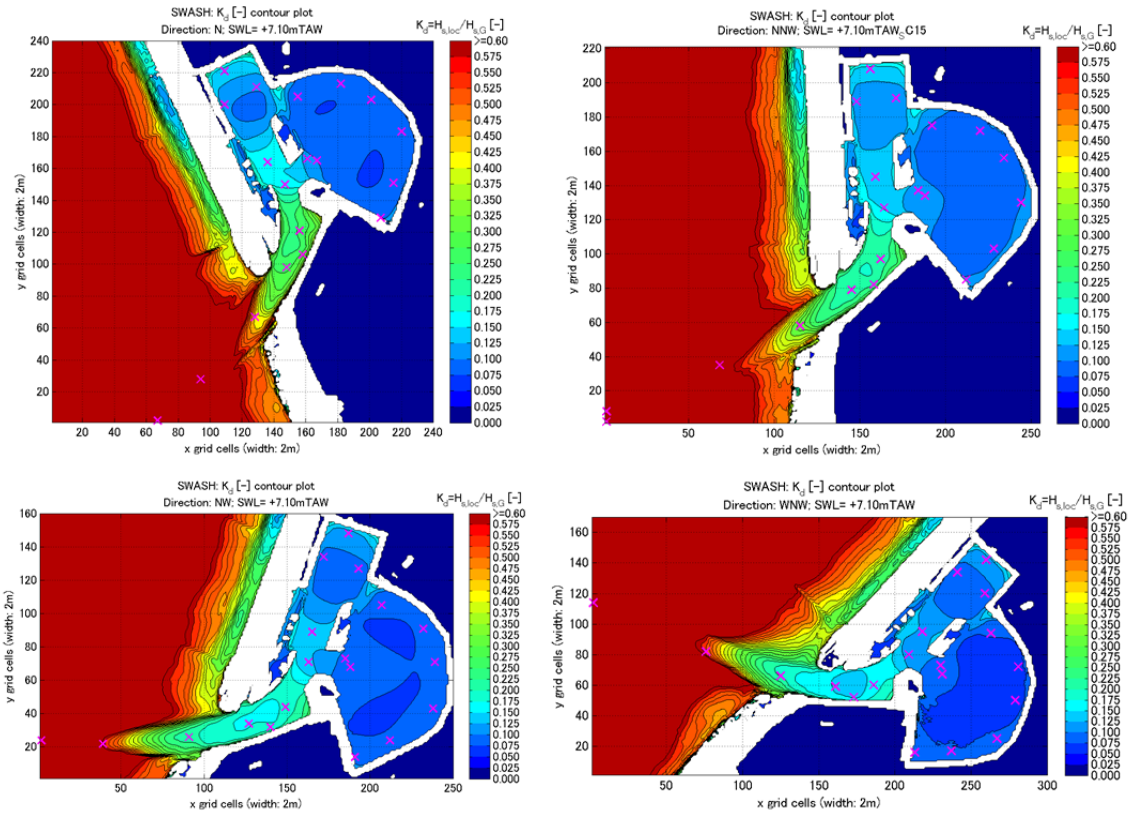

Figure 3-39: K_d contour plot zoomed to marina with indication of output locations. Result of the SWASH model. Comparison of wave directions N, NNW, NW and WNW.

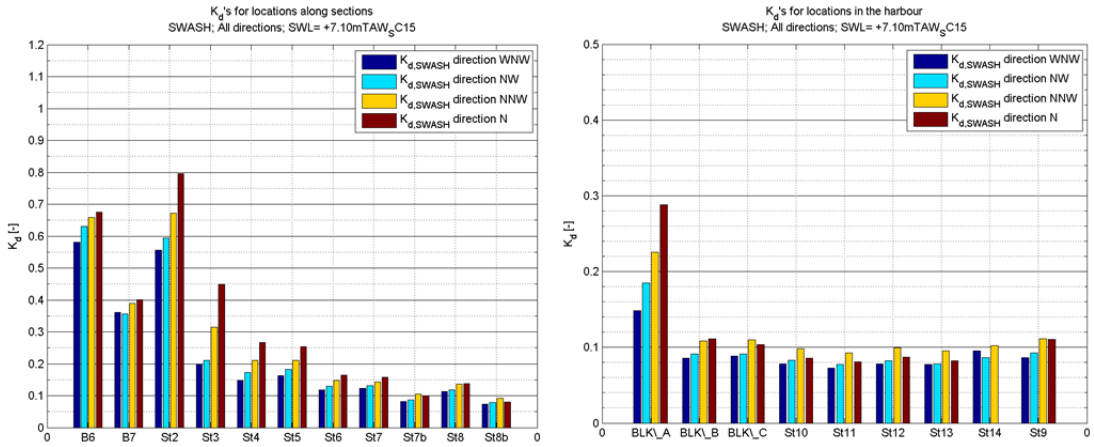

Figure 3-40: K_d-values of the locations along the sections (left) and in the marina (right). Result of the SWASH model. Comparison of wave directions N, NNW, NW and WNW.

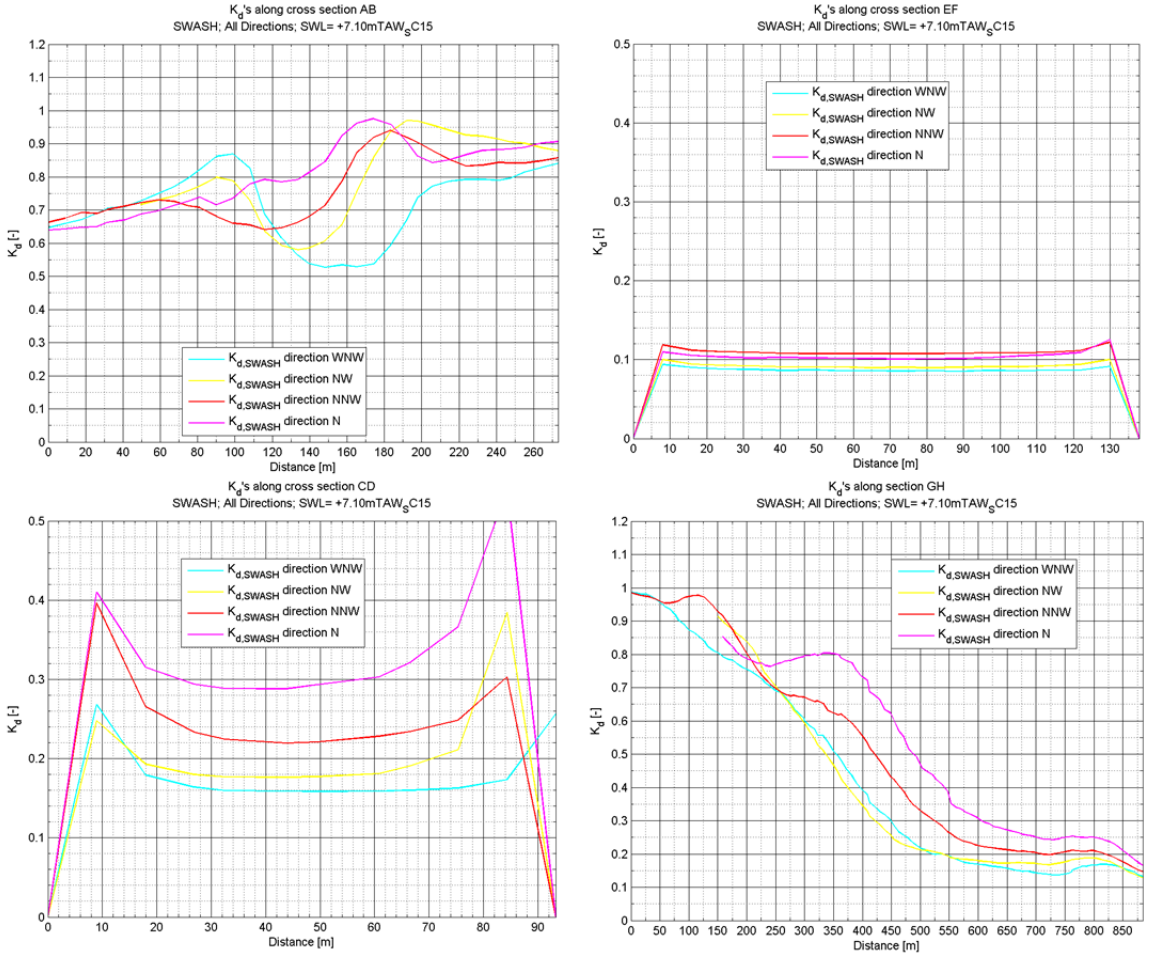

Figure 3-41: Comparison of the evolution of the K_d-value along the longitudinal section GH and cross sections AB, CD and EF for different wave directions. Result of the SWASH model.

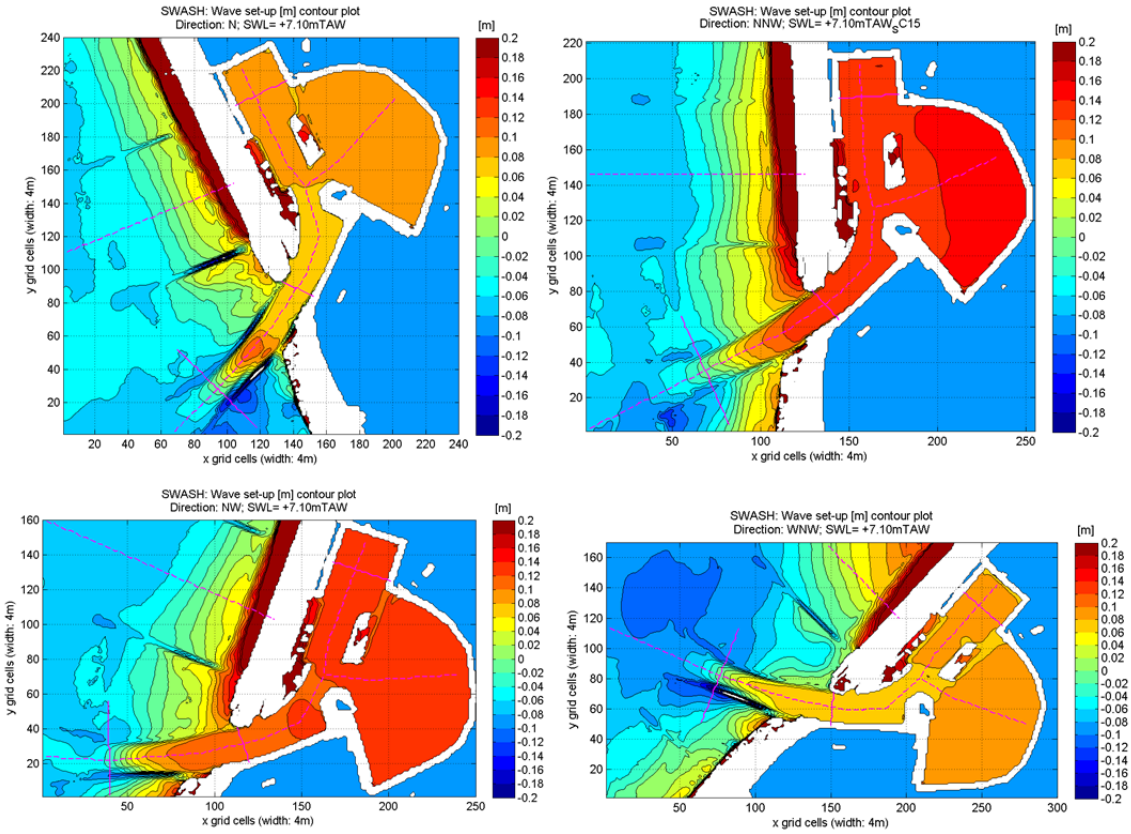

Figure 3-42: Wave set-up with different wave directions (N,NNW,NW and WNW) in the case of 1000 year storm condition with the SWASH model.

3.5.4 Directional spreading

Introduction

This chapter investigates the influence of short-crestedness on the wave climate in the marina.

The selected directional spreading is in total three cases, long crested wave (directional spreading 0°), short crested wave (directional spreading 15°), and another short crested wave (directional spreading 30°). 1000 year storm condition is used as a input wave condition for this investigation. The hydrodynamic boundary conditions are summarized in Table 3-13.

Table 3-13: Hydrodynamic boundary conditions for the sensitivity analysis “Directional spreading”.

SWL [mTAW]	d_{max} [m]	H_{m0} [m]	T_p [s]	Direction [-]	Directional spreading [°]		
+7.10	12.10	4.5	12.0	NNW	0	15	30

Mike 21 BW result

The K_d contour plots are shown in Figure 3-43. The comparison on the locations is shown in Figure 3-44 and the sections in Figure 3-45.

For each direction the following can be observed:

- The highest K_d values inside the marina can be seen for long crested waves.
- The K_d value becomes smaller when directional spreading increases.
- The difference between σ = 15° and σ = 30° is small.

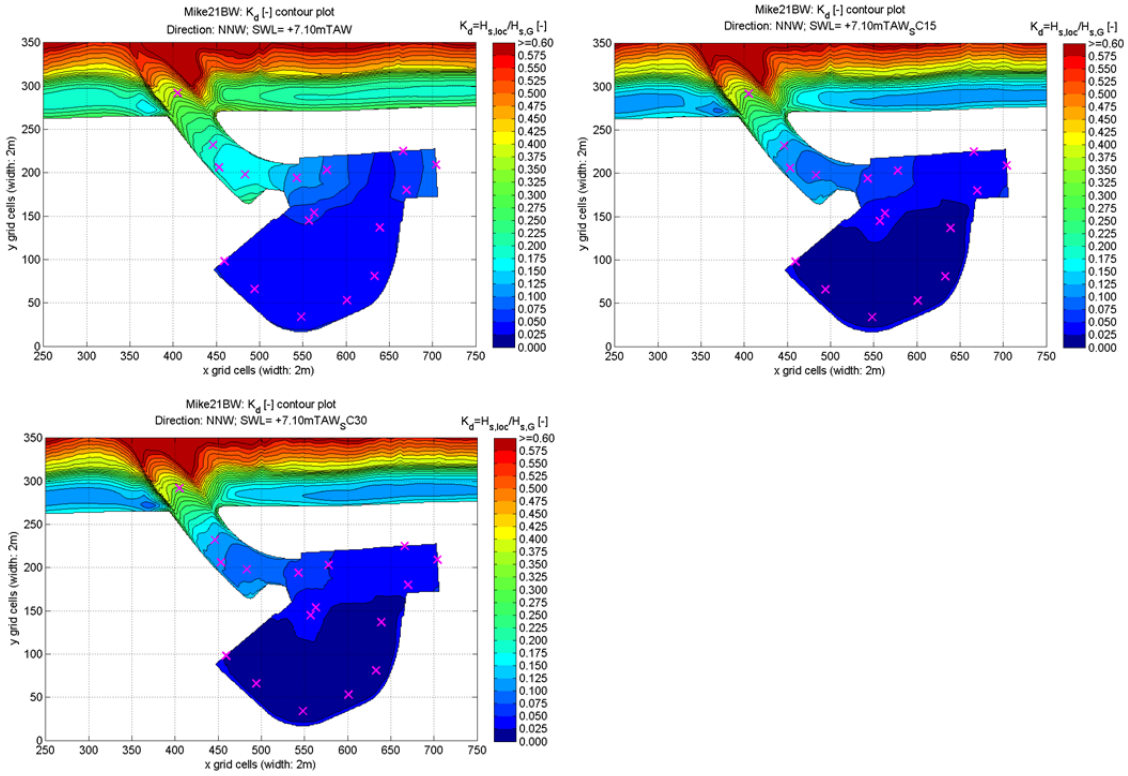

Figure 3-43: K_d contour plots zoomed to the marina of Blankenberge. Result of Mike 21 BW. Upper left: long crested waves, upper right: short crested waves (σ = 15°), lower: short crested waves (σ = 30°). For relative comparison only, since the absolute values are not valid (results are from an older model).

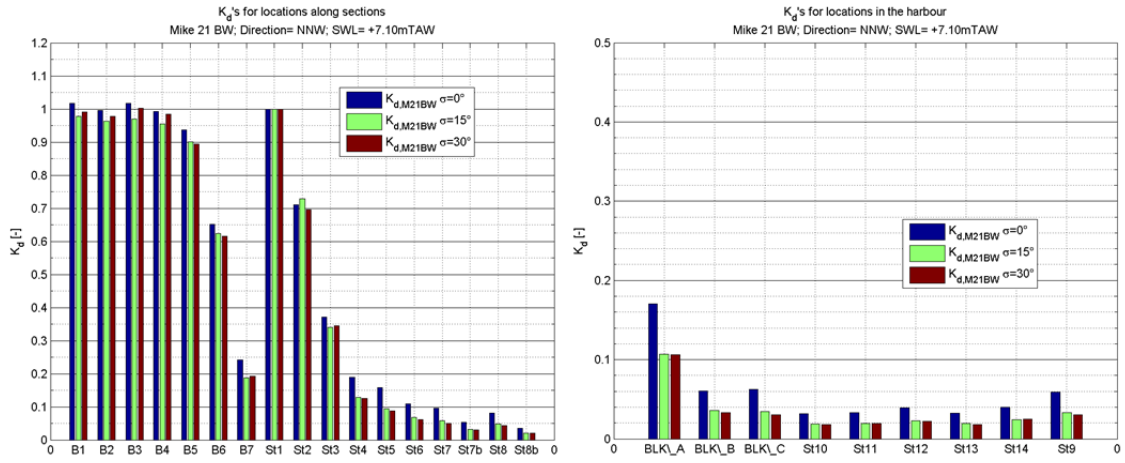

Figure 3-44: K_d-values of the locations along the sections (left) and in the marina (right). Comparison of long crested and short crested waves (15° and 30°). For direction NNW.

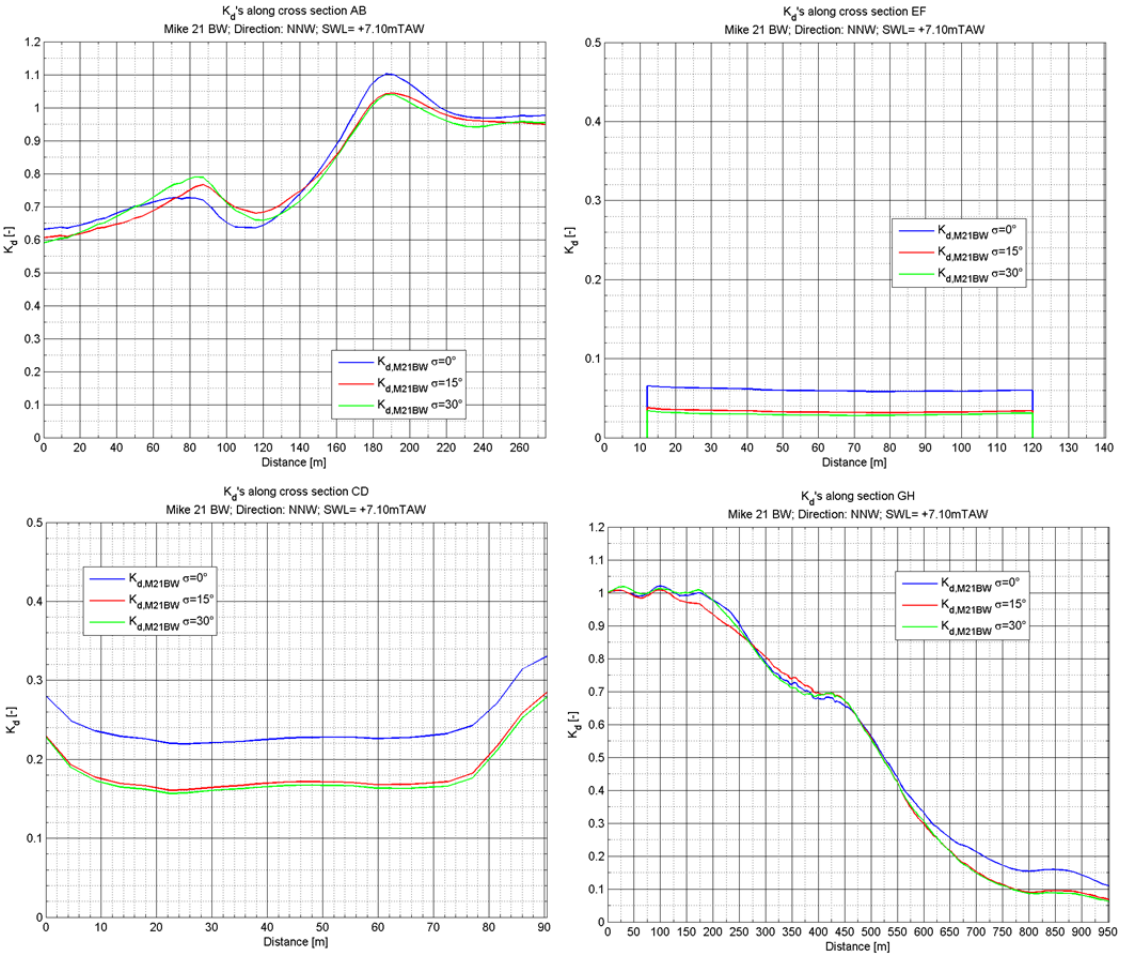

Figure 3-45: Comparison of the evolution of the K_d-value along the longitudinal section GH and cross sections AB, CD and EF. Comparison of long crested and short crested waves (15° and 30°). For direction NNW.

Note: these results are from an older model, but the same conclusions still apply for the current model.

SWASH model results

The K_d contour plots are shown in. The comparison on the locations is shown in and the sections in.

For each direction the following can be observed:

- The high K_d value inside the marina can be seen for long crested waves.
- The K_d value becomes smaller when directional spreading increases.
- The high wave set-up value is observed with long crested wave and short crested wave with directional spreading of 15 degree.
- The difference between σ = 15° and σ = 30° is relatively small compared to the difference between σ = 0° and σ = 15°.

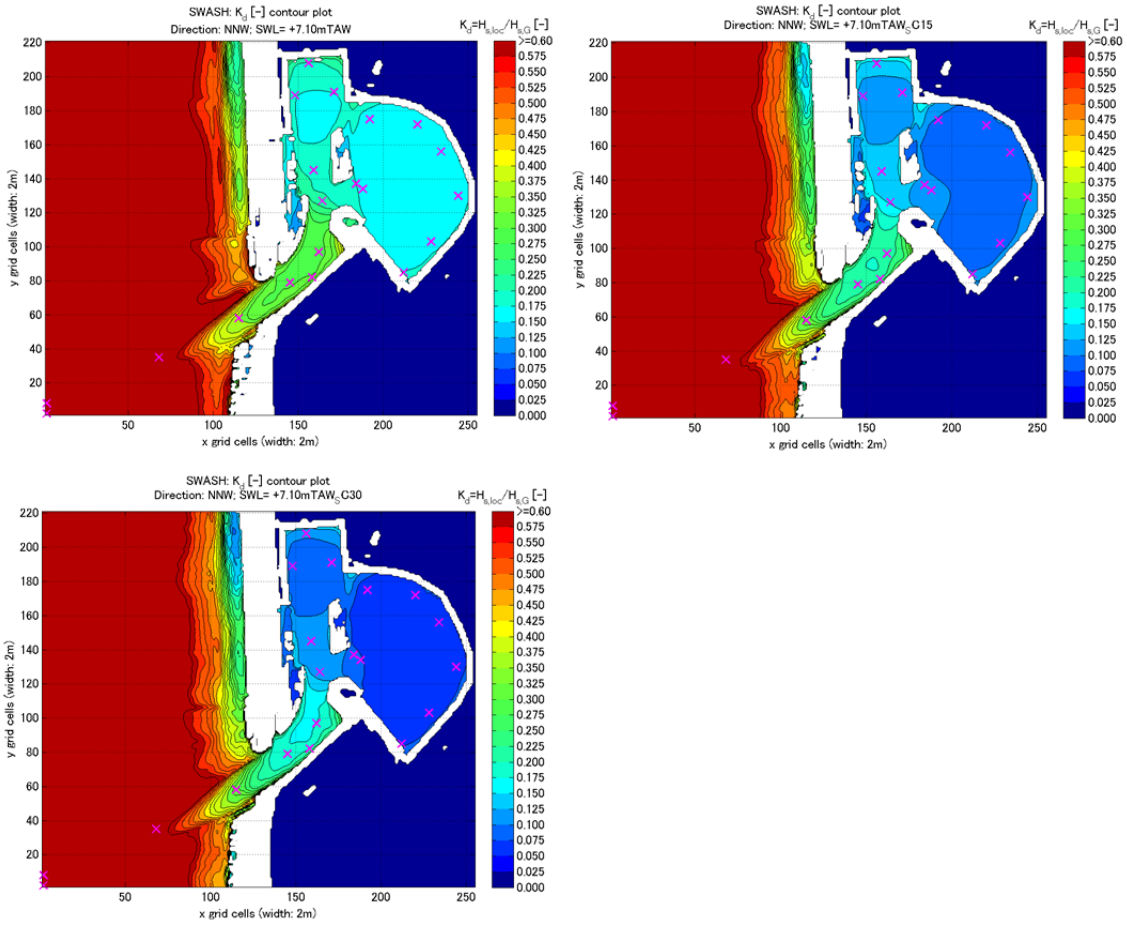

Figure 3-46: K_d contour plots from different directional spreading (long crested waves: 0°, short crested waves: 15° and 30°) in the case of 1000 year storm condition with SWASH model.

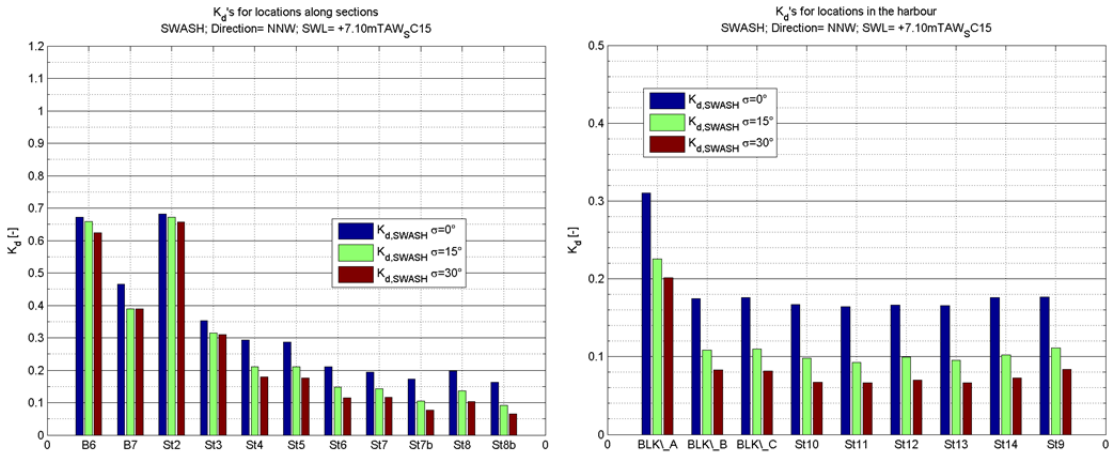

Figure 3-47: K_d-values of the locations along the sections (left) and in the marina (right). Comparison of long crested and short crested waves (15° and 30°). For direction NNW. SWASH model

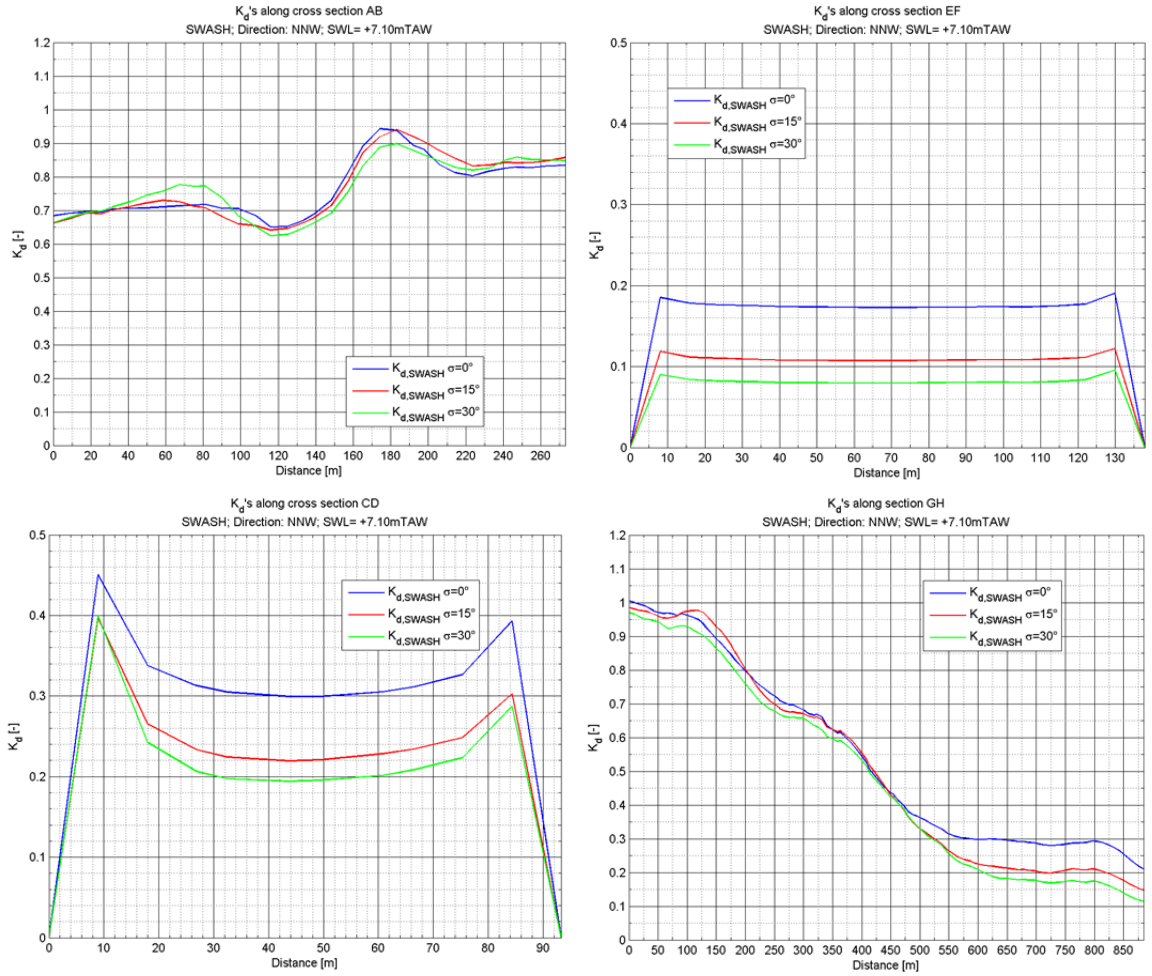

Figure 3-48: Comparison of the evolution of the K_d-value along the longitudinal section GH and cross sections AB, CD and EF. Comparison of long crested and short crested waves (15° and 30°). For direction NNW. SWASH model.

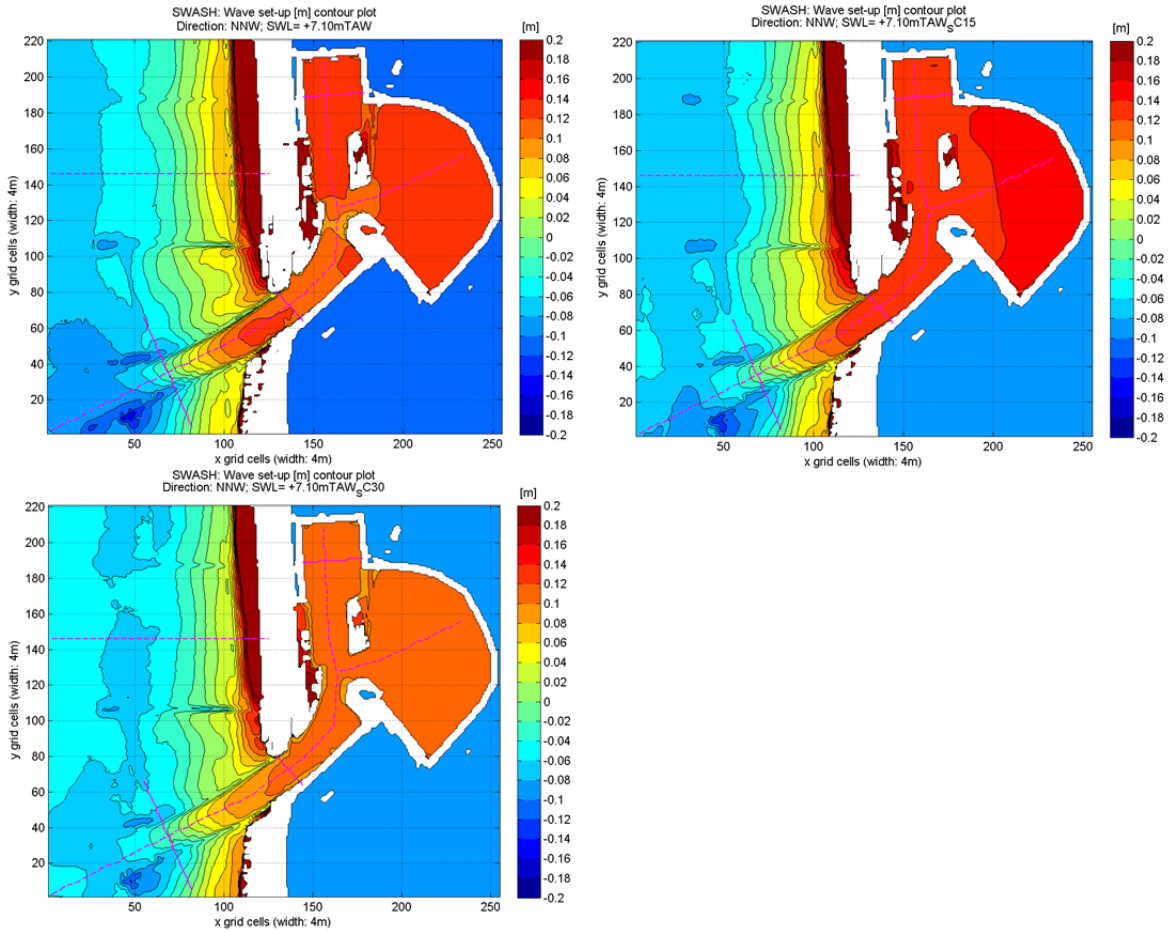

Figure 3-49: Wave set-up contour plots from different directional spreading (long crested waves: 0°, short crested waves: 15° and 30°) in the case of 1000 year storm condition with SWASH model.

3.5.5 Duration of simulation

The investigation of the influence of the duration of simulation is described in this section.

Time duration is normally decided based on statistical characteristics of the waves. It is known that 200 waves are statistically sufficient for the analysis of coastal engineering practices. However, this study area is including a shallow foreshore, which may transform short waves (high frequency waves) to long waves (low frequency waves). Thus, it is required to do a sensitivity analysis for the duration of the simulation time to see whether if the longer simulation time gives different wave parameter and spectrum shape. The influence of the wave trains can also be seen in this sensitivity analysis. This sensitivity analysis is conducted with Mike 21 BW model.

1000 year storm condition with the direction NNW is used for the wave condition for this investigation. In the standard runs for 1000 year storm simulations, a total of 200 waves (40 min) are used for the analysis. In addition to the 200 wave analysis, a 400 wave analysis (80 min) has also been conducted to see the influence of the duration of the simulation. All the other settings such as the output location of the time series of the water surface elevations are the same as used in the 1000 year storm condition simulation. The hydrodynamic boundary conditions are summarized in Table 3-14.

Table 3-14: Hydrodynamic boundary conditions for the sensitivity analysis “Duration of simulation”.

SWL [mTAW]	d_{max} [m]	H_{m0} [m]	T_p [s]	Directional spreading [°]	Direction [-]	Duration of simulation [min]	
+7.10	12.10	4.5	12.0	15	NNW	40	80

A comparison between 40 min simulation and 80 min simulation has been made for significant wave height, wave set-up, spectral wave period, wave spectrum and time series. These figures are shown in Figure 3-50, Figure 3-51 and Figure 3-52 respectively. From these figures, it is clear that the influence of the time duration for the simulation is negligible. Slight differences can be seen, but these are attributed by the difference of the wave trains. The wave trains are different for the 40 min simulation and 80 min simulation which can be seen in the Figure 3-52.

It is determined that the time duration in this study is 40 min (200 waves).

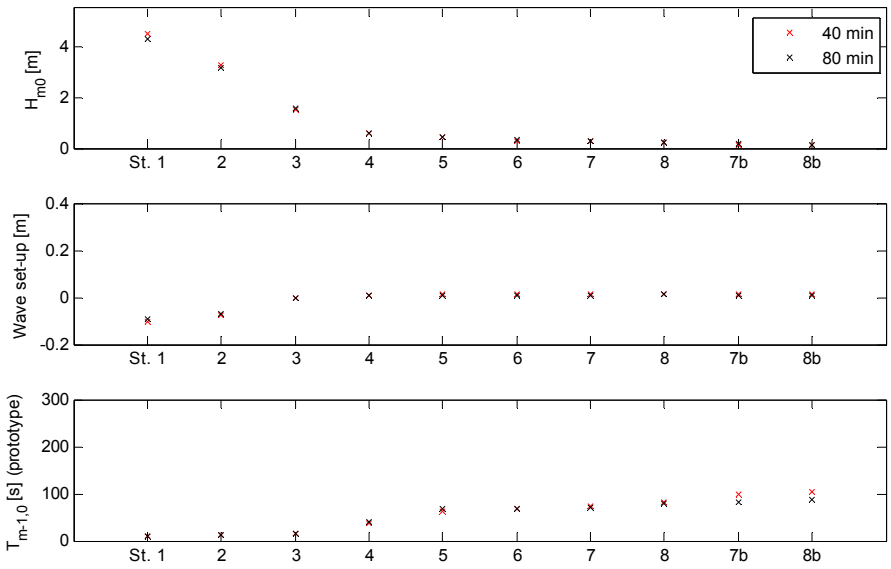

Figure 3-50: Comparison between 40 min simulation and 80 min simulation for significant wave height, wave set-up and spectral wave period

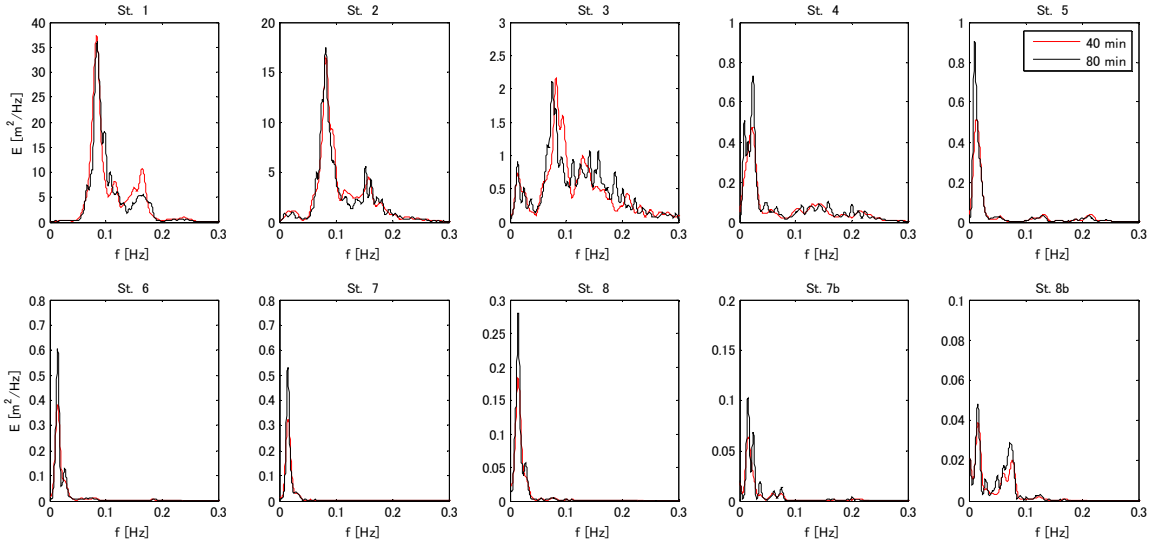

Figure 3-51: Comparison between 40 min simulation and 80 min simulation for wave spectrum

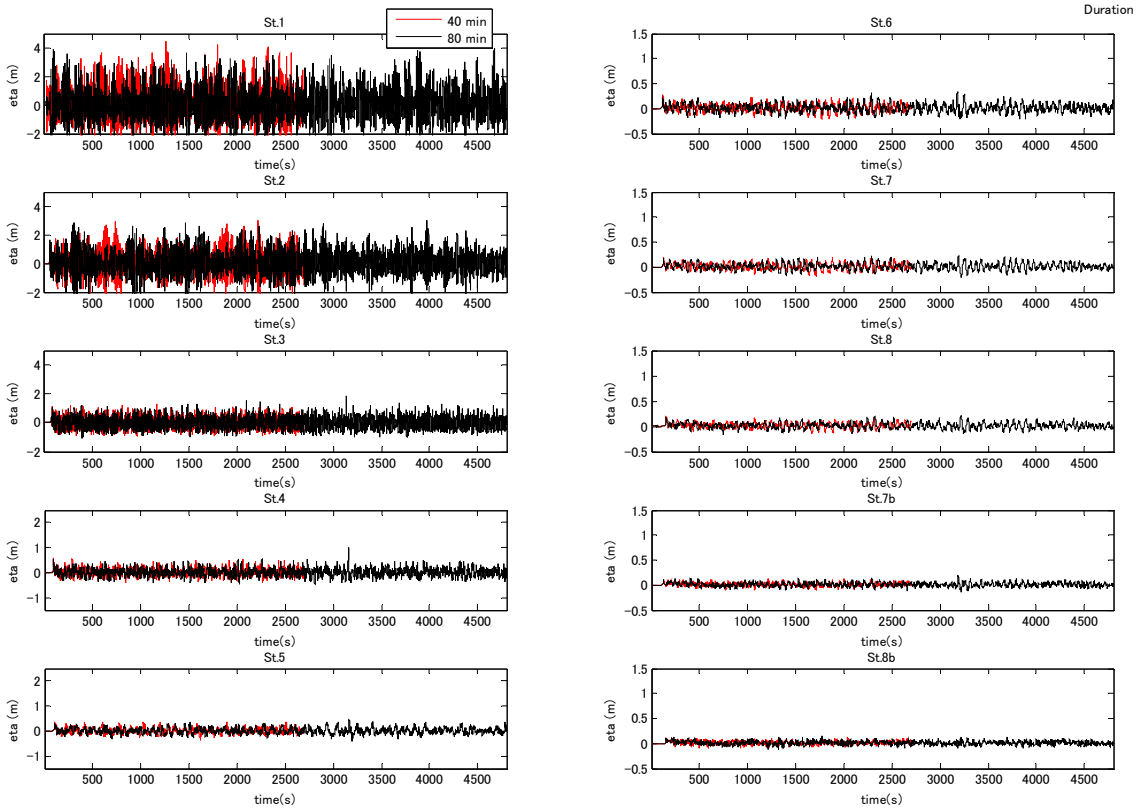

Figure 3-52: Comparison between 40 min simulation and 80 min simulation for time series

3.5.6 Conclusions

The following sensitivity analyses were performed:

- The influence of the time-extrapolation factor was analysed;
- The sensitivity of the wave direction at the boundary;
- The sensitivity of the directional spreading on the wave climate in the marina;
- The sensitivity of the length of the time series on the result of the generated long waves;

For the Mike 21 BW model a time-extrapolation factor had to be applied to obtain a numerically stable model. It introduces some dissipation over long propagation distances. The influence of this factor was therefore investigated for largest grid with orientation WNW. Comparison of the result for factors 0.80 and 0.90 showed almost no difference between the two. A time-extrapolation factor of 0.80 is used for the final models.

Sensitivity of wave directions has been investigated for the SWASH and Mike 21 BW model. The main conclusions from this sensitivity analysis are listed as follows.

- The wave direction of NNW has the highest K_d value inside the marina while N has the highest K_d value at the entrance channel in SWASH model, while N has the highest K_d value for both locations inside marina and at the entrance channel in Mike 21 BW model.
- When the wave direction becomes parallel to the entrance channel (e.g. NW, WNW and W), the incoming waves become small due to the effect of the wave refraction in the navigation channel.
- The K_d values of direction N become high at the entrance channel due to the wave reflection.
- The high K_d values of NNW in SWASH model can be explained by the wave reflection direction. The incoming waves of NNW are reflected at the west bank of the entrance channel almost 45 degrees. The reflected waves go directly into the marina. This can be the reason that the high K_d value is observed in NNW.
- The reflection of N in Mike 21 BW model might be overestimated due to the settings of the land boundary condition. The SWASH model uses the actual configuration which is a combination of the slope and the storm surge wall. On the other hand, the Mike 21 BW model took the slope less into account. This gives higher reflection for short waves.
- Wave set-up is high at the direction NNW and NW.

From the sensitivity analysis of wave directions, the worst condition can be direction N (Mike 21 BW) or NNW (SWASH). The extreme direction dependent wave height for the direction of NNW is higher than the direction of N. Therefore NNW was chosen for the worst case inside the marina. For the entrance area of the marina, other wave directions can be worse. The detailed analysis for wave boundary condition along the harbour including the locally generated wind wave is described in Chapter 5.

Sensitivity of directional spreading has been investigated for the SWASH and Mike 21 BW model. The main conclusions from this sensitivity analysis are listed as follows.

- The highest K_d values inside the marina can be seen for long crested waves.
- The K_d value becomes smaller when directional spreading increases.
- The highest wave set-up value is observed for the case of the short crested waves with $\sigma = 15°$.
- The difference of the K_d values between $\sigma = 15°$ and $\sigma = 30°$ is relatively small compared to the difference of the K_d values between $\sigma = 0°$ and $\sigma = 15°$.

A comparison between 40 min simulation and 80 min simulation has been made for significant wave height, wave set-up, spectral wave period, wave spectrum and time series. From this investigation it is clear that the influence of the time duration for the simulation is negligible. Slight differences can be seen, but these are attributed by the difference of the wave trains. The wave trains are different for the 40 min simulation and 80 min simulation. It is determined that the time duration in this study is 40 min (200 waves).

3.6 Validation

3.6.1 Introduction

Validation of the SWASH model of the Blankenberge harbour is described in this section. The validation is based on data from field measurements.

Field measurements

Field measurements were performed by IMDC (2011) in the harbour of Blankenberge during the period between February 2010 and April 2011 (excluding the summer months June, July and August). Pressure sensors of the type PDCR 1830 were placed at three positions located in the entrance and in the marina as shown in Figure 3-53.

Figure 3-53: The locations of the wave buoy and measurement points at the entrance and inside the marina. (© Google Earth)

Validation cases

Four conditions from the field measurements were chosen to compare with the numerical models. Since the Mike 21 BW model has to apply a cut-off frequency for the generation of the wave, measurement cases which have a higher wave period are chosen. These cases are listed in Table 3-15.

Table 3-15: Four validation cases extracted from the measurements

Case	Time	SWL [mTAW]	H_{m0} [m]	T_p [s]	Wave Direction [-]	Wind Direction [-]	Wind speed [m/s]
Validation 1	02:00-02:15, 25/09/2010	+4.91	2.3	9.1	NNW	NNW	14
Validation 2	15:15-15:30, 25/09/2010	+4.97	2.3	8.5	NW	WNW	15
Validation 3	10:45-11:00, 20/10/2010	+4.55	2.5	8.5	NNW	WNW	14
Validation 4	01:30-01:45, 24/12/2010	+4.61	2.7	8.5	N	NNE	18

Wave analysis

The analysis of the results in this chapter is done with the wave penetration coefficient K_d and wave spectrum.

The K_d value of the field measurements is calculated the equation shown as below.

$$K_d = \frac{H_{m0,loc}}{H_{m0,BLK/GB1}}$$

with $H_{m0,loc}$ the significant wave height at the considered location [m]
$H_{m0,BLK/GB1}$ the significant wave height at the wave buoy (BLK-GB1) location [m].

The same method for the analysis of the wave spectrum (a MATLAB code for SWASH results found in 'Test cases' at http://swash.sourceforge.net/) was used for SWASH and Mike 21 BW models, so that the model's spectrum outputs are the same in terms of degree of smoothing. The smoothing factor 40 was used for these analysis.

In the wave spectrum analysis, 15 minute measurement data is compared with 40 minute numerical model result. The duration of the field measurements and numerical models are different, so the energy of long waves can be underestimated for the field measurements. However, this differences is considered to be small. It is noted that the minimum wave frequency of the field measurements was 0.004 Hz, 250 s (IMDC, 2011).

Bathymetry

For the validation cases (+4.55 to +4.91 m TAW), the water level is lower than 1000 year storm (+7.1 m TAW) and 8m storm (+7.9 m TAW) conditions so that the bathymetries used in both models are almost the same (cf. no wave overtopping, no additional bottom friction).

3.6.2 Validation

Validation 1

The measurement data of 02:00, 25/09/2010 is used for the validation of numerical models, SWASH and Mike 21 BW. This is validation 1. The wave direction from the field measurements is NNW, significant wave height 2.3 m, peak wave period 9.1 s and water level +4.91 m TAW, respectively. The wind is also measured at the same time and the wind speed is 14 m/s and the wind direction is NNW. It is noted that the wind direction stays same direction longer period.

Figure 3-54 shows K_d contour plot of numerical models. The overall results of K_d value inside the marina from the SWASH model and the Mike 21 BW model show similar pattern and similar values.

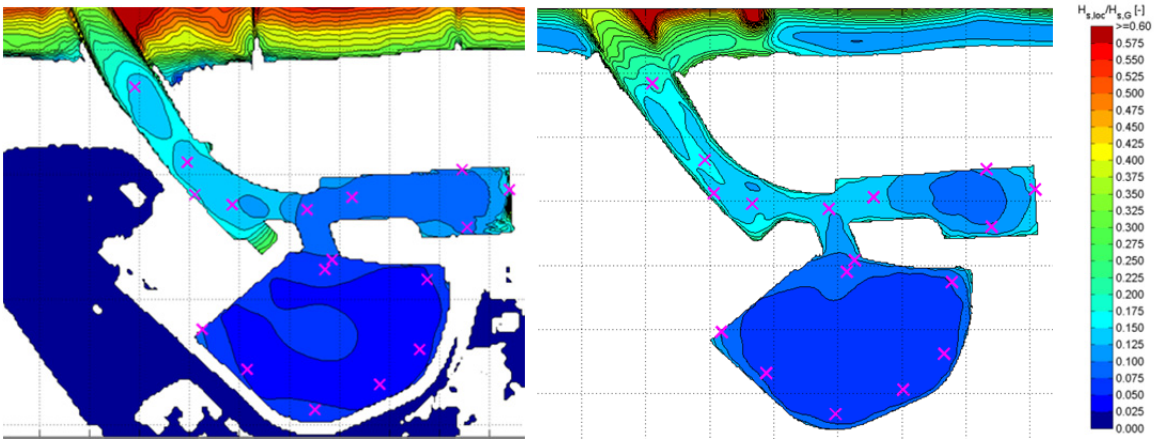

Figure 3-54: K_d contour plot inside the marina in the case of Validation 1. Left figure shows the SWASH model result and right figure shows the Mike 21 BW model (legend is the same in both figures).

Figure 3-54 shows K_d values for the numerical models and the field measurement at each station in the case of validation 1. In general, K_d values of measurement and numerical models have similar value as can be seen in Figure 3-54. The differences are less than 5 % in K_d value. This indicates that the models reproduced the measured waves reasonably well. However, the spectrum pattern for BLK-A shown in Figure 3-56 is somewhat different from what is obtained from numerical models. It appears that the wave energy in the high frequency component is still dominant in the field measurements, while both models show that most energy comes from the low frequency parts. This may result from locally generated wind waves, which are not accounted for in the numerical results.

SWAN was used to see the influence of locally wind generated waves. The result of the locally wind generated waves is shown in Figure 3-57. The absolute significant wave height value at BLK-A obtained by the SWAN model is about 15 cm and the wave period is less than 2.0 s, while the absolute value of the significant wave height in the measurement and the models at BLK-A is about 40 cm. Since the wave period generated by wind is less than 2.0 s, the relatively large energy at 0.1 to 0.3 Hz cannot be explained by the local wind generation.

Even though some differences at the high frequency spectrum are observed, it can be said that both models reproduced the measurement waves reasonably well.

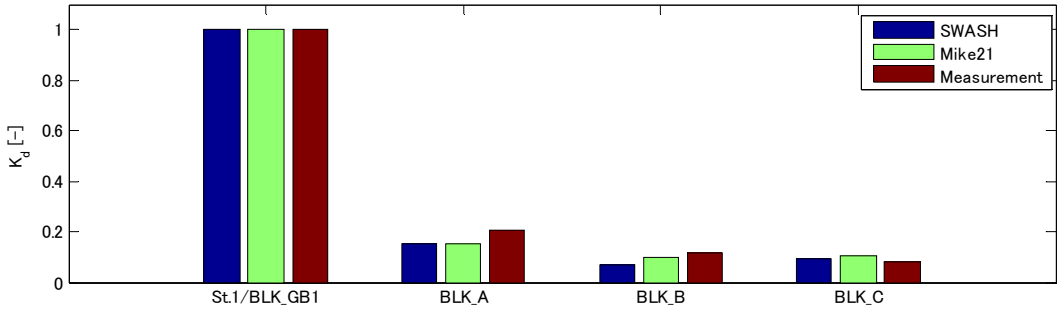

Figure 3-55: K_d value of numerical models and field measurements in the case of validation 1.

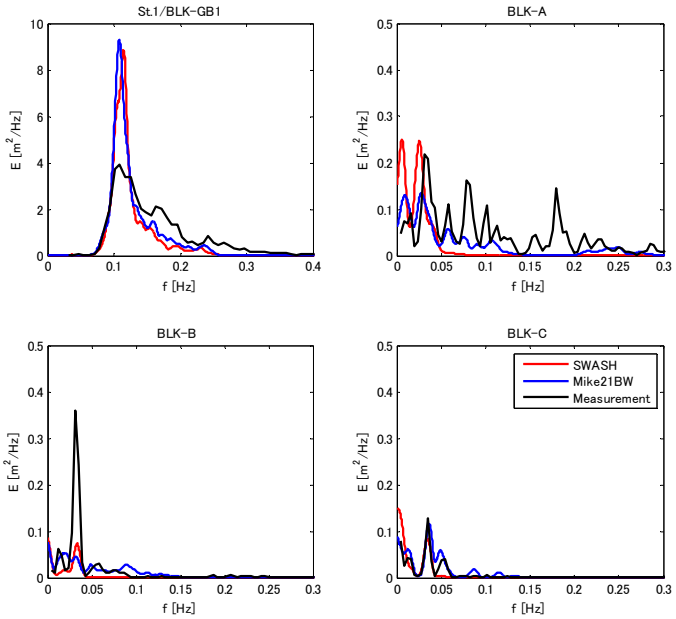

Figure 3-56 Wave spectrum of numerical models and field measurements in the case of validation 1 (NB: different axis scales for St.1/BLK-GB1).

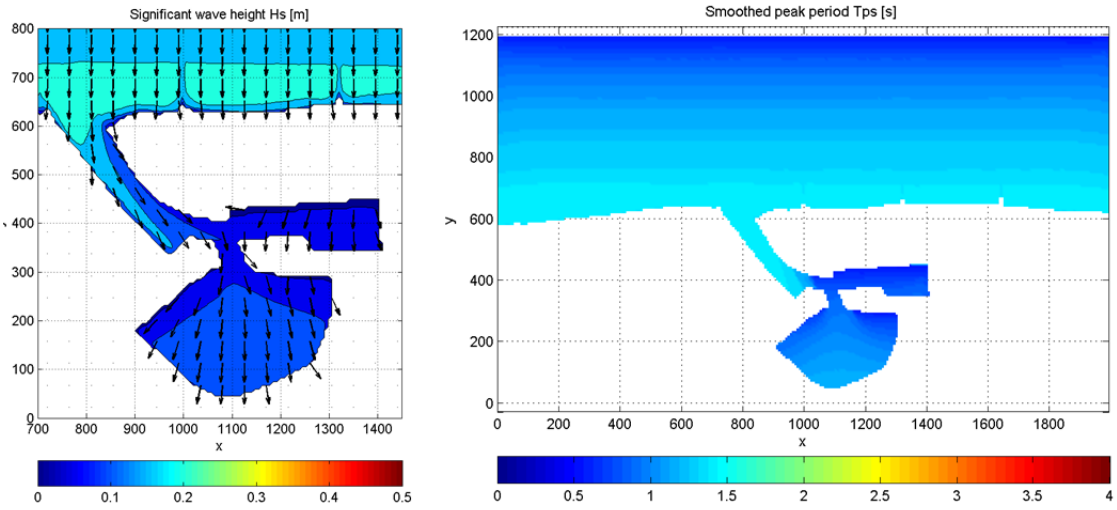

Figure 3-57 Significant wave height Hs (left) and smoothed peak period Tps (right) of local wind generated waves calculated by SWAN model. The Wind direction is NNW and the wind speed is 14 m/s.

Validation 2

The measurement data of 15:15, 25/09/2010 is used as validation 2. The wave direction from the field measurements is NW, significant wave height 2.3 m, peak wave period 8.5 s and water level +4.97 m TAW, respectively. The wind is also measured at the same time and the wind speed is 15 m/s and the wind direction is WNW.

Figure 3-62 shows the K_d contour plot from the numerical models. Slightly higher values can be seen in the SWASH model in the entire domain compared to the K_d value in the Mike 21 BW model. Figure 3-59 shows the K_d value plot from the numerical models and the field measurements. The largest difference in this case is about 10 % in the K_d value between Mike 21 BW and the measurement at BLK_A. However, the value at BLK_C of different models show similar value. Figure 3-60 shows the energy spectrum evaluated at the field measurement points. Slightly higher K_d values in the SWASH results than in the Mike 21 BW model can be explained by the spectrum. It seems that very long waves are generated in the SWASH model inside the marina, which gives higher values for K_d. Apart from the discussion of K_d values, again it is seen that the high frequency energy at BLK_A in the measurement is dominant as is observed in the validation 1. Still the pattern of numerical models and field measurements for the wave frequency at BLK_B and BLK_C is somewhat similar.

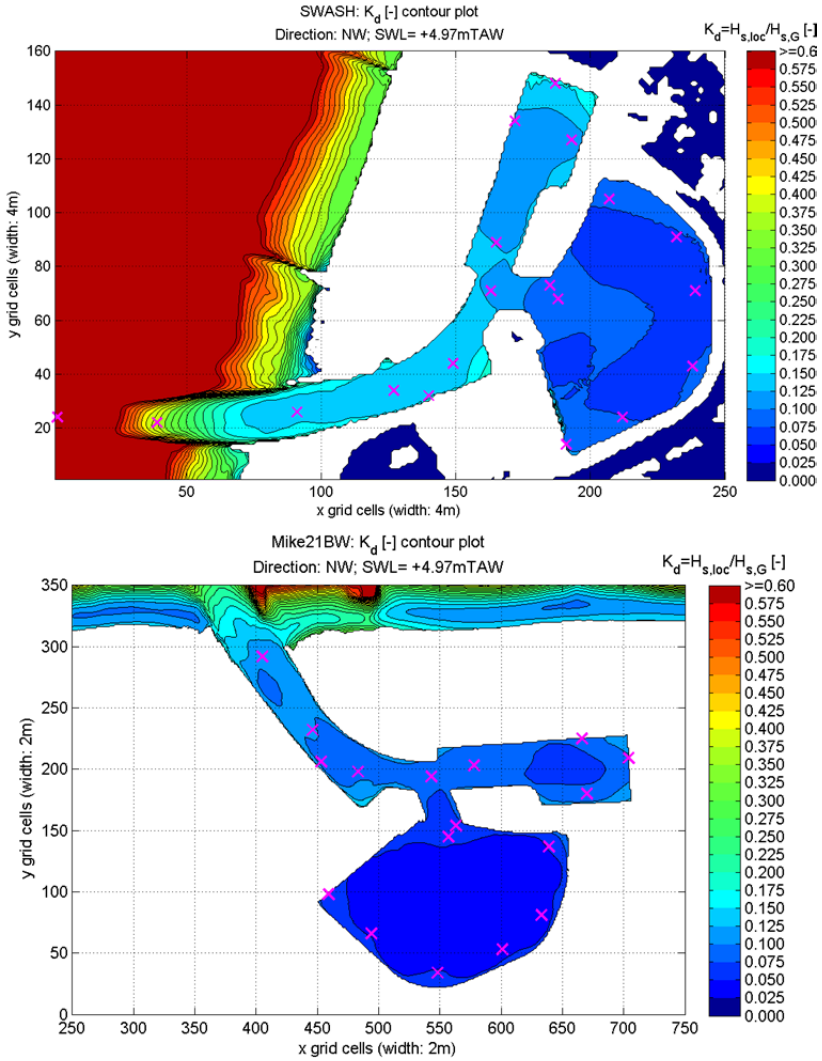

Figure 3-58: K_d contour plot inside the marina in the case of Validation 2. Upper figure shows the SWASH model result and lower figure shows the Mike 21 BW model.

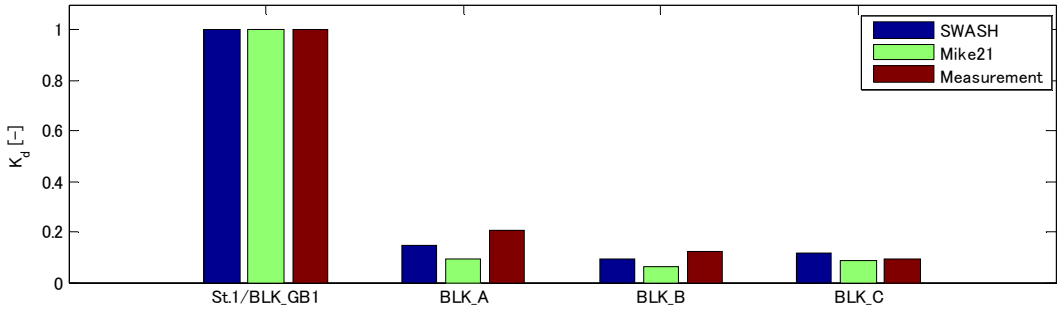

Figure 3-59: K_d value of numerical models and field measurements in the case of validation 2.

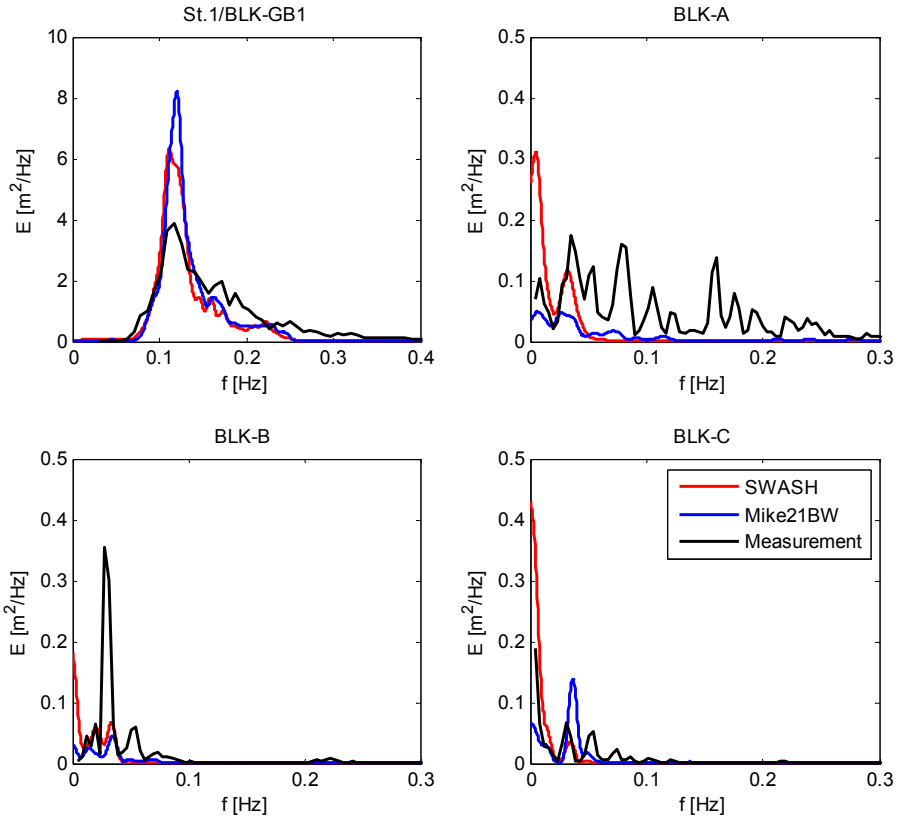

Figure 3-60 Wave spectrum of numerical models and field measurements in the case of validation 2.

Validation 3

The measurement data of 10:45-11:00, 20/10/2010 is used as validation 3. The wave direction from the measurements is NNW, significant wave height 2.5 m, peak wave period 8.5 s and water level +4.55 m TAW, respectively. The wind is also measured at the same time and the wind speed is 14 m/s and the wind direction is WNW.

The similar trends can be seen in this case as obtained in the validation 1.

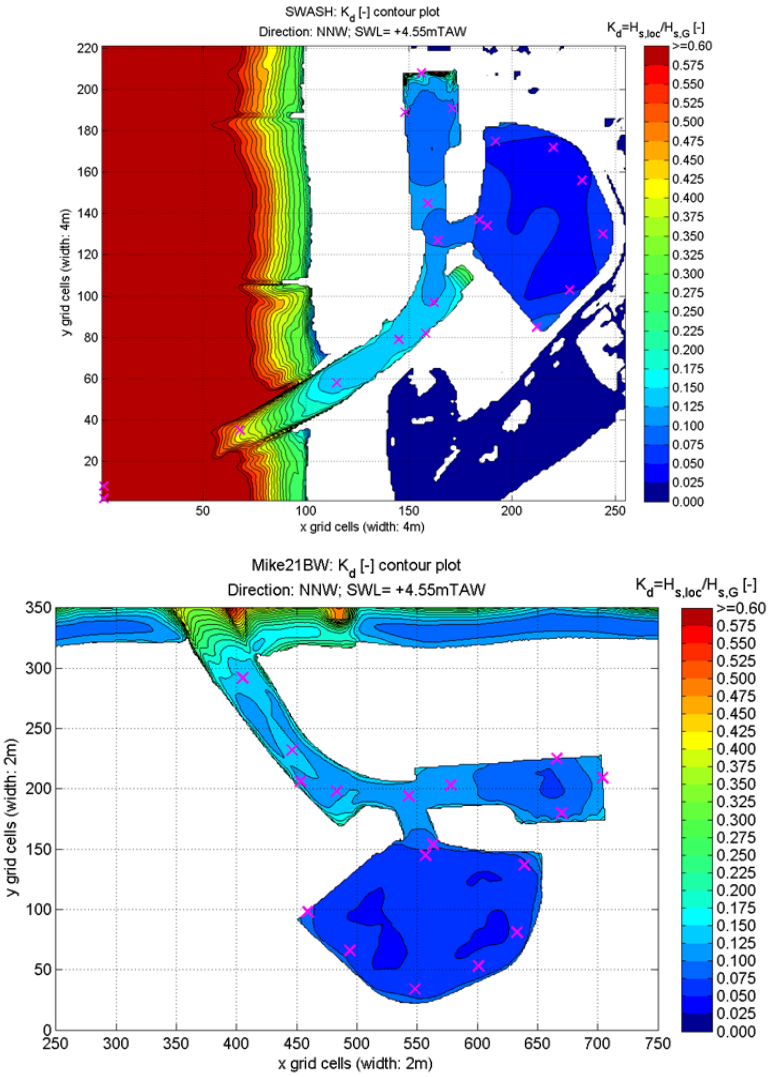

Figure 3-61: Kd contour plot inside the marina in the case of Validation 3. Upper figure shows the SWASH model result and lower figure shows the Mike 21 BW model.

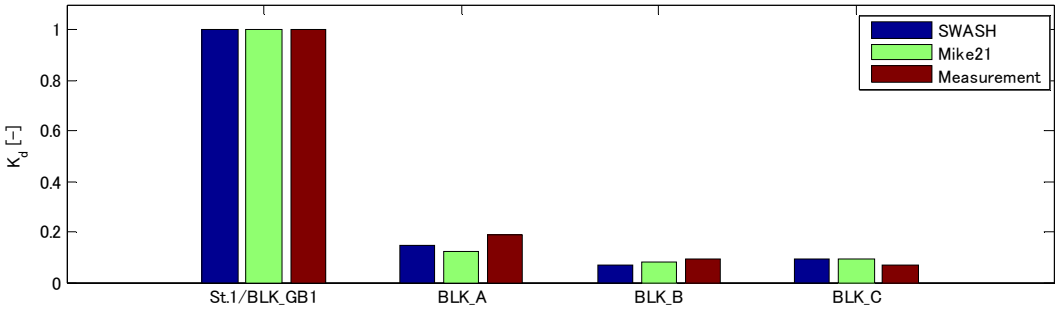

Figure 3-62: Kd value of numerical models and field measurements in the case of validation 3.

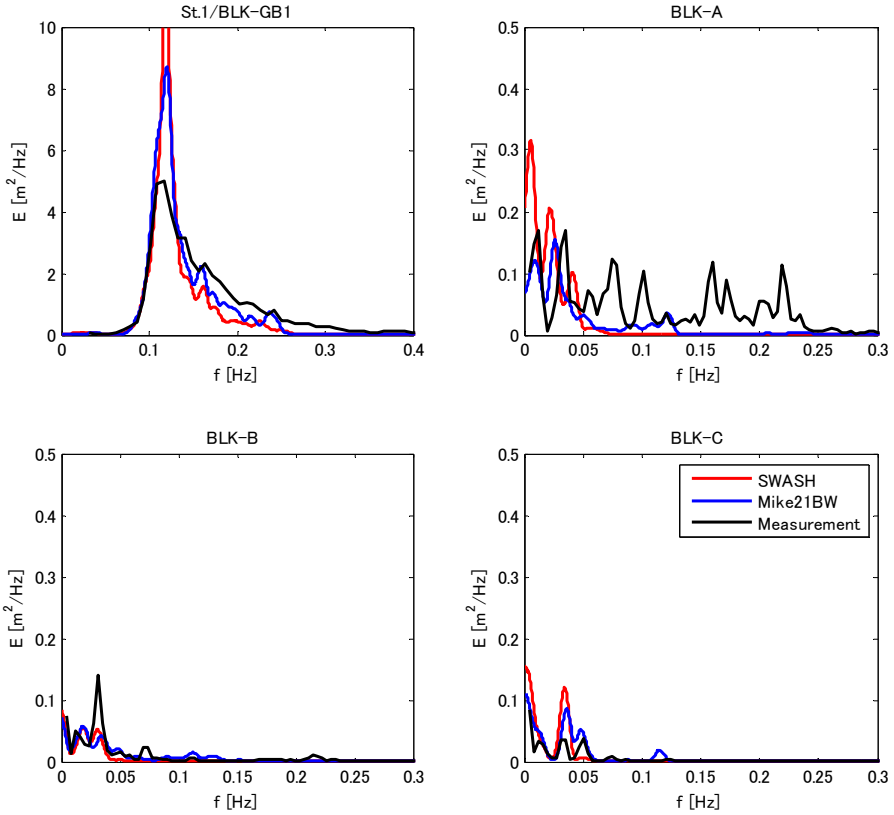

Figure 3-63 Wave spectrum of numerical models and field measurements in the case of validation 3.

Validation 4

The measurement data of 01:30-01:45, 24/12/2010 is used as validation 4. The wave direction from the measurements is N, significant wave height 2.7 m, peak wave period 8.5 s and water level +4.55 m TAW, respectively. The wind is also measured at the same time and the wind speed is 14 m/s and the wind direction is NNE.

Slightly different trends can be seen in this case. The field measurement's K_d value in the validation 1 to 3 were almost equivalent to the numerical model results, however the field measurement's K_d value in this case is lower than the K_d values in the numerical models. From this, it can be considered that the K_d value trend depends on the dominant wave directions.

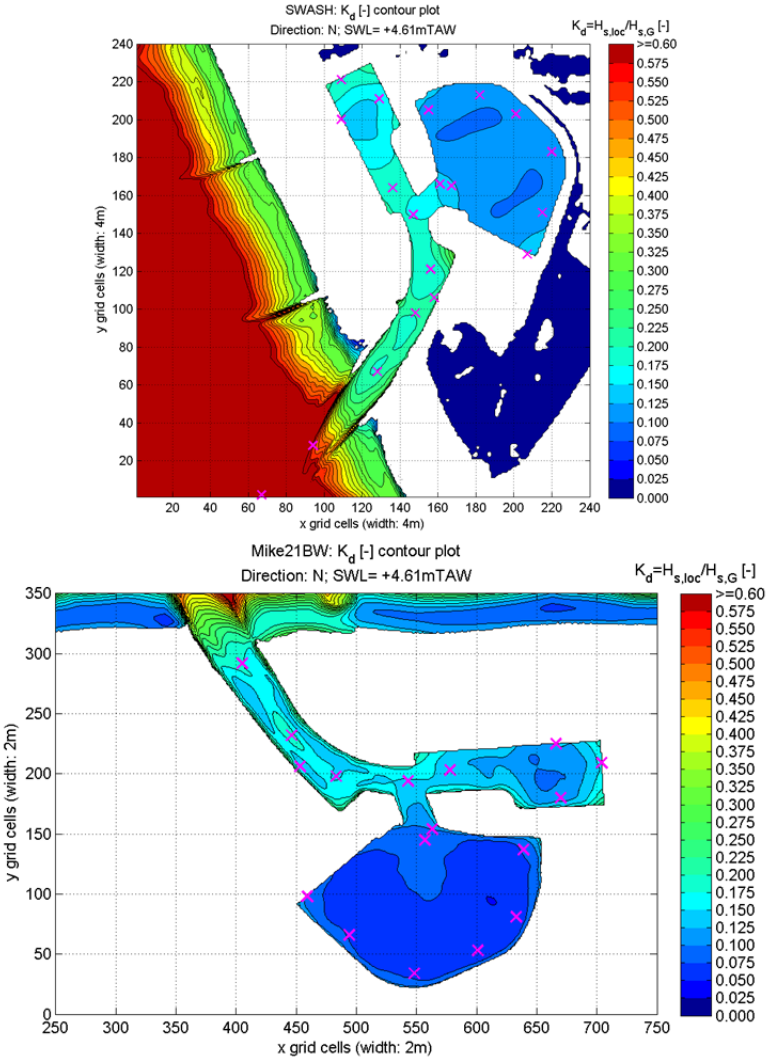

Figure 3-64: Kd contour plot inside the marina in the case of Validation 4. Upper figure shows the SWASH model result and lower figure shows the Mike 21 BW model.

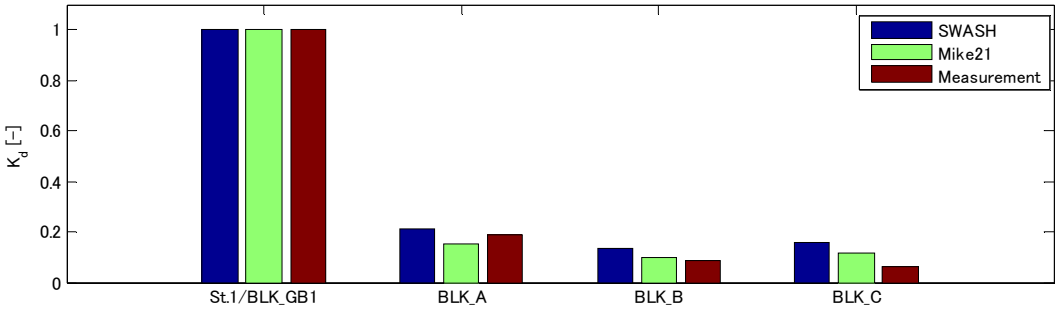

Figure 3-65: Kd value of numerical models and measurement in the case of validation 4.

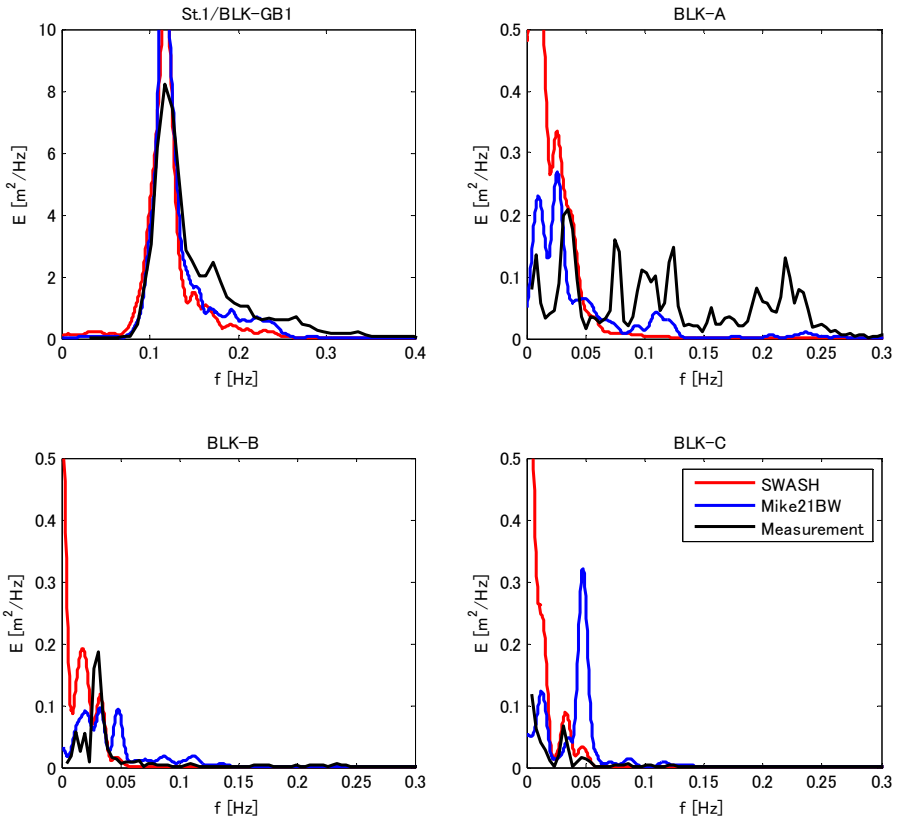

Figure 3-66 Wave spectrum of numerical models and measurement in the case of validation 2.

3.6.3 Conclusions

Four measurement period were used to validate the SWASH and Mike 21 BW model. The main conclusions from this validation are as follows.

- In general, both models are capable at reproducing the significant wave height with sufficient accuracy in each direction, N,NNW and NW, even though the non-linear effect can be high in the shallow marina. It was also found that the trend of the K_d values can depend on the dominant wave directions.
- The largest difference is about 10% in the K_d value (BLK_A in the validation 2 and BLK_C in the validation 4), which is almost equivalent to 0.2 to 0.3 m in significant wave height.
- Inside the marina, most of the high frequency energy is transferred to the low frequency. Peak values did not perfectly correspond to each other, but the shift of the peak frequency was shown reasonably well.
- It appears that the wave energy in the high frequency component is still dominant in the field measurements for BLK-A, even though numerical models show the high frequency component. The differences between the numerical models and the field measurements cannot be explained by locally generated wind waves calculated by SWAN model since its wave period is too low.

From these validations, it can be concluded that the both numerical models are suitable for the study of the wave penetration into Blankenberge marina. Thus it was determined that these models can be applied to the analysis of the wave penetration with the condition of 1000 year storm and 8m super storm.

3.7 Results and comparative analyses

3.7.1 Comparison Mike 21 BW and SWASH

In this section a comparison between SWASH model and Mike 21 BW model has been done.

The selected wave condition is a 1000 year storm condition with the directional spreading 15°. The hydrodynamic boundary conditions are summarized in Table 3-16.

Table 3-16: Hydrodynamic boundary conditions for the comparison between SWASH and Mike 21 BW

SWL [mTAW]	d_{max} [m]	H_{m0} [m]	T_p [s]	Direction [-]
+7.10	12.10	4.5	12.0	NNW

The K_d and the bathymetry contour plots are shown in Figure 3-67 and Figure 3-68 respectively. The comparison on the locations is shown in Figure 3-69 and the sections in Figure 3-70. The spectrum on the location is shown in Figure 3-71.

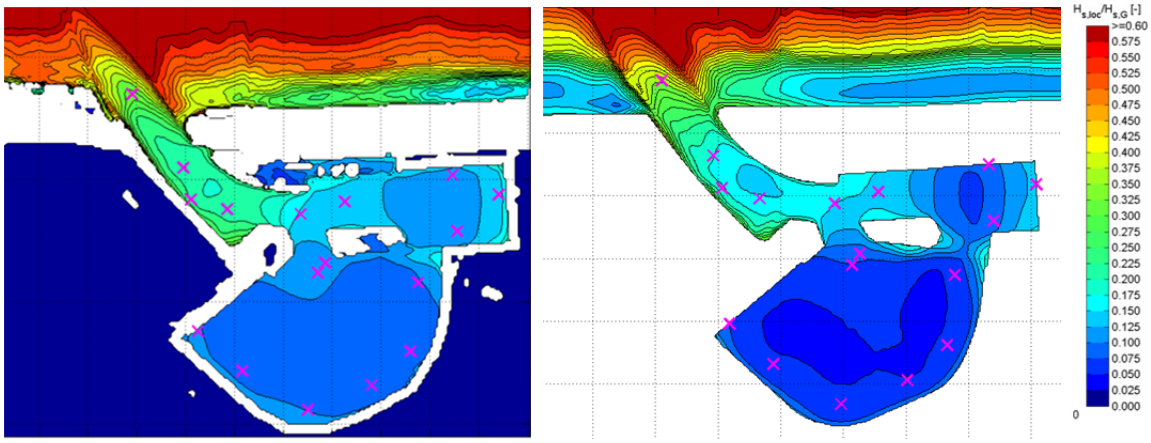

Figure 3-67: K_d contour plots for the SWASH model and the Mike 21 BW in the case of 1000 year storm condition with the directional spreading is 15 degree.

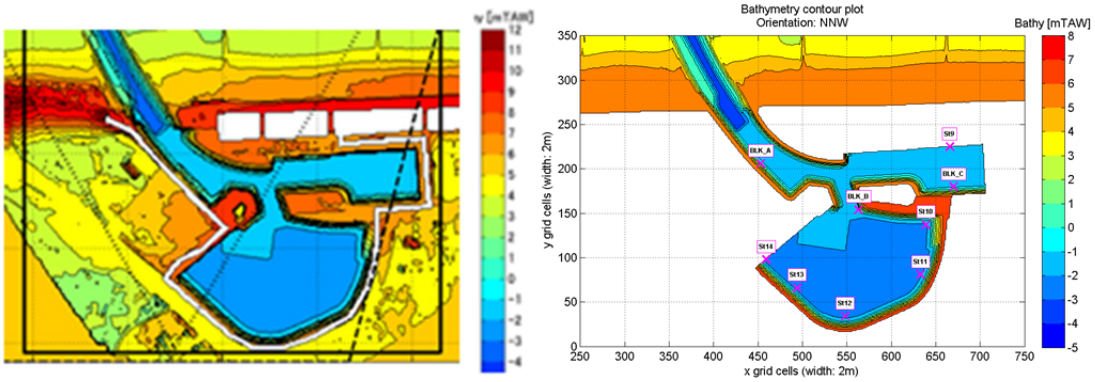

Figure 3-68: Bathymetry contour plots for the SWASH model and the Mike 21 BW.
(NB: The colour scale is different)

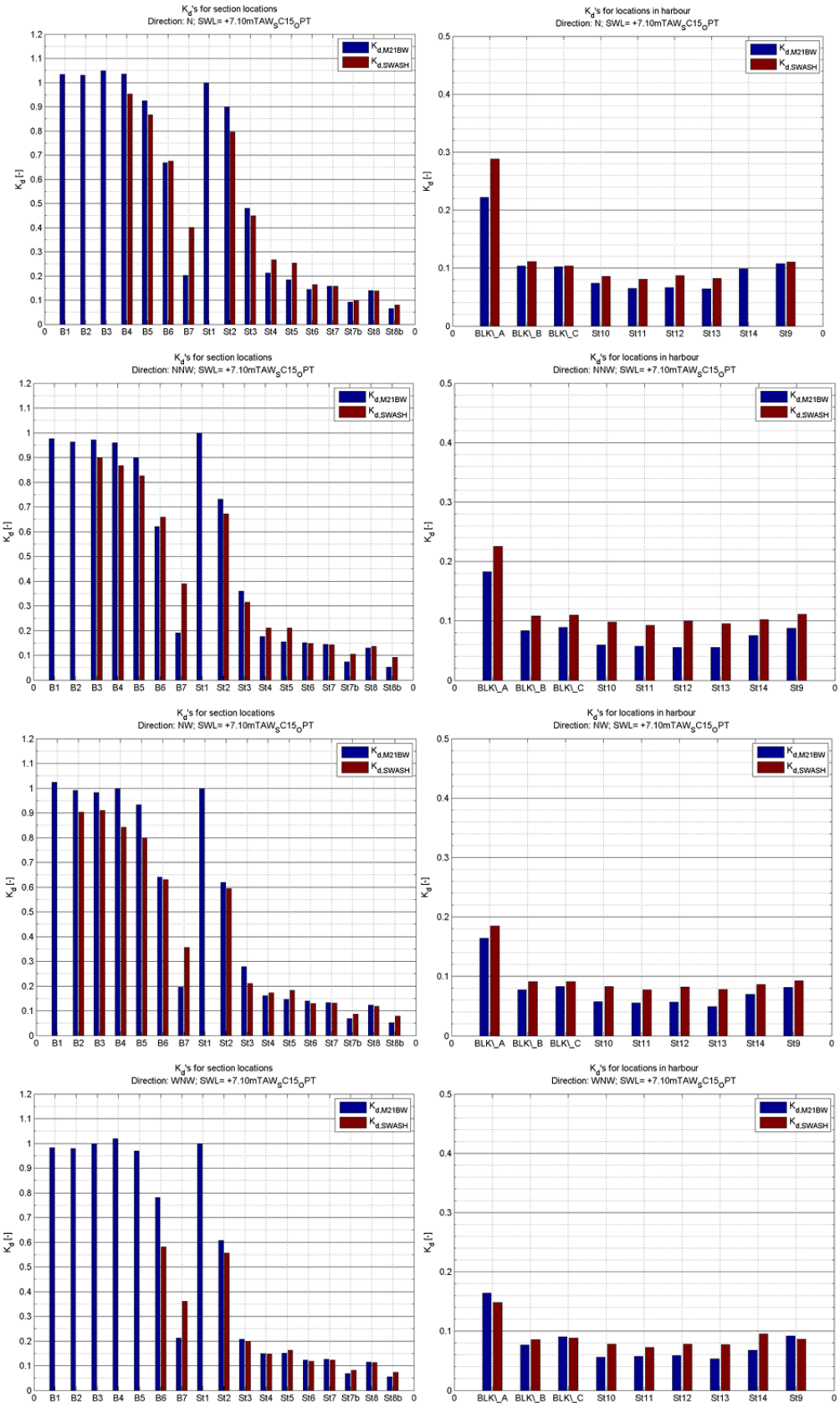

Figure 3-69: Comparison of K_d values between SWASH model and Mike 21 BW. Four directions (N,NNW,NW and WNW).

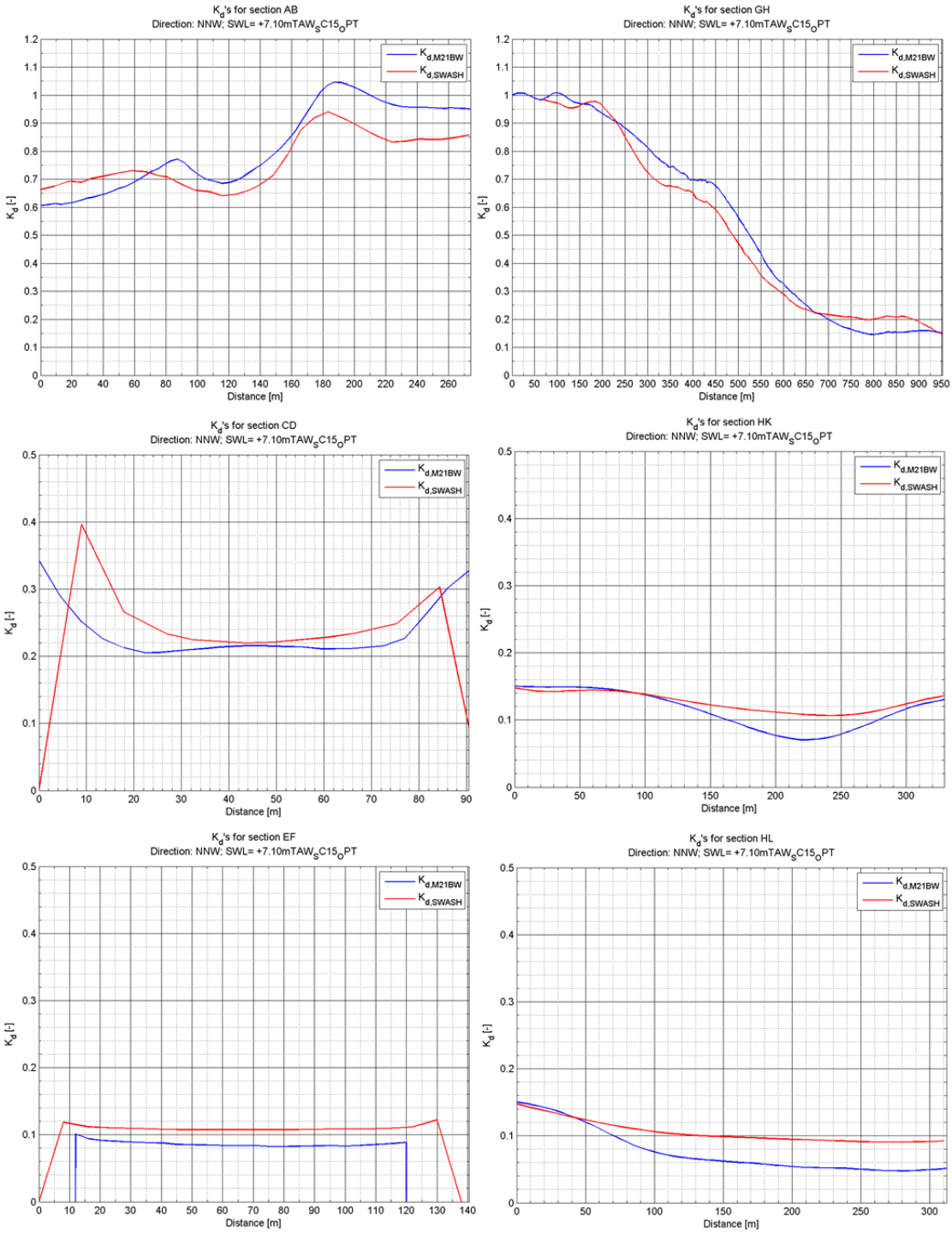

Figure 3-70: Comparison of K_d cross-sections (AB, CD, EF) and longitudinal sections (GH, HK, HL) between SWASH model and Mike 21 BW. For direction NNW.

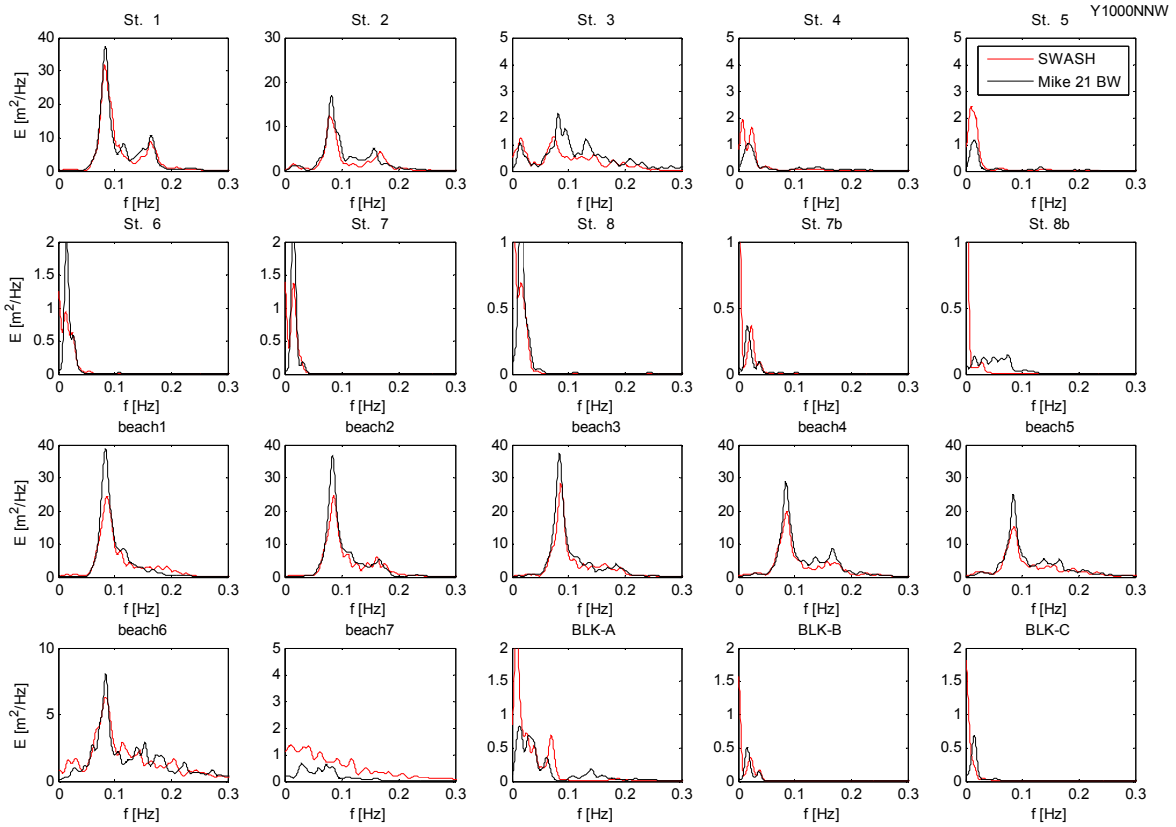

Figure 3-71: Comparison of wave spectrum between SWASH model and Mike 21 BW in the case of 1000 year storm condition with the directional spreading is 15 degree.

The comparison of the final models for the purpose of predicting the extreme wave climate in the harbour of Blankenberge in SWASH and Mike 21 BW shows that:

- The K_d-values of the SWASH model are slightly higher than the K_d-values of the Mike 21 BW model inside the marina. The higher K_d-value of the SWASH model could be explained by the differences of the generation of the long waves between the two models.

From the comparisons of both models and validation with the field measurements, it is recommended for the design of safety measures in the harbour to use the numerical results with care:

In favour of the SWASH model results is the fact that:

- SWASH uses the actual bathymetry since no minimum water depth is needed in the model.
- No sponge layers, additional bottom friction and low-pass filter were needed for numerical stability.

On the contrary:

- It is also possible that SWASH overestimates the generation of the long waves as it was seen in the validation with the field measurements;
- and the wave set-down is not correctly calculated in SWASH, since an offset based on the Mike 21 BW result has been applied.

Therefore it is wise to consider also the Mike 21 BW result since:

- The wave set-down is correctly calculated;
- The model behaviour is well known;
- The validation showed good results.

3.7.2 Resonance frequencies

Resonance happens when the resonance frequencies of (the docks in) the marina are excited. The resonance frequencies are determined by the geometry of the harbour. Usually these frequencies are in the lower range of frequencies or (very) long waves.

A practical method to determine the resonance frequencies of a harbour is described and successfully applied with Mike 21 BW[1] by Gierlevsen et al. (2001). A so called "White Noise" spectrum is made, which is a fictional spectrum with equal amounts of energy at all frequencies. A time series of surface elevations is made from this spectrum and imposed at the wave generation line. Only the waves with wave frequency around or equal to the resonance frequency will increase in energy. The peaks in the generated spectra in several locations in the harbour then provide the resonance frequencies of the marina. This is a very efficient and clear manner to determine the resonance frequencies of a random harbour geometry.

The "White Noise" spectrum for the white noise simulation for Blankenberge is made with equal amounts of energy at all frequencies between 0.001Hz-0.100Hz (= long wave frequency range). The resulting time series contains waves with a wave period between 10s and 1000s and all with the same wave height.

Table 3-17: Hydrodynamic boundary conditions of the "White Noise" simulation.

SWL [mTAW]	d_{max} [m]	H_{m0} [m]	T [s]	Direction [-]	Simulation duration	Mike 21 BW
+7.10	12.10	White Noise	10-1000	NNW	45min	X

The resulting wave spectra of locations BLK_A, BLK_B and BLK_C (i.e. field measurement locations, cf. Figure 3-11) are given in Figure 3-72. BLK_A is representative for the marina entrance area, BLK_B for the basin area and BLK_C for the yacht dock. In Table 3-18 the wave periods with the highest peaks in these spectra are given, they correspond with the resonance frequencies of the marina. Long waves with periods around 60s (=1min) and 600s (=10min) cause to most resonance in the harbour (highest peaks in the spectra). This is between 1min and 3min at the entrance area of the marina.

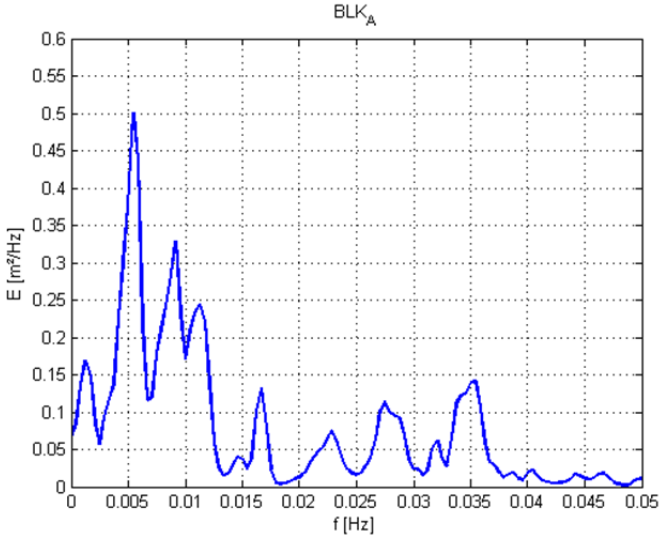

[1] The linear mild-slope wave model MILDwave, which was used in the previous harbour studies (Gruwez et al., 2011; Gruwez et al., 2012), is in theory also able to determine the resonance frequencies. However, during the analysis in this report, this was still being validated (Comm. Troch, 30/03/2012).

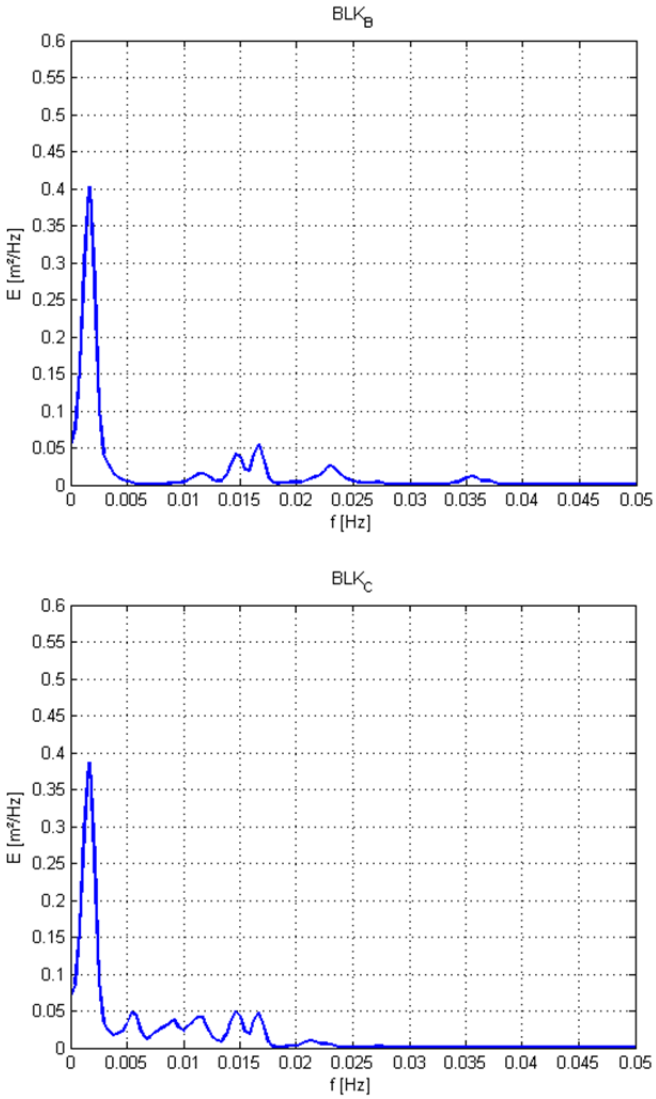

Figure 3-72: Spectra at locations BLK_A, BLK_B and BLK_C from the “White Noise” simulation.

Table 3-18: Wave periods around which resonance occurs in the marina of Blankenberge. Ordered according to importance, the first wave period causes the highest resonance.

Location [-]	Resonance periods [s]	Resonance period ranges [s]
BLK_A	185, 109, 89, 800, 28, 60, 36, 44	[80→200], [30→50]
BLK_B	600, 60, 69	[500→700], [60→70]
BLK_C	600, 69, 60, 185	[500→700], [80→200], [60→70]

The white noise simulation can only determine the resonance frequencies, but not whether or not long-period oscillations or resonance will actually develop under natural wave conditions. The wave period of the generated long waves are dependent on the offshore natural sea state. Long waves are generated by wave-wave interactions in shallow water and become free long waves where wave breaking occurs.

Next to and at the marina entrance very shallow water areas exist where long waves can be generated.

Because both models simulate the wave-wave-interactions inherently and also wave breaking is simulated, long waves will be generated and become free to excite some of the resonance frequencies determined here. The energy of long waves with wave period around these resonance frequencies will increase in the marina.

It is however possible that the offshore spectrum already contains energy in the long wave frequency range due to wave-wave interactions and wave breaking in shallow areas (e.g. offshore sand banks). This is not included in the JONSWAP spectrum which was imposed at the boundary of the final models, so it is possible that the long wave energy is underestimated.

3.7.3 Wave period

To investigate the evolution of the wave period into the harbour, the spectra of the points St1-8 along the longitudinal section (cf. Figure 3-8) are shown in Figure 3-73 for the wave conditions in Table 3-19.

Table 3-19: Hydrodynamic boundary conditions and wave penetration models for which the 1D spectra in output points St1-8 are investigated.

SWL [mTAW]	d_{max} [m]	H_{m0} [m]	T_p [s]	Direction [-]	SWASH	Mike 21 BW
+7.10	12.10	4.5	12.0	NNW	X	-

The evolution of the wave spectrum going into the harbour is such that energy is transferred to the lower frequencies (long wave generation due to wave-wave interactions) and the energy around the original peak frequency disappears (due to wave breaking and obstacles). On top of that, some lower frequencies are excited due to resonance in the harbour (cf. §3.7.2) causing the wave energy to increase for these lower frequencies.

In the entrance area the peak frequency is more or less the same as outside, but deeper into the harbour (yacht dock and basin) the lower frequencies dominate. It can be seen that the highest peaks correspond with some of the resonance frequencies determined in §3.7.2 (10min and 1min in case of St7 and St8, both located in the same dock as BLK_C).

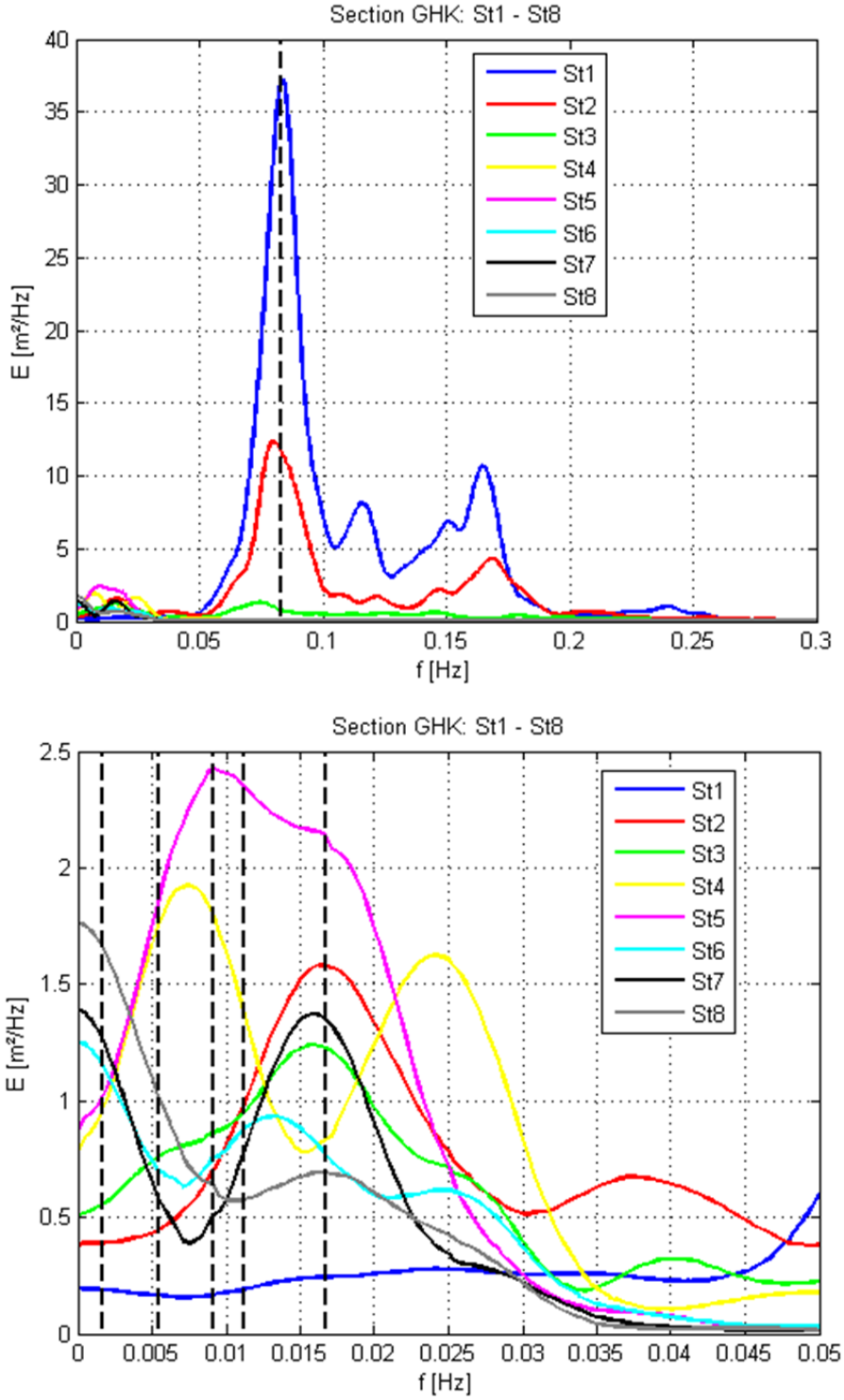

Figure 3-73: Wave spectra in locations St1 – St8, SWL = +7.10mTAW, NNW, SWASH result. Upper: complete spectrum with indication of the peak wave period 12.0s; lower: zoom to lower frequencies (long wave energy), including indication of the most important resonance frequencies from the white noise simulation.

3.7.4 Wave direction

Gruwez et al. (2011; 2012) describes three different ways to determine the wave direction from a phase-resolving wave model result. It appeared that only one method was practically applicable in the highly reflective environment of a harbour, namely looking at the perpendicular on the wave front of the first incoming wave (cf. Figure 3-74). The first incoming wave is considered, because otherwise the wave front is not discernible due to reflections in the harbour. Also the surface plot of the result with long crested waves is preferred because of a very clear wave front.

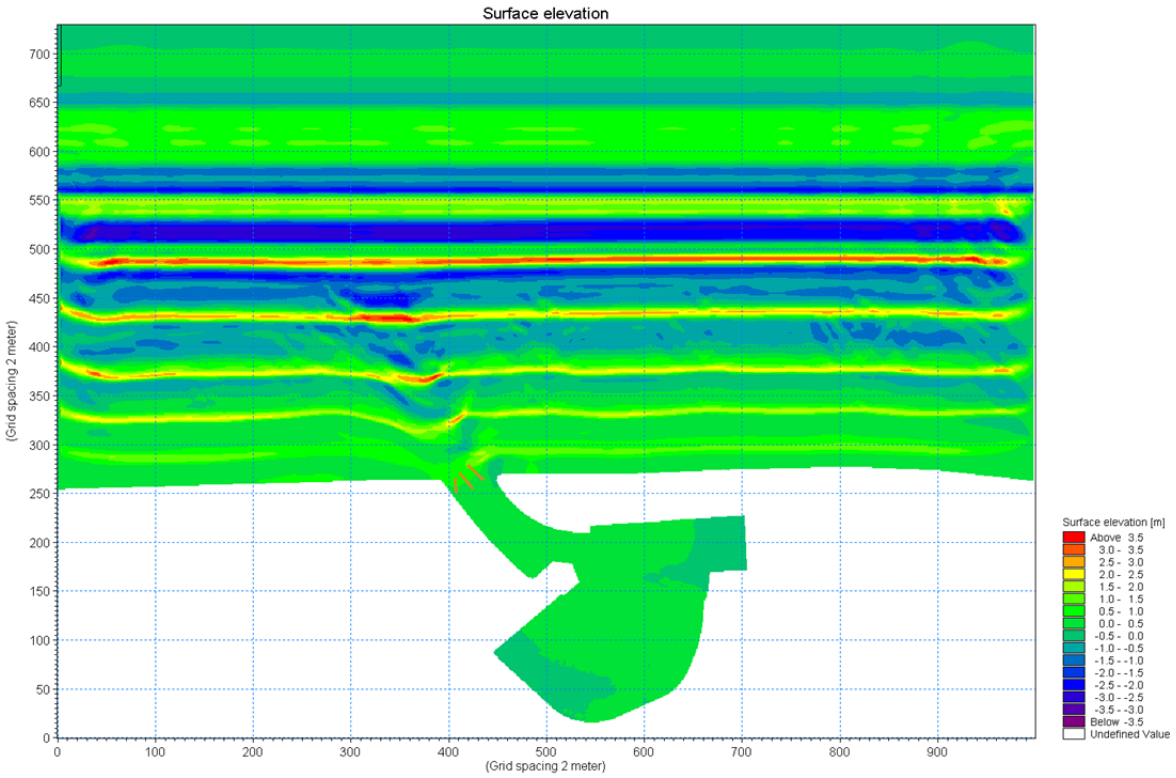

Figure 3-74: Example of a surface elevation plot where the wave front of the first incoming wave is visible (Mike 21 BW result with long crested waves). The red lines perpendicular to the wave front signify the wave direction.

This method is only useful for the short wave penetration at the entrance of the marina. Deeper into the marina (yacht dock and basin) only long wave energy remains. Because of the very large wave length of these waves (larger than the dimensions of the marina itself) no wave direction can be specified. These long waves have a very low wave steepness and the effect of the long waves is more like long oscillations or even an up and down movement of the complete water surface in the marina.

4 Local wind waves: phase-averaged wave modelling

4.1 Introduction

Locally generated waves determine the short (T<20.0s) wave climate in the areas of the marina where little or almost no wave penetration arrives. In §3.7.3 it was observed that the short wave penetration in the harbour is very limited in most of the marina where the boundary conditions are needed.

As discussed in §2 the phase-averaged model SWAN (TUDelft, 2010) is used for the modelling of the locally generated waves by extreme wind speeds. Gruwez et al. (2011; 2012) already showed that SWAN is suited for this purpose and the same methodology is applied here.

4.2 Bathymetry and calculation domain

4.2.1 Bathymetry

The bathymetry which was developed for the wave penetration model Mike 21 BW (SWL = +7.90mTAW) is used for the SWAN model (cf. Figure 4-1). For different water levels SWAN determines the new land boundary automatically (=land above SWL).

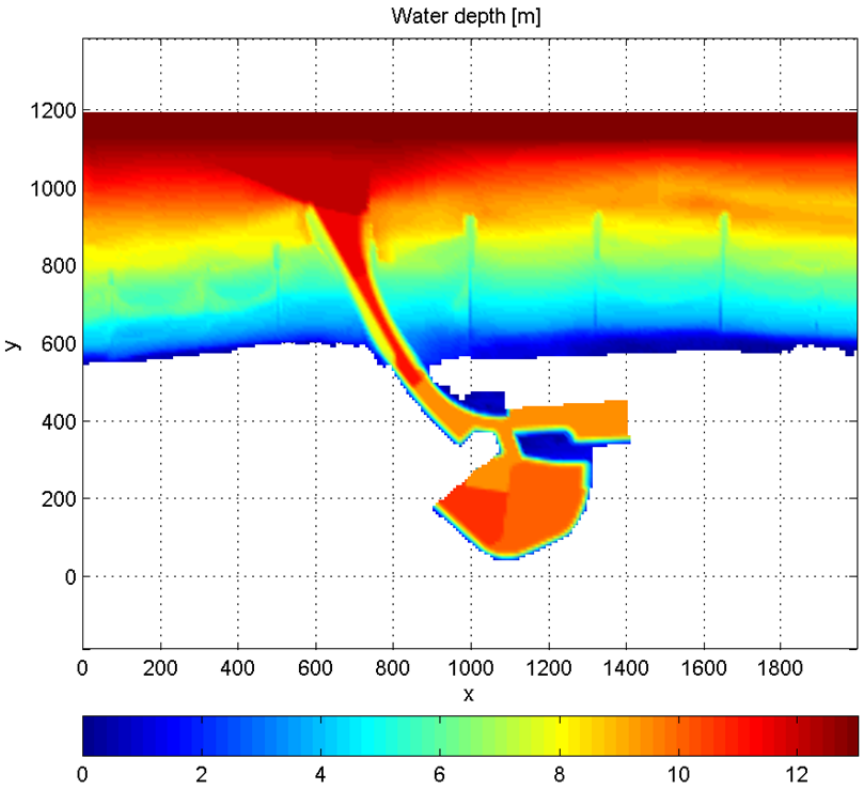

Figure 4-1: Water depth in the SWAN model for SWL +7.90mTAW.

4.2.2 Calculation domain

The calculation domain for the SWAN model is chosen to be the same as the wave penetration models oriented to NNW. This way the fetch length starts where the phase resolving wave modelling (i.e. without locally generated wind waves) starts.

4.3 Boundary conditions

4.3.1 Hydrodynamic boundary conditions

No incoming waves are imposed in the SWAN model. Waves are only allowed to exist by local generation due to the imposed wind speed and direction.

Because the marina of Blankenberge is close to the harbour of Zeebrugge, the same wind speeds for the 1000-year storm and super storms are used (Gruwez et al., 2012).

The wind speeds of the 1000-year storm are determined based on the statistics which were made for the 2-hour values in deep water (Technum et al., 2002). Two reduction factors are applied to these values: 0.9 to reduce the wind speed to 10m height above SWL (logarithmic profile) and 0.8 to take land effects into account (Gruwez et al., 2011). The resulting 1000-year wind speeds per wind direction are given in Table 4-1. For each wind direction a direction dependent still water level is given. They are based on those determined at Oostende but adapted according to the difference in spring tide between Oostende and Blankenberge (~0.10m).

Table 4-1: Boundary conditions for the SWAN simulations with only wind (RP = 1000 year)

Wind direction	SWL (incl. slr)	Wind speed	Wind speed (10m height)	Wind speed (land)
[-]	[m TAW]	[m/s]	[m/s]	[m/s]
NO	5.90	28.33	25.5	20.4
NNO	6.30	30.46	27.4	21.9
N	6.90	30.57	27.5	22.0
NNW	6.90	30.77	27.7	22.2
NW	6.90	29.98	27.0	24.3
WNW	6.80	33.43	30.1	24.1
W	6.60	35.53	32.0	25.6

The wind speeds of the super storms defined by Verwaest et al. (2008) are also modelled. These values were already reduced to 10m height above SWL, but the reduction factor of 0.8 due to land effects still has to be applied. The modified values are given in Table 4-2. These wind speeds belong to the wind direction of -33.75°N (average of NW and NNW) (Verwaest et al., 2008). Nevertheless, all wind directions[2] are modelled for each water level and corresponding wind speeds, like in Table 4-1, to be able to determine the worst direction.

[2] Remark: because the wind speeds of Verwaest et al. (2008) are direction dependent (for direction -33.75°), it is possible that they are an under- or overprediction for the other directions. Wind speeds of direction W are for example larger for the same return period.

Table 4-2: boundary conditions of the SWAN simulations with only wind for the water levels and wind speeds of the super storm defined by Verwaest et al. (2008)

SWL	**Wind speed (10m heigth)**	**Wind speed (land) NE, NNE, N, NNW, NW WNW, W**
[m TAW]	[m/s]	[m/s]
+6.40	25.6	20.5
+6.90	29.1	23.3
+7.40	32.6	26.1
+7.90	36.1	28.9

4.3.2 Structures

Structures such as breakwaters, quay walls and steep slopes of dikes are modelled in SWAN as obstacles with a certain transmission and reflection coefficient. Because only the incoming wave height is of interest in the results it was chosen not to include obstacles to model the structures. Not including obstacles causes the land boundary to be completely absorbing and no reflection is taken into account.

4.4 Numerical settings

The input file with all numerical settings is given in Annex 2 for water level +7.90mTAW.

A rectangular grid is applied with cell dimensions 7.5m x 7.5m. To be able to model the very short wind waves (T = 1.0s to 3.0s) the frequency range is chosen to include the higher frequencies: i.e. 0.05Hz – 2.49Hz.

4.5 Results

SWAN simulations are performed with all the boundary conditions from §4.3.1 resulting in 35 modelled cases.

An example of a result of the SWAN model is given in Figure 4-2 and Figure 4-3.

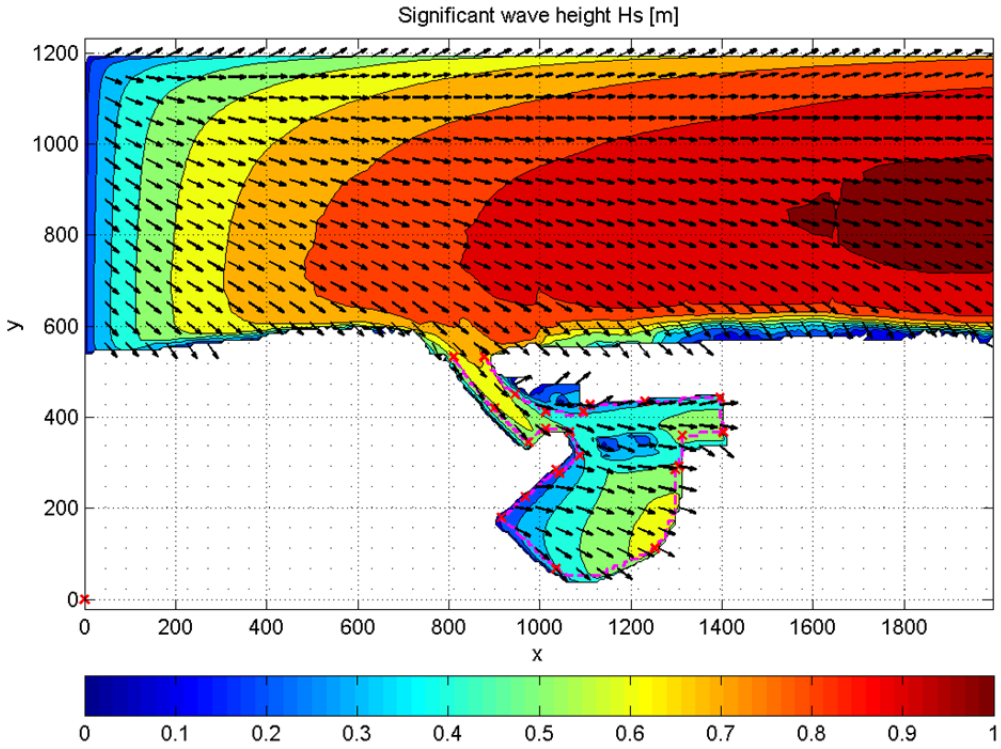

Figure 4-2: Contour plot of the significant wave height Hs [m] of the locally generated wind waves in the marina of Blankenberge. Result of a super storm with SWL = +7.90mTAW and wind direction W. The black arrows indicate the mean wave direction. The magenta coloured slash-slash line is the output section and the red crosses indicate the boundaries of each section.

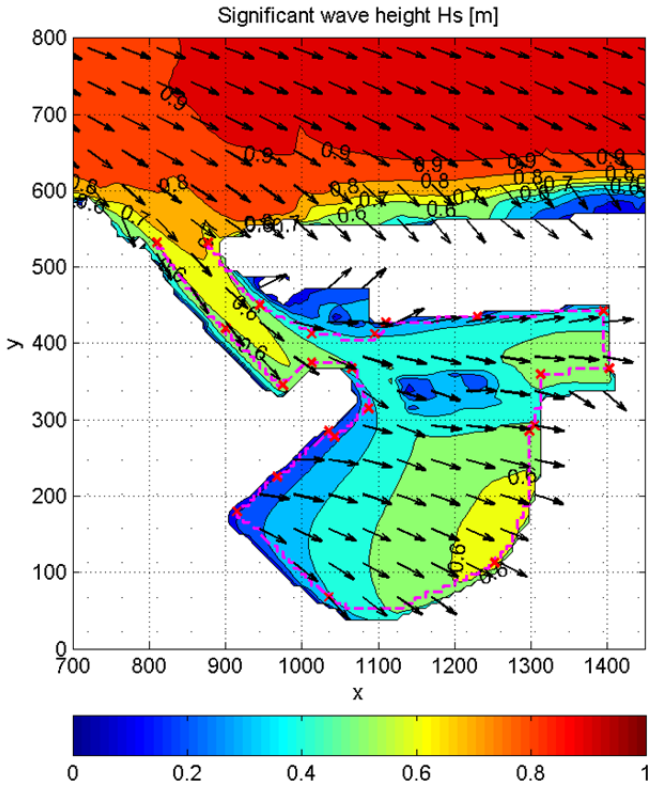

Figure 4-3: Same as Figure 4-2, but zoom to the marina.

The minimum and maximum H_{m0} is determined in each zone along the complete boundary of the marina (cf. Figure 5-4). The maximum $H_{m0,min}$ and $H_{m0,max}$ SWAN result for all directions is given in Table 4-3 for the 1000-year storm and in Table 4-4 and Table 4-5 for the super storms. The direction dependent results are also made available on the digital CD-rom. Also the most disadvantageous (i.e. most perpendicular to the structure) wave direction occurring for all wind directions is given.

Table 4-3: Minimum and maximum significant wave height Hs from the SWAN model for each zone and for the highest result of all wind directions. (RP = 1000yrs)

	RP = 1000j		Wave direction
Zone	min. Hs	max. Hs	
[-]	[m]	[m]	[°perpendicular]
1	0.39	0.54	0
2	0.40	0.45	0
3	0.44	0.49	0
4	0.42	0.47	0
5	0.28	0.42	0
6	0.25	0.29	60
7	0.26	0.28	60
8	0.21	0.31	60
9	0.22	0.33	60
10	0.32	0.41	0
11	0.35	0.52	0
12	0.39	0.52	0
13	0.35	0.39	0
14	0.10	0.38	0
15	0.38	0.44	0
16	0.35	0.44	0
17	0.27	0.35	80
18	0.17	0.29	80
19	0.20	0.37	80
20	0.33	0.40	80
21	0.36	0.46	80
22	0.41	0.55	80

Table 4-4: Minimum and maximum significant wave height Hs from the SWAN model for each zone and for the highest result of all wind directions. (+6.40mTAW and +6.90mTAW super storms)

	SWL = +6.40mTAW		SWL = +6.90mTAW		Wave direction
Zone	min. Hs	max. Hs	min. Hs	max. Hs	
[-]	[m]	[m]	[m]	[m]	[°perpendicular]
1	0.33	0.48	0.42	0.60	0
2	0.33	0.37	0.40	0.46	0
3	0.36	0.38	0.43	0.46	0
4	0.31	0.36	0.37	0.43	0
5	0.27	0.31	0.33	0.37	0

6	0.26	0.30	0.33	0.36	60
7	0.26	0.29	0.32	0.35	60
8	0.21	0.31	0.25	0.38	60
9	0.22	0.33	0.26	0.40	60
10	0.32	0.37	0.39	0.46	0
11	0.31	0.37	0.38	0.45	0
12	0.28	0.38	0.34	0.45	0
13	0.26	0.28	0.31	0.34	0
14	0.00	0.28	0.10	0.33	0
15	0.28	0.31	0.33	0.38	0
16	0.25	0.32	0.30	0.38	0
17	0.19	0.25	0.23	0.30	80
18	0.17	0.24	0.21	0.29	80
19	0.20	0.29	0.24	0.34	80
20	0.24	0.29	0.30	0.36	80
21	0.26	0.34	0.33	0.41	80
22	0.30	0.42	0.37	0.52	80

Table 4-5: Minimum and maximum significant wave height Hs from the SWAN model for each zone and for the highest result of all wind directions. (+7.40mTAW and +7.90mTAW super storms)

	SWL = +7.40mTAW		**SWL = +7.90mTAW**		**Wave direction**
Zone	**min. Hs**	**max. Hs**	**min. Hs**	**max. Hs**	
[-]	**[m]**	**[m]**	**[m]**	**[m]**	**[°perpendicular]**
1	0.51	0.73	0.61	0.87	0
2	0.47	0.54	0.56	0.64	0
3	0.50	0.54	0.58	0.62	0
4	0.43	0.50	0.50	0.58	0
5	0.39	0.43	0.46	0.50	0
6	0.39	0.44	0.47	0.53	60
7	0.38	0.43	0.46	0.51	60
8	0.30	0.46	0.35	0.54	60
9	0.31	0.48	0.36	0.57	60
10	0.47	0.55	0.56	0.65	0
11	0.47	0.54	0.58	0.65	0
12	0.43	0.54	0.54	0.64	0
13	0.41	0.43	0.53	0.54	0
14	0.31	0.41	0.45	0.53	0
15	0.41	0.44	0.52	0.53	0
16	0.35	0.45	0.44	0.53	0
17	0.27	0.35	0.32	0.44	80
18	0.25	0.34	0.29	0.40	80
19	0.29	0.38	0.34	0.45	80

20	0.31	0.42	0.39	0.47	80
21	0.38	0.50	0.43	0.56	80
22	0.45	0.66	0.51	0.82	80

Due to the small available fetch lengths inside the marina, the locally wind generated significant wave heights are relatively low (H_{m0} = ~0.50m). But because the short wave penetration is very low or even negligible for the yacht dock and basin (not marina entrance), these local wind waves become important in the total extreme wave climate (cf. §5).

The average wave period $T_{m-1,0}$ of these wind waves varies between 0.50s and 2.50s for the complete marina.

4.6 Conclusions

A SWAN model was made of the marina of Blankenberge to model the local generation of waves by extreme wind speeds. No reflection of the structures in the harbour is modelled to obtain only the incoming wave height necessary for the design of the storm retaining walls. In total 35 simulations were performed providing the results for all direction dependent 1000-year and super storm wind speeds.

The result is a rather low significant wave height (H_{m0} order of magnitude ~0.50m) due to the limited available fetch lengths inside the marina. The minimum and maximum values per defined quay wall zone are available on the CD-rom for each modelled wind direction.

The average wave period $T_{m-1,0}$ of these wind waves varies between 0.50s and 2.50s for the complete marina.

5 Superposition wave penetration and local wind waves

5.1 Method

The simulation of wave penetration and locally generated waves was decoupled. To obtain the total wave climate in the harbour both components are brought back together by using the superposition method proposed by van der Meer et al. (2002):

$$H_{m0} = \sqrt{H_{m0,1}^2 + H_{m0,2}^2}$$

With H_{m0} the significant wave height including wave penetration and local wind waves [m]
$H_{m0,1}$ the significant wave height of the wave penetration models SWASH or Mike 21 BW [m]
$H_{m0,2}$ The locally generated significant wave height generated by the extreme wind speed (SWAN result) [m]

In the spectra of the wave penetration models (cf. Annex 5) a significant part of the total wave energy can be found at low frequencies corresponding to generated long wave energy (non-linear wave-wave interactions) and resonance (cf. §3.7.2). This is particularly the case deeper into the marina, in the tidal docks (yachting dock and basin).

This low frequency wave energy contains waves with very high wave periods (approximately 600s and 60s, cf. §3.7.2 and §3.7.3) and therefore very long wave lengths (respectively 5550m and 550m) which are even larger than the dimensions of the marina and/or considered dock (order of magnitude: 300m-400m). The long wave energy therefore causes a slow up and down movement of the complete water body of the marina/dock. Because this kind of long wave energy is usually treated separately from the short wave energy in the design, the long wave energy is separated from the short wave energy. A separation period of 30s was chosen[3]: T>30s for long wave energy and T<30s for short wave energy (e.g. Figure 5-1).

Based on the short wave energy the significant wave height of the short waves $H_{m0,hf}$ is determined. This wave height is combined with the wave height of the locally generated wind waves (SWAN result) using the previously explained superposition method of van der Meer et al. (2002). Based on the long wave energy and the wave setup the maximum surface elevation is determined. This is done by applying a 30s moving average filter to the time series (cf. Figure 5-2) in each point along the complete boundary inside the harbour. The result is the maximum surface elevation due to long waves including the wave setup. This value can then be used to increase the still water level in the design[4].

[3] To compare: Van Gent and Giarrusso (2005) used T=25s as the separation period.
[4] Keep in mind though that the maximum surface elevation due to long waves is only temporary (dependent on the wave period) and using this value to increase the still water level could therefore be too conservative for some design cases. The wave setup part on the other hand is constant during the complete storm and should always be taken into account.

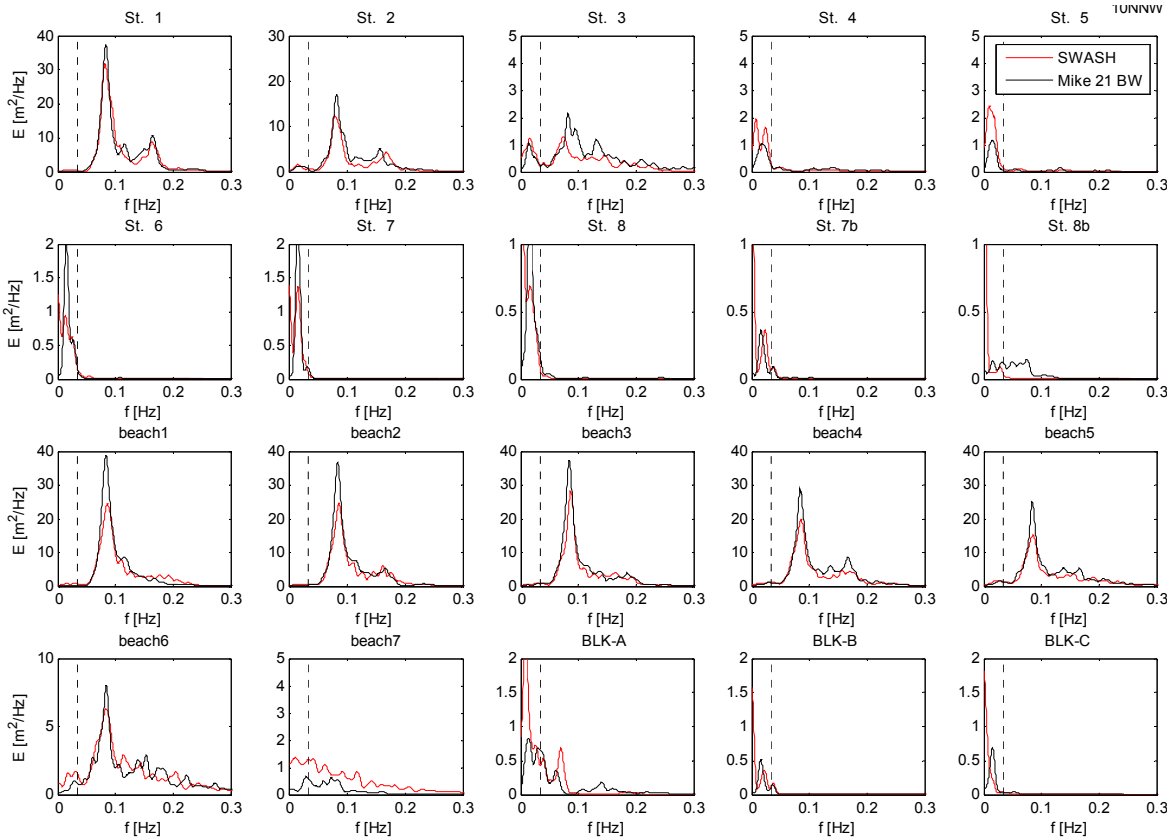

Figure 5-1: Wave spectra in some points outside and inside the marina. With indication of the separation frequency (=1/30s).

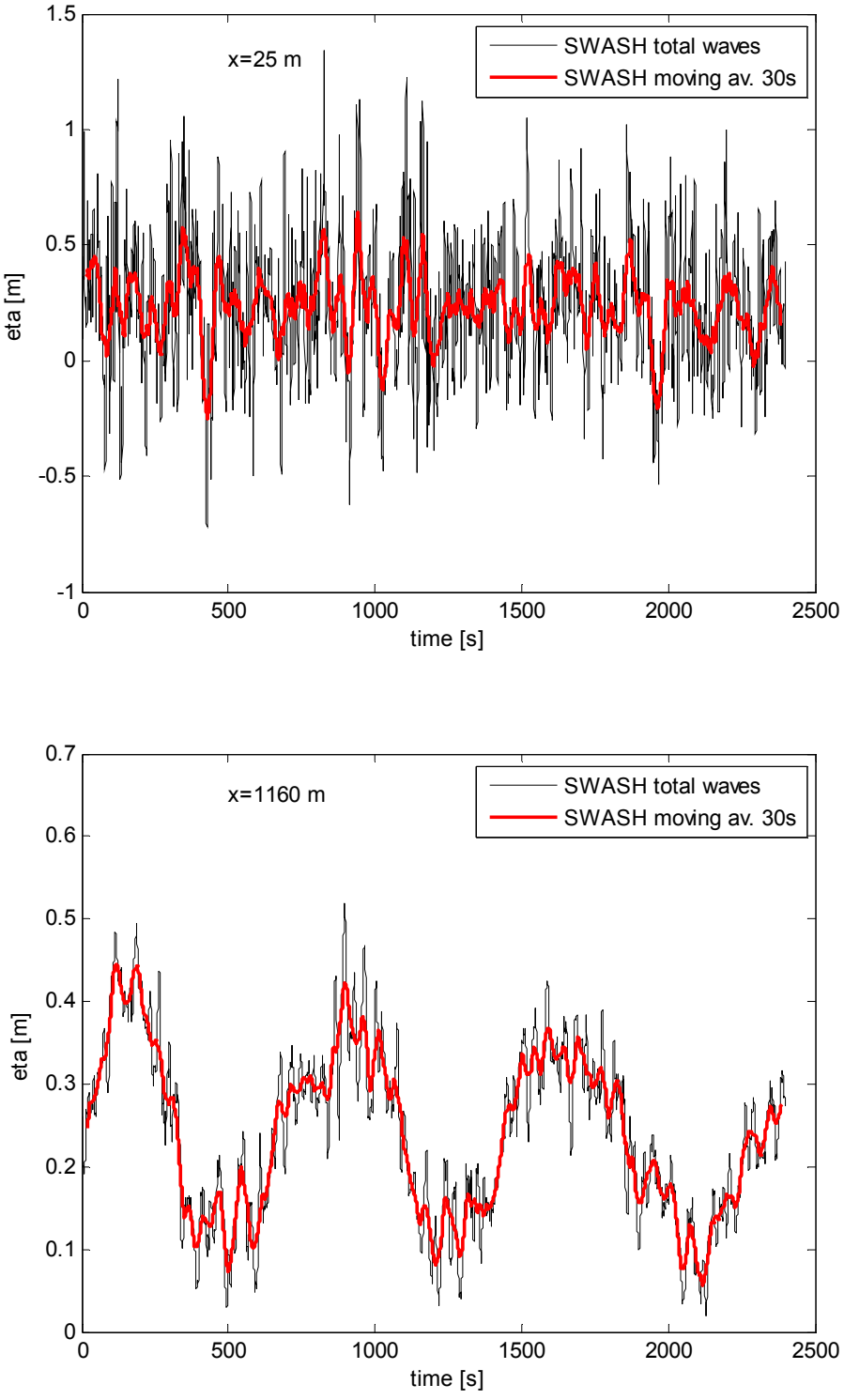

Figure 5-2: Time series and 30s moving average filtered time series of a location at the entrance (upper figure) and in the marina (the old “Spuikom”, lower figure).

5.2 Results per quay wall zone

An overview of the results is given along the complete boundary of the marina. The boundary (cf. Figure 5-3) is divided in 22 quay zones for which the hydrodynamic boundary conditions are determined. The zones are defined in Figure 5-4.

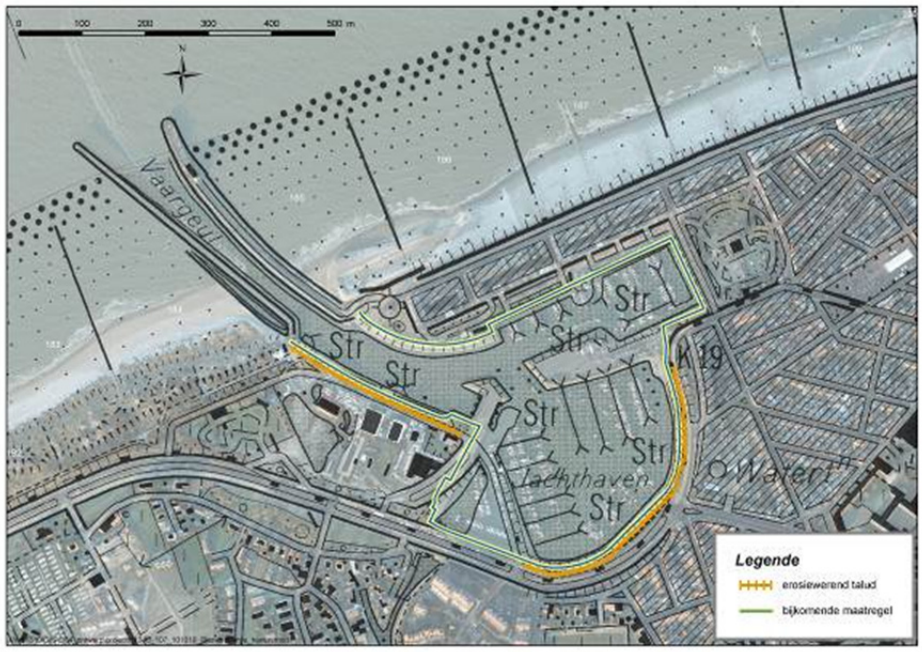

Figure 5-3: Trajectory of existing or planned storm retaining walls along the boundary of the marina of Blankenberge (Coastal Division, 2011).

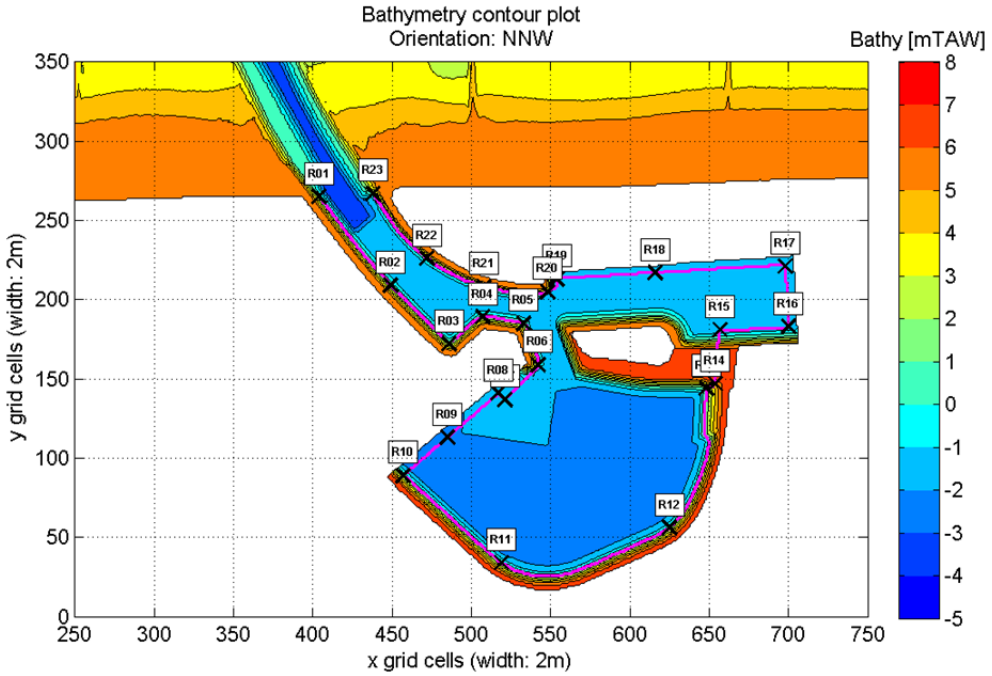

Figure 5-4: Zoom of the bathymetry (from Mike 21BW and SWL=+7.10mTAW) of the marina of Blankenberge with indication of the section along which results are extracted. Division of the marina boundary into different quay wall zones for which the hydrodynamic boundary conditions are determined (e.g. zone 11 is between points R11 and R12).

As discussed in §5.1 the results are given for the short wave and long wave energy separately.

For the short wave energy part of the spectrum:

The minimum and maximum significant wave height is given for each quay wall zone (cf. Figure 5-4) of each wave penetration model separately (only short wave energy, T<30s) and superposed together with the SWAN result.

The overview tables are limited to the 1000-year water level +7.10mTAW (cf. Table 5-1 and Table 5-2) and the +7.90mTAW super storm (cf. Table 5-3). The result from the wave penetration models for the +7.90mTAW storm is limited to wave direction NNW, because not all wave directions were modelled. For wave direction NNW the highest wave penetration was found (cf. §3.5.3) for zones along the boundary for which presently boundary conditions are needed. For the eastern (i.e. zones 20-22) and western dikes (i.e. zones 1-4) at the entrance of the marina, other offshore wave directions can give higher (primarily direction N, cf. §3.5.3) wave heights, so for these zones the values in the overview of +7.90mTAW are an underestimation. For 1000-year conditions also a table overview is made based on maxima of all directions (cf. Table 5-2). This is possible because all directions were modelled for the 1000-year storm.

The results of the locally generated waves however are available for all wind directions and super storm water levels. The maximum and minimum values given in the tables are therefore of all directions. The results for each wind direction separately are also available on the included CD-ROM.

The superposition for each zone is done by combining the minima and maxima of each type of model. This gives a conservative value for the maxima but not necessarily for the minima, because the location of the maxima and minima of the wave penetration and local wind waves do not occur at the same locations within the considered zone (Comm. Monbaliu, 2011).

The tables also include an estimation of the direction of the incoming waves for each zone. The wave directions are given relative to the perpendicular of the considered quay zone.

It is however discouraged to use the values directly from these tables as boundary conditions for the design. An expert judgement is still needed for each zone to determine the wave conditions for the design.

For the long wave energy part of the spectrum:

The minimum (η_{min}) and maximum (η_{max}) value along each zone of the maximum surface elevation due to long waves and wave setup in each point of the zone is given. This value can be used to increase the still water level in design formulas.

Note: It is important to keep in mind that the increase of the water level due to long waves is not constant in time, but oscillates. In the tables the maximum increase of water level is given. This could be too conservative in some design cases.

Table 5-1: Overview of the minimum and maximum significant wave heights along the defined zones in the marina. SWAN (all directions), SWASH (NNW) and Mike 21BW (NNW) results. Superposition of SWASH and SWAN and of Mike 21BW and SWAN. 1000-year storm.

T1000	SWAN		SWASH		SWASH		SWASH & SWAN		Mike 21BW		Mike 21BW		Mike 21BW & SWAN		
			Short waves (T < 30s)		Long waves (T > 30s)		Short waves (T < 30s)		Short waves (T < 30s)		Long waves (T > 30s)				
Direction	All directions		NNW		NNW				NNW		NNW				
Return period [year]	1000		1000		1000				1000		1000				
Water level [m TAW]	~6.9		7.1		7.1				7.1		7.1				
Hm0,inc [m]	0.00		4.50		4.50				4.50		4.50				
Tp [s]	-		12.0		12.0				12.0		12.0				
	min	max	σ = 15°		σ = 15°				σ = 15°		σ = 15°				
generated $T_{m-1,0}$ [s]	0.50	2.00													
															Wave direction
Quay zone	Hs,min [m]	Hs,max [m]	Hs,min [m]	Hs,max [m]	ηmin [m]	ηmax [m]	Hs,min [m]	Hs,max [m]	Hs,min [m]	Hs,max [m]	ηmin [m]	ηmax [m]	Hs,min [m]	Hs,max [m]	[°perpendicular]
1	0.39	0.54	0.57	1.07	0.51	0.57	0.69	1.20	0.68	1.69	0.25	0.31	0.78	1.77	0
2	0.40	0.45	0.50	0.61	0.54	0.64	0.64	0.76	0.65	1.12	0.29	0.33	0.76	1.20	0
3	0.44	0.49	0.29	0.63	0.58	0.64	0.53	0.80	0.44	1.16	0.26	0.35	0.62	1.26	0
4	0.42	0.47	0.26	0.30	0.49	0.58	0.49	0.56	0.38	0.63	0.23	0.26	0.56	0.79	0
5	0.28	0.42	0.19	0.27	0.40	0.48	0.34	0.50	0.22	0.53	0.13	0.24	0.35	0.67	0
6	0.25	0.29	0.11	0.23	0.34	0.40	0.27	0.37	0.17	0.22	0.10	0.13	0.30	0.36	60
7	0.26	0.28	0.12	0.14	0.34	0.35	0.28	0.32	0.20	0.21	0.10	0.10	0.32	0.35	60
8	0.21	0.31	0.10	0.14	0.34	0.35	0.23	0.34	0.18	0.23	0.10	0.12	0.27	0.38	60
9	0.22	0.33	0.08	0.12	0.33	0.35	0.23	0.35	0.15	0.28	0.12	0.13	0.26	0.43	60
10	0.32	0.41	0.09	0.14	0.33	0.35	0.33	0.43	0.21	0.40	0.12	0.14	0.38	0.57	0
11	0.35	0.52	0.08	0.16	0.34	0.36	0.36	0.54	0.17	0.39	0.11	0.12	0.39	0.65	0
12	0.39	0.52	0.07	0.14	0.34	0.35	0.39	0.54	0.15	0.24	0.10	0.12	0.41	0.57	0
13	0.35	0.39	0.09	0.12	0.35	0.36	0.36	0.40	0.18	0.19	0.12	0.13	0.39	0.43	0
14	0.10	0.38	0.09	0.27	0.34	0.37	0.13	0.47	0.22	0.30	0.14	0.18	0.24	0.48	0
15	0.38	0.44	0.05	0.09	0.36	0.44	0.39	0.44	0.18	0.25	0.18	0.28	0.42	0.50	0
16	0.35	0.44	0.06	0.08	0.44	0.45	0.35	0.44	0.17	0.25	0.26	0.28	0.39	0.50	0
17	0.27	0.35	0.08	0.12	0.36	0.45	0.28	0.37	0.16	0.22	0.15	0.26	0.31	0.41	80
18	0.17	0.29	0.10	0.15	0.39	0.46	0.20	0.33	0.19	0.23	0.16	0.24	0.25	0.37	80
19	0.20	0.37	0.14	0.25	0.47	0.48	0.25	0.44	0.21	0.23	0.23	0.24	0.29	0.43	80
20	0.33	0.40	0.25	0.37	0.48	0.58	0.42	0.55	0.25	0.35	0.24	0.26	0.42	0.53	80
21	0.36	0.46	0.32	0.56	0.54	0.61	0.48	0.72	0.33	0.45	0.26	0.29	0.49	0.64	80
22	0.41	0.55	0.40	1.18	0.53	0.57	0.57	1.30	0.45	0.85	0.23	0.29	0.61	1.02	80

Table 5-2: Overview of the minimum and maximum significant wave heights along the defined zones in the marina. SWAN (all directions), SWASH (all directions) and Mike 21BW (all directions) results. Superposition of SWASH and SWAN and of Mike 21BW and SWAN. 1000-year storm.

T1000	SWAN		SWASH		SWASH		SWASH & SWAN		Mike 21BW		Mike 21BW		Mike 21BW & SWAN		
			Short waves (T < 30s)		Long waves (T > 30s)		Short waves (T < 30s)		Short waves (T < 30s)		Long waves (T > 30s)				
Direction	All directions		All directions		All directions				All directions		All directions				
Return period [year]	1000		1000		1000				1000		1000				
Water level [m TAW]	~6.9		7.1		7.1				7.1		7.1				
Hm0,inc [m]	0.00		4.50		4.50				4.50		4.50				
Tp [s]	-		12.0		12.0				12.0		12.0				
	min	max	σ = 15°		σ = 15°				σ = 15°		σ = 15°				
generated $T_{m-1,0}$ [s]	0.50	2.50													
															Wave direction
Quay zone	Hs,min [m]	Hs,max [m]	Hs,min [m]	Hs,max [m]	ηmin [m]	ηmax [m]	Hs,min [m]	Hs,max [m]	Hs,min [m]	Hs,max [m]	ηmin [m]	ηmax [m]	Hs,min [m]	Hs,max [m]	[°perpendicular]
1	0.39	0.54	0.71	1.18	0.51	0.73	0.81	1.30	0.77	1.96	0.31	0.37	0.86	2.03	0
2	0.40	0.45	0.50	0.75	0.71	0.79	0.64	0.88	0.70	1.22	0.37	0.41	0.80	1.30	0
3	0.44	0.49	0.38	0.69	0.61	0.73	0.58	0.84	0.47	1.26	0.38	0.43	0.64	1.36	0
4	0.42	0.47	0.26	0.38	0.49	0.61	0.49	0.61	0.41	0.72	0.36	0.39	0.58	0.86	0
5	0.28	0.42	0.21	0.27	0.40	0.48	0.35	0.50	0.24	0.58	0.15	0.36	0.37	0.72	0
6	0.25	0.29	0.12	0.30	0.34	0.40	0.28	0.42	0.20	0.24	0.16	0.19	0.32	0.38	60
7	0.26	0.28	0.46	0.71	0.34	0.35	0.52	0.77	0.21	0.23	0.16	0.16	0.33	0.36	60
8	0.21	0.31	0.12	0.44	0.34	0.35	0.24	0.54	0.20	0.25	0.15	0.16	0.29	0.40	60
9	0.22	0.33	0.08	0.20	0.33	0.35	0.23	0.38	0.17	0.28	0.15	0.15	0.27	0.43	60
10	0.32	0.41	0.09	0.14	0.33	0.35	0.33	0.43	0.21	0.40	0.15	0.15	0.38	0.57	0
11	0.35	0.52	0.08	0.16	0.34	0.36	0.36	0.54	0.17	0.39	0.15	0.15	0.39	0.65	0
12	0.39	0.52	0.10	0.14	0.34	0.35	0.40	0.54	0.15	0.28	0.14	0.15	0.41	0.59	0
13	0.35	0.39	0.12	0.18	0.35	0.36	0.37	0.42	0.21	0.22	0.15	0.16	0.41	0.44	0
14	0.10	0.38	0.09	0.27	0.34	0.37	0.13	0.47	0.22	0.30	0.16	0.19	0.24	0.48	0
15	0.38	0.44	0.05	0.09	0.36	0.44	0.39	0.44	0.19	0.33	0.19	0.28	0.43	0.55	0
16	0.35	0.44	0.06	0.08	0.44	0.45	0.35	0.44	0.17	0.33	0.26	0.28	0.39	0.55	0
17	0.27	0.35	0.08	0.13	0.36	0.45	0.28	0.37	0.18	0.24	0.18	0.27	0.32	0.42	80
18	0.17	0.29	0.10	0.17	0.39	0.46	0.20	0.34	0.20	0.28	0.18	0.26	0.26	0.40	80
19	0.20	0.37	0.15	0.25	0.47	0.48	0.25	0.44	0.25	0.28	0.26	0.26	0.32	0.46	80
20	0.33	0.40	0.25	0.52	0.48	0.59	0.42	0.65	0.30	0.38	0.27	0.30	0.45	0.55	80
21	0.36	0.46	0.46	0.77	0.59	0.78	0.58	0.89	0.38	0.49	0.30	0.38	0.52	0.67	80
22	0.41	0.55	0.55	1.79	0.53	0.75	0.68	1.87	0.49	0.96	0.31	0.38	0.64	1.11	80

Table 5-3: Overview of the minimum and maximum significant wave heights along the defined zones in the marina. SWAN (all directions), SWASH (NNW) and Mike 21BW (NNW) results. Superposition of SWASH and SWAN and of Mike 21BW and SWAN. +7.90mTAW super storm.

+7.90m TAW	SWAN		SWASH		SWASH		SWASH & SWAN		Mike 21BW		Mike 21BW		Mike 21BW & SWAN		
			Short waves (T < 30s)		Long waves (T > 30s)				Short waves (T < 30s)		Long waves (T > 30s)				
Direction	**All directions**		**NNW**		**NNW**				**NNW**		**NNW**				
Return period [year]	-		-		-				-		-				
Water level [m TAW]	7.90		7.90		7.90				7.90		7.90				
Hm0,inc [m]	0.00		5.00		5.00				5.00		5.00				
Tp [s]	-		12.0		12.0				12.0		12.0				
	min	**max**	σ = 15°		σ = 15°				σ = 15°		σ = 15°				
gegenereerde $T_{m-1,0}$ [s]	0.50	2.50													
															Wave direction
Quay zone	**Hs,min [m]**	**Hs,max [m]**	**Hs,min [m]**	**Hs,max [m]**	**ηmin [m]**	**ηmax [m]**	**Hs,min [m]**	**Hs,max [m]**	**Hs,min [m]**	**Hs,max [m]**	**ηmin [m]**	**ηmax [m]**	**Hs,min [m]**	**Hs,max [m]**	**[°perpendicular]**
1	0.61	0.87	0.92	1.51	0.62	0.67	1.11	1.74	1.55	2.75	0.29	0.35	1.67	2.89	0
2	0.56	0.64	0.54	0.94	0.68	0.78	0.77	1.14	1.13	2.25	0.29	0.43	1.26	2.34	0
3	0.58	0.62	0.48	0.66	0.69	0.78	0.75	0.91	0.87	1.75	0.30	0.38	1.04	1.86	0
4	0.50	0.58	0.33	0.46	0.50	0.68	0.60	0.74	0.68	1.16	0.25	0.30	0.85	1.30	0
5	0.46	0.50	0.26	0.35	0.41	0.50	0.53	0.61	0.34	0.83	0.12	0.25	0.58	0.97	0
6	0.47	0.53	0.17	0.27	0.39	0.41	0.50	0.59	0.21	0.34	0.10	0.12	0.51	0.63	60
7	0.46	0.51	0.19	0.23	0.40	0.41	0.50	0.56	0.23	0.24	0.10	0.10	0.51	0.56	60
8	0.35	0.54	0.17	0.23	0.40	0.41	0.39	0.59	0.21	0.25	0.10	0.12	0.41	0.60	60
9	0.36	0.57	0.12	0.17	0.40	0.44	0.38	0.59	0.20	0.30	0.12	0.14	0.41	0.64	60
10	0.56	0.65	0.13	0.21	0.41	0.46	0.57	0.68	0.24	0.45	0.10	0.14	0.61	0.79	0
11	0.58	0.65	0.15	0.20	0.45	0.47	0.60	0.68	0.20	0.49	0.11	0.13	0.62	0.81	0
12	0.54	0.64	0.14	0.21	0.40	0.45	0.56	0.67	0.19	0.24	0.11	0.13	0.57	0.68	0
13	0.53	0.54	0.16	0.19	0.40	0.41	0.55	0.57	0.21	0.21	0.12	0.12	0.57	0.58	0
14	0.45	0.53	0.16	0.34	0.41	0.50	0.48	0.63	0.22	0.32	0.14	0.18	0.51	0.62	0
15	0.52	0.53	0.15	0.19	0.50	0.58	0.54	0.56	0.20	0.28	0.16	0.26	0.56	0.60	0
16	0.44	0.53	0.15	0.22	0.59	0.60	0.46	0.58	0.21	0.28	0.24	0.26	0.48	0.60	0
17	0.32	0.44	0.19	0.26	0.43	0.60	0.37	0.51	0.22	0.32	0.10	0.24	0.39	0.54	80
18	0.29	0.40	0.20	0.27	0.46	0.56	0.35	0.48	0.28	0.35	0.13	0.25	0.40	0.53	80
19	0.34	0.45	0.24	0.30	0.52	0.55	0.42	0.54	0.35	0.48	0.25	0.25	0.49	0.66	80
20	0.39	0.47	0.29	0.38	0.52	0.66	0.49	0.60	0.57	0.68	0.25	0.28	0.69	0.83	80
21	0.43	0.56	0.36	0.69	0.66	0.73	0.56	0.89	0.63	0.83	0.27	0.31	0.76	1.00	80
22	0.51	0.82	0.67	1.94	0.62	0.68	0.84	2.11	0.83	1.75	0.26	0.30	0.97	1.93	80

6 Conclusions

For the design of the storm retaining walls in the marina of Blankenberge and the risk analysis, hydrodynamic boundary conditions are needed along the complete boundary of the marina. The boundary conditions are needed for a 1000-year storm and several super storms defined by the risk analysis.

Corresponding to the method applied for the harbours of Oostende and Zeebrugge, the wave modelling was decoupled to the modelling of the wave penetration and local generation of waves by the extreme wind speed.
The wave penetration was modelled with the well-known and validated Boussinesq model Mike 21 BW, but also with the new model SWASH based on the non-linear shallow water equations. Due to the many shallow areas of Blankenberge non-linear effects were considered to be important and therefore the linear model MILDwave was not used this time.
The local generation of waves by extreme wind speeds was once again modelled with SWAN.

The same method as for the case of Oostende and Zeebrugge was used for setting up the Mike 21 BW model. Like in the case of Oostende, due to the many shallow areas several (numerical) measures were needed to make the model numerically stable:

- A minimum water depth of 1.50m (1.00m in case of the validation runs) was established in the bathymetry to be able to disable the wave run-up module (which causes too many numerical instabilities);
- Sponge layers at the western beach/bank just outside the marina entrance;
- An artificially high bottom friction on the beaches on both sides of the harbour;
- A numerical low-pass filter in the shallowest parts of the calculation domain.

The location and degree of dissipation was chosen as much as possible such that it has a small effect on the results.

For SWASH this is the first application of the model to simulate wave penetration in a harbour. SWASH is suitable for the calculation of the shallow water phenomenon where the non-linear effect is dominant. The benefit to apply the SWASH model to this practice is that the non-linear effect plays an important role in this study. Also other benefits are the model does not need to have many measures to stabilise the computation. For example, there is no need to put the minimum depth and even it is possible to calculate wave overtopping over a structure. Also a cut-off frequency is not necessary for the wave generation and also no low-pass filter is needed.

Validation with the Wenduine case showed that wave set-down was best modelled by Mike 21 BW. Conversely, the wave setup is underestimated due to the influence of the numerical measures for stability in the shallow areas. On the other hand SWASH overestimated the wave set-down and –up for the Wenduine case.
The wave set-down result of Mike 21 BW in the final 2DH models is used as the reference for the offset of the SWASH result, causing the wave setup to be better predicted by SWASH (i.e. not overestimated).

The main conclusions of the sensitivity analyses are:

- Changing the time-extrapolation factor used in Mike 21 BW for stability has almost no effect on the results;
- Wave direction NNW is the worst direction according to the SWASH result. For Mike 21 BW this is N and NNW.
- Directional spreading: long crested waves cause the highest wave penetration. Short crested waves cause both lower wave penetration and lower resonance. The biggest difference has been found between long crested waves and short crested waves. The difference between directional spreading 15° and 30° is small in comparison. Short crested waves are more

realistic, so a directional spreading of 15° is used for the final models which more or less corresponds to the calculated value of Goda's method (~11°). 15° was also chosen because the results are higher and therefore safer than the results with directional spreading of 30°.

Validation of the SWASH and Mike 21 BW model with 4 field measurements shows that both models generally predict the wave penetration and long wave generation well:

- In general, both models are capable at reproducing the significant wave height with sufficient accuracy in each direction (N,NNW and NW), even though the non-linear effect can be high in the shallow marina. It was also found that the trend of the K_d-values can depend on the dominant wave directions.

- The largest difference is about 10% in K_d value (BLK_A in the validation 2 and BLK_C in the validation 4), which is almost equivalent to 0.2 m to 0.3 m in significant wave height. In the other cases the difference is smaller (lower than 5%).

- Inside the marina, most of the high frequency energy is disappeared and some of it transferred to the lower frequencies. The absolute energy values did not perfectly correspond to each other, but the shift and position of the peak frequencies was reproduced reasonably well by both models. Especially the SWASH model seems to overestimate the energy of the long waves.

- It appears that the wave energy in the high frequency component is still dominant in the field measurements at location BLK_A (positioned in the marina entrance). Both numerical models (especially Mike 21 BW) also show the high frequency components, but with less wave energy than in the field measurements. The differences between the numerical models and the field measurements cannot be explained by locally generated wind waves calculated by SWAN model since their wave periods are too low.

The comparison of the final models for the purpose of predicting the extreme wave climate in the harbour of Blankenberge in SWASH and Mike 21 BW shows:

- The K_d-values of the SWASH model are somewhat higher than the K_d-values of the Mike 21 BW model, but overall a good agreement is found.

- It seems that the differences of the K_d-value pattern start already outside the marina in the navigation channel. This may be attributed to the bathymetric differences (Mike 21 BW model uses the a minimum water depth of 1.5 m) or due to differences in the workings of the wave breaking module of each model.

- The higher K_d-value of the SWASH model in the southern part of the entrance channel can be explained by wave overtopping. Since the land level of the east bank is about +9.0 m TAW, some big waves overtop the east bank. This phenomena is most important in the case of +7.90mTAW storm conditions. The wave overtopping is not include in the Mike model.

The model results also gave:

- The resonance frequencies: they were identified in the harbour by doing a white noise simulation (equal energies at all frequencies) with Mike 21 BW. In the yacht dock and basin of the marina the main resonance frequencies are around 600s (=10min) and 60s (=1min);

- The wave period: the evolution of the wave period was investigated by looking at the evolution of the wave spectra along the longitudinal section GHK, which runs from St1 (offshore from marina) towards St8 (end of yacht dock). The short wave energy almost completely disappears (due to wave breaking and the presence of obstacles) and the long wave frequencies begin to dominate the wave climate due to resonance. The peak long wave frequencies correspond with some of the resonance frequencies determined in the white noise simulation.

- The wave direction: at the entrance of the harbour (where there is still short wave energy) the wave direction is determined based on the perpendicular on the wave front of the first incoming wave.
  Deeper into the marina (yacht dock and basin) only long wave energy remains. Because of the very large wave length of these waves (larger than the dimensions of the marina itself) no wave direction can be specified for these long waves. These long waves have a very low wave steepness and the effect of the long waves is more like long oscillations or an up and down movement of the complete water surface in the marina.

From the comparisons of both models and validation with the field measurements, it is recommended for the design of safety measures in the harbour to use the numerical results with care:

In favour of the SWASH model results is the fact that:

- SWASH uses the actual bathymetry since no minimum water depth is needed in the model.
- No sponge layers, additional bottom friction and low-pass filter were needed for numerical stability.

On the contrary:

- It is also possible that SWASH overestimates the generation of the long waves as it was seen in the validation with the field measurements;
- and the wave set-down is not correctly calculated in SWASH, since an offset based on the Mike 21 BW result has been applied.

Therefore it is wise to consider also the Mike 21 BW result since:

- The wave setdown is correctly calculated;
- The model behaviour is well known;
- The validation showed good results.

The SWAN results of the locally generated wave climate due to the extreme wind speeds is given along the complete boundary of the marina divided in quay wall zones. These results are also important because almost no short wave energy penetrates into the yacht dock and basin.

Finally the short wave penetration was superposed with the locally generated waves to obtain the total wave climate. This was done for the 1000-year conditions and the +7.90mTAW super storm. The results were given based on the minimum and maximum significant wave height along each quay wall zone. Per zone, the maximum values of all wind and wave directions for each model were given. This was only possible for the 1000-year storm. For the +7.90mTAW storm, only NNW was modelled with the wave penetration models. This means that for some zones (primarily at the marina entrance) the wave height could still be higher for other wave directions.

Because the long wave energy is a big part (or even the biggest part in some cases) of the wave climate, the long wave energy was separated from the total wave spectrum. This means that H_{m0} values were obtained which represent only the short waves (e.g. T<30s) and which were used for the superposition with the SWAN results. Taking the long wave energy into account was done by increasing the still water level with a constant value corresponding with the highest surface elevation due to long wave energy and wave setup. However, increasing the water level with the maximum surface elevation of the long waves could be too conservative in some cases as it is not continuous (in contrast to the wave setup). An expert judgement is needed to determine the hydrodynamic boundary conditions which depends on the kind of analysis or design to be done.

7 Data Sources

Afdeling Kust (2011a). Database of all bottom level field measurements.

Afdeling Kust (2011b). Plan with dredging depths for the marina of Blankenberge. *Blankenberge in wgs84 utm31.dwg*

Afdeling Kust (2011c). Plan of renovation area (club house) in the marina of Blankenberge. *plan 2-3_aangepast na aanbesteding_v6.pdf*

Afdeling Kust (2011d). *Collection of scanned original plan including cross section of the structure in the marina of Blankenberge.*

8 References

Afdeling Kust (2012). *"Verslag vergadering 25 januari 2012: Voortgangsoverleg extreem golfklimaat in de kusthavens: Blankenberge en Zeebrugge."*

Beltrami, G. M., De Girolamo, P., Pellegrini, G (2003). *"Influence of Dredged Channels on Wave Penetration into Harbours: The Malamocco Inlet Case."* Coastal Structures.

Booij, N.; Ris, R.C.; Holthuijsen, L.H. (1999). *"A third-generation wave model for coastal regions, Part I, Model description and validation."* J. Geoph. Research, Vol. 104, pp.7649-7666

DHI (2009). *"Mike 21 BW: Boussinesq Waves Module User Guide."*

Gierlevsen, T.; Hebsgaard, M.; Kirkegaard, J. (2001). *"Wave disturbance modelling in the port of Sines, Portugal – with special emphasis on long period oscillations".* Paper for International Conference on Port and Maritime R&D and Technology, Singapore, 29-31 October 2001.

Goda Y. (2010). *"Random Seas and Design of Maritime Structures"*. Advanced Series on Ocean Engineering, Vol 33.

Gruwez, V.; Bolle, A.; Hassan, W.; Verwaest, T.; Mostaert, F. (2011). "*Numerieke modellering van het extreem golfklimaat in de Belgische havens. Deel 1: Haven van Oostende."* Versie 2_0. WL Rapporten, 769_03. Waterbouwkundig Laboratorium & IMDC (I/RA/11273/11.113/VGR).

Gruwez, V.; Bolle, A.; Hassan, W.; Verwaest, T.; Mostaert, F. (2012). "*Numerieke modellering van het extreem golfklimaat in de Belgische havens. Deel 2: Haven van Zeebrugge."* Versie 2_0. WL Rapporten, 769_03. Waterbouwkundig Laboratorium & IMDC (I/RA/11273/12.016/VGR).

IMDC (2011). *"Golfmetingen in de havens van Nieuwpoort, Blankenberge en Zeebrugge."* In opdracht van Afdeling Kust. I/RA/11348/11.084/SDO

Jensen M.S. (2004). *"Breaking of waves over a Steep Bottom Slope".* Phd Thesis. Aalborg University.

Madsen, P.A.; Murray R.; Sørensen, O.R. (1991). *"A new form of the Boussinesq equations with improved dispersion characteristics."* Coastal Engineering, Vol. 15, pp. 371-388.

Madsen, P.A.; Sørensen, O.R. (1992). *"A new form of the Boussinesq equations with improved dispersion characteristics. Part 2. A slowly-varying bathymetry."* Coastal Engineering, Vol. 18, pp. 183-204.

Radder, A.C. and Dingemans, M.W. (1985). *"Canonical equations for almost periodic, weakly nonlinear gravity waves."* Wave Motion, Vol. 7, pp. 473-485.

Suzuki, T., Verwaest, T., Hassan, W., Veale, W., Trouw, K and Troch, P. (2011) The applicability of SWASH for modelling wave transformation and wave overtopping: A case study for the Flemish coast, Proceedings of ACOMEN 2011.

SWASH Team (2011). SWASH user manual; version 1.05.

Technum, IMDC en Alkyon (2002). *"Structureel herstel van de kustverdediging te Oostende en verbetering van de haventoegang naar de haven van Oostende: Hydrodynamische randvoorwaarden voor het ontwerp. Waterstanden en golfklimaat".* 26-30070-200/SR002

Troch, P. (1998). "MILDwave – A numerical model for propagation and transformation of linear water waves." Intern rapport, AWW-UGent.

TUDelft (2010). *"SWAN (Simulating WAves Nearshore); a third generation wave model"* Copyright © 1993-2011, Delft University of Technology.

van der Meer, J.W.; Langenberg, J.W.; Breteler, M.K.; Hurdle, D.P.; den Heijer, F. (2002). *"Wave*

boundary conditions and overtopping in complex areas." Coastal Engineering, 2002, pp. 2092-2104

Van Gent, R.A. M.; Giarrusso, C. C. (2005). *"Influence of foreshore mobility on wave boundary conditions."* Proc. Waves 2005, ASCE.

Veale, W., Suzuki, T., Spiesschaert, T., Verwaest, T., Mostaert, F. (2011). SUSCOD Pilot 1: Wenduine Wave Overtopping Scale Model: interim results report. Version 2.0. WL Rapporten, 759_02a. Flanders Hydraulics Research: Antwerp. IV, 27 + 7 p. Appendices pp.

Verwaest, T.; Van Poucke, Ph.; Vanderkimpen, P.; Van der Biest, K.; Reyns, J.; Peeters, P.; Kellens W.; Vanneuville, W.; Mostaert, F. (2008). "*Overstromingsrisico's aan de Vlaamse kust: Evaluatie van de zeewering. Deel 1: Methodologie."* WL Rapporten, 718/2A. Waterbouwkundig Laboratorium & Universiteit Gent & Soresma-Haecon: Borgerhout, België.

Zijlema, M., Stelling, G.S. and Smit P. (2011) SWASH: An operational public domain code for simulating wave fields and rapidly varied flows in coastal waters. Coastal Engineering, 58: 992-1012.

ANNEX 1: MEMO HYDRODYNAMIC BOUNDARY CONDITIONS

Nota

Datum: 21/02/2012

Aan: Waterbouwkundig Laboratorium

Auteur: Vincent Gruwez, Toon Verwaest

Documentref: **I/NO/11273/11.341/VGR/ v1.0**

Betreft : 11273 - Hydrodynamische randvoorwaarden voor de golfindringingsmodellen (ZBG en BLK)

Inhoudstafel

International Marine & Dredging Consultants nv
Coveliersstraat 15 - B 2600, Antwerpen tel +32 3 270 92 95 - fax +32 3 235 67 11 – E-mail: info@imdc.be

0. INLEIDING

In deze nota worden de hydrodynamische randvoorwaarden voor de havens Blankenberge en Zeebrugge bepaald die gebruikt zullen worden voor de golfindringingsmodellen binnen project 11273. Naar analogie met de randvoorwaarden die voor de haven van Oostende werden gebruikt, zijn nodig:

- T1000: de 1000-jarige hydrodynamische randvoorwaarden bepaald op basis van de 98 stormen uit IMDC *et al.* (2004) en IMDC (2008).
- Superstormen: de hydrodynamische randvoorwaarden horende bij de superstormen bepaald voor de risicoberekeningen (Verwaest et al., 2008)

1. HAVEN VAN ZEEBRUGGE

1.1 HYDRODYNAMISCHE RANDVOORWAARDEN VOOR T1000

IMDC (2008) stelde een SWAN model op om een eerste benadering van de hydraulische randvoorwaarden in de haven te bekomen. 98 extreme condities (cf. Bijlage A) werden daarbij gemodelleerd met gekende kans van voorkomen zodat in elk uitvoerpunt aan de kust of in de havens de extreme waarden curve voor de significante golfhoogte opnieuw opgesteld kon worden. In deze simulaties werd telkens ook uitvoer in punten buiten de haven opgevraagd. Het is één van deze punten die gebruikt zal worden om de hydrodynamische randvoorwaarden voor de golfindringingsmodellen te bepalen.

In Figuur 1-1 zijn de beschikbare uitvoerpunten weergegeven.

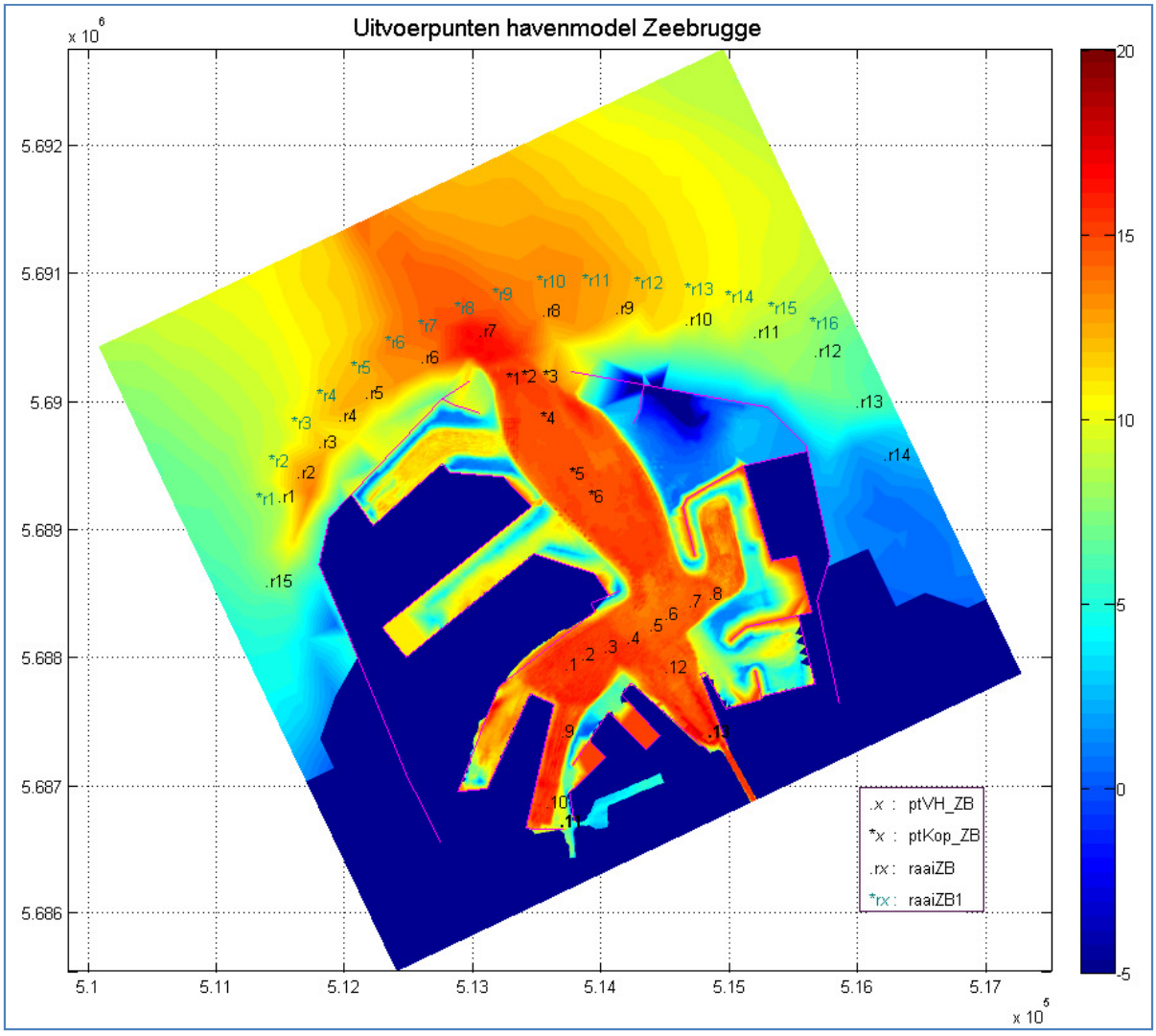

Figuur 1-1: Bathymetrie en rekengebied van het SWAN nestmodel voor de haven van Zeebrugge met aanduiding van de beschikbare uitvoerpunten (IMDC, 2008).

Punt r7 op raaiZB (cf. Figuur 1-1) wordt gebruikt als referentiepunt voor de randvoorwaarden van de golfindringingsmodellen. Het punt ligt net buiten de ingang van de haven zodat dit punt tegelijk een goede representatie is van de golfcondities die de haven binnenkomen en nog geen invloed van structuren van de haven ondervindt. Het punt ligt bovendien in de vaargeul.

De extreme waarden curve voor de significante golfhoogte in punt r7, opgesteld aan de hand van de 98 stormen volgens de methode beschreven door IMDC (2008), is weergegeven in Figuur 1-2. Zowel de richtingsonafhankelijke curve als de curve voor elke richting is weergegeven.

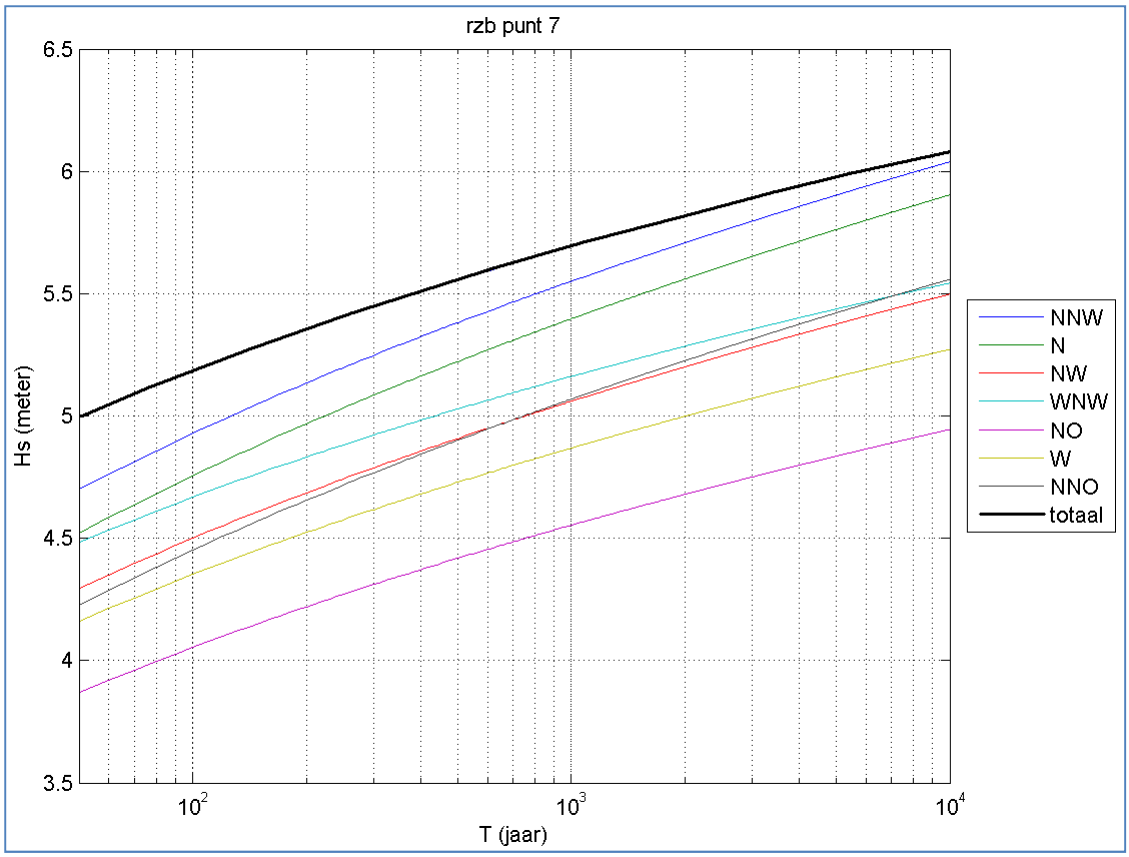

Figuur 1-2: Significante golfhoogte H_s (=H_{m0}) vs terugkeerperiode T voor punt r7 (raaiZB).

De richtingsonafhankelijke condities worden gekozen voor de golfindringingsmodellen om te vermijden dat bij elke richtingswijziging de golfcondities gewijzigd moeten worden. Andere golfcondities en waterstand kunnen er immers voor zorgen dat een nieuw rekenrooster opgesteld moet worden en/of dat een nieuwe tijdstap geldt. De richtingsonafhankelijke golfcondities gebruiken is een conservatieve aanname. Uit Figuur 1-2 blijkt dat voor T = 1000j richting NNW niet veel afwijkt van de richtingsonafhankelijke waarde (resp. $H_{m0,1000j}$ = 5.55m en 5.69m), echter richting NW eerder wel ($H_{m0,1000j,NW}$ = 5.08m). NNW en NW zijn waarschijnlijk de belangrijkste richtingen voor golfindringing diep in de haven van Zeebrugge.

De richtingsonafhankelijke hydrodynamische randvoorwaarden voor T = 1000j in punt r7 zijn gegeven in Tabel 1-1. De waterstand in deze tabel is zonder zeespiegelstijging en wordt gegeven door IMDC (2008). Ter vergelijking, de 1000-jarige waterstand zonder zeespiegelrijzing van Oostende is 6.90mTAW. Met een verschil in springtij HW van ongeveer 0.10m tussen Oostende en Zeebrugge is de 1000-jarige waterstand voor Zeebrugge van 6.81mTAW inderdaad een verwachte waarde.

Tabel 1-1: De hydrodynamische condities in punt r7 voor de storm met terugkeerperiode 1000 jaar (IMDC, 2008)

Punt	X_p	Y_p	H_{m0}	T_p	SWL	bodem
[-]	[m UTM31 WGS84]	[m UTM31 WGS84]	[m]	[s]	[m TAW]	[m TAW]
r7	513053.000	5690550.000	5.69	11.78	6.81	-16.22

De hydrodynamische randvoorwaarden uit Tabel 1-1 worden afgerond voor gebruik in de golfindringingsmodellen (cf. Tabel 1-2). De waterstand werd daarbij verhoogd met een zeespiegelrijzing van 0.30m voor hoogwater in 50 jaar (2050) (IMDC *et al.*, 2003). Er wordt geen rekening gehouden met een waterstandsverhoging door lange golfoscillaties, buistoten,… . De invloed van de zeespiegelrijzing op de golfcondities wordt verwaarloosd zoals ook werd aangenomen door IMDC (2008).

Tabel 1-2: De richtingsonafhankelijke hydrodynamische condities in punt r7 voor de storm met terugkeerperiode 1000 jaar. Waterstand inclusief zeespiegelstijging en lange golfoscillaties. Waarden bestemd voor de kalibratie van de randvoorwaarden in de golfindringingsmodellen voor Zeebrugge.

Parameter	Waarde
H_{m0} [m]	5.70
T_p [s]	12.0
SWL [m TAW]	+7.10

De randvoorwaarden aan de golfgeneratielijn van de golfindringingsmodellen kunnen dan gekalibreerd worden totdat in punt r7 de gewenste 1000-jarige golfcondities uit Tabel 1-2 worden bekomen.

1.2 HYDRODYNAMISCHE RANDVOORWAARDEN VOOR DE SUPERSTORMEN

Er is een springtijverschil van 0.10m tussen Oostende en Zeebrugge. Daarom worden de superstormwaterstanden van Oostende met 0.10m verlaagd resulterend in de superstormwaterstanden voor Zeebrugge. Deze waarden zijn zonder zeespiegelrijzing.

Gebruik makend van de resultaten van de golfvoortplantingsmodelleringen van de verschillende superstormen met het swan2D kustzonemodel uitgevoerd in het kader van de risicoberekeningen ter onderbouwing van het kustveiligheidsplan voor wat betreft de variatie van H_{m0} met het stormvloedniveau worden de golfrandvoorwaarden voor de verschillende superstormen afgeleid vertrekkende van deze voor de 1000-jarige storm. Dit is consistent met

de werkwijze die aangehouden is voor de haven van Oostende. Voor de golfperiode wordt T_p=12s aangehouden voor elk van de superstormen (vanwege dezelfde redenen als bij de case Oostende; cf. het hiervoor genoemde rapport Gruwez et al. 2011)

De resulterende hydrodynamische randvoorwaarden voor de superstormen worden gegeven in Tabel 1-3.

Tabel 1-3: De hydrodynamische randvoorwaarden van de superstormen voor Zeebrugge.

SWL [mTAW]	H_{m0} [m]	T_p [s]
+6.40	5,50	12.0
+6.90	5,70	12.0
+7.40	5,90	12.0
+7.90	6,20	12.0

2. HAVEN VAN BLANKENBERGE

2.1 HYDRODYNAMISCHE RANDVOORWAARDEN VOOR T1000

Dezelfde methode wordt gevolgd zoals in §1.1. Ook voor de haven van Blankenberge zijn reeds uitvoerpunten buiten de haven beschikbaar (cf. Figuur 2-1).

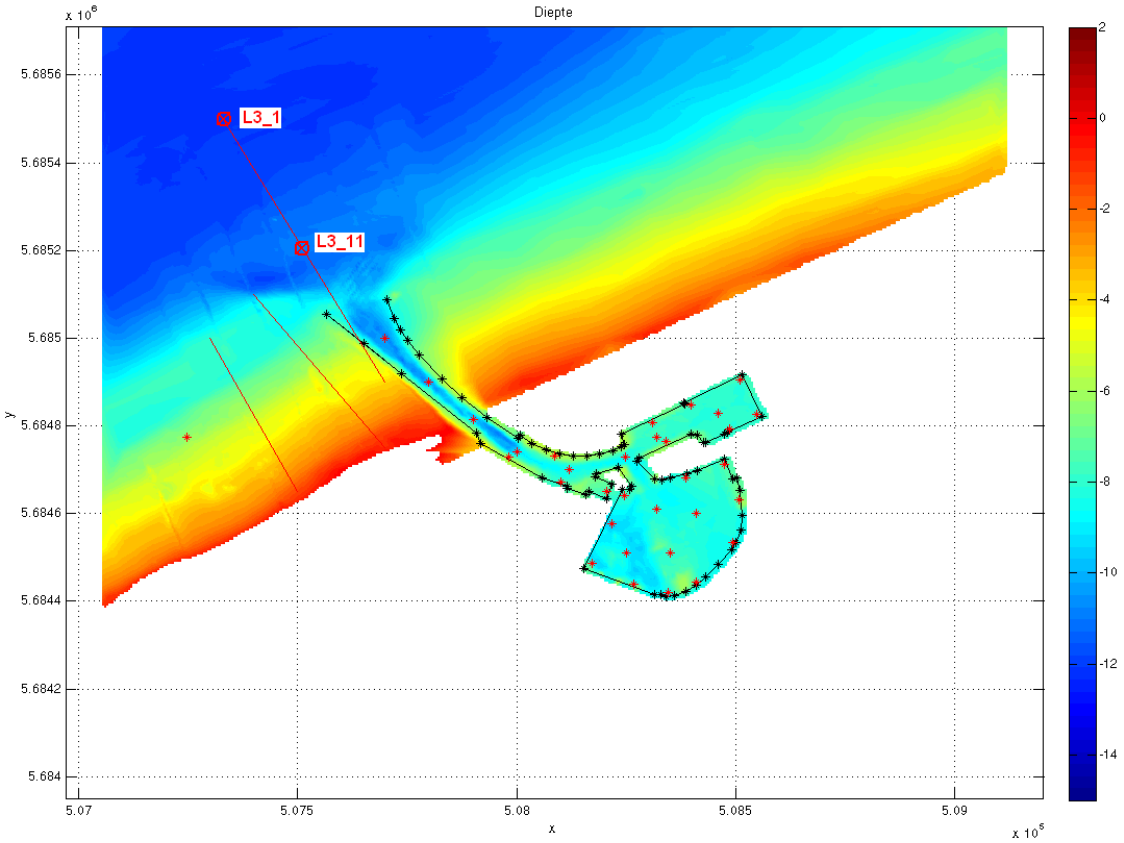

Figuur 2-1: Bathymetrie en rekengebied van het SWAN nestmodel voor de haven van Blankenberge met aanduiding van de beschikbare uitvoerpunten (IMDC, 2008).

De onderste van de twee cirkel-kruis aanduidingen op de raai die meest zeewaarts reikt (punt L3_11, cf. Figuur 2-1) wordt gebruikt als referentiepunt voor de randvoorwaarden van de golfindringingsmodellen. Het punt ligt net buiten de ingang van de haven zodat dit punt tegelijk een goede representatie is van de golfcondities die de haven binnenkomen en nog geen invloed van structuren van de haven ondervindt. Het punt wordt vergeleken met het meest offshore punt L3_1.

De extreme waarden curven voor de significante golfhoogte in beide punten, opgesteld aan de hand van de 98 stormen volgens de methode beschreven door IMDC (2008), zijn weergegeven in Figuur 2-2. Zowel de richtingsonafhankelijke curve als de curve voor elke richting is weergegeven.

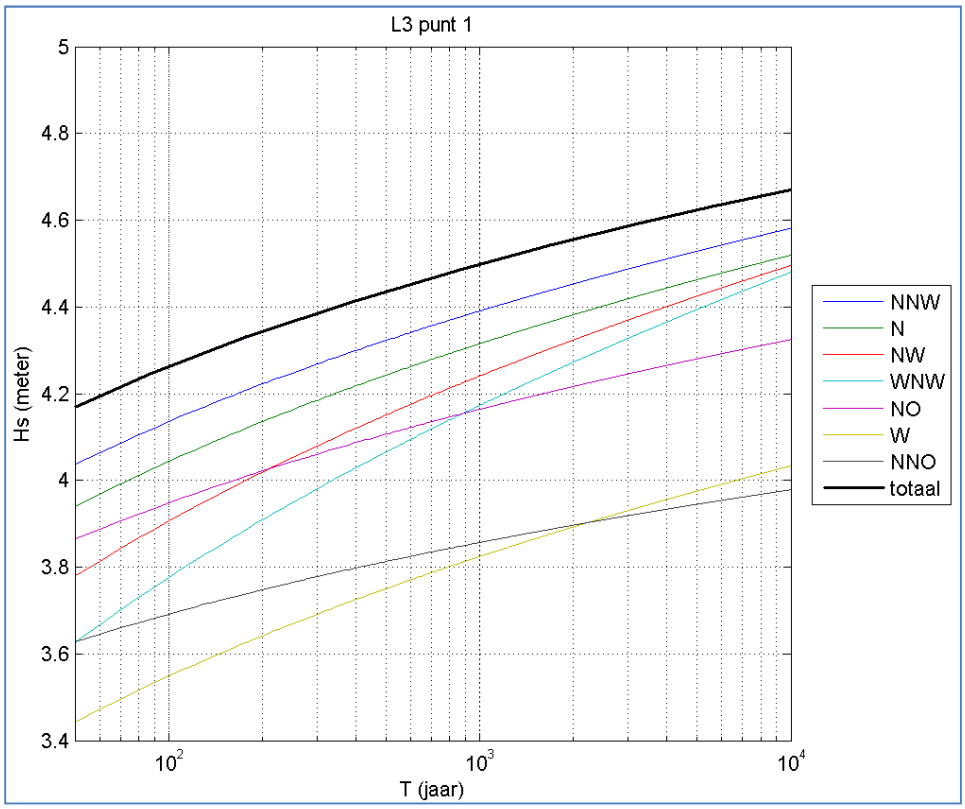

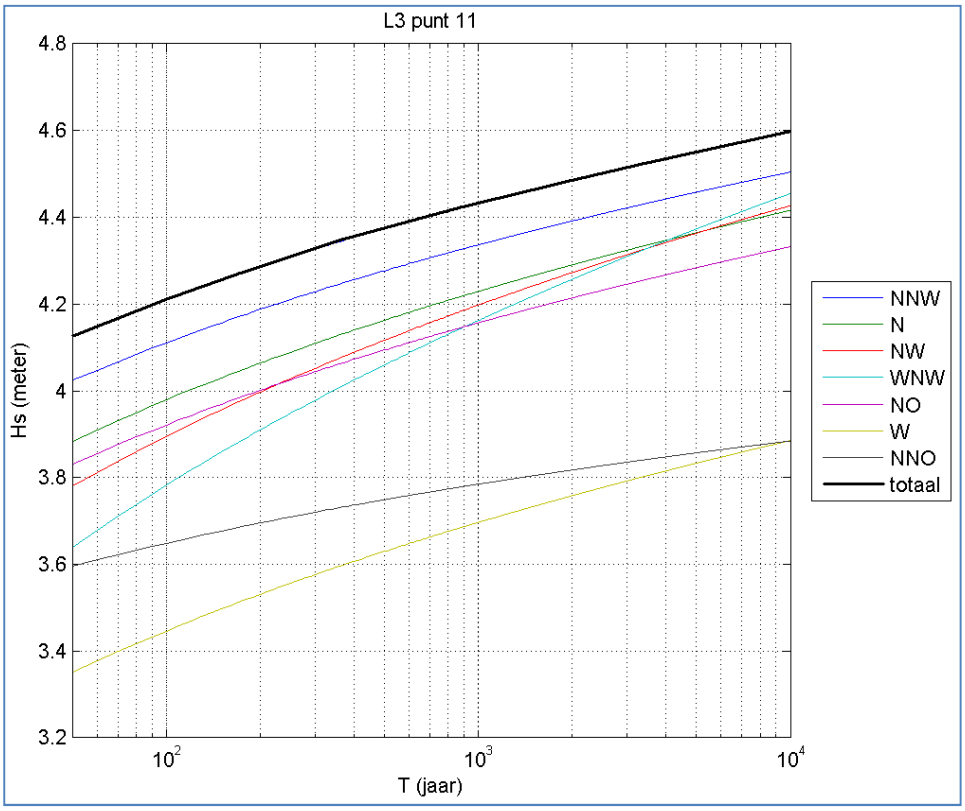

Figuur 2-2: Significante golfhoogte H_s (=H_{m0}) vs terugkeerperiode T voor punt L3_1 (boven) en L3_11 (onder).

De condities voor retourperiode 1000 jaar in beide punten zijn gegeven in Tabel 2-1.

Tabel 2-1: De hydrodynamische condities in punten buiten de haven voor de storm met terugkeerperiode 1000 jaar (IMDC, 2008)

Punt	X_p	Y_p	H_{m0}	T_p	SWL	bodem
[-]	[m UTM31 WGS84]	[m UTM31 WGS84]	[m]	[s]	[m TAW]	[m TAW]
L3_1	507330.000	5685500.000	4.50	11.81	6.84	-5.70
L3_11	507515.000	5685200.000	4.43	11.77	6.83	-4.58

De golfcondities verschillen weinig in beide punten. Punt L3_11 wordt gekozen als referentiepunt voor kalibratie van de randvoorwaarden in de golfindringingsmodellen omdat dit punt het dichtst bij de haven ligt zodat de grootte van het rekendomein beperkt kan worden.

De condities werden afgerond en aangepast zoals besproken in §1.1 naar de waarden gegeven in Tabel 2-2.

Tabel 2-2: De richtingsonafhankelijke hydrodynamische condities in punt L3_11 voor de storm met terugkeerperiode 1000 jaar. Waterstand inclusief zeespiegelstijging en lange golfoscillaties. Waarden bestemd voor de kalibratie van de randvoorwaarden in de golfindringingsmodellen.

Parameter	Waarde
H_{m0} [m]	4.50
T_p [s]	12.0
SWL [m TAW]	+7.10

2.2 HYDRODYNAMISCHE RANDVOORWAARDEN VOOR DE SUPERSTORMEN

Omdat Blankenberge nabij Zeebrugge ligt, wordt eenzelfde verschil van 0.10m van het springtij met Oostende ondersteld. De superstormwaterstanden van Zeebrugge gelden dan ook voor Blankenberge. Deze waarden zijn zonder zeespiegelrijzing.

Voor het bepalen van de golfcondities wordt een analoge manier gevolgd als in §1.2.

De resulterende hydrodynamische randvoorwaarden voor de superstormen worden gegeven in Tabel 2-3.

Tabel 2-3: De hydrodynamische randvoorwaarden van de superstormen voor Zeebrugge.

SWL [mTAW]	H_{m0} [m]	T_p [s]
+6.40	4,30	12.0
+6.90	4,50	12.0
+7.40	4,70	12.0
+7.90	5,00	12.0

3. REFERENTIES

IMDC, WLH, KUL (2003). Hydraulisch randvoorwaardenboek Vlaamse Kust (2004), I/RA/11226/03041/KTR, in opdracht van Afdeling Kust.

IMDC (2008). Geïntegreerd Kustveiligheidsplan: Leidraad Toetsen 2007, I/RA/11310/07.129/ABO, in opdracht van Afdeling Kust.

Verwaest, T.; Van Poucke, Ph.; Vanderkimpen, P.; Van der Biest, K.; Reyns, J.; Peeters, P.; Kellens W.; Vanneuville, W.; Mostaert, F. (2008). Overstromingsrisico's aan de Vlaamse kust: Evaluatie van de zeewering. Deel 1: Methodologie. WL Rapporten, 718/2A. Waterbouwkundig Laboratorium & Universiteit Gent & Soresma-Haecon: Borgerhout, België.

Bijlage A Randvoorwaarden voor het SWAN model voor de kust

Tabel A-3-1: Overzicht van de parameters voor de 98 stormen (IMDC et al., 2003).

	Hm0 [m]	*Tp [s]*	*Golfrichting [°]*	*Waterstand [m TAW]*	*Windsnelheid [m/s]*	*Windricht. [°N]*	*Kans p [-]*
aNNW	4.507	9.758	333.658	5.62	22.357	337.5	1.957E-06
bNNW	4.763	10.025	333.543	5.76	23.386	337.5	1.097E-06
cNNW	5.019	10.286	333.439	5.91	24.44	337.5	6.019E-07
dNNW	5.276	10.54	333.338	6.07	25.518	337.5	3.237E-07
eNNW	5.536	10.788	333.237	6.22	26.615	337.5	1.708E-07
fNNW	5.793	11.03	333.155	6.39	27.733	337.5	8.855E-08
gNNW	6.05	11.268	333.079	6.56	28.868	337.5	4.514E-08
hNNW	6.305	11.5	332.992	6.73	30.019	337.5	2.264E-08
iNNW	6.566	11.728	332.91	6.9	31.187	337.5	1.119E-08
jNNW	6.828	11.951	332.829	7.08	32.369	337.5	5.446E-09
kNNW	7.093	12.17	332.746	7.27	33.565	337.5	2.614E-09
lNNW	7.362	12.386	332.647	7.45	34.775	337.5	1.238E-09
mNNW	7.636	12.598	332.547	7.64	35.997	337.5	5.785E-10
nNNW	7.911	12.806	332.444	7.84	37.232	337.5	2.670E-10
aN	4.431	9.758	-8.87	5.52	22.303	0	1.420E-06
bN	4.684	10.025	-9.098	5.65	23.409	0	7.892E-07
cN	4.93	10.286	-9.497	5.79	24.534	0	4.308E-07
dN	5.177	10.54	-9.84	5.94	25.677	0	2.312E-07
eN	5.422	10.788	-10.204	6.08	26.835	0	1.222E-07
fN	5.668	11.03	-10.527	6.23	28.007	0	6.366E-08
gN	5.91	11.268	-10.927	6.39	29.192	0	3.271E-08
hN	6.158	11.5	-11.199	6.54	30.39	0	1.659E-08
iN	6.406	11.728	-11.488	6.7	31.599	0	8.312E-09

	Hm0 [m]	*Tp [s]*	*Golfrichting [°]*	*Waterstand [m TAW]*	*Windsnelheid [m/s]*	*Windricht. [°N]*	*Kans p [-]*
jN	6.658	11.951	-11.724	6.86	32.819	0	4.116E-09
kN	6.919	12.17	-11.839	7.03	34.048	0	2.016E-09
lN	7.185	12.386	-11.943	7.19	35.287	0	9.768E-10
mN	7.456	12.598	-12.08	7.36	36.536	0	4.684E-10
nN	7.728	12.806	-12.246	7.53	37.792	0	2.224E-10
aNW	4.442	9.758	315.378	6.02	23.494	315	4.044E-07
bNW	4.592	9.919	315.409	6.12	24.116	315	2.556E-07
cNW	4.741	10.078	315.443	6.22	24.728	315	1.617E-07
dNW	4.891	10.234	315.453	6.33	25.331	315	1.023E-07
eNW	5.042	10.388	315.476	6.44	25.925	315	6.483E-08
fNW	5.192	10.54	315.506	6.55	26.512	315	4.110E-08
gNW	5.343	10.689	315.537	6.66	27.091	315	2.608E-08
hNW	5.494	10.837	315.557	6.78	27.664	315	1.655E-08
iNW	5.647	10.982	315.562	6.91	28.231	315	1.051E-08
jNW	5.799	11.126	315.571	7.02	28.791	315	6.682E-09
kNW	5.952	11.268	315.587	7.16	29.346	315	4.249E-09
lNW	6.106	11.408	315.585	7.29	29.896	315	2.703E-09
mNW	6.26	11.546	315.581	7.42	30.441	315	1.720E-09
nNW	6.415	11.683	315.577	7.57	30.98	315	1.095E-09
aWNW	4.287	9.758	298.638	5.69	22.468	292.5	2.375E-06
bWNW	4.589	10.078	298.429	5.79	23.44	292.5	1.375E-06
cWNW	4.883	10.388	298.465	5.9	24.404	292.5	7.949E-07
dWNW	5.177	10.689	298.517	6	25.36	292.5	4.591E-07
eWNW	5.472	10.982	298.577	6.1	26.31	292.5	2.649E-07

	Hm0 [m]	*Tp [s]*	*Golfrichting [°]*	*Waterstand [m TAW]*	*Windsnelheid [m/s]*	*Windricht. [°N]*	*Kans p [-]*
fWNW	5.77	11.268	298.596	6.2	27.254	292.5	1.528E-07
gWNW	6.075	11.546	298.541	6.3	28.192	292.5	8.801E-08
hWNW	6.388	11.818	298.382	6.4	29.125	292.5	5.067E-08
iWNW	6.708	12.083	298.218	6.51	30.053	292.5	2.915E-08
jWNW	7.038	12.343	298.073	6.61	30.977	292.5	1.676E-08
kWNW	7.384	12.598	297.882	6.71	31.896	292.5	9.633E-09
lWNW	7.753	12.847	297.595	6.81	32.811	292.5	5.533E-09
mWNW	8.151	13.092	297.24	6.92	33.722	292.5	3.177E-09
nWNW	8.583	13.332	296.86	7.02	34.629	292.5	1.823E-09
aNO	4.235	9.758	31.041	5.24	22.763	45	5.508E-07
bNO	4.5	10.025	31.111	5.32	23.582	45	3.254E-07
cNO	4.776	10.286	31.294	5.4	24.398	45	1.918E-07
dNO	5.064	10.54	31.69	5.48	25.209	45	1.129E-07
eNO	5.402	10.788	32.859	5.57	26.017	45	6.629E-08
fNO	5.752	11.03	33.861	5.65	26.822	45	3.886E-08
gNO	6.102	11.268	34.821	5.73	27.623	45	2.275E-08
hNO	6.469	11.5	35.868	5.81	28.421	45	1.330E-08
iNO	6.838	11.728	36.754	5.89	29.217	45	7.762E-09
jNO	7.192	11.951	37.357	5.98	30.01	45	4.525E-09
kNO	7.548	12.17	37.846	6.06	30.8	45	2.635E-09
lNO	7.924	12.386	38.453	6.14	31.587	45	1.533E-09
mNO	8.322	12.598	39.121	6.23	32.372	45	8.905E-10
nNO	8.742	12.806	39.853	6.31	33.155	45	5.168E-10
aW	4.313	10.286	285.524	5.81	25.776	270	9.188E-07

	Hm0 [m]	*Tp [s]*	*Golfrichting [°]*	*Waterstand [m TAW]*	*Windsnelheid [m/s]*	*Windricht. [°N]*	*Kans p [-]*
bW	4.553	10.54	284.986	5.88	26.615	270	5.838E-07
cW	4.793	10.788	284.494	5.96	27.451	270	3.694E-07
dW	5.04	11.03	283.913	6.04	28.284	270	2.329E-07
eW	5.289	11.268	283.328	6.11	29.115	270	1.463E-07
fW	5.534	11.5	282.981	6.19	29.943	270	9.166E-08
gW	5.779	11.728	282.69	6.27	30.768	270	5.724E-08
hW	6.043	11.951	282.118	6.35	31.591	270	3.564E-08
iW	6.324	12.17	281.412	6.43	32.412	270	2.214E-08
jW	6.626	12.386	280.693	6.51	33.23	270	1.371E-08
kW	6.956	12.598	279.732	6.59	34.046	270	8.477E-09
lW	7.305	12.806	278.749	6.67	34.859	270	5.227E-09
mW	7.671	13.011	277.915	6.75	35.671	270	3.216E-09
nW	8.045	13.212	277.151	6.83	36.48	270	1.975E-09
aNNO	4.184	9.758	6.207	5.49	23.693	22.5	5.988E-07
bNNO	4.425	10.025	5.868	5.59	24.602	22.5	3.690E-07
cNNO	4.696	10.286	6.312	5.68	25.499	22.5	2.282E-07
dNNO	4.949	10.54	6.241	5.78	26.387	22.5	1.416E-07
eNNO	5.223	10.788	6.624	5.87	27.264	22.5	8.810E-08
fNNO	5.48	11.03	6.553	5.97	28.134	22.5	5.497E-08
gNNO	5.736	11.268	6.445	6.06	28.995	22.5	3.438E-08
hNNO	5.998	11.5	6.377	6.15	29.849	22.5	2.155E-08
iNNO	6.268	11.728	6.443	6.25	30.696	22.5	1.354E-08
jNNO	6.545	11.951	6.519	6.34	31.536	22.5	8.519E-09
kNNO	6.825	12.17	6.559	6.43	32.371	22.5	5.372E-09

	Hm0 [m]	*Tp [s]*	*Golfrichting [°]*	*Waterstand [m TAW]*	*Windsnelheid [m/s]*	*Windricht. [°N]*	*Kans p [-]*
lNNO	7.117	12.386	6.705	6.52	33.2	22.5	3.393E-09
mNNO	7.456	12.598	7.527	6.61	34.023	22.5	2.146E-09
nNNO	7.64	12.806	6.129	6.71	36.274	22.5	1.360E-09

ANNEX 2: OVERVIEW STRUCTURES

	plan nr	name + type of structure	tan(α)	bottom level	water depth	crest level	level of berm	berm width	crest existing wall	material of structure
	[-]	[-]	[-]	[m TAW]	[m]	[m TAW]	[m TAW]	[m]	[m TAW]	[-]
1	Blankenberge - v	Havengeul W: glooiing	1/2	-1.62	9.52	8.40	6.10	2.50	-	gemetselde breuksteen
2	plan2-AB-ontwo	Spuisluis	1/2	-1.62	9.52	8.60	-	-	-	gemetselde betonblokken
3	BSK.0002	Spuikom: kaaimuur	vert	-1.62	9.52	8.35	-	-	-	stalen damplanken
4	BSK.0002	Spuikom: kaaimuur	vert	-2.72	10.62	7.55	7.55	15.00	-	stalen damplanken
5	BSK.0001	Spuikom: glooiing	1/2	-1.62	9.52	6.80	6.80	6.00	7.15	gemetselde betonstraatstenen
6	694 B	Spuikom: glooiing	1/2	-1.62	9.52	6.80	6.80	6.00	7.15	gemetselde getrilde betonstenen
7	1249	Spuikom parking: glooiing	1/1.75	-1.62	9.52	6.90	6.90	2.00	7.40	gemetselde getrilde betonstenen
8	1162	Toegang spuikom: glooiir	1/2	-1.62	9.52					gemetselde getrilde betonstenen
9	opmeting '83	Toegang tijdok Z: glooiing	1/1.75	-1.62	9.52	7.50	5.40	4.15	-	breuksteen/gemetselde rode baks
10	opmeting '83	Tijdok Z: glooiing	1/1.75	-1.62	9.52	6.00	6.00	6.00	6.75	breuksteen/gemetselde rode baks
11	streefdieptenplat	Tijdok O: kaaimuur	vert	-1.62	9.52	6.50	6.50	20.00	-	metselwerk
12	BVD.0001	Tijdok N: glooiing met ka	1/1.75	-1.62	9.52	6.40	6.40	25.00	-	gemetselde breuksteen
13	BVD.0002	Tijdok N: glooiing met ka	vert	-1.62	9.52	6.40	6.40	25.00	-	stalen damplanken
14	807	Tijdok N: glooiing met ka	2/3	-1.62	9.52	6.40	6.40	-	-	gemetselde breuksteen
15	807/streefdiepte	Havengeul O: glooiing	1/2	-1.62	9.52	7.40	5.80	4.00	-	bak-/breuksteenmetselwerk

ANNEX 3: INPUT SWAN MODEL

```
$*********************************HEADING*************************************
$
PROJ 'blankenberge' 'ew'
$proto bestand voor de superstormen voor haven blankenberge met enkel wind
$
$*******************************MODEL INPUT***********************************
$
SET LEVEL    {SWL}
SET NAUT
MODE STATIONARY
MODE TWOD
$
CGRID 0 0 0 1995 1192.5 266 159 CIRCLE 64 0.05 2.49 41
$
INPGRID BOTTOM 0 0 0 999 599 2 2 EXC -20
READ BOTTOM -1 '..\..\..\Bathymetry\BLK_A1_2m_I05_mild_wall_VGR_SWAN.txt' 1 16 FREE
$
$
GEN3 KOMEN AGROW
BREAK CON 1.00 0.73
FRIC JON 0.0670
$
NUM STOPC STAT 50
$
$
$
$
$*********************************MODEL OUTPUT**********************************

$
OUTPUT OPTIONS TABLE 16 BLOCK 9 6

$
 BLOCK   'COMPGRID' NOHEAD  'ew_32_NNW_V29_R337_L790_xp.blk'  LAY-OUT 1  XP

 BLOCK   'COMPGRID' NOHEAD  'ew_32_NNW_V29_R337_L790_yp.blk'  LAY-OUT 1  YP

 BLOCK   'COMPGRID' NOHEAD  'ew_32_NNW_V29_R337_L790_dep.blk'  LAY-OUT 1  DEP

 BLOCK   'COMPGRID' NOHEAD  'ew_32_NNW_V29_R337_L790_hs.blk'  LAY-OUT 1  HS

 BLOCK   'COMPGRID' NOHEAD  'ew_32_NNW_V29_R337_L790_tmm10.blk'  LAY-OUT 1  TMM10

 BLOCK   'COMPGRID' NOHEAD  'ew_32_NNW_V29_R337_L790_per.blk'  LAY-OUT 1  PER
 BLOCK   'COMPGRID' NOHEAD  'ew_32_NNW_V29_R337_L790_rtp.blk'  LAY-OUT 1  RTP
 BLOCK   'COMPGRID' NOHEAD  'ew_32_NNW_V29_R337_L790_tps.blk'  LAY-OUT 1  TPS
 BLOCK   'COMPGRID' NOHEAD  'ew_32_NNW_V29_R337_L790_dspr.blk'  LAY-OUT 1  DSPR
 BLOCK   'COMPGRID' NOHEAD  'ew_32_NNW_V29_R337_L790_dir.blk'  LAY-OUT 1  DIR
 BLOCK   'COMPGRID' NOHEAD  'ew_32_NNW_V29_R337_L790_pdir.blk'  LAY-OUT 1  PDIR
 BLOCK   'COMPGRID' NOHEAD  'ew_32_NNW_V29_R337_L790_ubot.blk'  LAY-OUT 1  UBOT
 BLOCK   'COMPGRID' NOHEAD  'ew_32_NNW_V29_R337_L790_urms.blk'  LAY-OUT 1  URMS
 BLOCK   'COMPGRID' NOHEAD  'ew_32_NNW_V29_R337_L790_dhsign.blk'  LAY-OUT 1  DHSIGN
 BLOCK   'COMPGRID' NOHEAD  'ew_32_NNW_V29_R337_L790_drtm01.blk'  LAY-OUT 1  DRTM01
$
$
WIND    {wvs}      {wdir}
COMPUTE
STOP
$
```

ANNEX 4: INPUT SWASH MODEL

```
$*************HEADING*************************************
$
$ Scale 1/1, 1000 year storm NNW
$
PROJ 'A1_10_NNW_MUS' '01'
$
$***********MODEL INPUT**********************************

$ Water level
SET LEVEL 7.00 ! 7.10-0.10 (set-down)
MODE NONST TWOD

$ Coordinates (1D)
CGRID 0. 400. 0. 1240. 1400. 310 350

$ Bottom (1D)
INPGRID BOTTOM 0. 0. 0. 620 1100 2.0 2.0
READINP BOTTOM -1. 'A1_2m_NNW.bot' 1 0 FREE !

$ Initial state
INIT zero

$ Wave conditions
BOUN SHAPespec JON
BOUN SIDE W CCW BTYPE WEAK CON SPECT 4.5 12.0 0.0 10.0
BOUN SIDE E CCW BTYPE RADIATION

$ Physics
FRIC MANN 0.020
VISC Horizontal SMAG 0.1
Break 0.4 ! 0.4: spilling
NONHYDROSTATIC ! Non-hydrostatic

$ Numerics
DISCRET UPW MUS
TIMEI 0.1 0.4 ! Explicit
$
```

```
$********** OUTPUT REQUESTS *************************
$
GROUP 'OUT1' 51 305 95 315
BLOCK 'OUT1' NOHEAD '2dcaltest.mat' WATL OUTPUT 000000.000 0.4 SEC
GROUP 'COMPGRD'    1 310     1 350
BLOCK 'COMPGRD' NOHEAD 'CaldepNNW70.mat' BOTL OUTPUT 000000.000 3600.0 SEC
POINTS 'WG'       FILE 'WG_NNW.loc'
TABLE    'WG'       NOHEAD 'A1_10_NNW_MUS.tbl' TSEC DIST BOTL WATL OUTPUT 000000.000 0.2 SEC
$
TEST 1,0
COMPUTE 000000.000 0.02 SEC 005000.000
STOP
```

ANNEX 5: CALCULATION RESULTS

Validation 1, +4.91 m TAW, Wave direction NNW

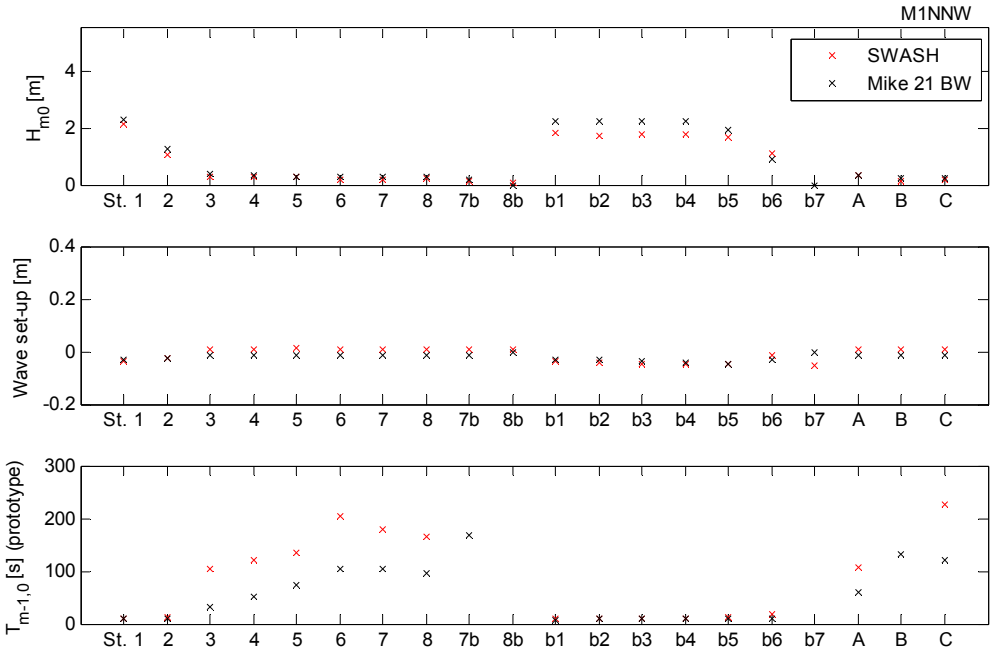

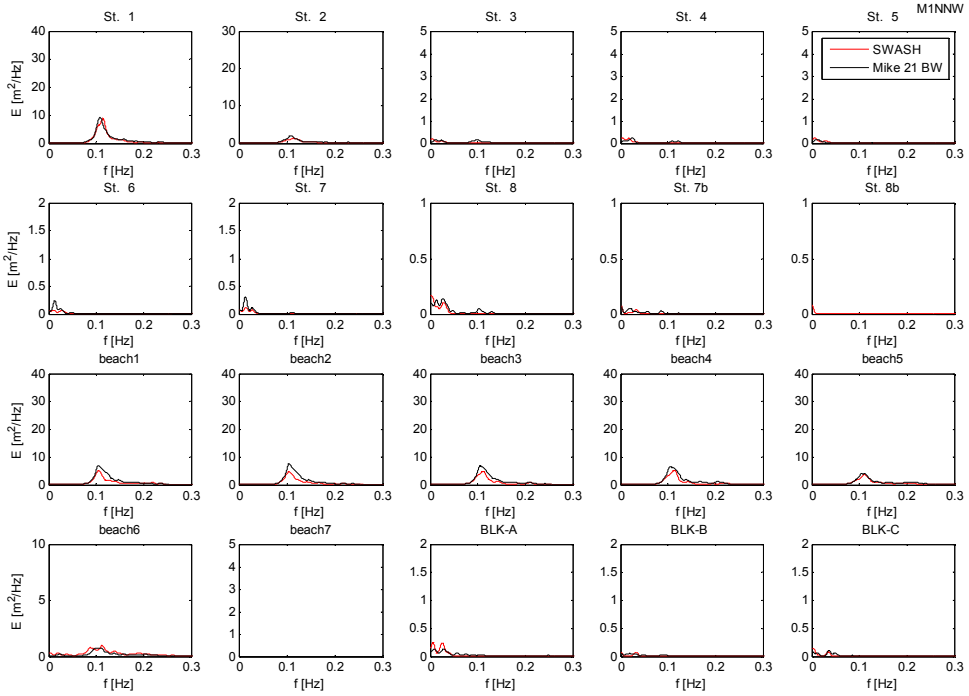

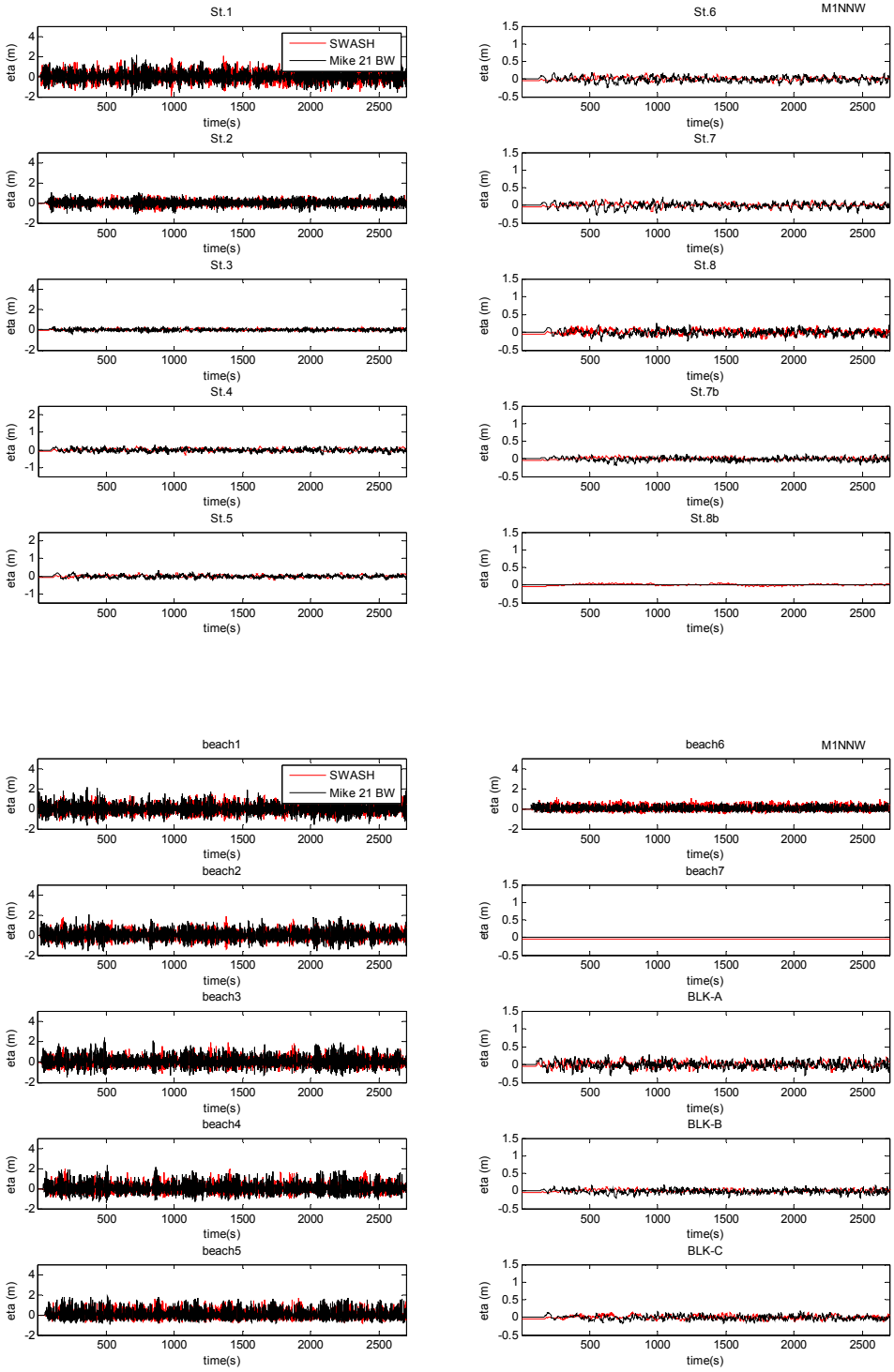

Validation 2, +4.97 m TAW, Wave direction NW

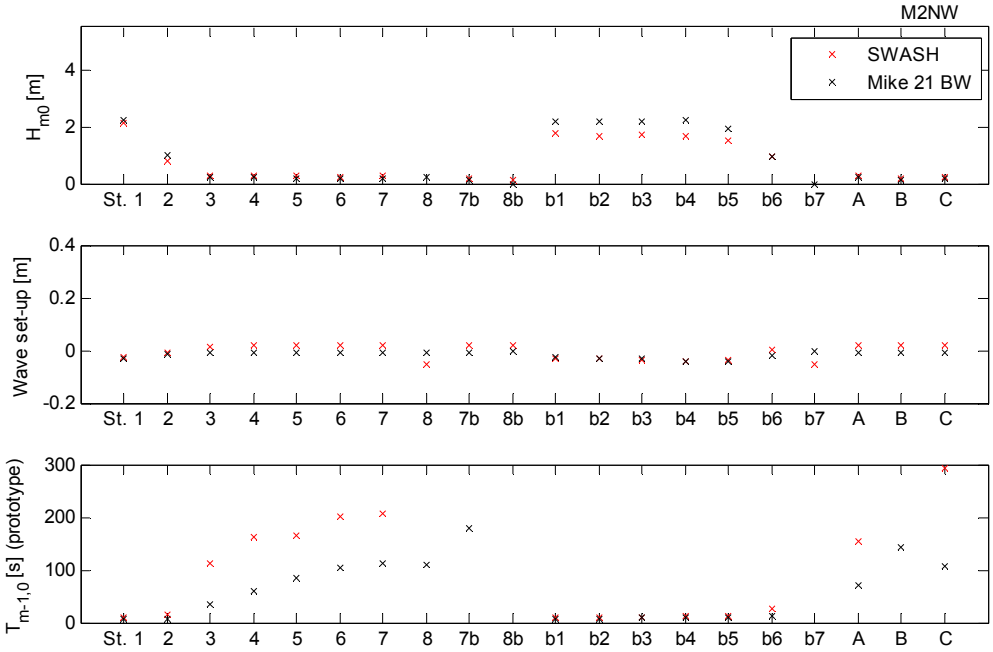

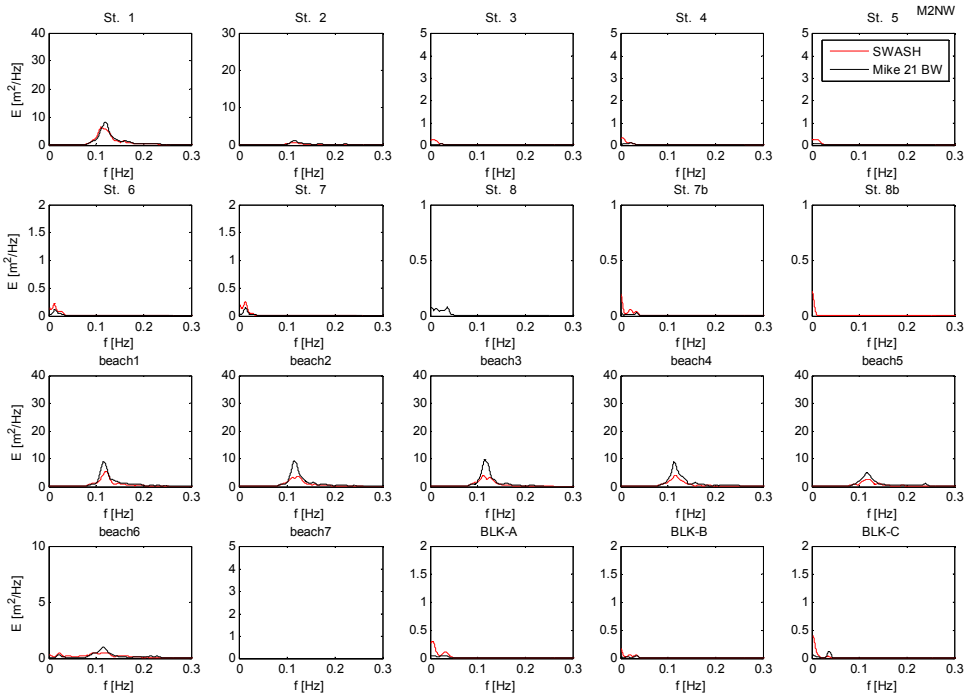

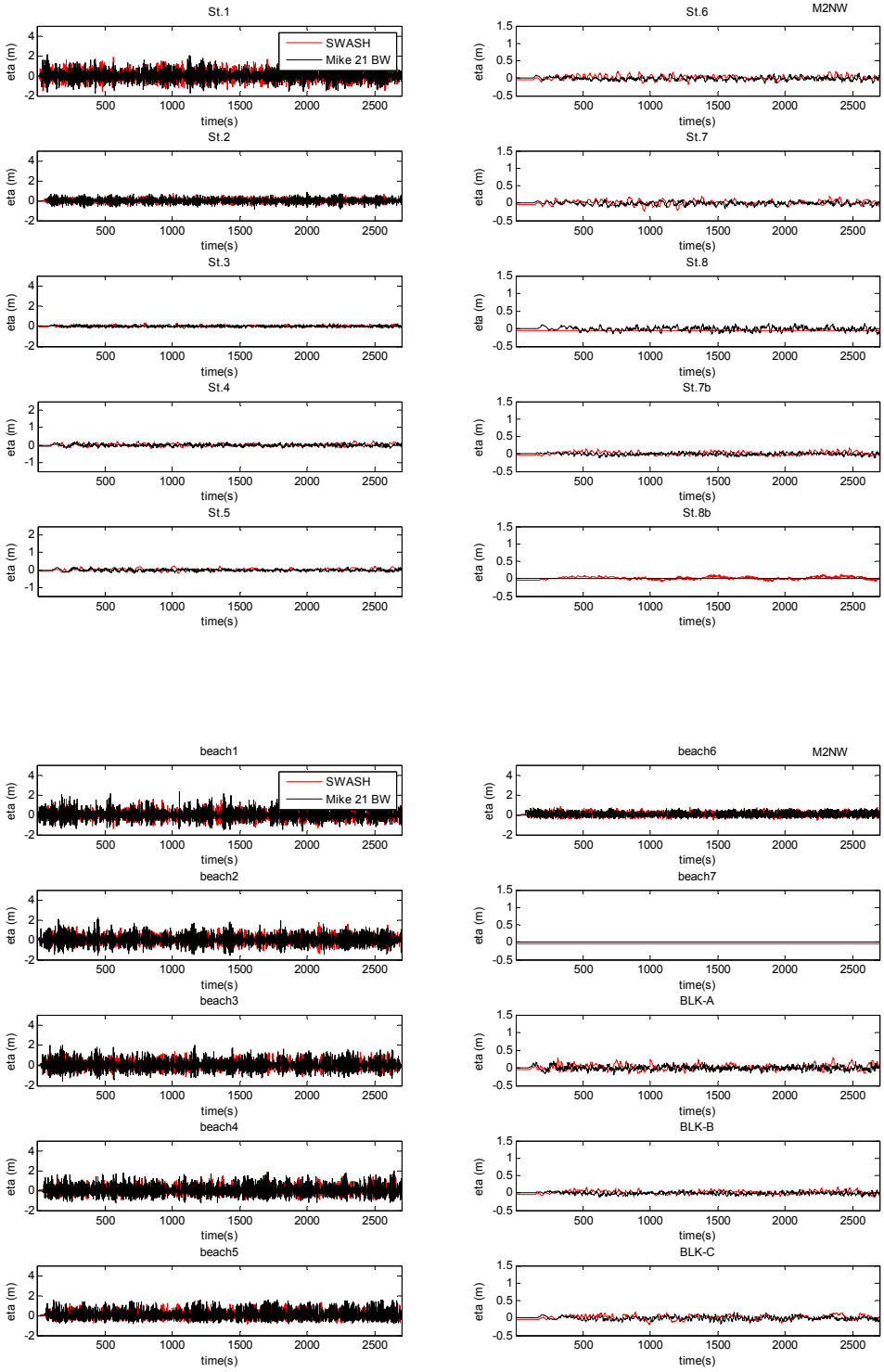

Validation 3, +4.55 m TAW, Wave direction NNW

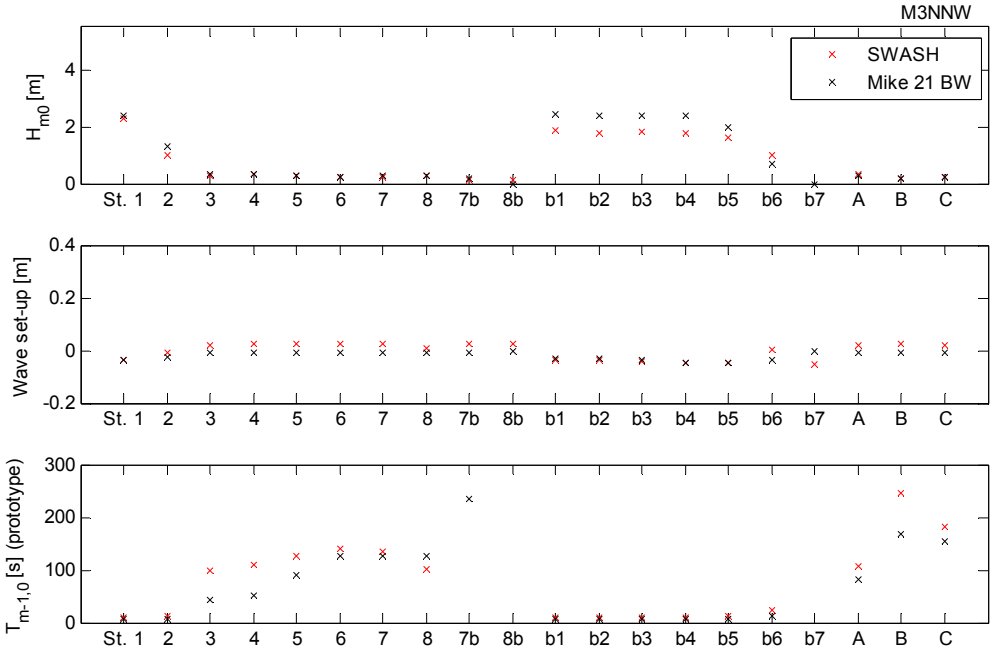

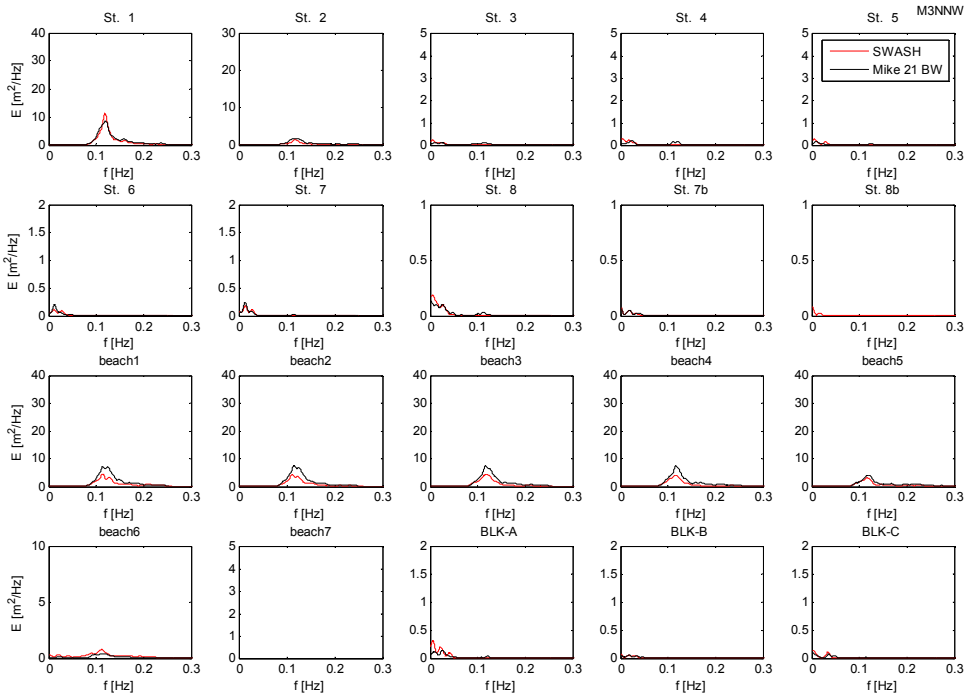

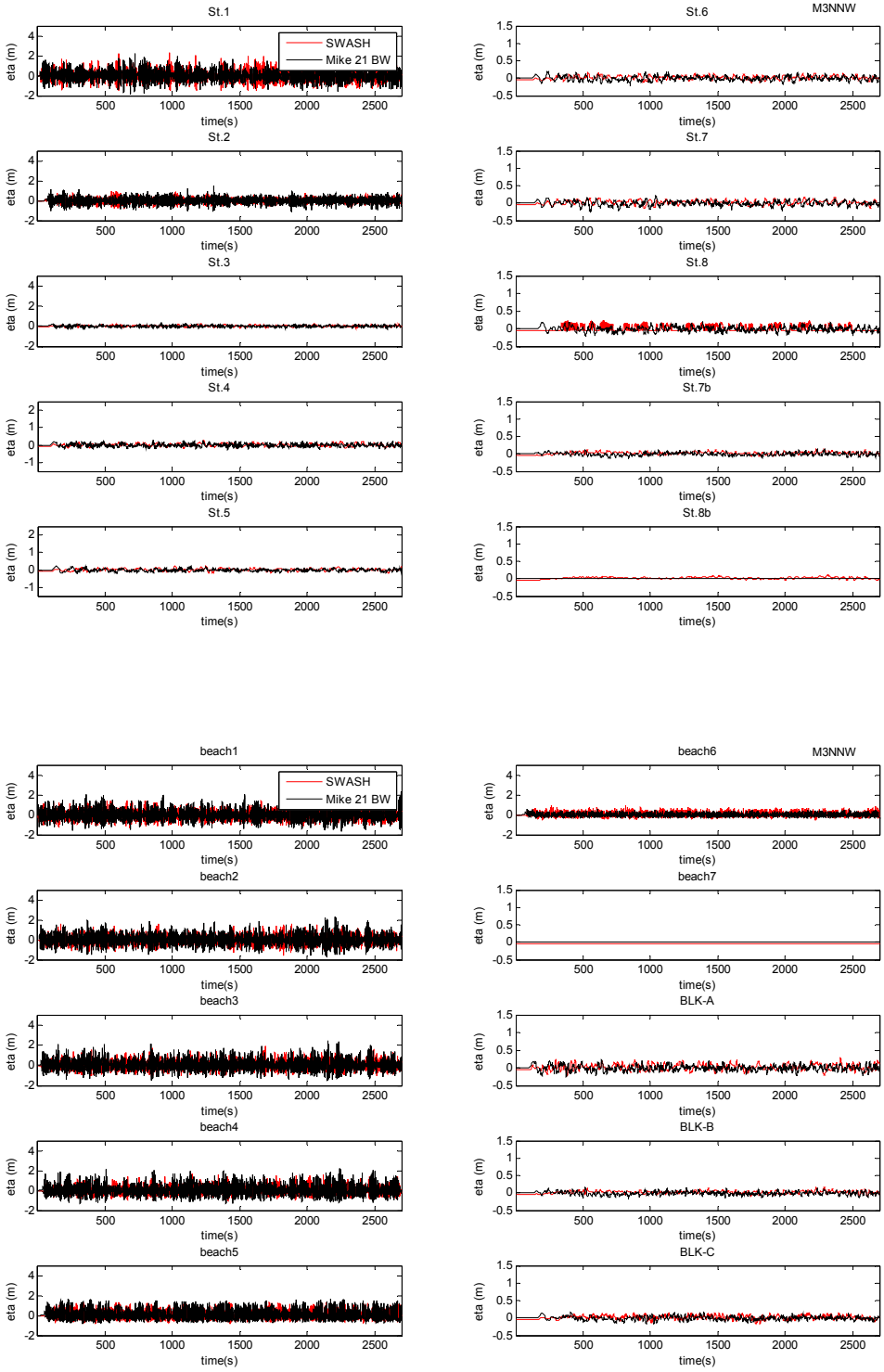

Validation 4, +4.61 m TAW, Wave direction N

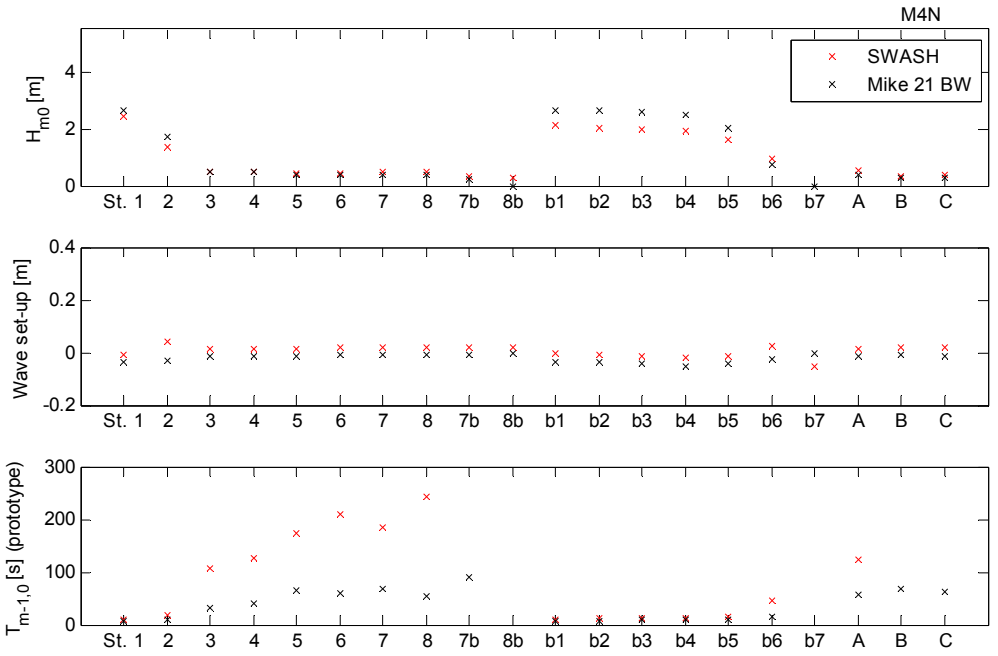

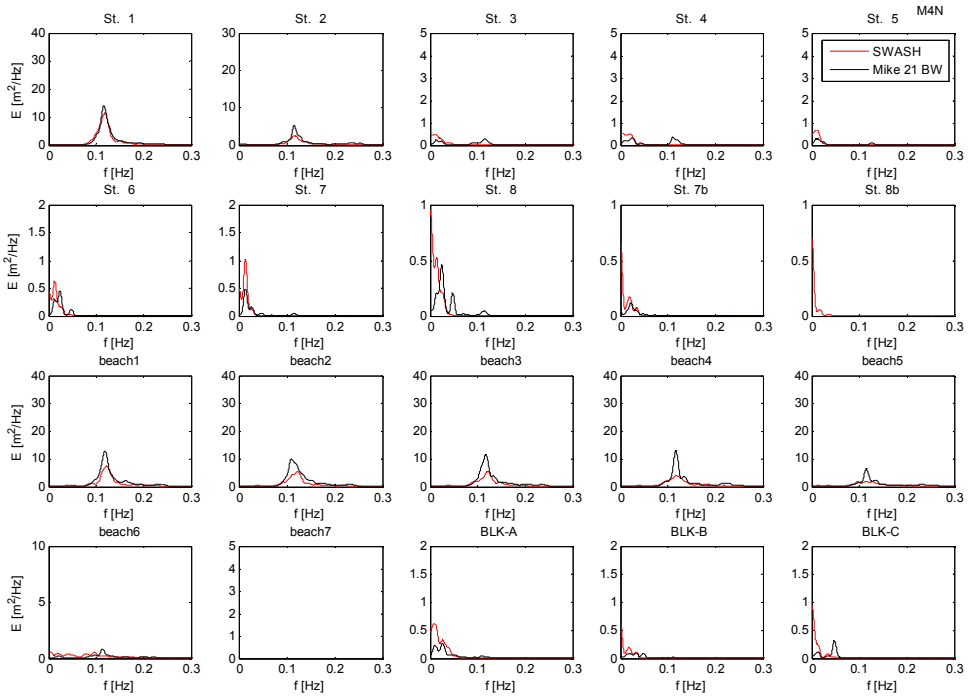

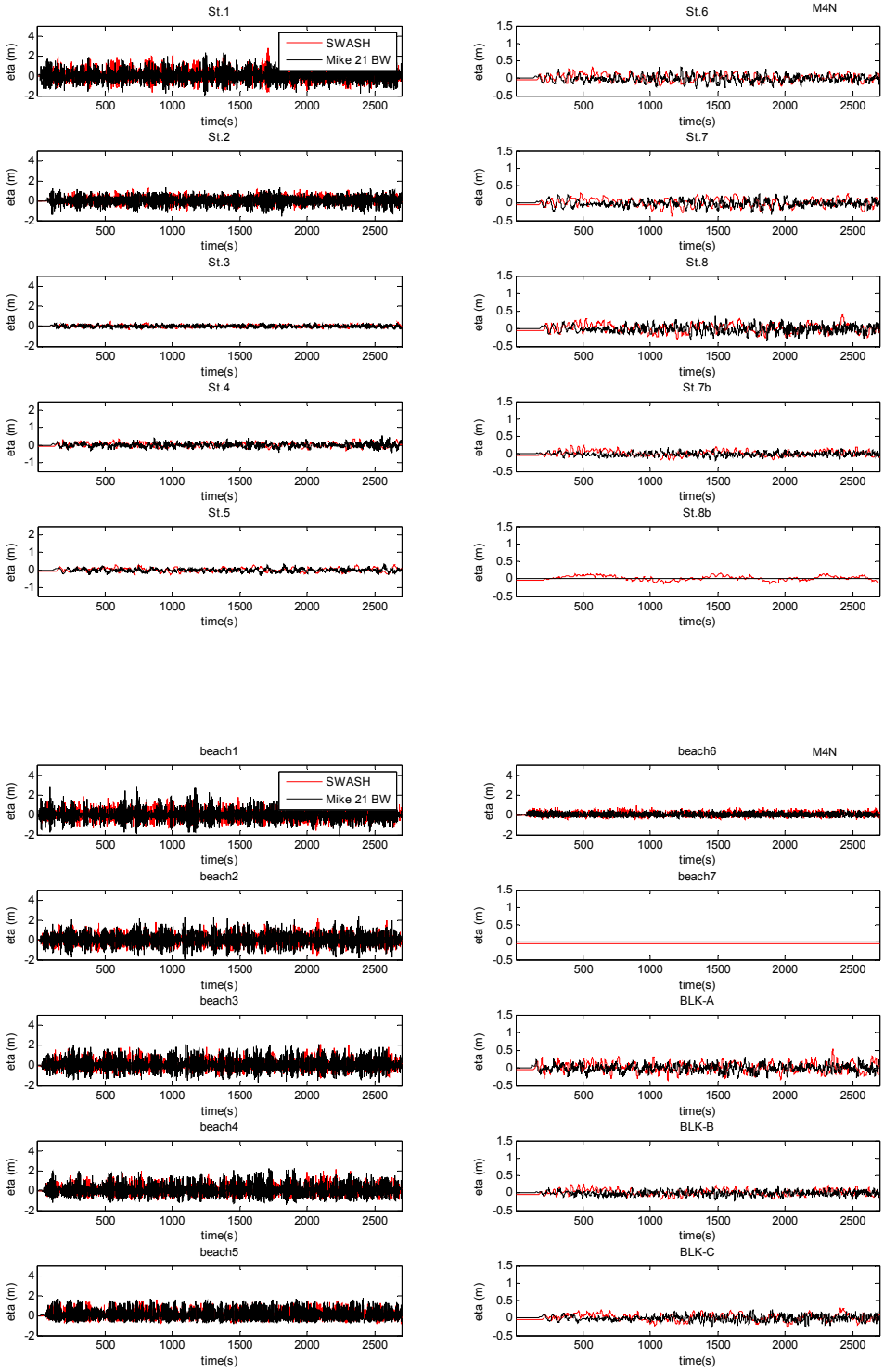

1000 year storm, Wave direction N

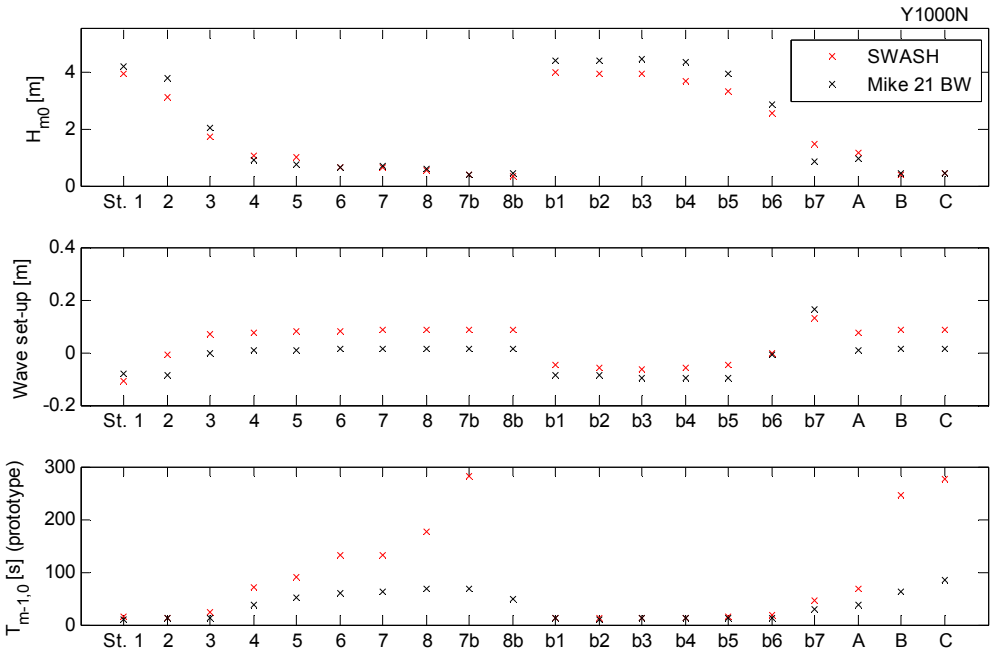

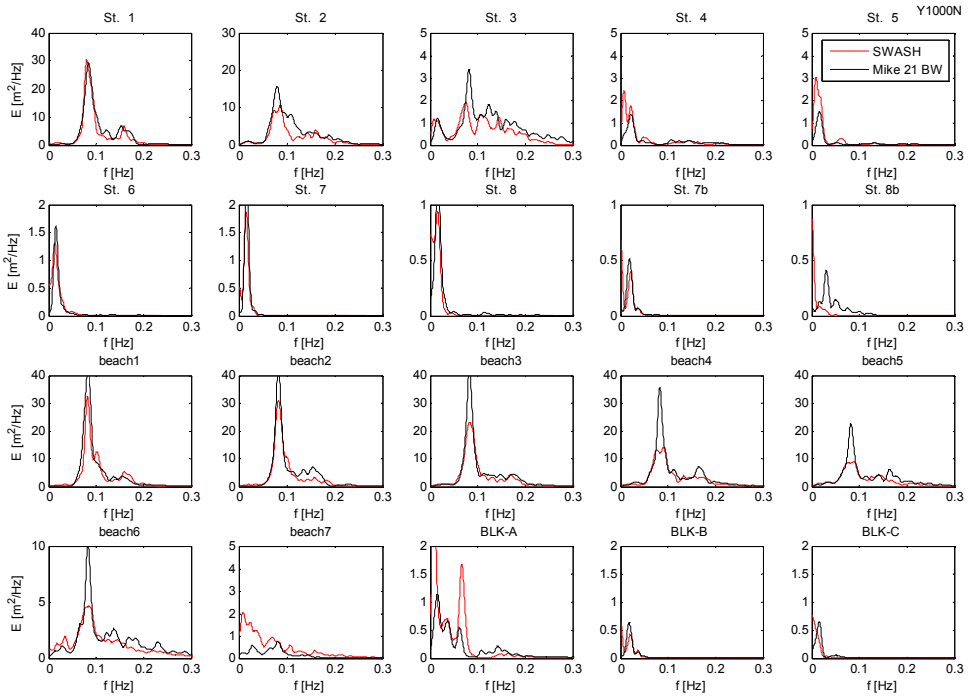

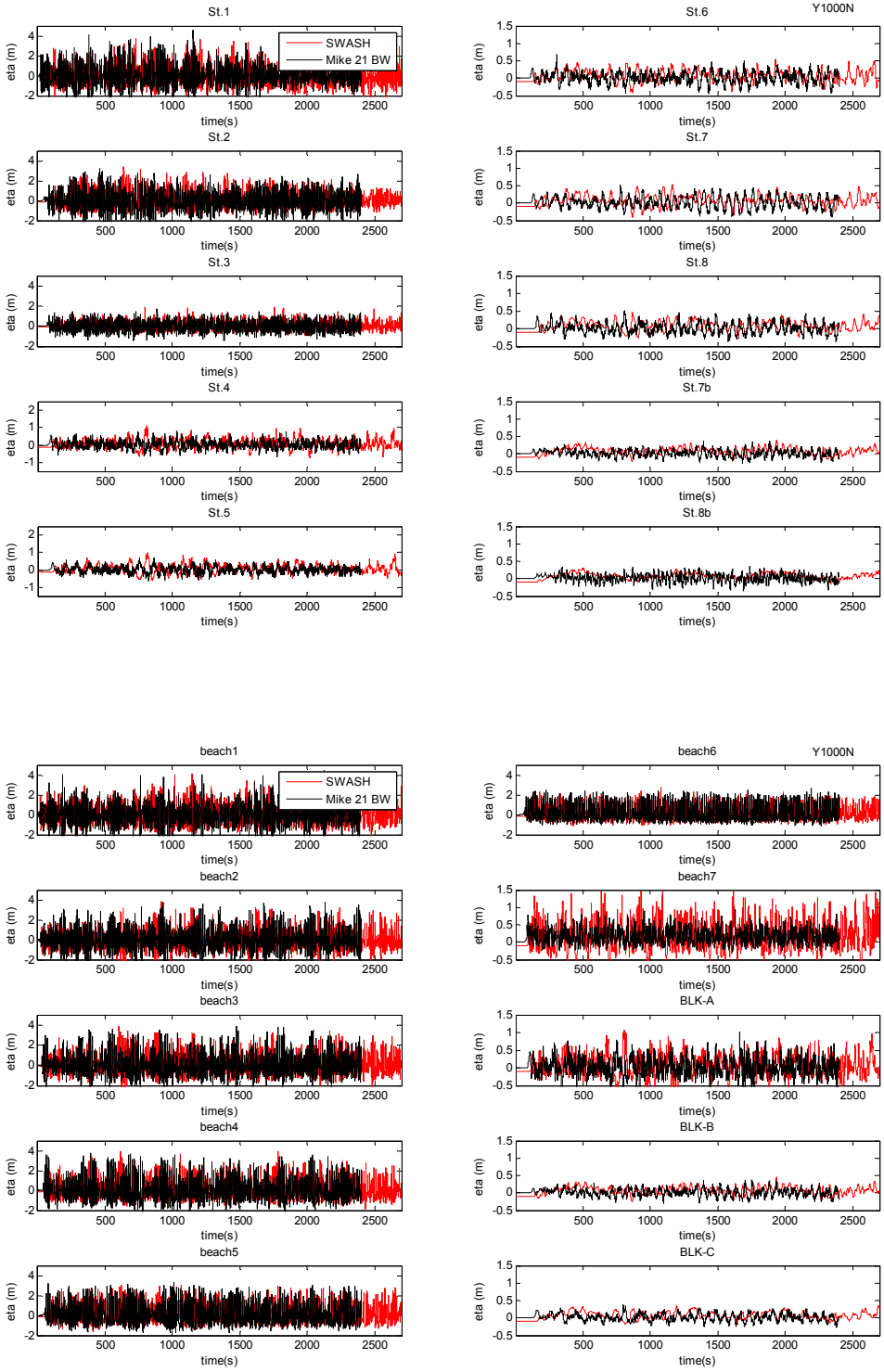

1000 year storm, Wave direction NNW, Long crested

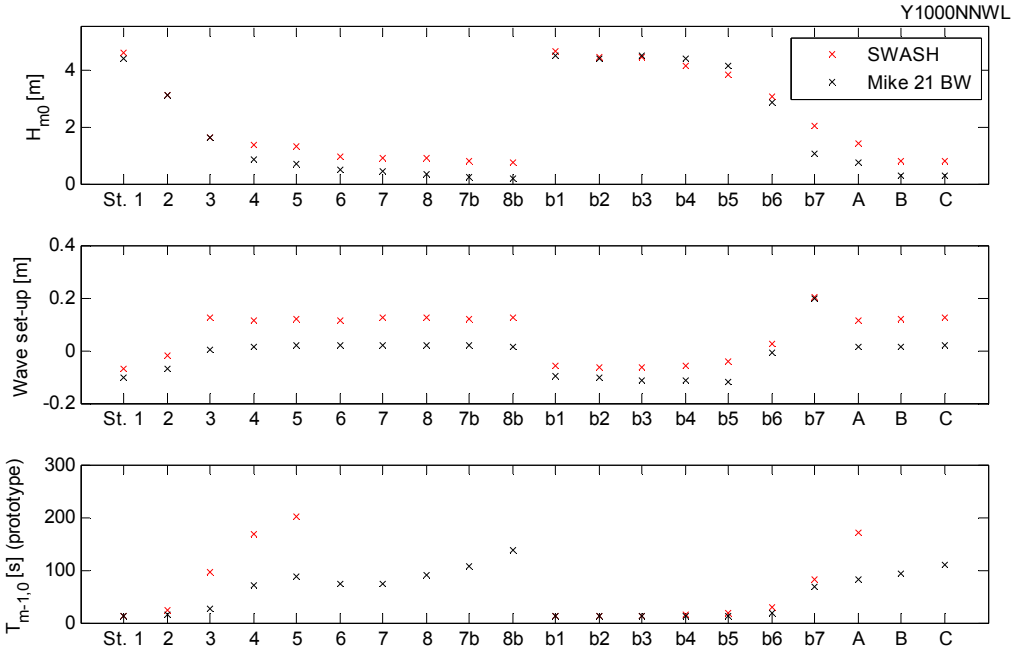

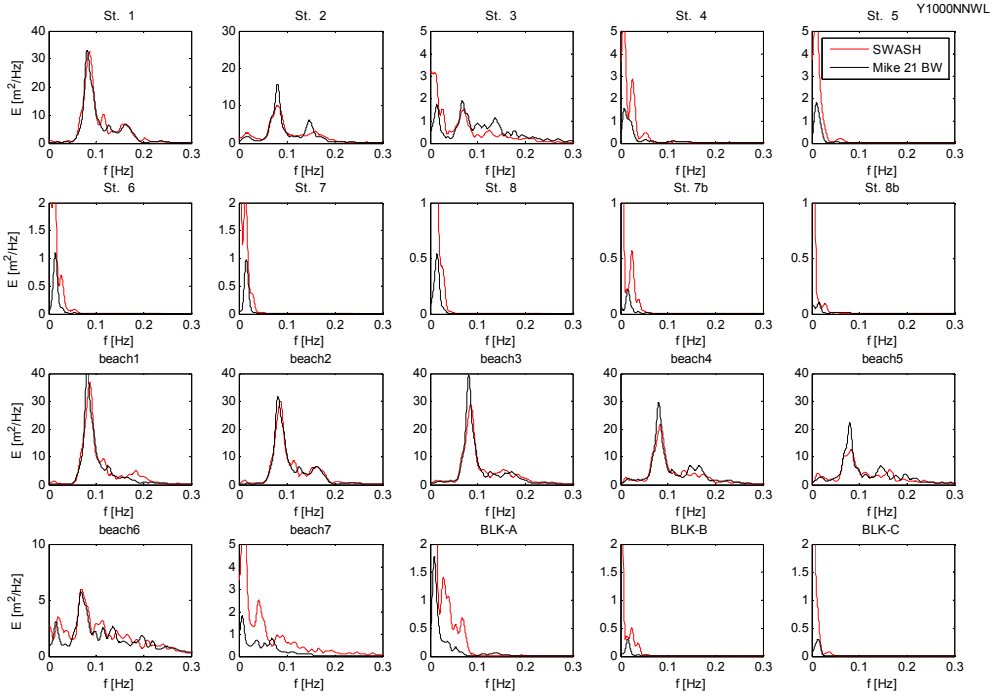

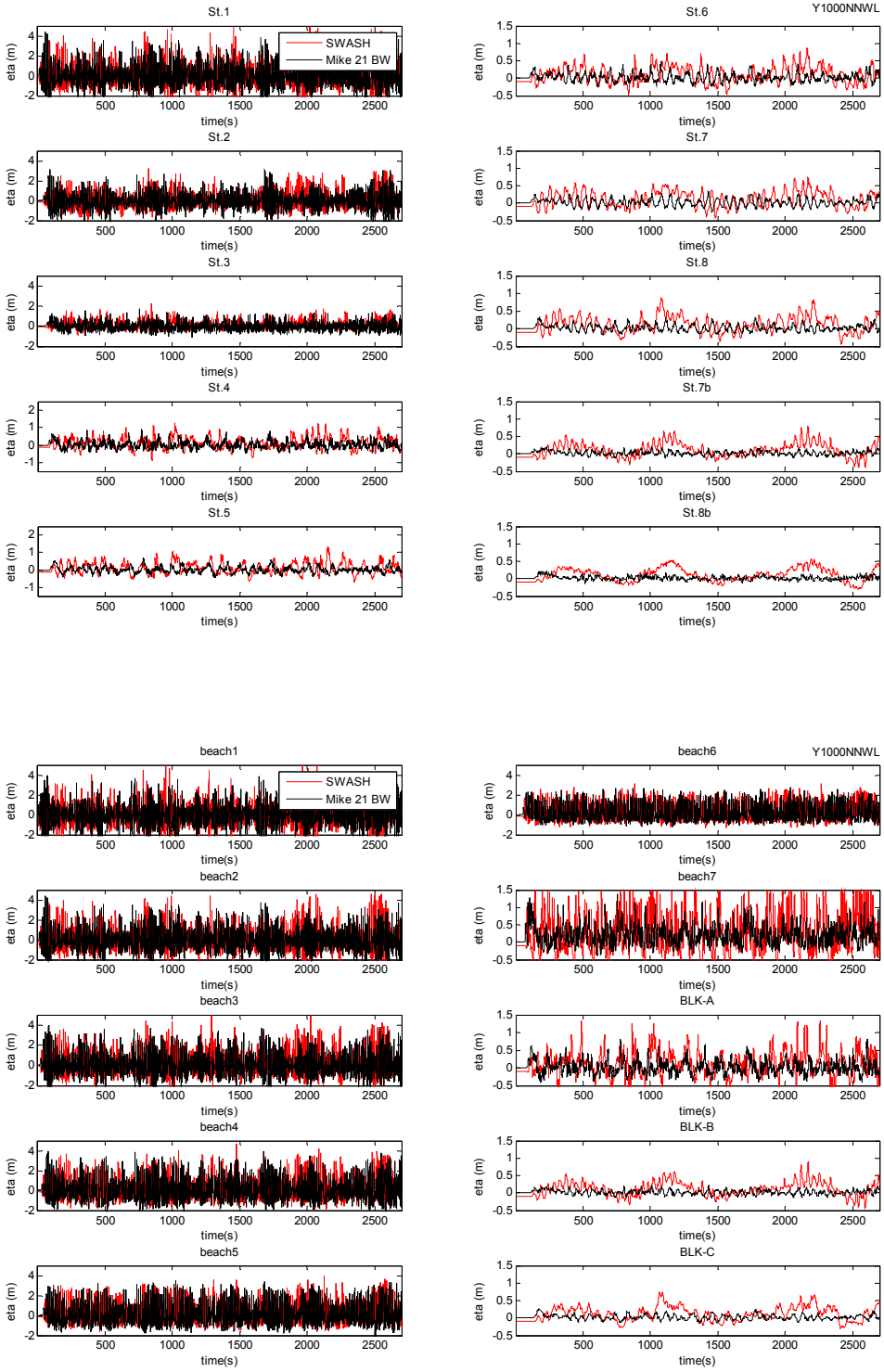

1000 year storm, Wave direction NNW, Short crested (15 deg.)

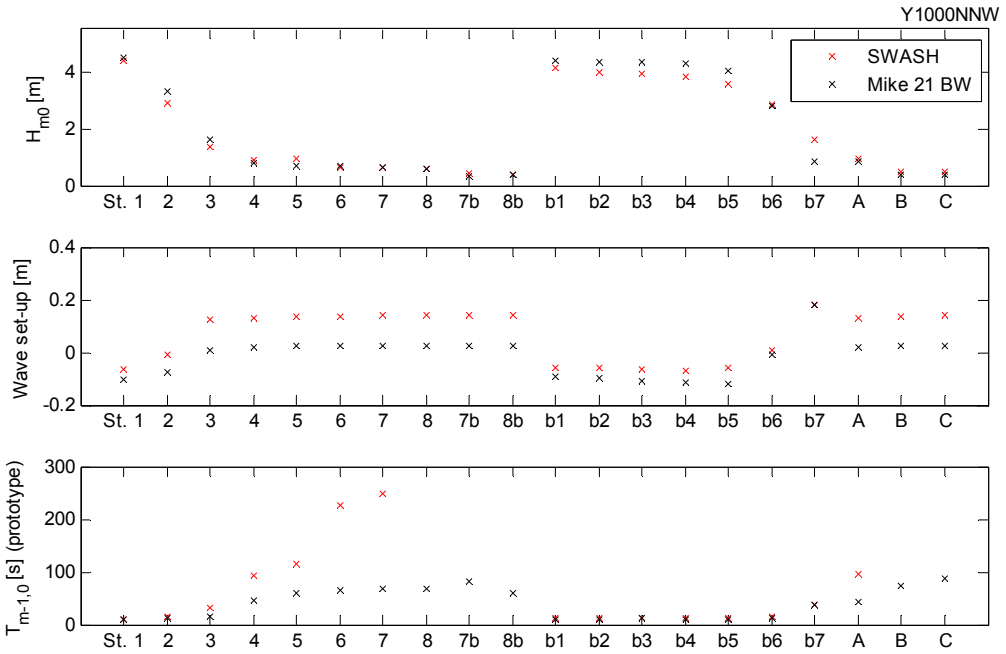

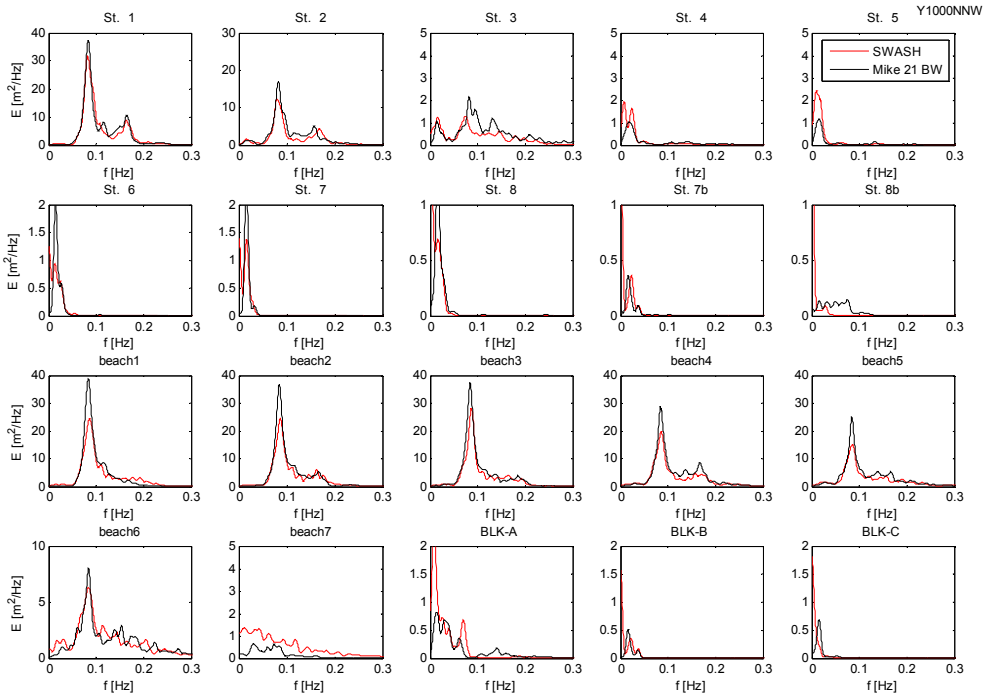

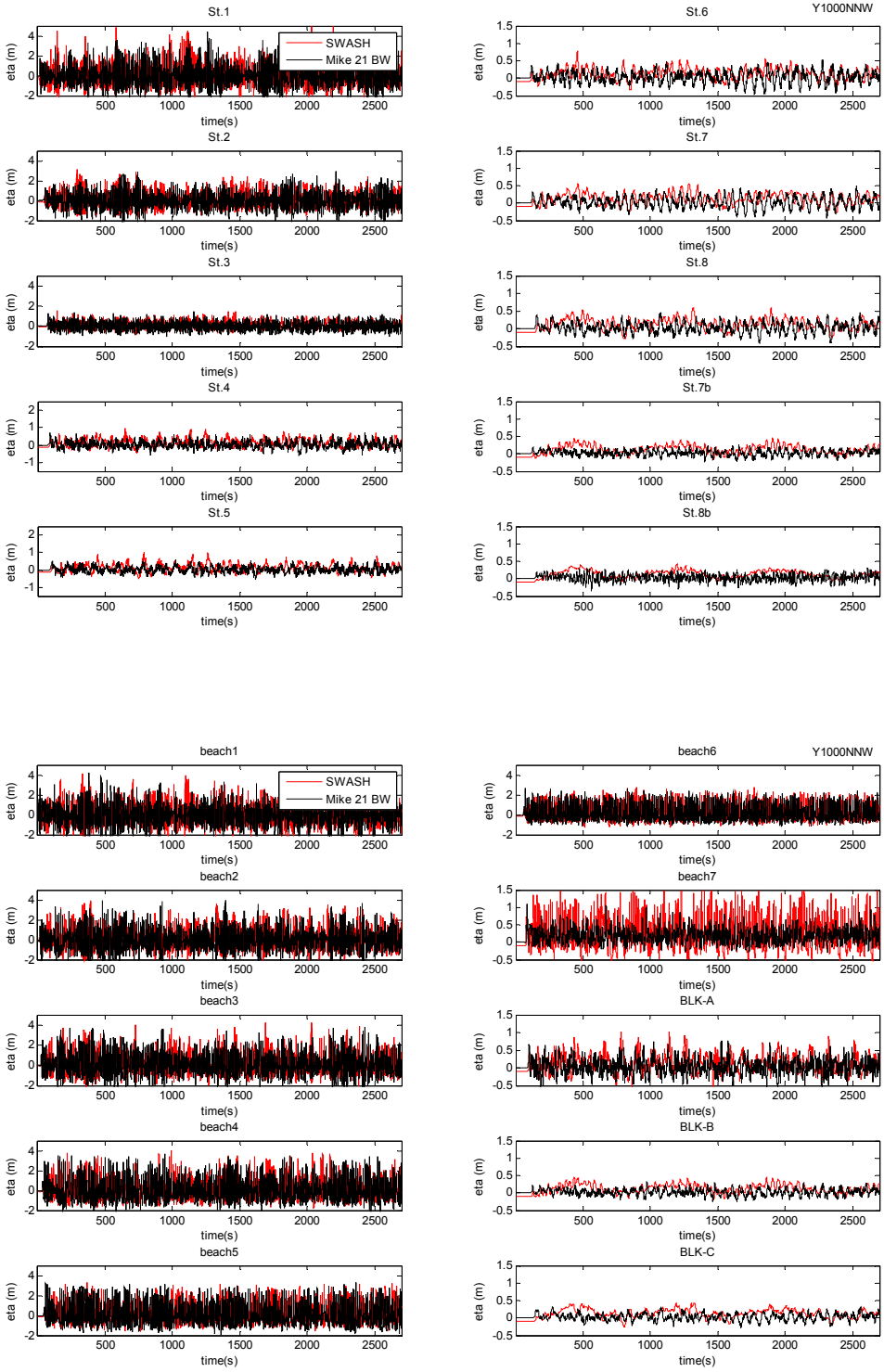

1000 year storm, Wave direction NNW, Short crested (30 deg.)

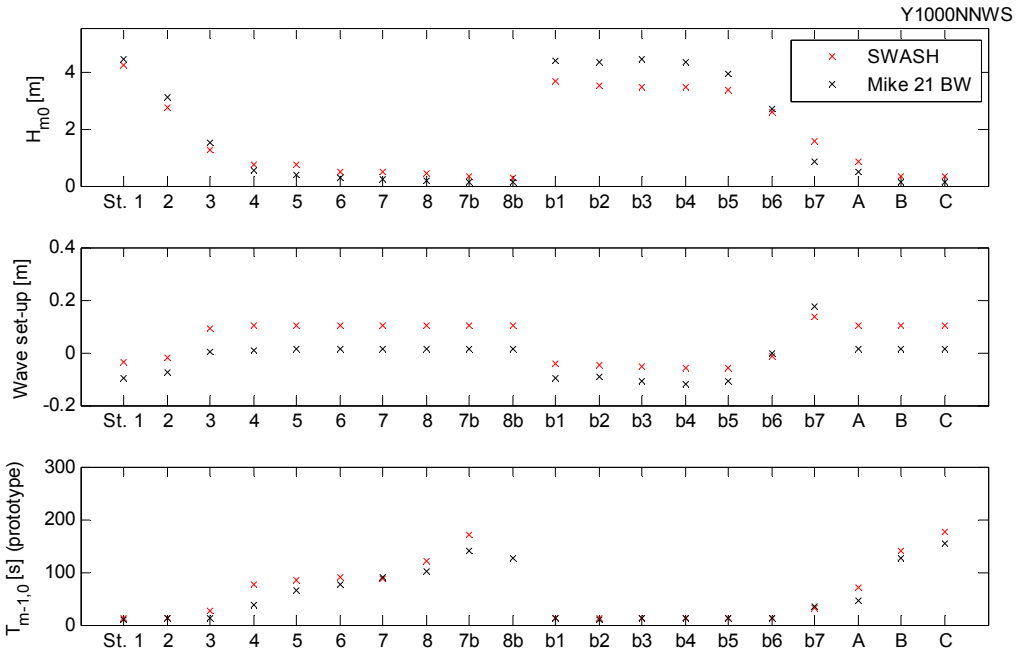

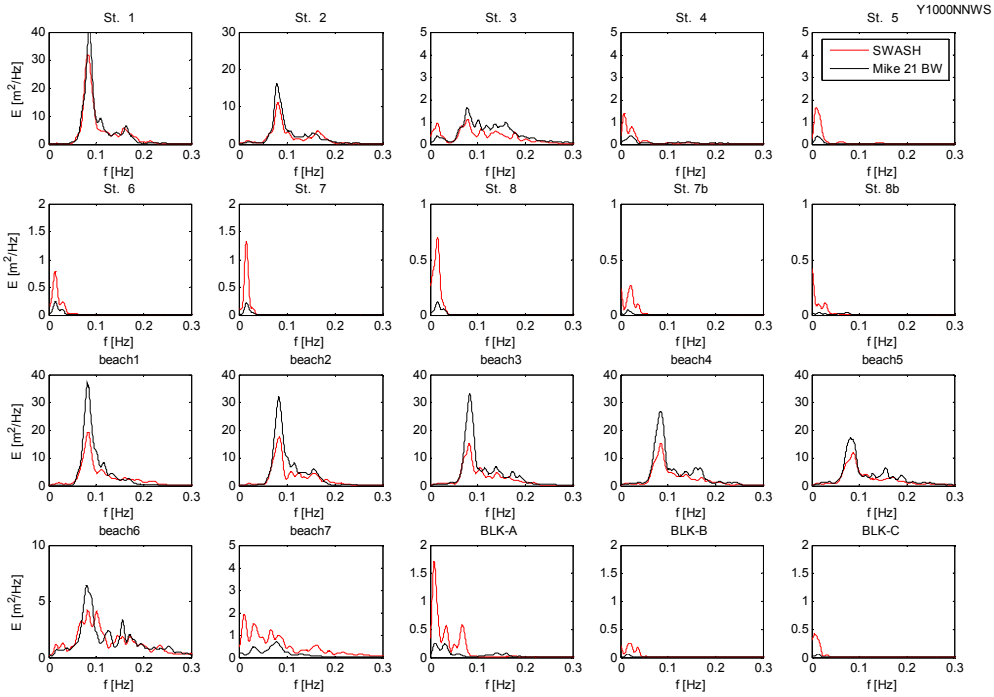

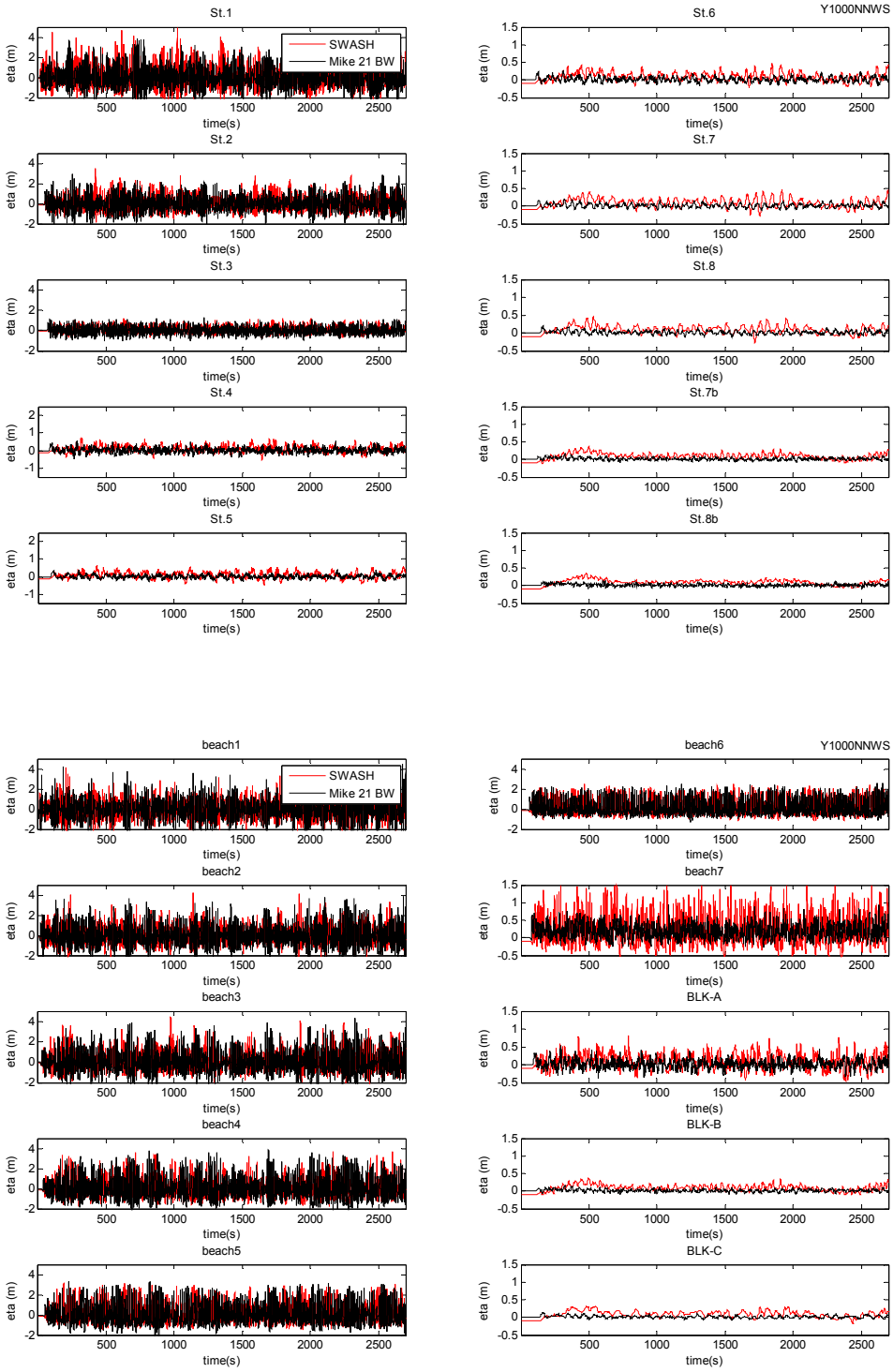

1000 year storm, Wave direction: NW

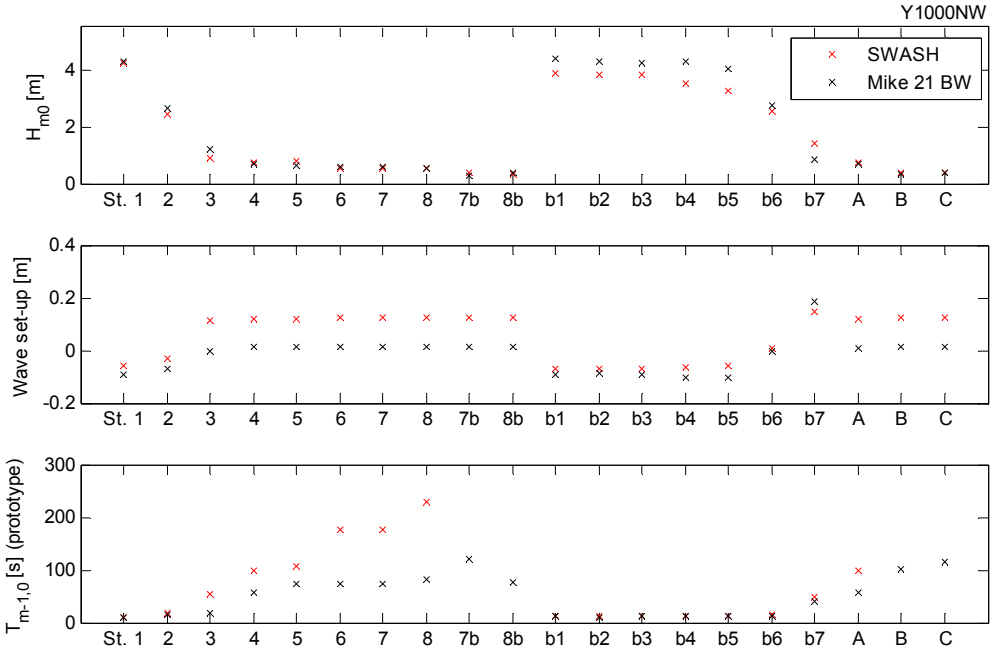

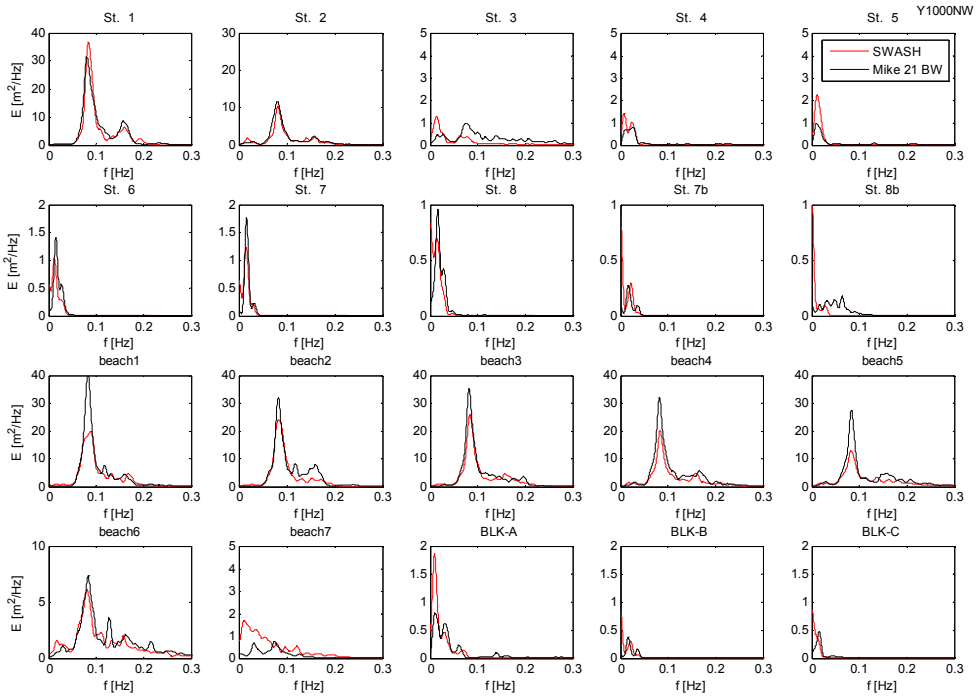

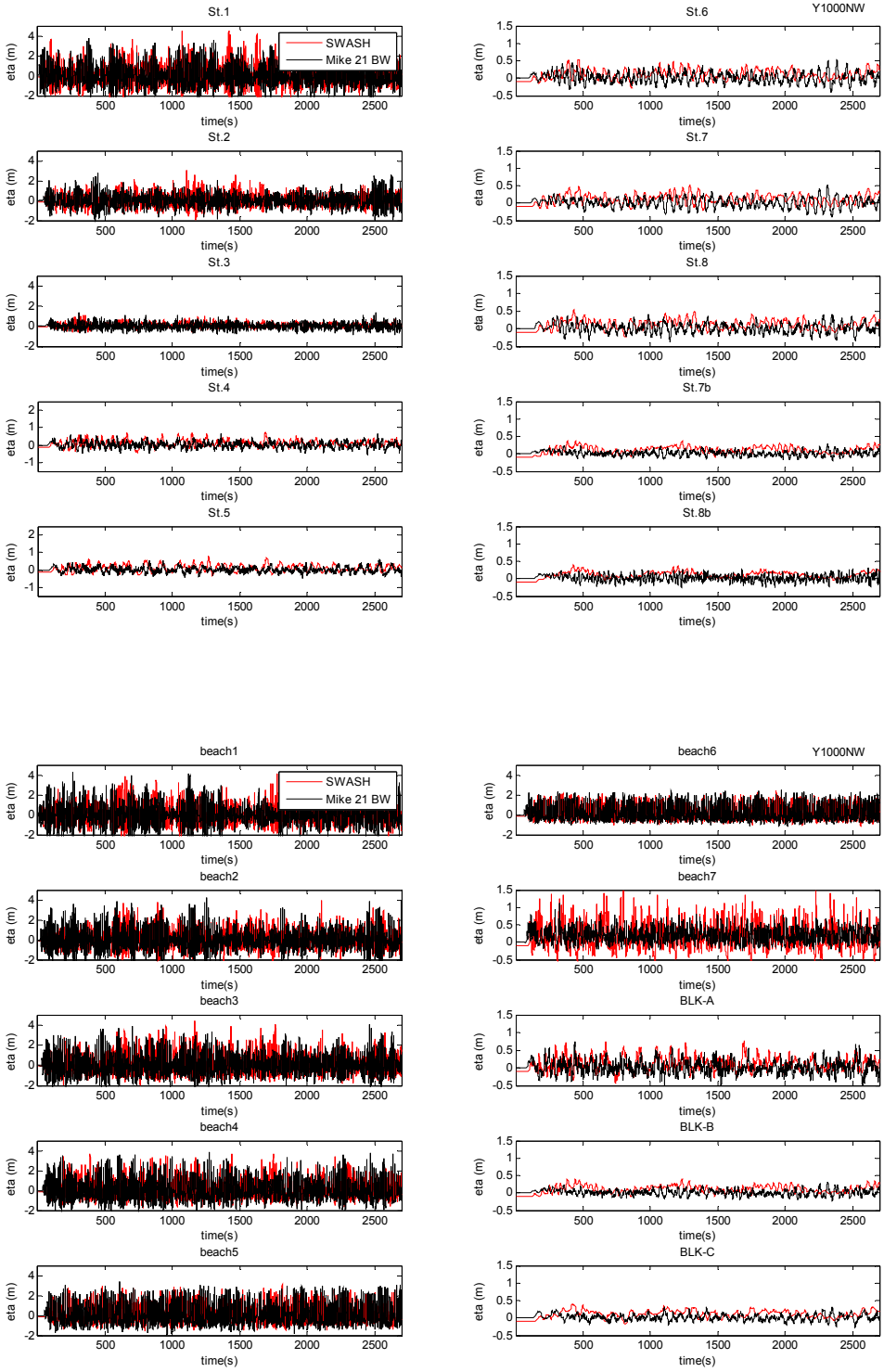

1000 year storm, Wave direction WNW

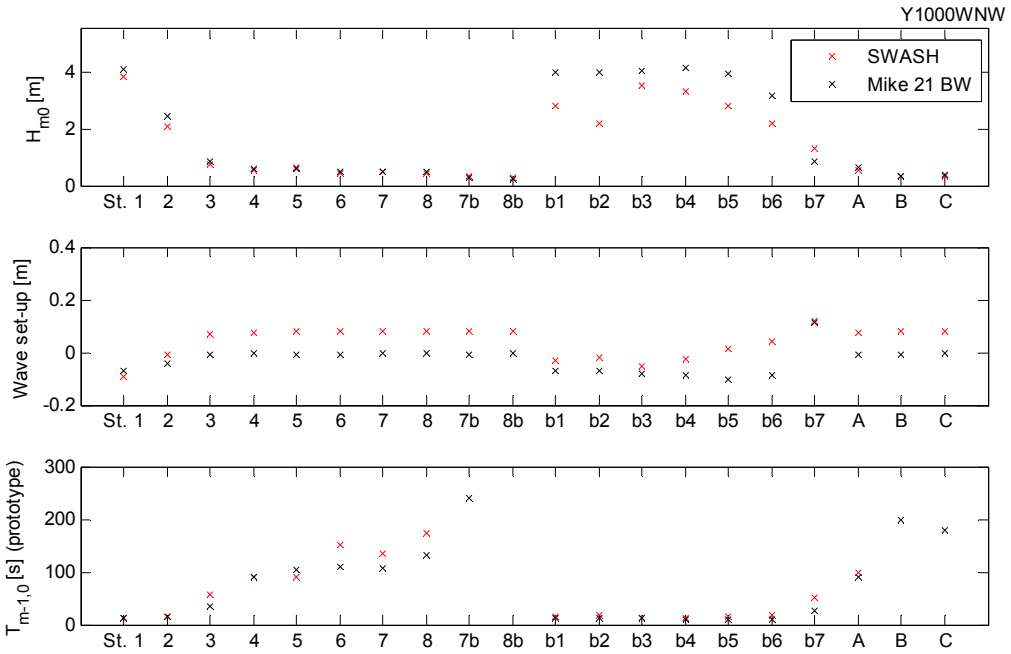

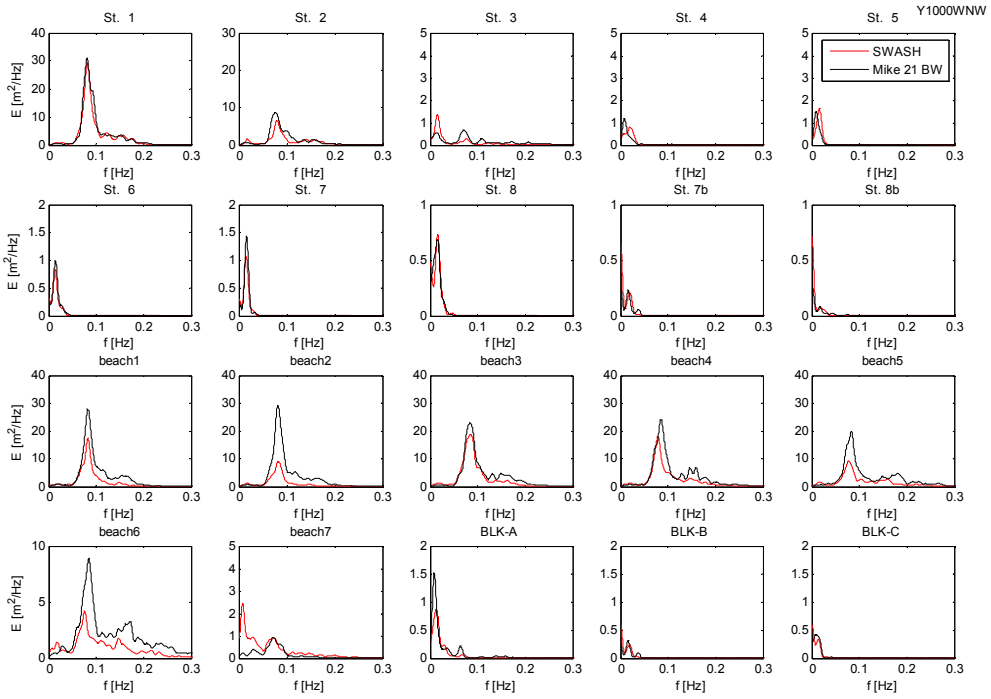

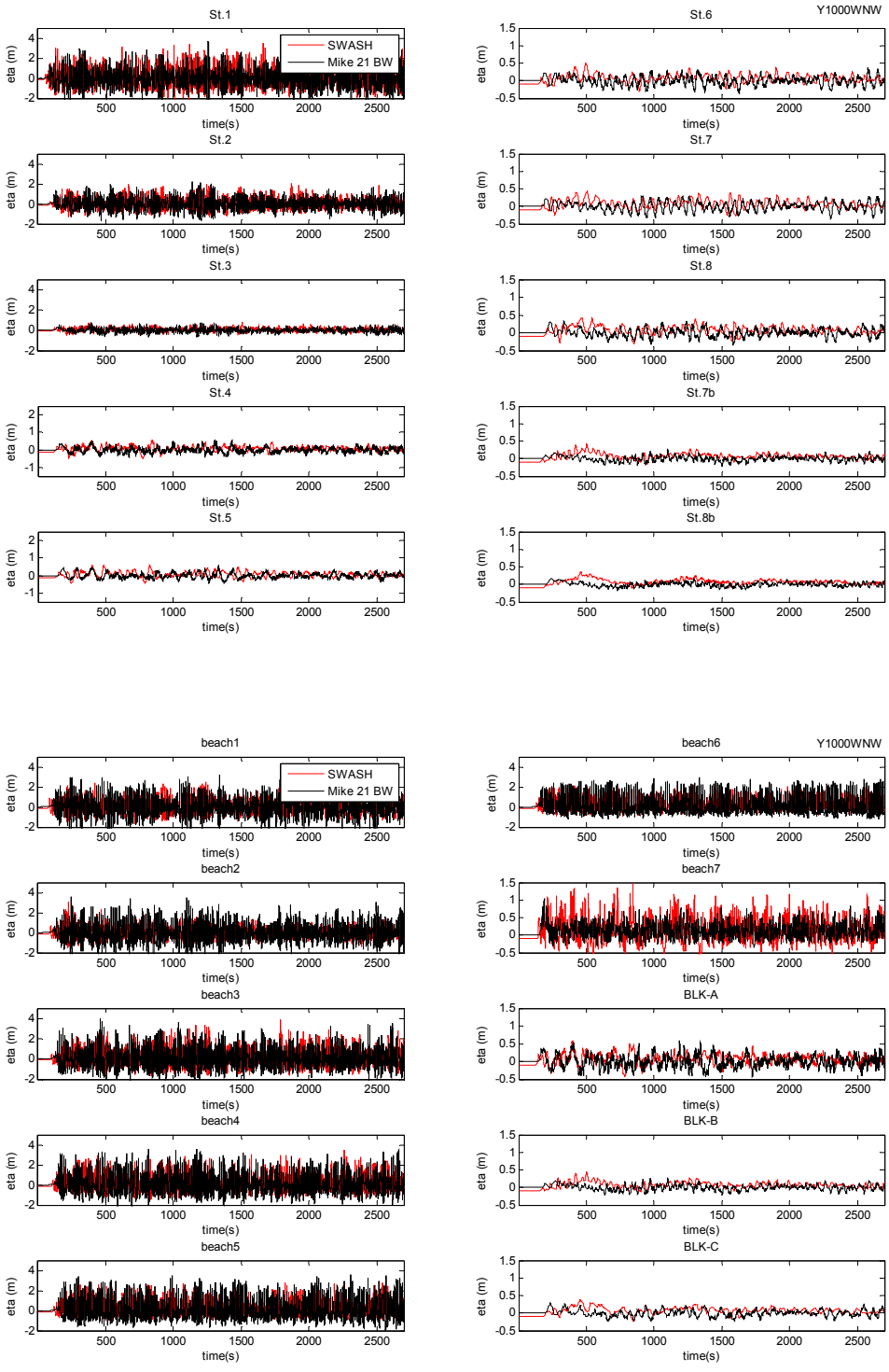

8m super storm, Wave direction NNW, Long crested

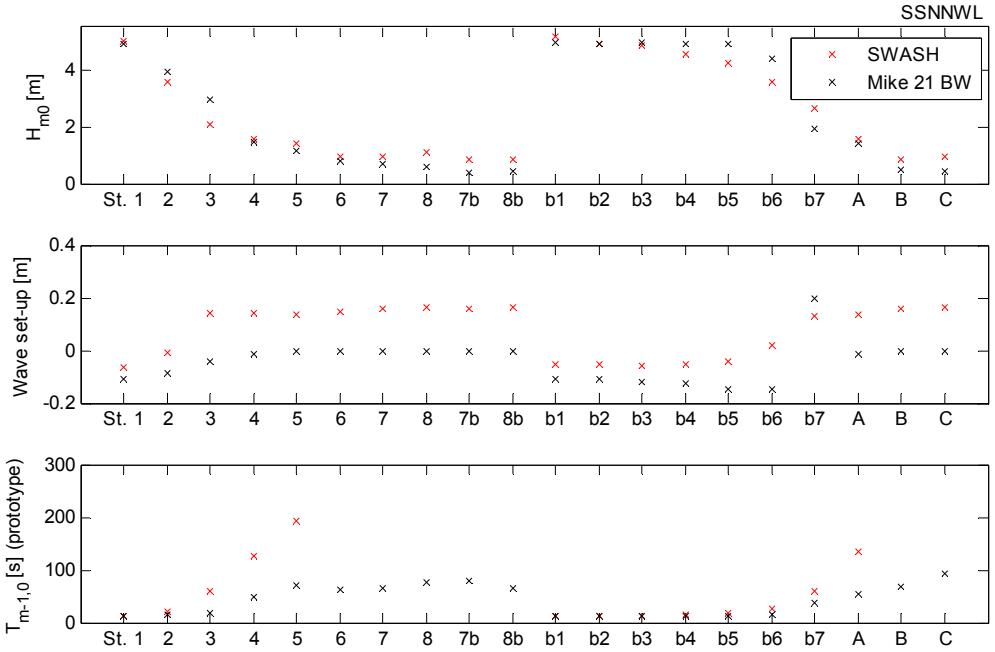

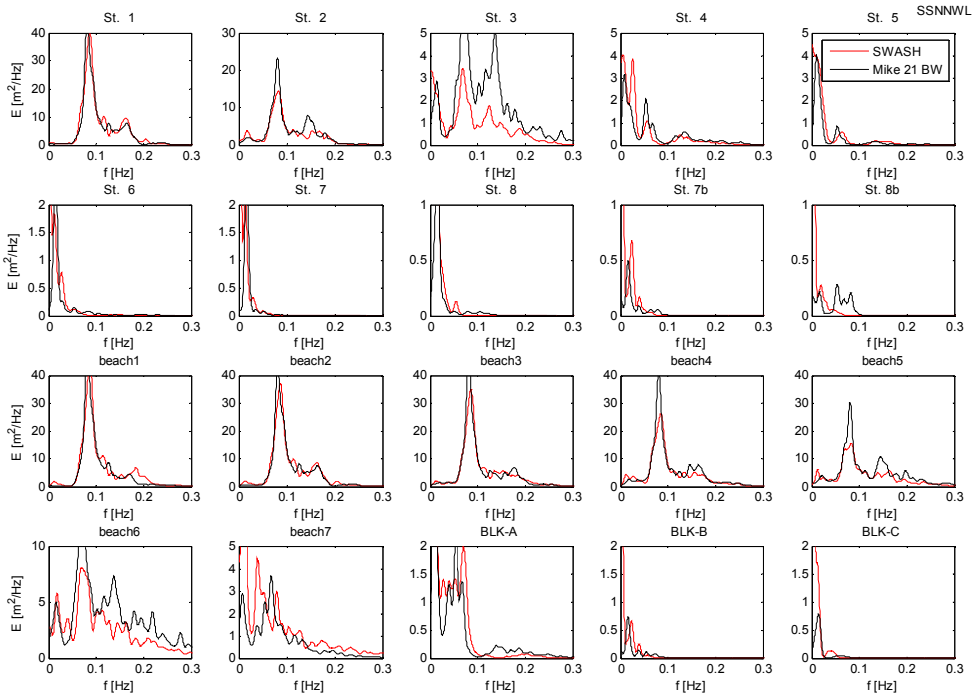

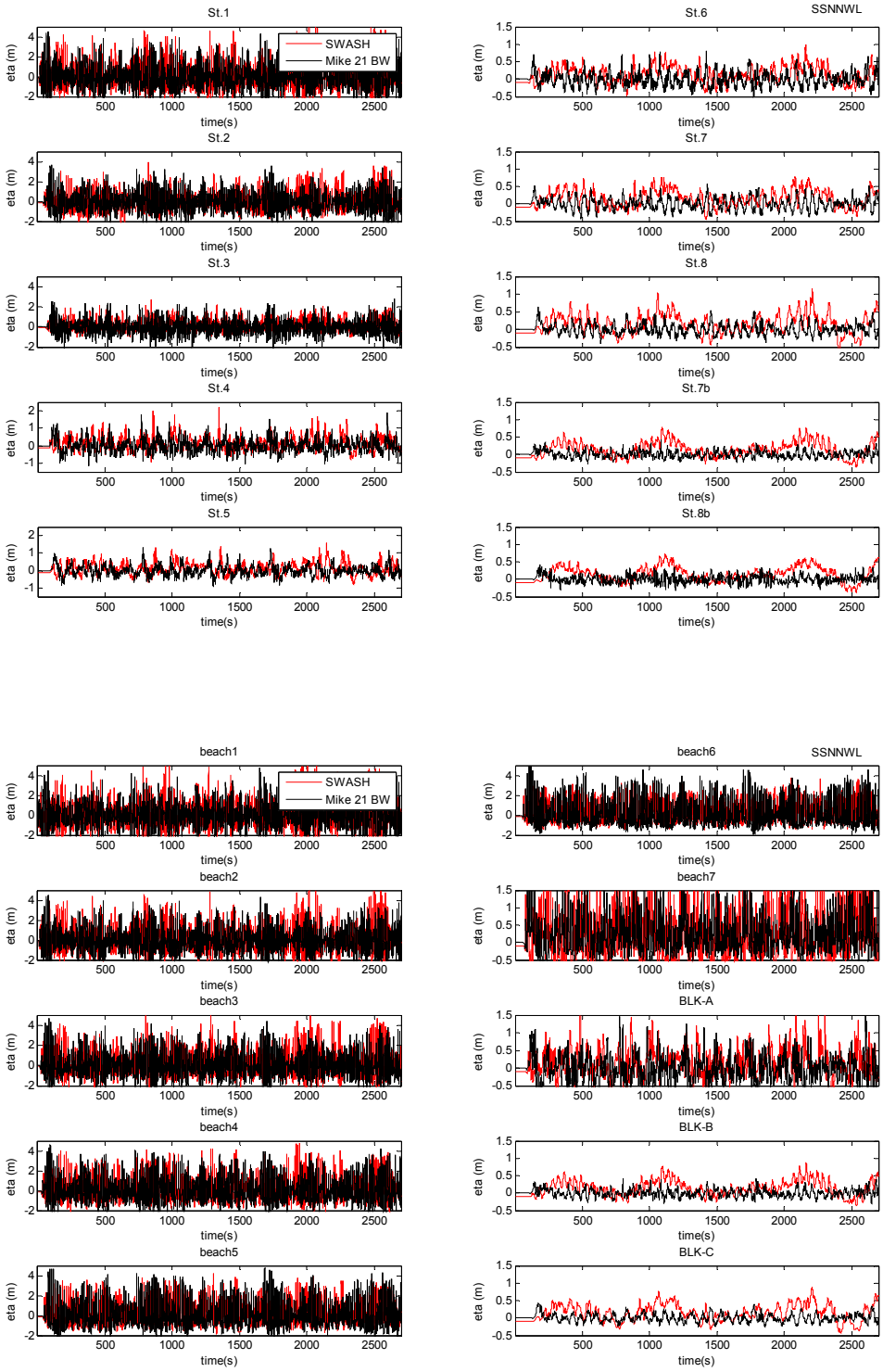

8m super storm, Wave direction NNW, Short crested (15 deg.)

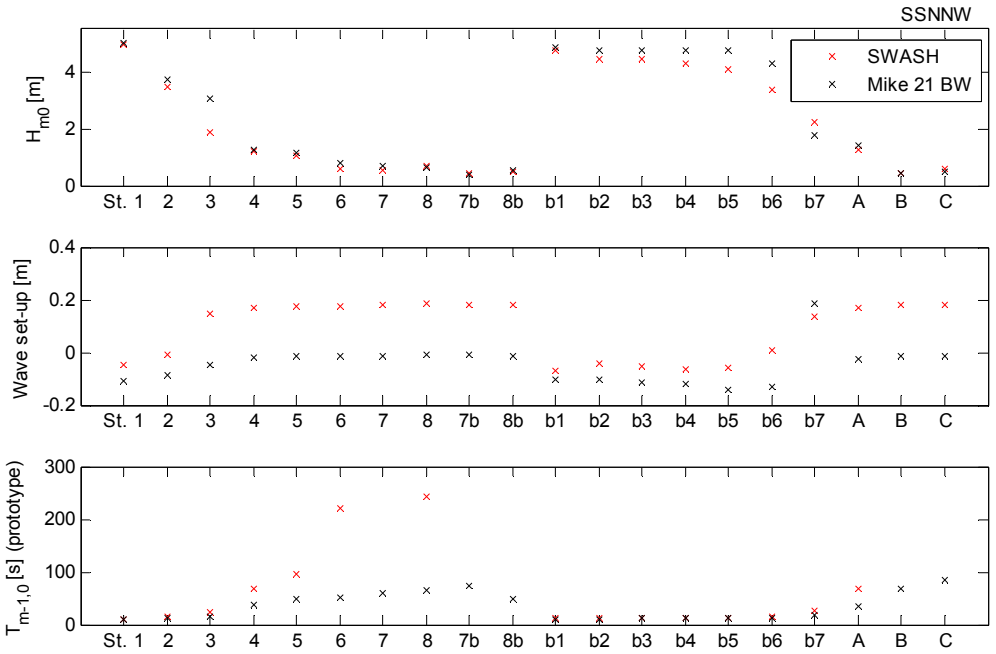

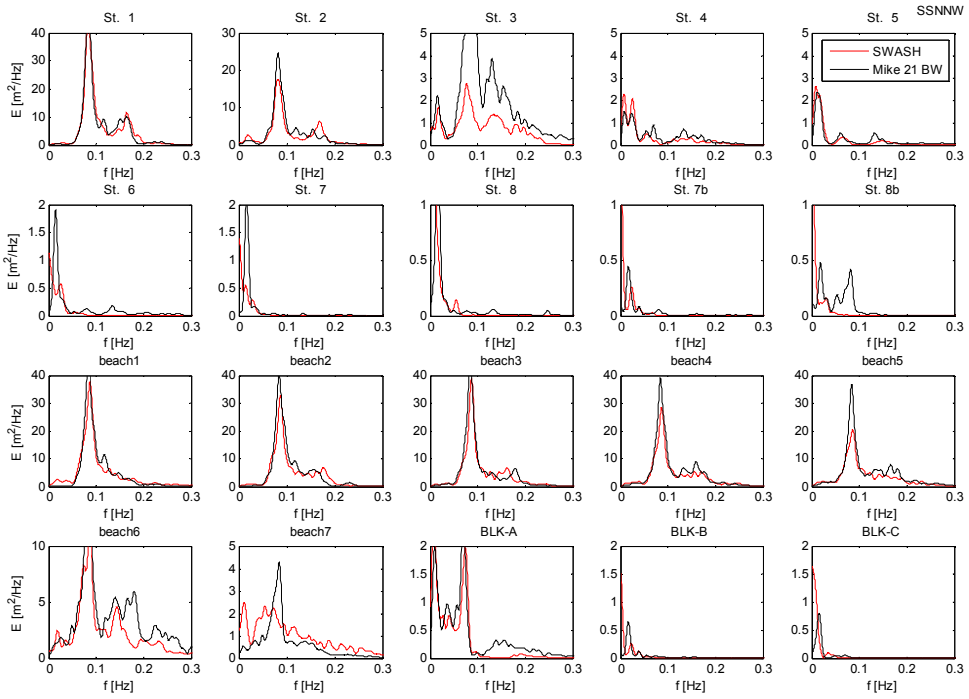

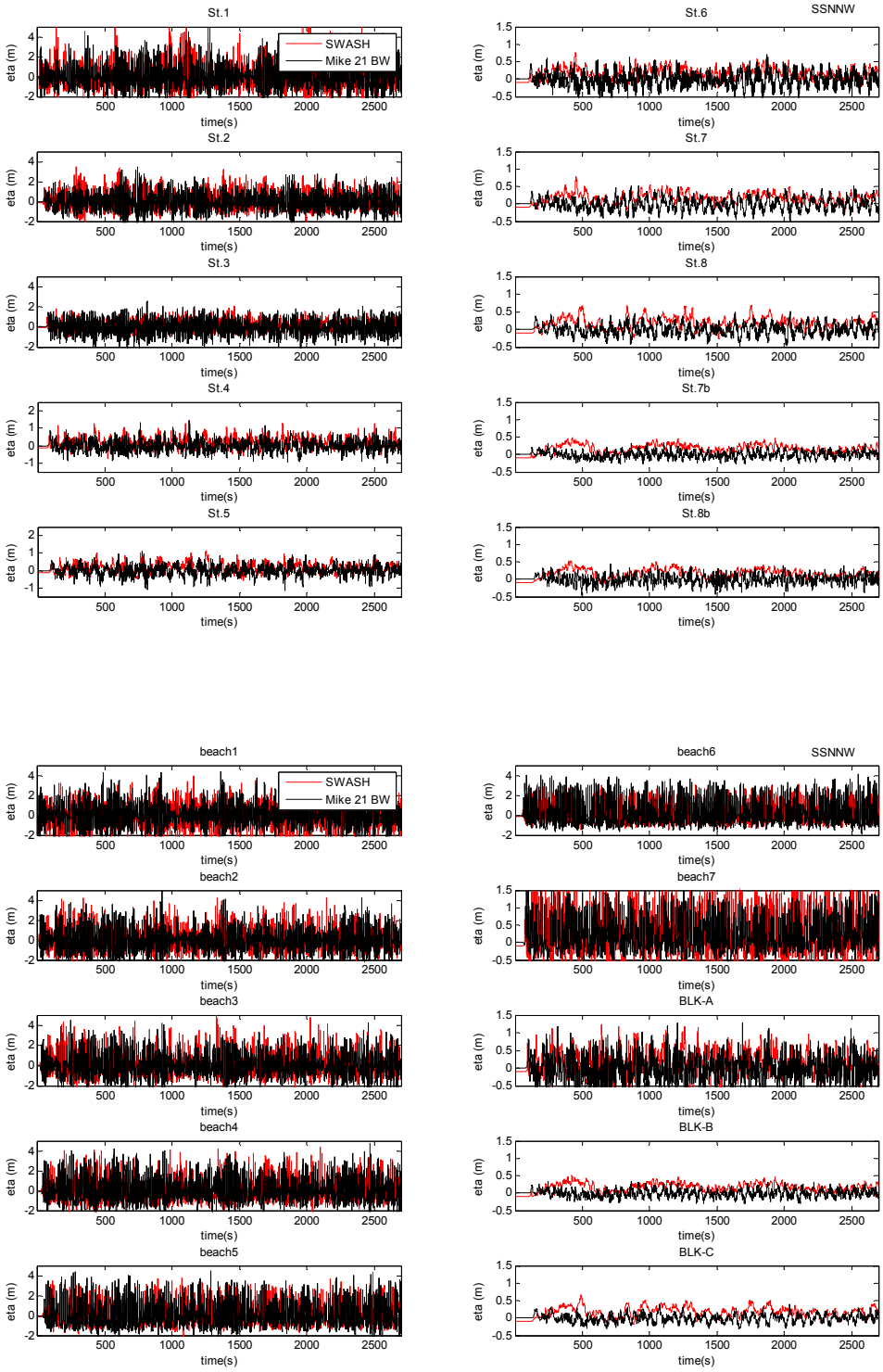

8m super storm, Wave direction NNW, Short crested (30 deg.)

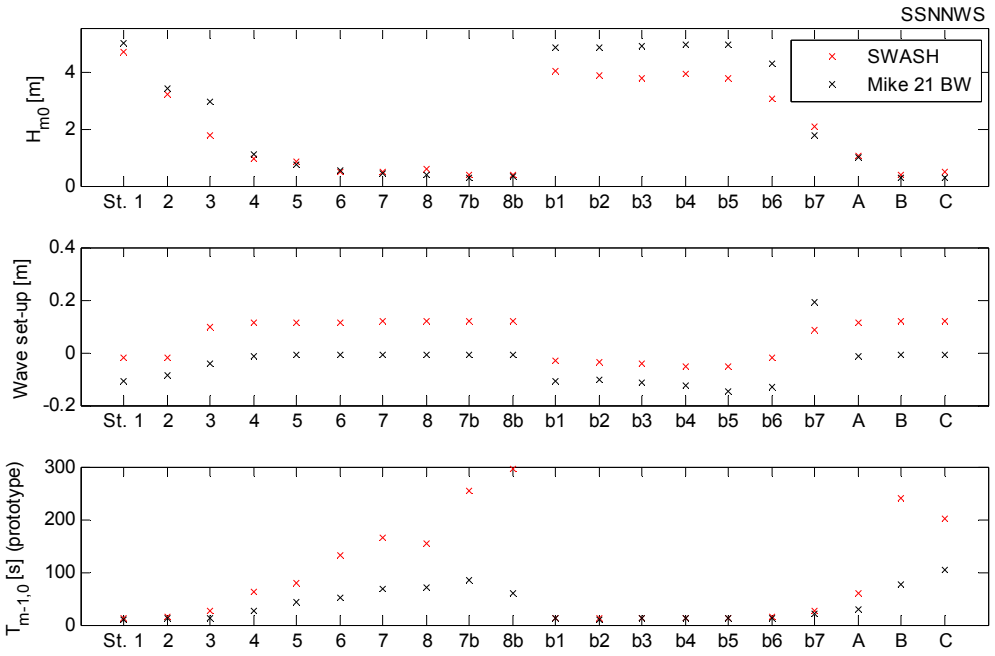

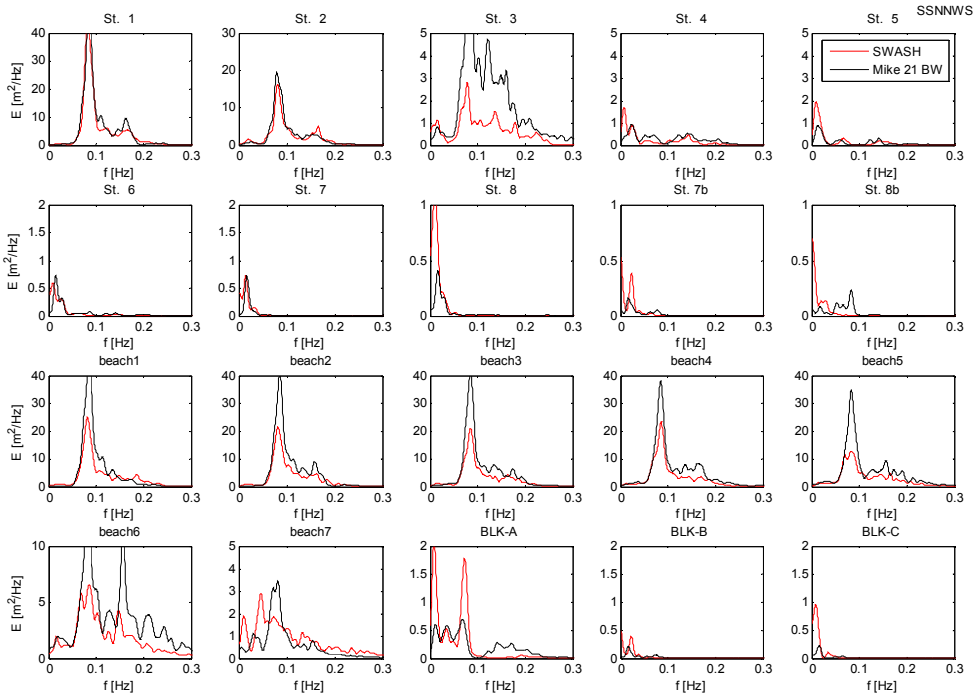

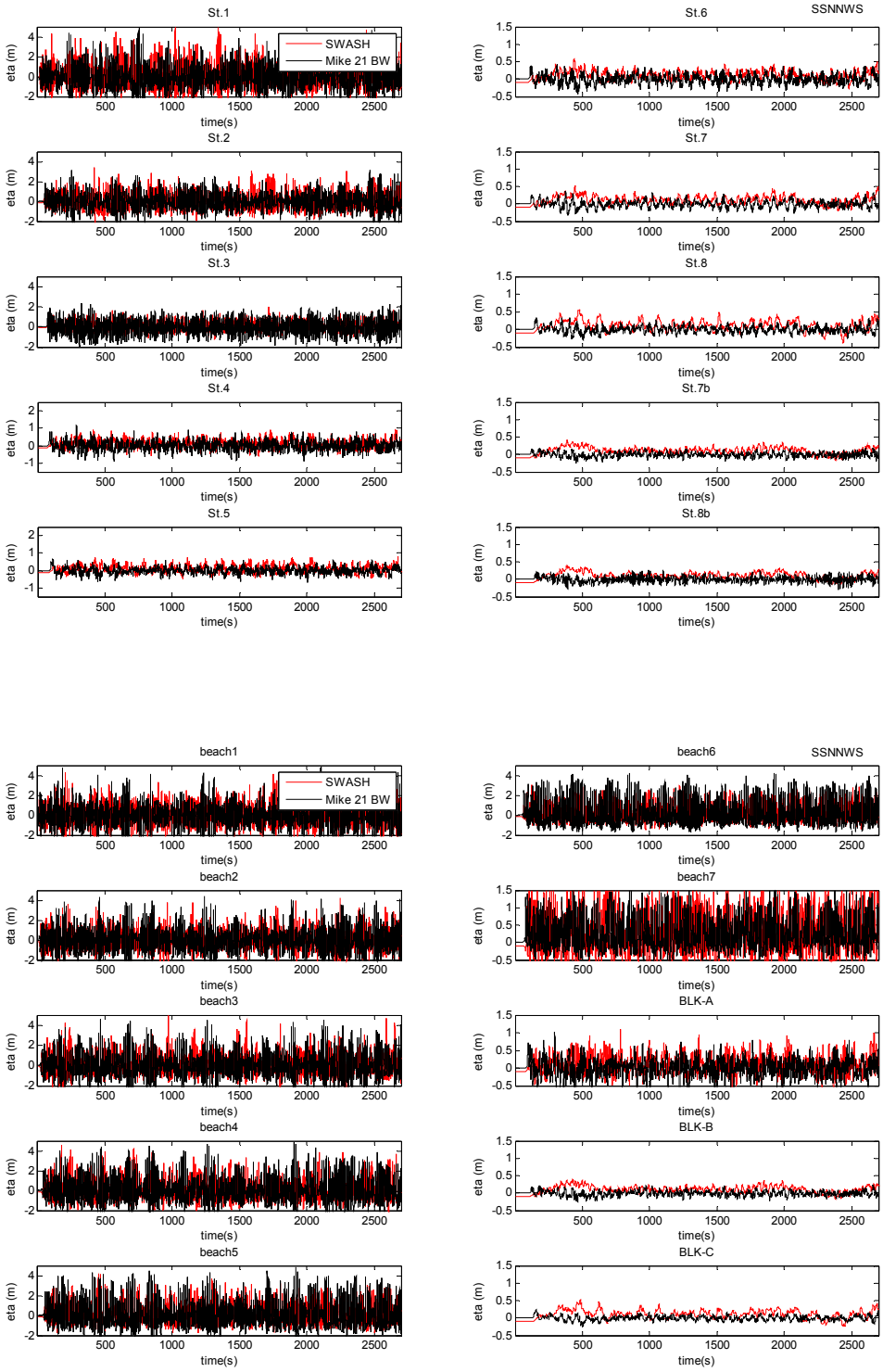

White noise

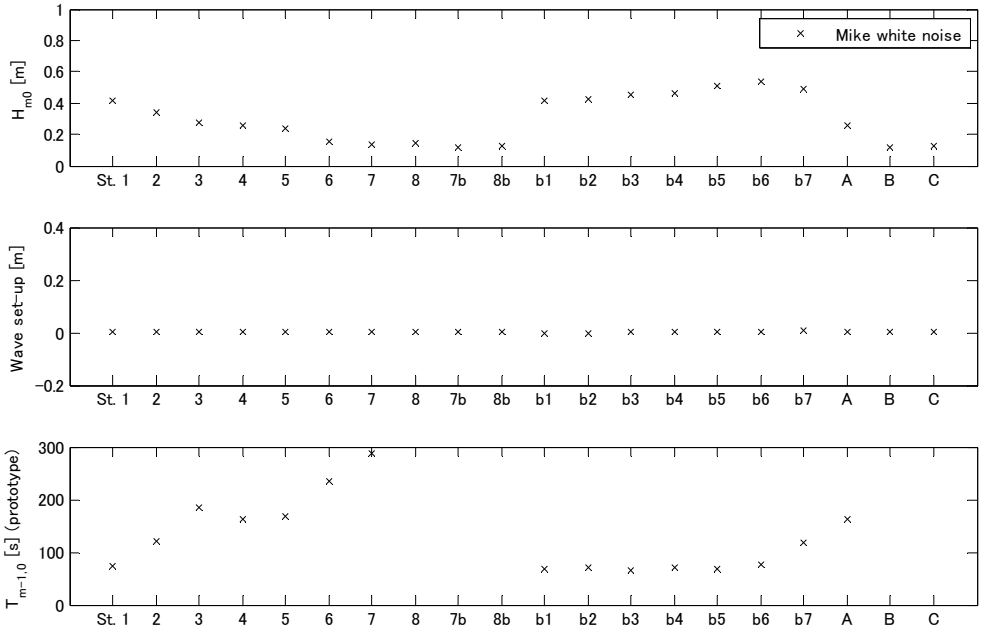

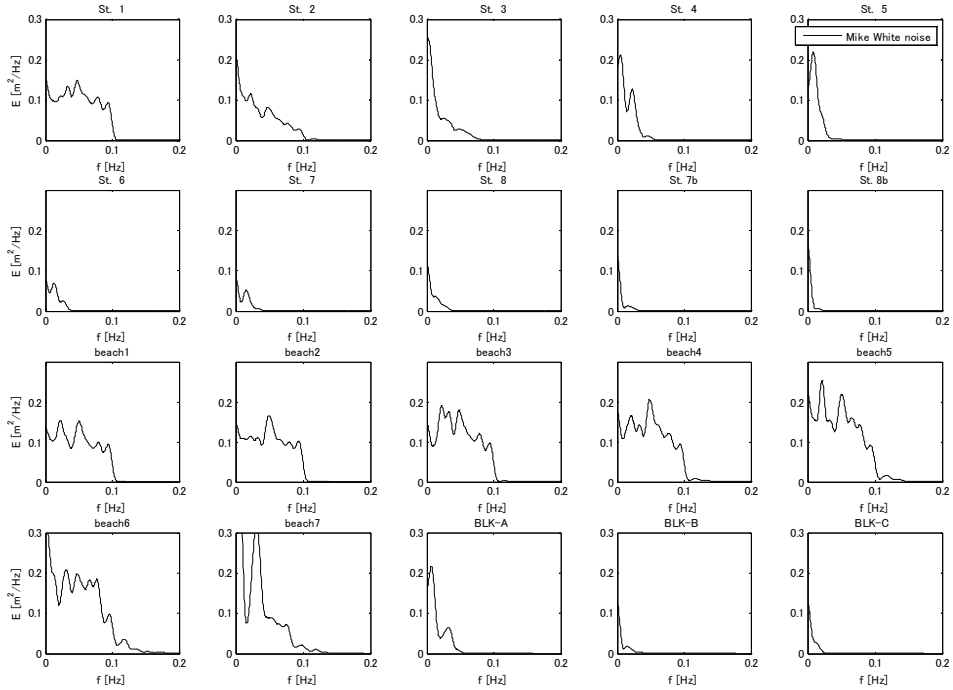

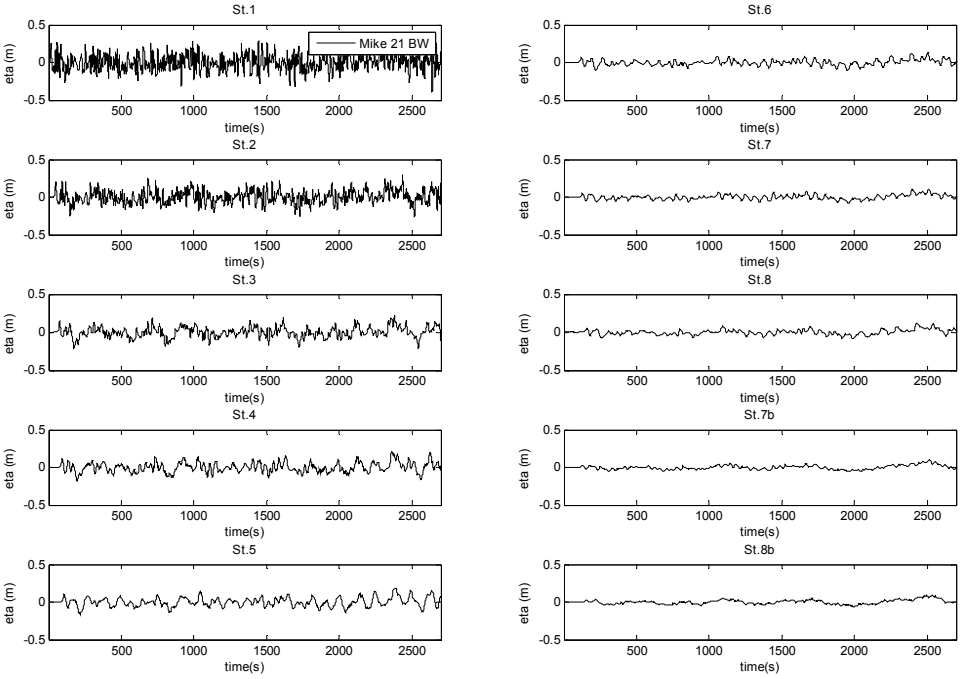

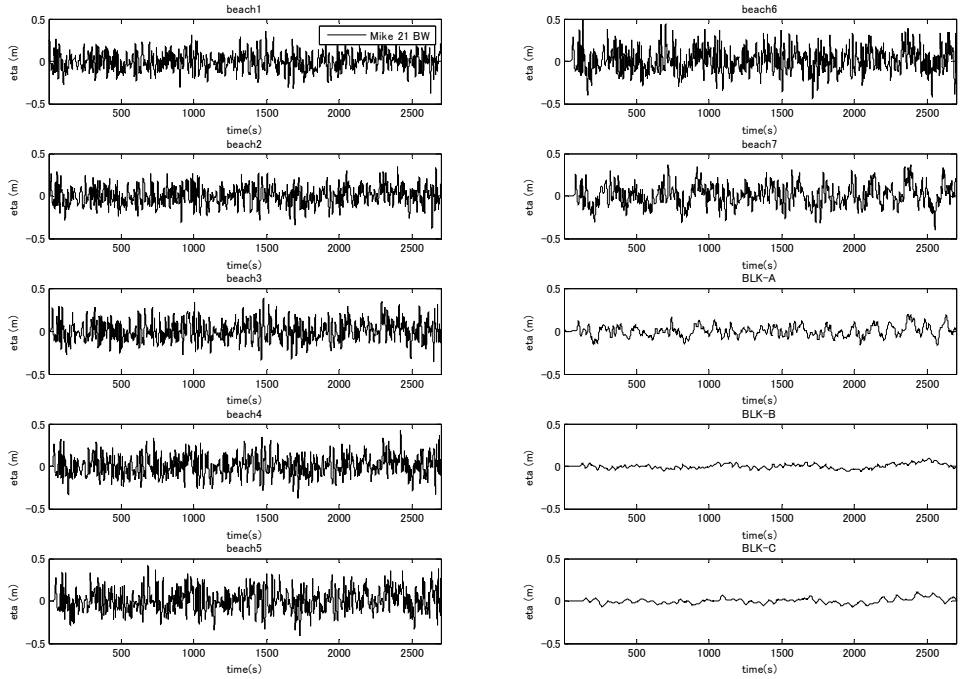

Waterbouwkundig Laboratorium

Flanders Hydraulics Research

Berchemlei 115
B-2140 Antwerp
Tel. +32 (0)3 224 60 35
Fax +32 (0)3 224 60 36
E-mail: waterbouwkundiglabo@vlaanderen.be
www.watlab.be